PROGRAMMING THE TOMATO GENOME WITH LED LIGHT

JANUARY 2019

STEVEN JAMES GRUNDY BSc Hons

SUPERVISORS: Prof. GRAHAM SEYMOUR, Prof. CHUNGUI LU and Dr. ERIK MURCHIE

A thesis submitted to The University of Nottingham for the degree of Doctor of Philosophy

The University of Nottingham

School of Biosciences

Sutton Bonington Campus,

Leicestershire,

LE12 5RD

Abstract

Light quality has a profound effect on many aspects of plant growth and development. An extremely important breakthrough has been made with light-emitting diode (LED) technology which now is playing an increasing role in horticultural lighting. A key feature is that the spectral output of LEDs can be adjusted, which makes it possible to intercept light at high efficiency and drive photosynthesis to produce adequate crop yield and quality. The LEDs lighting opens up tremendous opportunities for researchers, farmers, and breeders. Currently, the effects of different LED light on plant growth, especially, on morphological and physiological changes in different crops have been studied. However, very little is known about the regulatory mechanisms and correlations between these changes at the omics level by integrative systems biology approach.

In this study, the influence of light quality on yield, morphology, pigment metabolism and photosynthetic performance was evaluated in *Solanum lycopersicum* cv. Micro-Tom. Transcriptomic analysis (RNA-Seq) and gene co-expression networks have been conducted to identify differentially expressed genes and key genes regulated by light quality. Growing Micro-Tom from germination to harvest under red (R), blue (B), red/blue (RB), or red/blue/green (RBG) LED lights, as well as fluorescent tube (Fl) lighting, the R spectrum produced plants with shade-avoidance type growth, with significantly increased height, elongated petioles, a reduction of photosynthesis, and a reduction in yield and fruit soluble sugar content compared to RB and RBG grown plants. The transcriptomic analysis shows that Fl drastically altered the transcriptome compared to any LED light spectra, with 6623, 8805, and 5942 genes differentially expressed in pair-wise comparisons between Fl with R, B, and RBG, respectively, and 3528 genes commonly differentially expressed between all LED comparisons. Between R, B, and RBG. In R transcriptome, the expression of RvB and RvRBG differentially expressed genes, the expression of growth promoting hormone biosynthesis and signalling genes was enhanced, as well as the expression of cell-wall modifying enzymes and transcription factors which regulate growth. Additionally, plants grown under R had reduced photosynthetic and pigment related

gene expression, while plants grown under B had reduced expression of defense, biotic stress-responsive genes, and a reactive oxygen species signalling gene. The resultant co-expression network included 17 co-expression modules, of which 9 genes were associated with the biosynthesis of anthocyanin. Anthocyanin biosynthesis genes were co-expressed together, along with a known transcription factor ANTHOCYANINLESS and an APETELAa ERF transcription factor, with zero expression of these genes in B, low levels in R, and high expression in RBG. Twelve differentially expressed genes were identified from the RNA-Seq study as candidate genes of interest for gene functional studies. To further validate the regulation of these genes by light, RNA was harvest weekly from Micro-Tom plant grown under the same light qualities, and a qRT-PCR time-course of gene expression of these genes was conducted to establish which genes are consistently differentially regulated by light. Five genes were found to be consistently differentially regulated by light: a cell-wall modifying gene XYLOGLUCAN ENOTRANSGLUCOSYLASE HYDROLASE 16, cytokinin catabolic gene CYTOKININ DEHYDROGENASE/KINASE 6, a C2H2 transcription factor, a MYB-RELATED transcription factor, and HAT4 BZIP transcription factor. In the future, the function of these genes will be studied through *Agrobacterium*-mediated gene silencing in Micro-Tom. Additionally, a second RNA-Seq experiment studying the effect of supplemental green LED light added to a background of RB, which was found to induce an early transcriptional response with 1190 genes differentially expressed. However, this response was transient, as after one day and seven days 305 and 270 genes were differentially expressed, respectively. These data provide a basis for understanding light signalling in tomato, and the extensive transcriptional reprogramming which underpins the adaptive response of tomato morphology, biochemistry, and development in response to spectral quality. The observation of the effects of LED spectra on the transcriptome as well as the effect of LED spectra on yield in tomato are novel and have a meaningful consequence for the identification of molecular markers which regulate important plant traits, which can be targeted for improved crop yield and quality.

Acknowledgments

First of all, I would like to express my sincere gratitude to my supervisor, Prof. Chungui Lu, for his patient guidance, motivation and advice throughout my time as his student. Despite leaving the University, his support and encouragement throughout my Ph.D. has been essential to this research. I would also like to thank my second supervisor, Dr. Erik Murchie, for his constructive suggestions and reassurance. Also, my earnest thanks to Prof. Graham Seymour, for adopting me as his student when I lost my primary supervisor and giving me space and support to continue with my research.

A special thanks to my colleagues and friends on SB, who greatly improved my work: life balance and made work enjoyable. Alex, Stuart, and Jack, the lunch banter and constant arguing was an incredible distraction from the stress of Ph.D. life. To my friends at Gateway, especially Rosie, Heather, and Emma: the caffeine, sugar, and gossip were endless sources of energy and positivity.

Last but not least I would like to thank my family: my mother, sister, and Christina, for their unconditional love and support. To my mother, you are the embodiment of hard work and resilience, and I could never have made it this far without your sacrifice. Finally, to my partner Christina, without you finishing this would have been impossible. You were the best part of every bad day and your moral support gave me the strength to carry on through the hard times.

Table of Contents

Abstract - 1 -

Acknowledgements ..... - 3 -

Table of Contents ..... - 4 -

List of Tables - 11 -

List of Figures- 13 -

List of Abbreviations ..... - 17 -

1 LITERATURE REVIEW 1

1.1 LED light benefits over traditional agricultural light sources 1

1.1.1 Introduction 1

1.1.2 Benefits of LED lighting over traditionally used horticultural lighting 2

1.1.3 Plant morphology and developmental responses to spectral quality 3

1.2 Light Signalling in Plants 4

1.2.1 Plants adaptively respond to their light environment 4

1.2.2 Introduction to Light Signalling and Photoreceptor Families 6

1.3 Phytochrome-mediated red light signalling 7

1.3.1 Cryptochrome-mediated blue light signalling 8

1.3.2 Phototropins 11

1.3.3 Zeitlupe Family 12

1.3.4 Light signalling components involved in phytochrome and cryptochrome signalling 13

1.3.5 Integration of light and hormone signalling controls development 15

1.4 Adaptive response to light 20

1.4.1 Photoreceptor role in seed germination and photomorphogenesis 21
1.4.2 Photoreceptor regulation of plant architecture 22
1.4.3 Photoreceptor regulation in photosynthesis and photoprotection 25
1.4.4 Photoreceptor, photoperiod and flowering.....28
1.4.5 Fruit quality 29
1.5 Manipulating light signalling components to improve crop yield 30
1.6 Transcriptomic studies into light signalling.....34
1.6.1 Transcriptomic studies of light and photoreceptor signalling.....34
1.6.2 Transcriptomic studies of light signalling in crop species 34
1.6.3 Transcriptomic studies in tomato 35
1.6.4 RNA-Sequencing technology overview.....37
1.7 Tomato is a model species and important crop.....40
1.7.1 Tomato as an important crop.....40
1.7.2 Tomato as a model species for genetic studies.....40
1.8 Aims and objectives of this project.....41
2 GENERAL METHODS.....42
2.1 Plant materials and general growing conditions 42
2.2 LED lights.....42
2.2.1 Comparison of the spectral distributions of LED and fluorescent lights.....42
2.2.2 Spectral distribution of LED lights used for chapters 3,4, and 5 .43
2.3 Total RNA extraction.....46
2.3.1 Determination of RNA concentrations.....48
2.4 RNA-Sequencing processing and bioinformatics.....48
2.4.1 RNA extraction and libraries prep for RNA-Sequencing 48
2.4.2 Mapping of Illumina reads 49
2.4.3 Quality assessment and unsupervised analysis 49

2.4.4 PCA + Hierarchical clustering 49
2.4.5 Differential expression analysis (EdgeR) 49
2.4.6 Gene-Set Enrichment Analysis (GSEA) 50
2.5 qRT-PCR 50
2.5.1 cDNA synthesis 50
2.5.2 qRT-PCR analysis 51
2.6 Primer design and efficiency 52
3 PHENOPTYPING MICRO-TOM GROWN UNDER VARYING LED SPECTRA QUALITIES 53
3.1 Introduction 53
3.2 Methods 56
3.2.1 Plant materials and growth conditions 56
3.2.2 Morphological measurements 56
3.2.3 Photosynthesis analysis and chlorophyll measurements 57
3.2.4 Measurement of leaf optical properties 58
3.2.5 Pigment content analysis 59
3.3 Results 61
3.3.1 Plant growth analysis at vegetative stage 61
3.3.2 Plant growth analysis at harvest 65
3.3.3 Photosynthesis and chlorophyll fluorescence analysis 74
3.3.4 Whole plant chlorophyll fluorescence analysis 80
3.3.5 Analysis of leaf optical properties 83
3.3.6 Pigment content analysis 85
3.4 Discussion 87
3.4.1 Photosynthesis, biomass accumulation, and yield 87
3.4.2 Relationship between optical properties of plant and pigment metabolism 89

3.4.3 Monochromatic R grown plants exhibit LBL induced shade avoidance phenotype....90
3.4.4 Fluorescent tube lighting vs LEDs....91
3.4.5 Addition of green light to mixed red and blue LED seems to not be improving agronomically important traits....91
3.5 Conclusion....92
4 TRANSCRIPTOMIC ANALYSIS OF MICRO-TOM GROWN UNDER DIFFERENT LIGHT SPECTRA....94
4.1 INTRODUCTION....94
4.1.1 Overview of previous chapter....94
4.1.2 Light re-programmes transcriptome....95
4.1.3 Gene regulatory networks....96
4.1.4 Aims and objectives....97
4.2 METHODS....98
4.2.1 Sample collection and Illumina sequencing....98
4.2.2 Mapping of Illumina reads....99
4.2.3 Quality assessment and unsupervised analysis....99
4.2.4 PCA + Hierarchical clustering....99
4.2.5 Differential expression analysis (EdgeR)....99
4.2.6 *Gene-Set Enrichment Analysis (GSEA)*....100
4.2.7 *Gene co-expression Network modelling*....101
4.2.8 qRT-PCR validation of RNA-Sequencing results....101
4.3 RESULTS....102
4.3.1 Summary of RNA-Seq Libraries and Alignment to Genome....102
4.3.2 Quality assessment of transcriptome data....103
4.3.3 Unsupervised analysis of Transcriptomic data....104
4.3.4 Transcriptomic analysis of MT grown under different spectral qualities.....105

4.3.5 Hierarchical clustering of RvBvRBG DEGs 118
4.3.6 Transcription factor analysis 120
4.3.7 Investigation of Pathways of Interest 131
4.3.8 Differential gene expression analysis between Micro-Tom grown under Fluorescent light compared to LED lighting. 150
4.3.9 Co-Expression network modelling 153
4.3.10 qRT-PCR confirmation of RNA-Seq data 157
4.4 Discussion 159
4.4.1 Effect of LED spectra on Micro-Tom leaf transcriptome 159
4.4.2 Co-action of red and blue light up-regulates pigment metabolism 166
4.4.3 Fluorescent tube lighting elicited vastly different transcriptome to LEDs 168
4.4.4 Unexplained variance between RB and RBG transcriptome 169
4.4.5 Conclusions 170
5 Investigating Genes of Interest and Candidate Gene Selection 172
5.1 Introduction 172
5.1.1 Review of Candidate Genes of Interest 172
5.1.2 Aims 179
5.2 Methods 179
5.2.1 Plant materials and growing conditions 179
5.2.2 qRT-PCR gene expression analysis 180
5.3 Results 181
5.4 Discussion 183
5.4.1 Future work: characterisation of gene function 184
5.5 Conclusions 184
6 TRANSCRIPTOMIC ANALYSIS OF THE EFFECT OF SUPPLEMENTAL GREEN LIGHT ON MICRO-TOM 186

6.1 INTRODUCTION 186
6.1.1 Cryptochrome-dependent green light effect 186
6.1.2 Other photoreceptor-dependent green light effect 187
6.1.3 Aims and hypotheses 187
6.2 METHODS 188
6.2.1 Plant materials and growth conditions 188
6.2.2 Sample collection and Illumina sequencing 189
6.2.3 Bioinformatics on RNA-Seq data 189
6.3 RESULTS 191
6.3.1 Summary of RNA-Seq Libraries and Alignment to Genome 191
6.3.2 Quality assessment of RNA-Seq libraries 192
6.3.3 Unsupervised analysis of transcriptomic data 193
6.3.4 Differential expression analysis 195
6.3.5 TOP DEGs 200
6.3.6 Gene enrichment analysis of DE gene sets 203
6.3.7 Pathways analysis 208
6.4 DISCUSSION 217
6.4.1 Experimental context 217
6.4.2 Immediate transient response to green light supplementation 218
6.4.3 Limitations of this experiment 220
6.5 Conclusions 221
7 GENERAL DISCUSSION AND CONCLUSIONS 222
7.1 Introduction 222
7.1.1 Blue light is essential for tomato development 223
7.1.2 Defence related gene expression 224
7.1.3 Co-action of red and blue light necessary for pigment production 225

7.1.4 Green light did not significantly alter morphology, physiology or gene expression 226
7.1.5 Targeted improvement of crops 227
7.2 Future work 229
7.2.1 Functional characterisation of candidate light signalling genes. 229
7.2.2 Further understanding of the post-translational mechanisms at the apex of the transcriptional network 229
7.2.3 Quantitative investigation of effects of varying doses green light on Micro-Tom 230
7.3 Conclusions 231
8 Supplementary Information 233
8.1 Supplementary data for Chapter 6 233
8.1.1 Quality assessment of chapter 6 RNA-Seq data 233
8.1.2 Full gene enrichment tables 237
8.2 RNA-Seq (Chapter 4) 247
8.2.1 Quality assessment of RNA-Seq data 247
8.2.2 Full gene enrichment tables 252
9 References 266

List of Tables

Table 1-1 Summary of phytochrome and cryptochrome gene function studies in different crop species 33
Table 3-1 Leaf absorption within different regions of visible light spectrum 84
Table 4-1 Primer sequences for qRT-PCR validation of RNA-Seq 101
Table 4-2 Summary statistics for RNA-Sequencing 102
Table 4-3 Top 10 most highly up- and down- regulated genes in RvBvRBG comparisons 112
Table 4-4 Top 5 most highly differentially up- and down- regulated transcription factors RvBvRBG 122
Table 4-5 Transcription factor target enrichment analysis of genes up or down-regulated in RvB DEGs 128
Table 4-6 Transcription factor target enrichment analysis of genes up or down-regulated in RvRBG DEGs 129
Table 4-7 Transcription factor target enrichment analysis of genes up or down-regulated in BvRBG DEGs 130
Table 4-8 light signalling and circadian clock gene expression 133
Table 4-9 Photosynthesis and photoprotection DEA between RvBvRBG 138
Table 4-10 Differential expression of chlorophyll metabolism genes between R, B, and RBG 140
Table 4-11 Hormone biosynthesis and signalling genes differentially expressed in response to spectral quality 146
Table 4-12 DEA of plant pathogen interaction keg pathway genes between R, B, and RBG 149
Table 4-13 Expression of anthocyanin metabolism genes and correlation coefficient of expression of genes compared to anthocyanin content 156
Table 4-14 Assessment of the variation in expression of candidate reference genes within RNA-Seq dataset. 157
Table 5-1 RNAseq differential expression analysis results for genes of interest in RvBvRBG leaf samples 173
Table 5-2 Primer sequences of primers designed for qRT-PCR 180

Table 6-1 Summary of sequencing and alignment of RNA libraries.....192
Table 6-2 Top 10 differentially up- and down- regulated genes in RBGvRB at each time-point.....200
Table 6-3Photosynthesis related gene expression.....212
Table 6-4 Porphyrin and chlorophyll metabolic genes.....215
Table 6-5 Plant hormone metabolism and signalling genes DE between RBG and RB 216
Table 8-1 Enriched GO and KEGG terms significantly down-regulated in TvC_4h 237
Table 8-2 Enriched GO and KEGG terms significantly up-regulated in TvC_4h.....240
Table 8-3 Enriched terms significantly down-regulated in TvC_1d genes 241
Table 8-4 Enriched terms significantly up-regulated in TvC_1d genes 243
Table 8-5 Enriched terms significantly down-regulated in TvC_7d genes 244
Table 8-6 Enriched terms significantly up-regulated in TvC_7d genes 245
Table 8-7 RvB up-regulated gene functional enrichment.....252
Table 8-8 RvB down-regulated gene functional enrichment.....254
Table 8-9 RvRBG up-regulated functional enrichment.....256
Table 8-10 RvRBG down-regulated genes functional enrichment.....258
Table 8-11 BvRBG up-regulated genes functional enrichment.....260
Table 8-12 BvRBG down-regulated genes functional enrichment.....262
Table 8-13 FlvLED shared DE genes GO and KEGG enrichment.....263

List of Figures

Figure 1-1 Quantum energy distribution of full sunlight and underneath canopy shade.. 5
Figure 1-2 Reaction scheme of phytochrome Photocycle.. 8
Figure 1-3 Reaction scheme of cryptochrome photocycle.....10
Figure 1-4 Model of light, brassinosteroid, auxin, and gibberellin signal integration through PIF4-BZR1-DELLA module......19
Figure 1-5 Possible fates of light energy absorbed by chloroplast (Muller, 2001).....27
Figure 1-6 Typical RNA-Sequencing workflow from mRNA through library preparation to RNA-Sequencing generation of expression level of genes. 39
Figure 2-1 Comparison of spectral distribution of two LED light lamps and fluorescent light tube.....43
Figure 2-2 Spectral distribution of light treatments. 45
Figure 3-1 Morphological and physiology changes of Micro-Tom plants grown under different spectral qualities at vegetative stage. 62
Figure 3-2 Fresh and dry weight of Micro-Tom grown under different light spectra at vegetative stage. 64
Figure 3-3 Plant growth analysis during different developmental stages when grown under different spectral qualities..... 66
Figure 3-4 Leaf morphological analysis of plants grown under varying spectral qualities at harvest DAE93. 69
Figure 3-5 Biomass accumulation and partitioning of Micro-Tom plants grown under different light spectral conditions. at 93 DAE. 71
Figure 3-6 Fruit quality analysis of Micro-Tom grown under varying light spectral conditions. 73
Figure 3-7 Photosynthetic light curve of Micro-Tom plants grown under varying light spectra. 75
Figure 3-8 Quantum yield of photosynthesis of Micro-Tom plants leaves grown under different light spectra. 76
Figure 3-9 Photosynthesis and Chlorophyll fluorescence analysis of Micro-Tom leaves at different irradiances. 79

Figure 3-10 Whole plant chlorophyll fluorescence light curve of dark-adapted Micro-Tom plants grown under varying light spectra.. 82
Figure 3-11Absorption spectrum of tomato leaves grown under different light spectra.. 84
Figure 3-12 Pigment content analysis of Micro-Tom grown under different light spectra.. 86
Figure 4-1 PCA and Hierarchical clustering of RNA-Seq data.. 104
Figure 4-2 RvBvRBG differential expression analysis summary and comparison of overlap in DE gene sets. A.....107
Figure 4-3 Volcano plot of differentially expressed genes in RvBvRBG pair-wise compairons. 108
Figure 4-4 Hierarchical clustering with heatmap of RvBvRBG differentially expressed genes. 118
Figure 4-5 Gene expression of differentially expressed transcription factors between RvBvRBG in pair-wise comparisons. 124
Figure 4-6 RvBvRBG heatmap of differential expression overlayed onto 'Circadian Rhythm' KEGG pathway.....132
Figure 4-7 Heatmap of DEGs between RvBvRBG in photosynthesis related GO terms.. 136
Figure 4-8 RvBvRBG heatmap of differential expression overlayed onto 'Carbon Fixation in Photosynthetic Organisms' KEGG pathway. 137
Figure 4-9 Plant hormone signal transduction gene expression pathway overlay.. 144
Figure 4-10 Log-fold change of auxin responsive genes in RvBvRBG comparison.. 145
Figure 4-11 Plant-pathogen interaction gene expression pathway overlay. 148
Figure 4-12 Differential expression analysis of Micro-Tom grown under Fluorescent tube lighting in comparison to LEDs. 150
Figure 4-13 Hierarchical clustering of genes commonly differentially expressed between Fl and LED transcriptomes.. 152
Figure 4-14 Global view of co-expression network built from gene expression of Micro-Tom leaves grown under varying spectral qualities.. 153
Figure 4-15Co-expression network of anthocyanin biosynthesis genes.. 155

Figure 4-16 Gene expression of anthocyanin metabolism genes and transcription factor Anthocyanin-less as well as anthocyanin content on leaf tissue of Micro-Tom plants grown under varying spectral qualities.. 156
Figure 4-17 qRT-PCR validation of RNA-Seq data.. 158
Figure 5-1 Expression of gene Solyc06g053290.1 and height of plants grown under varying spectral qualities.. 177
Figure 5-2 qRT-PCR gene expression analysis of candidate genes differentially expressed in micro-tom leaves under varying spectral qualities over time-course....182
Figure 6-1 Spectral output of LED lights for both control and treatment conditions. 189
Figure 6-2 PCA and Hierarchical clustering of time-course data.. 195
Figure 6-3 Summary of up and down-regulated genes between treatment and control at each time-point for all DEGs. 198
Figure 6-4Volcano plot of differential expression between Treatment and control throughout time-course. 199
Figure 6-5. Tree-map of enriched Biological Process GO terms in down-regulated genes between TvC after 4hours. 206
Figure 6-6 Tree-map of enriched Biological Process GO terms in down-regulated genes between TvC after 1 day. 207
Figure 6-7 Key genes' expression heatmap of TvC overlayed onto KEGG photosynthesis pathway maps.. 210
Figure 6-8 Key genes' expression heatmap of TvC overlayed onto KEGG 'carbon fixation in photosynthetic organisms' map. 211
Figure 6-9 Heatmap overlay of time-course key genes' expression of TvC onto 'Porpyhrin and Chlorophyll metabolism' KEGG map.. 214
Figure 8-1 Sensitivity plot of normalized unfiltered transcriptome data. 233
Figure 8-2 Density plot of the effect of filtering genes on log-CPM distribution on RNA-Seq transcriptomes.. 234
Figure 8-3 Mean expression for compared against GC content and gene length for transcriptomic data.. 235
Figure 8-4 Normalization of RNA-Seq count data.. 236
Figure 8-5 Sensitivity plot of % genes which fall into different count per million (CPM) ranges in RNA-Seq samples from Micro-Tom grown under different spectral qualities. 247

Figure 8-6 Effect of filtering on log-CPM distribution of RNA-Seq samples from Micro-Tom grown under different spectral qualities.. 248
Figure 8-7 GC and length Bias in RNA-Seq samples from Micro-Tom grown under different spectral qualities.. 249
Figure 8-8 Biotype detection of RNA-Seq samples from Micro-Tom leaves grown under different spectral qualities. 250
Figure 8-9 Effect of normalization on log-CPM distribution of RNA-Seq samples from Micro-Tom grown under different spectral qualities.. 251

List of Abbreviations

LED- Light-emitting diode

R – Red (660nm)

B - Blue (450nm)

G – Green (520nm)

Fr – Far-red (720nm)

RB- Red and blue

RBG – Red, blue and green

Fl – Fluorescent tube lighting

LBL – Low blue light

PAR – Photosynthetically active radiation (400-700nm)

PHY- Phytochrome

CRY- Cryptochrome

PIF – Phytochrome-interacting factor

NPQ – Non-photochemical quenching

ΦPSII – Quantum efficiency of PSII

Pn – Net photosynthetic rate

J/ ETR- Electron transport rate

FDR – False discovery rate

DEA – Differential expression analysis

DEG – Differentially expressed gene

qP – Photochemical quenching

ETR – Electron transport rate

1 LITERATURE REVIEW

1.1 LED light benefits over traditional agricultural light sources

1.1.1 Introduction

Over the past decade, advancements in light emitting diodes (LED) lighting technology have drastically improved the technology; reducing the production cost, increasing the energy-use efficiency, and the maximum luminous flux (Morrow, 2008). In its current state, LED lighting has tremendous potential to replace traditionally used horticultural lighting as supplemental or sole-source lighting in crop production (Morrow, 2008). LED lights to offer substantial advantages over traditionally used horticulture lighting, including increased luminous efficacy, superior lifetime, reduced size, and a cooler emitting temperature (Massa et al, 2008). They are unique in that they allow us to target individual photoreceptors. Unlike other artificial light sources - high-pressure sodium or fluorescent light which provide a broad ‘white light’ spectrum, they are narrow band devices which allow us to precisely control not only the quantity but also spectral quality. They are also more easily controllable and can be placed closer to the plants as they don’t produce heat in their beam.

Spectral quality, the relative proportion of different wavelengths within emitted light, has been shown to drastically affect plant growth and productivity. (Goins, 1997; Massa et al, 2008; Morrow, 2008). The ability of LED lights to produce a range of specific wavelengths including blue (450nm), green (520nm), red (660nm) and far-red (720nm) leads to the possibility of developing ‘spectral recipes’ designed to optimize crop growth and development. In the following section, I will outline the benefits of LED lights over traditionally used horticultural lighting, and the research conducted into using LED lights and optimizing spectral recipes to improve crop productivity and quality.

1.1.2 Benefits of LED lighting over traditionally used horticultural lighting

LEDs have increased luminous efficacy compared to traditional horticultural lighting, meaning they have a high energy use efficiency and therefore can reduce both the cost of lighting and the carbon-footprint in horticulture. A recent life cycle assessment of LED and high-intensity discharge lighting for greenhouse crop production of tomatoes found white-LEDs achieved an energy efficiency of 95% compared to HPS and incandescent lighting which had an efficiency of 58.3% and 11.4% respectively (Hao Zhang, Burr, & Zhao, 2017). In addition to increased energy efficiency, LEDs were found to be substantially more environmentally friendly, with the life cycle assessment (LCA) revealing a 40% reduction in contribution to global warming potential if LEDs are adopted over HID lighting (HID), mostly achieved through reduced energy consumption (Hao Zhang et al., 2017). LED light performance, in terms of energy-use efficiency and maximum light intensity, has increased dramatically over the past decade, and is projected to continue to both increases in efficiency and reduce in manufacturing and running costs (Haitz & Tsao, 2011).

Another benefit of LED lights interlinked to its energy-use efficiency is its cool emitting temperature, as LEDs emit substantially less heat than alternative agricultural lighting. The reduced temperature not only improves energy efficiency through a reduction in waste heat energy produced but also permits LEDs to be placed closer to the plant canopy, increasing the light energy absorbed by the leaf which therefore leads to increased overall productivity (Nelson & Bugbee, 2014). With the rise of vertical farming systems for vegetable production, the ability to reduce the distance between light source and plant allows for increased light intensity reaching the plant while also increasing the density at which growing compartments can be stacked, while in a glasshouse setting, LEDs can be used for intra-canopy or close-proximity supplemental lighting.

1.1.3 Plant morphology and developmental responses to spectral quality

Early studies into the use of LEDs as sole-source lighting for controlled environment agriculture began in 1991 and were performed by NASA, which had the goal of improving space-based plant growth systems. Due to the fact that only red LED light technology had advanced to the point that it could provide sufficient light intensity (~40µmol m^2s^{-1}), initial studies focused on red light with the supplementation of blue fluorescent lamps (Massa, Kim, Wheeler, & Mitchell, 2008). This early work investigated the physiological response and yield of plants such as wheat (Goins, Yorio, Sanwo, & Brown, 1997), radish, lettuce, spinach (Bula et al., 1991; Yorio, Goins, Kagie, Wheeler, & Sager, 2001), and peppers to LED light (Brown, Schuerger, & Sager, 1995; Morrow, 2008). This research established that although red light was sufficient for a plant to complete its life cycle, the addition of a small threshold amount of blue light was necessary for optimal growth and morphology, and drastically improved yield compared to monochromatic red light alone (Brown et al., 1995; Goins et al., 1997).

Plant responses to blue light can be categorized into either quantitative (dose-dependent) or qualitative (threshold) responses. While only a small amount of blue light is necessary to alleviate photosynthetic dysfunction, photosynthesis in several crop species has been shown to be controlled quantitatively by blue light ((Hogewoning et al., 2010)). In cucumbers, for example, the maximum rate of photosynthesis increased proportionally with blue light percentage increased up to 50%, while the maximum quantum yield of CO_2 fixation (the amount of CO_2 fixed per photon of light absorbed) increased with blue light percentage peaking at 30% (Hogewoning et al., 2010). The morphological change under reduced ratio of red to blue light showed that plant height decreased substantially with the introduction of a small fraction of blue light, and then continued to decrease to a lesser extent proportionally to blue light percentage, as did leaf mass per area and chlorophyll content (R. Hernández & Kubota, 2016). In lettuce plants transferred from white light to various combinations of red and blue LED light conditions, results showed that 100% of red LEDs produced the highest biomass, while pigment content increased proportionally with the proportion of blue light, as did phytonutrient content including flavonoids and antioxidants (Son & Oh, 2013). Moreover, supplementary blue light

has been shown to improve the nutritional quality of several leafy vegetables through stimulating the accumulation of antioxidants including vitamin C, carotenoids, anthocyanin, and polyphenol (Olle & Viršile, 2013). The growth of tomato seedlings under various LED light qualities has been examined (Ricardo Hernández, Eguchi, Deveci, & Kubota, 2016; X. Y. Liu, Chang, Guo, Xu, & Li, 2011). Hernandez (2016) found that increasing the % of blue light in red+blue LED light spectra reduced hypocotyl growth and increased shoot dry mass. Liu (2011) Cherry tomato seedlings were grown under varying spectral qualities were identified toexhibit a significantly higher quantum yield of photosynthesis, and a higher biomass accumulation when grown under blue, red + blue, or red + blue + green LED light compared to those grown under red light (Liu Xiaoying, 2012). Monochromatic red grew Micro-Tom also exhibited extreme shade avoidance apical growth, and an even greater reduction of the maximum photosynthetic rate as well as reduced chlorophyll content (Liu Xiaoying, 2012). The current studies on effects of light quality on tomatoes using sole-source lighting, which is necessary to precisely control spectral quality, have been limited to the study of seedlings, and therefore the effect of light at later developmental stages and its influence on yield and quality have yet to be established.

1.2 Light Signalling in Plants

1.2.1 Plants adaptively respond to their light environment

The spectral quality of the natural light environment surrounding a plant can vary greatly depending on the geographical location, time of day, season and habitat. As sessile organisms, plants are often in competition for resources (light, water, and nutrition) with their surrounding neighbors. They rely on the absorption of photosynthetically active radiation (PAR, between 400-700nm) to drive photosynthetic assimilation of energy-rich organic compounds which in turn fuel plant growth. Light for photosynthesis is absorbed by photosynthetic pigments within the thylakoid membrane of plant chloroplasts, predominantly chlorophyll *a* and *b*, which absorb most efficiently within the red and blue portion of the visible light spectrum. Plants often grow at high-vegetation densities in which competition for available light occurs as canopies close and leaves of neighboring plants block off the

light, thereby shading the lower-levels of the canopy. The effect of canopy shading on the quantum energy distribution that shaded plants intercept is presented in **Figure 1-1**. As light passes into the canopy and through the upper-level leaves, the relative proportion of different wavelengths of light changes as the red and blue wavelengths are preferentially absorbed by chlorophyll. Therefore, the transmitted (shaded) light is depleted in red and blue, while enriched in far-red and green wavelengths (Folta & Maruhnich, 2007). Plants are able to sense ambient light quality and respond to shade by inducing a set of morphological and development responses aimed at both out-grow shading, as well as increasing photosynthetic efficiency and light capture. These responses to shade are collectively known as the shade avoidances responses (SAR), and include the elongation of stems and petioles, upward leaf movement, and increased apical dominance (Ballaré & Casal, 2000; de Wit et al., 2016; Keuskamp et al., 2011; Smith, 1982; Smith & Whitelam, 1997).

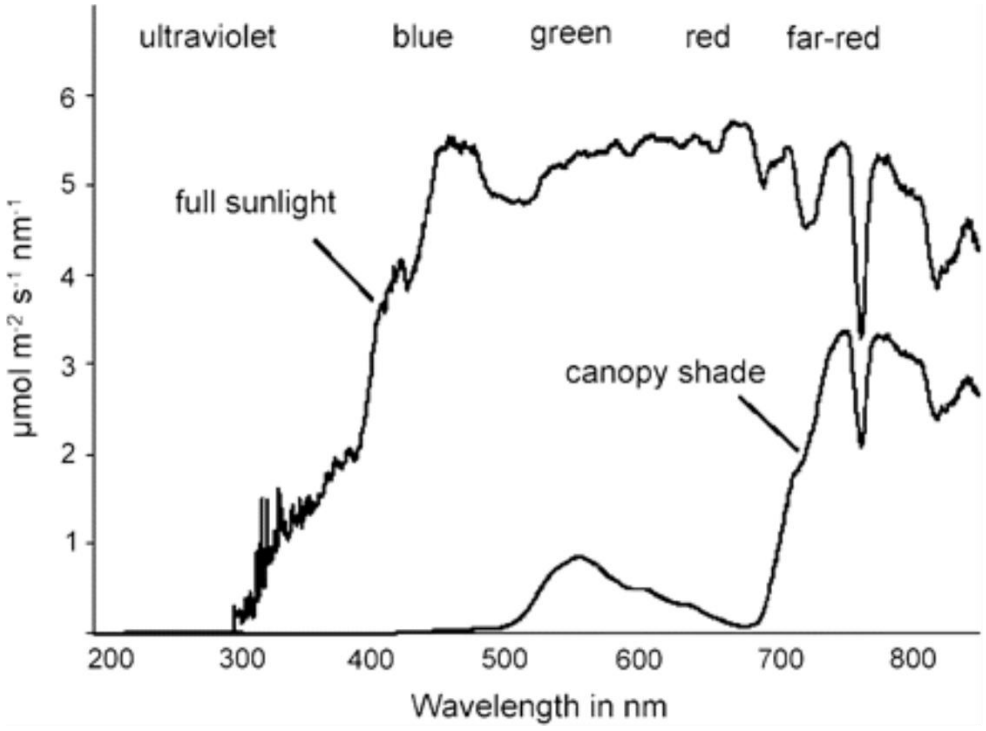


Figure 1-1 Quantum energy distribution of full sunlight and underneath canopy shade. Figure and data from Folta & Maruhnich, 2007 (doi:10.1093/jxb/erm130). Light conditions were measured at noon in mid-April in Gainesville, FL (29.67° N), using a StellarNet spectroradiometer.

Plants perceive the changes in spectral quality through multiple light cues which are perceived primarily through the phytochrome and cryptochrome photoreceptor systems and integrated together to adjust the plant's response to its

ambient light environment (de Wit et al., 2016). The red and far-red sensing phytochrome photosensory system integrates information on R: FR ratio, R+FR irradiance intensity, and end-of-day far-red. In addition to the phytochrome-mediated photosensory mechanisms, cryptochromes have been shown to mediate a similar but distinct shade avoidance response to low-blue light (LBL), as well as to low blue: green ratio elicited by a green light photo-reversible inactivation of cryptochromes analogous to that of the phytochrome R: FR switch (Banerjee et al., 2007; J. P. Bouly et al., 2007; Sellaro et al., 2010; Tingting Zhang, Maruhnich, & Folta, 2011). Transcriptome analysis indicates that the genetic regulatory pathways induced by different spectral qualities are distinct despite the involvement of the same bHLH transcription factors (Pedmale et al., 2016). Phytochrome and cryptochromes both have common physical interactions with key photomorphogenic signal transduction elements such as COP1/DET and phytochrome-interacting factors (PIFs). The physical and indirect interactions between the two photoreceptor classes cause cross-talk between phy-mediated red light and cry-mediated blue light signalling networks (de Wit et al., 2016; Keller et al., 2011).

1.2.2 Introduction to Light Signalling and Photoreceptor Families

Spectral quality, quantity, direction and duration of incident light signals are perceived through a complex photosensory system incorporating multiple families of photoreceptors which play distinct roles in coordinately regulating photosynthesis, plant growth, and development. The perception of light through the photosensory system initiates intracellular signal transduction cascades that lead adaptive changes at a cellular, tissue, and organism-wide level through a series of light-regulated genes in nuclear (Jigang Li, Li, Wang, & Deng, 2011). There are 5 major classes of photoreceptors which have been characterized to date. The first, Phytochromes (phys), are a well-characterized family responsible for sensing red and far-red light (600-750nm) (Butler, Hendricks, & Siegelman, 1964; Jigang Li et al., 2011). Three separate families that all coordinately regulate the response to blue/UVA (320-500nm) are Cryptochromes (cry) (Ahmad & Cashmore, 1993) , Phototropins (phots), and Zeitlupe (ztls) families (J. M. Christie, Blackwood, Petersen, & Sullivan, 2015). Finally, a UV-B (280-320nm) receptor (UVR8) has recently been characterized, but will not be discussed in this review. These photoreceptors convey light signals which

regulate dynamic reversible processes such as photosynthesis, chloroplast movement and phototropism, as well as entrainment of the circadian clock, and regulating important developmental transitions such as germination, de-etiolation, and floral initiation. In the next sections I will describe each photoreceptor family, but focusing mainly on the phytochrome and cryptochrome families.

1.3 Phytochrome-mediated red light signalling

Red/Far-red light sensing in higher plants is mediated by a structurally conserved group of photoreceptors, the phytochromes (Butler et al., 1964; Clack, Mathews, & Sharrock, 1994; Mathews & Sharrock, 1997). The photosensory activity of phytochromes derives from their reversible photoconversion between two conformations: the biologically inactive red-light (660nm) absorbing ground state (Pr) and the biologically active far-red (720nm) absorbing photoactivated state (Pfr), with dark-reversion of photo-active phytochrome back to its inactive state under prolonged darkness, as illustrated in **Figure 1-2** (Quail, 2002). Upon photoactivation, the active phytochrome molecule translocates to the nucleus where it interacts with various signalling elements to control light-regulated gene expression by transcriptional, post-transcriptional and post-translational mechanisms (Galvão & Fankhauser, 2015; Kircher et al., 1999). The number of phytochromes varies between species- such as 5 phytochromes (PHYA-E) in Arabidopsis; 5 phytochromes (PHYA, B1, B2, E, and F) in tomato; and 3 phytochromes (PHYA-C) in rice (Mathews & Sharrock, 1997). Phytochromes can be separated into two distinct groups: Phytochrome A is a type I (photolabile) phytochrome, and upon activation is rapidly degraded, whilst phytochromes B-E are type II (photostable) phytochromes (Smith, 1995; Li et al, 2011). Phytochrome A is the most abundant of the phytochromes in dark-grown seedling, however, it is rapidly degraded upon exposure to light, whilst phyB is the most abundant phytochrome in light-grown seedlings (Quail, 1994; Li et al, 2011). Phytochromes have pleiotropic effects throughout all stages of plant development, controlling important developmental processes including germination, de-etiolation, the transition from vegetative growth to flowering, as well as integrating with several

hormone signalling networks which regulate metabolism, resource partitioning, and resistance to abiotic stress (Casal, 2013; OS Lau and Deng, 2010).



Figure 1-2 Reaction scheme of phytochrome Photocycle. Ovals represent phytochrome chromophore with conformational state denoted by the Pr- the inactive red light absorbing, and Pf- far-red light absorbing active state. Black arrow indicates dark-reversion which occurs in prolonged darkness.

The cell autonomous early-signalling events involved in phytochrome signalling have been well characterized in *Arabidopsis* (Quail, 2002). Once in the nucleus, photoactive phytochromes interact with a series of early signalling elements to mediate this phytochrome-induced transcriptional reprogramming. Two distinct mechanisms have been identified as major hubs underpinning the phytochrome signalling network: suppression of the COP1/SPA multimeric E3 ubiquitin ligase complex and interaction with a family of phytochrome-interacting bHLH transcription factor. Phytochrome and cryptochrome signals both integrate through several common signalling components including direct interactions with several PIFs and COP1/SPA genes. The nature of these interactions and the mechanisms through which both phytochrome and cryptochrome signalling occur (transduction pathway) are dissected in **Section 1.3.4**.

1.3.1 Cryptochrome-mediated blue light signalling

Cryptochromes are a family of Blue/UV-A flavoproteins ubiquitous within both plant and animal kingdoms, and share homology to an ancient family of flavoproteins, the photolyases, which are involved in the repair of UV light-damaged DNA (Cashmore, Jarillo, Wu, & Liu, 1999). Arabidopsis contains three cryptochromes: CRY1, CRY2, and CRY3 (also known as CRY-DASH). CRY-3 is localized in both the mitochondria and chloroplast and appears to function in DNA repair (Kleine, Kindgren, Benedict, Hendrickson, & Strand, 2007; Sato et al., 2012).

CRY1 and CRY2, on the other hand, are predominately localized in the nucleus and do not function in DNA repair, instead of controlling various aspects of plant growth and development in response to blue light (J. M. Christie et al., 2015). Cry2 completes its post-translational life cycle in the nucleus, and is primarily responsible for transducing blue light signals under low irradiance, as the photoactivated cry2 is quickly degraded by the ubiquitin-proteasome system (Kleiner, Kircher, Harter, & Batschauer, 1999; Zuo et al., 2012). Cry1 exhibits greater photostability and is responsible for signalling in response to a broad range of blue-light intensities (Ahmad, Jarillo, Smirnova, & Cashmore, 1998). In addition to its role as a blue light receptor, cryptochromes have also been established as a sensor of B:G ratio. B:G ratio is a well-established signal of the degree of foliar shade, and low B:G induces cryptochrome-dependent shade-avoidance responses in a mechanism analogous to that of the phytochrome R: FR photo reversion (Sellaro et al., 2010).

Cryptochrome domain organization and activation chemistry

The cryptochromes of higher plants comprise of an N-terminal photosensory domain (PHD) and a C-terminal extension (CCE). The PHD region is responsible for dimerization and photo-activation, mediated through non-covalently binding two chromophores: A flavin adenosine dinucleotide (FAD) and 5,10-methyltetrahydrofolate (MTHF) (Cashmore et al., 1999). The FAD is the primary blue-light absorbing pigment that is essential for cryptochrome function, whilst MTHF functions as an accessory pigment, improving absorbance of the cryptochrome within the UV-A spectral region (J. M. Christie et al., 2015). Despite the CEE appearing largely unstructured, transgenic Arabidopsis expressing the CCE domain, removed from the PHR, exhibited a phenotype of constitutive blue light activation, indicating that the CCE is an effector module, and that blue-light activation of the PHR region releases its inhibition of the CCE activity, allowing it to interact with nuclear signalling elements to transduce the blue-light signal (H. Q. Yang et al., 2000).

The mechanism through which cryptochromes function as sensors of blue and green signals has been established (**Figure 1-3**). Cryptochromes are synthesized in a biologically inactive oxidized-FAD state, which accumulates in the dark. Upon illumination, absorption of blue-light triggers the semi-photoreduction of FAD

through intramolecular electron transfer and subsequent proton transfer, transforming the cryptochrome into its active semi-quinone FADH· state (Banerjee et al., 2007; J. Bouly et al., 2007). Adopting the photoexcited semi-quinone state causes a shift in the absorbance spectra of the pigment, as well as conformational changes which activate it allowing interactions with signalling elements to transduce the blue-light signal (Banerjee et al., 2007). Prolonged darkness causes a reversion back to the oxidized ground state of the cryptochrome, however absorption of green light by FADH· domain of the photo-activated cryptochrome causes a further reduction of the FAD semi-quinine, transforming the cryptochrome into a third fully reduced FADH- state with attenuated biological signalling activity (Banerjee et al., 2007).

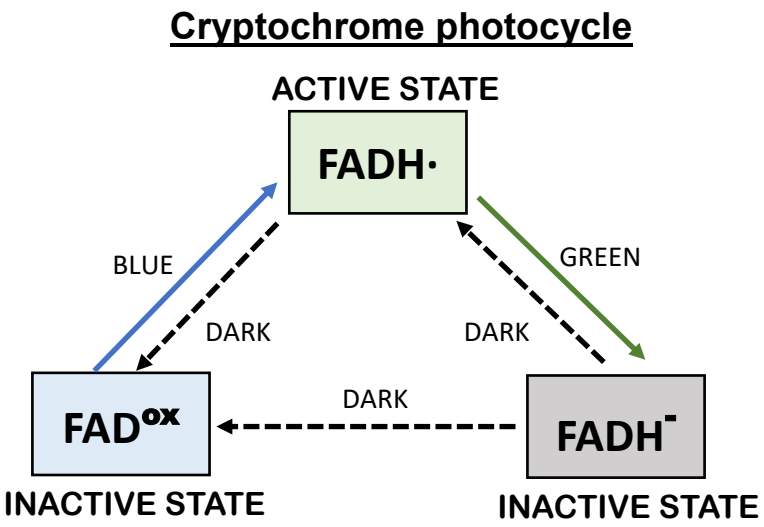


Figure 1-3 Reaction scheme of cryptochrome photocycle. Each box represents a different cryptochrome conformation denoted by the state of its FAD chromophore between oxidized (FAD^{ox}), semi-quinone intermediate (FADH$^{\cdot}$), and fully reduced (FADH^{-}). Arrows indicate the direction of change of state, while blue and green lines represent absorption of blue and green light, respectively, required to trigger conformational change. Black lines indicate dark-reversion change in conformational state.

1.3.2 Phototropins

The phototropin family is the second group of blue light receptors, named for their discovery through mutant screening of an *Arabidopsis* line, in which a deleterious mutation to the NPH1 locus disrupted the perception of phototropic stimuli (Liscum & Briggs, 1995). Subsequent experiments identified NPH1 as a 120kDa serine-threonine kinase, which non-covalently binds two flavin mononucleotides (FMN) that act as chromophores to enable blue light sensing (Sakai et al., 2001). There are two phototropins in *Arabidopsis*, phot1, and phot2, that exhibit partial redundancy in their function, the former being responsible for inducing phototropism at low-blue light irradiances, whilst the latter appears to function over a broad range of fluorescence (J. M. Christie et al., 2015; Sakai et al., 2001).

Aside from phototropism, phototropins are responsible for mediating chloroplast avoidance of high intensity light, regulation of stomatal opening, playing a role in regulating leaf positioning and expansion, inhibition of hypocotyl growth of de-etiolated seedlings, and optimisation of leaf photosynthetic efficiency (J. M. Christie et al., 2015; Kagawa et al., 2001; Kinoshita, Doi, & Suetsugu, 2001; Sakai et al., 2001). In contrast to cryptochromes which are nuclear-localised and function primarily through coordinately regulating gene expression based on light quality, phototropins act through phosphorylation of signalling components in various sub-cellular locations, excluding the nucleus, to coordinate a variety of blue light adaptive responses without a significant degree of transcriptional regulation (J. Christie, Suetsugu, Sullivan, & Wada, 2017; Sakamoto & Briggs, 2002). The signalling events following blue-light photo-activation of phototropins are still poorly understood, however increasing evidence has implicated phototropins phosphorylation of NPH3/RPT2-Like family proteins as integral for eliciting several phototropin responses and involving regulation of auxin distribution and signalling (J. M. Christie et al., 2015; J. Christie et al., 2017).

Phototropin signalling

Phot1 and phot2 both re-localize away from the plasma membrane upon photoactivation; a fraction of phot1 moves into the cytosol in all cell-types except for guard cells, while photo-activated phot2 associates with the Golgi apparatus (S. G.

Kong et al., 2006; Wan et al., 2008). Additionally, phot2 and to a lesser extent phot1 have been identified to exhibit blue-light dependent associations with the outer-chloroplast membrane (S. G. Kong et al., 2013). To date, very few downstream signalling elements in phototropin-mediated response to blue-light irradiation have been identified for Arabidopsis, all of which are phosphorylated by the C-terminal serine/kinase domain of phototropins. Phototropin phosphorylation of BLUS1 is a critical step in stomatal opening in guard cells under blue light irradiation, initiating a cascade that triggers membrane hyperpolarization and influx of K+, causing guard cells to swell, and therefore promoting stomatal opening (J. M. Christie et al., 2015; Takemiya et al., 2013). The two other proteins phosphorylated by phototropins are ABCB19 and phytochrome substrate kinase family members (PKS), and in both cases blue-light dependent photoactivation of phot1 triggers the phosphorylation of these proteins, enhancing their activity and phototropic responses (J. M. Christie et al., 2015; Demarsy et al., 2012).

1.3.3 Zeitlupe Family

Aside from phototropins, there is a second group of LOV-domain containing blue-light photoreceptors present in higher plants, which are collectively grouped as the Zeitlupe family (ZTL). The ZTL family consists of three members: The Zeitlupe (ZTL); Flavin-binding Kelch repeat F-box 1 (FKF1); and LOV kelch protein 2 (LKP2). The ZTLs consist of an N-terminal LOV photosensory domain, an F-BOX in its center and C-terminal Kelch repeats (ul Hassan et al 2015).

ZTL activation chemistry and signalling

The ZTL's photosensory domain and mode of activation are similar to that described in phototropins; In its inactive state, an FMN chromophore is non-covalently bound to its LOV domain. Excitation of the FMN chromophore by blue light triggers a conformational change in the ZTL, thereby activating it. However, ZTLs exhibit markedly different relaxation kinetics to phototropins as, in contrast to the fast dark reversion exhibited in phototropins, the photoexcited state of ztl and fkf are believed to decay over several hours, possibly the result of these important clock-related genes being tuned to sense day-night transitions (Galvao and Fankhauser, 2015; Pudasaini and Zoltowski, 2013).

The activated ZTLs mechanism of signal transduction is distinct from those observed or predicted in other photoreceptor families. The F-box and Kelch domains are important elements within E3 ubiquitin ligases, as the former domain enables interaction with target proteins whilst the latter confers ubiquitin ligase activity, and this activity has been observed *in vivo* (ul Hassan et al, 2015), and through these domains the ZTLs modulate the protein stability of their target proteins. The function of ZTLs is primarily associated with the circadian clock and perception of the photoperiod, and several signalling components of individual ZTL photoreceptors are core clock components.

1.3.4 Light signalling components involved in phytochrome and cryptochrome signalling

The primary mechanism through which both phytochrome and cryptochromes transduce the red and blue light signals is through interaction with a series of light signalling components. The two most integral light signalling components are 1) repression of the COP1/SPA E3 ubiquitin ligase, 2) inhibition of the bHLH family of transcription factors.

COP1/SPA E3 ubiquitin ligase. A major mechanism of photoreceptor mediated signal transduction is through selective protein degradation of various positive and negative regulators within the light signalling pathway (Wei and Deng, 1996; Ma et al, 2002; Tsai, 2014). COP1, named for the constitutive photomorphogenic phenotype exhibited in *cop*1 mutant lines which harbor deleterious mutations within this gene (Wei and Deng, 1996). COP1 forms a component of a multimeric E3 ligase located within the nucleus which interacts directly with several transcription factors that are positive regulators of photomorphogenesis, such as HY5 , HYH, HFR1, PAR1 and PAR2, targeting them for 26S proteasome-mediated degradation (Saijo et al., 2003; J. Yang et al., 2005; P. Zhou et al., 2014). Photoactive phytochrome A and B inhibit COP1 activity, preventing it from degrading its target genes, which leads to an increased abundance of positive regulators of photomorphogenesis (Ma et al, 2002). The COP1/SPA E3 ligase complex is a hub of light signalling as phytochromes and cryptochromes interact with COP1 and other

constituents of the complex to repress its activity in a light-dependent manner (Ma et al, 2002; Saijo et al, 2003).

Phytochromes A and B are able to interact with COP1, as well as another important component of the complex, known as SPA (Suppressor of PHYA) (Saijo et al, 2003). Other sub-components of the E3 ligase include *de-etiolated 1* (*det1*) and several other proteins, to which deleterious mutations to their genes result in complete or partial *cop* phenotypes (Wei and Deng, 1996). Comparison of expression profiles between the *cop1* and *det1* knock-out lines and the constitutively active phytochrome B mutant line *yhb* in darkness revealed the importance of COP1 in the red-light response, identifying a 30% overlap in misregulated genes (Hu et al, 2009). Cryptochromes initiate light signal transduction through suppression of the COP1/SPA, although the mechanism of activation differs between cryptochrome 1 and 2, with the form interacting with SPA but not COP1, while the latter has a strong affinity for COP1 and substantially reduced interaction with SPA (Holtkotte, Ponnu, Ahmad, & Hoecker, 2017; B. Liu, Zuo, Liu, Liu, & Lin, 2011). One COP1 regulated transcription factor, ELONGATED HYPOCOTYL 5 (HY5), has been identified as a core transcriptional regulator of photomorphogenesis, directly binding to and regulating the expression of over 1100 including other transcription factors to promote photomorphogenesis, photosynthesis, and pigment synthesis (Toledo-Ortiz et al., 2014; Huiyong Zhang et al., 2011).

Phytochrome Interacting Factors. First identified in Arabidopsis, it is now known that phytochrome-interacting factors (PIFs) are a small sub-family of Phytochrome-Interacting basic Helix-Loop-Helix (bHLH) transcription factors which are responsible for negatively regulating the expression of a large subset of genes in response to red-light signals perceived by the phytochrome (Heim et al., 2003; P. Leivar et al., 2009; Pablo Leivar et al., 2008; M. Ni, Tepperman, & Quail, 1998) as well as blue light signals perceived by cryptochromes photoreceptors (Pedmale et al., 2016). Several PIF-like (PIL) proteins interact with not only phytochromes but also cryptochromes to transduce both red/far-red and blue light signal ((Pedmale et al., 2016)). The trademark bHLH domain is a DNA-binding domain, and where examined, PIFs have been identified to bind specifically to core DNA G-box (CACGTG) and PBE-box (CACATG) motifs of target promoter genes (Y. Zhang et al., 2013). Predicted within 13 of the 15 members of the bHLH sub-family, and

validated within 7 members, were a conserved N-terminal active phyB binding (APB) domain which provides phyB specific binding (Heim et al., 2003; Rajnish Khanna et al., 2004). PIF1 and PIF3 have also been proven to bind PHYA, mediated through a separate Active Phytochrome A binding (APA) domain(Al-Sady, Ni, Kircher, Schäfer, & Quail, 2006).

The mechanism of both phytochrome and cryptochrome signal transduction through the PIF pathways is now well understood. For phytochromes, light-induced activation of PhyB triggers the degradation of PIFs, through direct physical interaction resulting in trans-phosphorylation of the transcription factor. The phosphorylation of the PIF and formation of the PHYB-PIF complex promotes poly-ubiquitination of PIF by E3 ligases, resulting in the degradation of both the PIF and phytochrome though the ubiquitin-proteasome system (Al-Sady et al., 2006; W. Ni et al., 2014). The degradation of PIFs relieves their suppression of a large subset of light-regulated genes, whilst concomitant proteolysis of PhyB provides an attenuation mechanism to prevent excessive signalling (Ni et al, 2014). Genetic studies using an Arabidopsis quadruple (PIF1, 3, 4 and 5) PIF-mutant (PIFq) identified the degree of misregulation in genome-wide expression through comparison of dark and light-grown mutants to its wild-type counterpart (P. Leivar et al., 2009). The critical role of PIFs was highlighted by the fact that 80% of gene expression changes in the dark-grown PIFq mutant were normally induced by white-light in wild-type seedlings (Leivar et al, 2009). In fact, PIFs bind to the common g-box motif as HY5, acting antagonistically in an activation-suppression module which is at the apex of the light-regulated transcriptional network (Toledo-Ortiz et al., 2014). Despite some functional redundancy, specific roles of PIFs have been established such as PIF4/PIF4 promotion of LBL shade avoidance, PIF7 low R:FR response and PIF4 high-temperature response (Koini et al., 2009; L. Li et al., 2012; Pedmale et al., 2016).

1.3.5 Integration of light and hormone signalling controls development

Plant growth and development at every stage of its life cycle is regulated by interconnected signal transduction pathways that integrate environmental and endogenous hormone signals to elicit specific cellular responses in a coordinated manner. The effect of light on plant growth and development can often be mimicked,

exaggerated, or abolished by application of exogenous hormones or biosynthesis inhibitors as well as by mutations to hormone metabolic genes (García-Martinez & Gil, 2001). Light and hormone signalling are tightly integrated, with multiple photoreceptors identified to mediate growth and developmental responses through altering phytohormones levels or through altering hormone distribution or sensitivity. In fact, light and hormone signalling pathways converge at multiple levels, and the integration of these signals dictates the responsiveness of tissues to light or hormones. A central integrator of light and hormone signalling has been identified in the conserved family of phytochrome-interacting factors (PIFs), which not only directly interact with cryptochromes and phytochromes but also several integral components in auxin, gibberellin, and brassinosteroid signalling pathways. In the following section, I discuss the roles of several phytohormones in light signalling as this is integral to understanding the mechanism through which photoreceptors transduce light signals to adaptively respond to light signals.

Auxin

Auxins are core positive regulators of growth, regulating cell division and expansion, as well as developmental processes including organogenesis, tissue patterning, and tropic responses. Light controls auxin abundance, distribution, and perception to coordinate plant growth and development in response to light. PIFs 4,5, and 7 promote auxin-mediated growth through promotion of auxin biosynthesis by direct binding to YUCCA genes, which encodes an enzyme that catalyzes the rate-limiting step in auxin biosynthesis (Hornitschek et al., 2012; L. Li et al., 2012). Consistent with this, YUCCA quintuplet silenced transgenic line exhibits a suppressed R: FR shade-avoidance response on both a phenotypic and transcriptomic level (Nozue et al., 2015). Auxin distribution is also essential for R: FR SAR responses, as silencing of PIN3 auxin efflux carrier, completely inhibited low R: FR induced SAR response but did not affect response to low-blue light (Keuskamp, Pollmann, Voesenek, Peeters, & Pierik, 2010; Keuskamp et al., 2011). Both cryptochromes and phytochromes also act antagonistically with auxin through interference with auxin signalling networks. They have both been shown to directly bind to AUX/IAAs, core negative components in auxin signalling, and stabilize them to prevent auxin-stimulated degradation via TIR1 (F. Xu et al., 2018). In addition to

this, PIFs directly bind to and alter the expression of several auxin early-signalling genes including AUX/IAA and SAURs in response to both red and blue light signals (N. Sun et al., 2016).

Auxin has also been identified to antagonistically regulate cytokinin signalling in response to light to coordinate cell growth. In *Arabidopsis*, auxin-induced signalling in responses to low R: FR induced shade avoidance upregulates cytokinin catabolic genes, cytokinin oxidase/dehydrogenase (CKX), which reduced cytokinin levels thereby arresting leaf development to allow plants to redirect resources towards apical growth (Carabelli et al., 2007).

Gibberellin and Brassinosteroids

In addition to auxin, two other growth-promoting hormones, brassinosteroids, and gibberellins are important regulators of light signalling. Gene functional studies have shown that mutants defective in auxin, brassinosteroids or gibberellin biosynthesis or signalling genes exhibit defective photomorphogenesis (Alabadi, 2004; J Li, Nagpal, Vitart, McMorris, & Chory, 1996). LBL induced a reduction in petiole elongation and was strongly inhibited in both DELLA mutant *gai1* and brassinosteroid receptor mutant *bri1*, which have defective responses to gibberellin and brassinosteroid, respectively (Keller et al., 2011). A common integration point between hormones GA and BR with phytochrome and cryptochrome photoreceptors has been identified involving PIF4 which is depicted in **Figure 1-4**. In shade, low R, low R: FR ratio, low B or low B:G ratio led to the inactivation of PHYB and CRY photoreceptors which released their inhibition of PIFs (J. P. Bouly et al., 2007; de Wit et al., 2016). When BR levels were high, brassinosteroid receptor kinase BRI1 initiated a signal transduction cascade leading to dephosphorylation and subsequent activation of BR-responsive transcription factor family BZR1, which then translocated to the nucleus and regulates growth-promoting gene expression. PIF4 interacted with BZR1 to form a heterodimer, and the PIF4-BZR1 have been identified to co-regulate a large number of common growth-promoting genes interdependently, although each factor has unique target genes (Eunkyoo Oh, Zhu, & Wang, 2012). Gibberellin elicited promotion of growth regulating genes through inducing the degradation of DELLA proteins, which were negative regulators that inactivate a plethora of transcription factors including PIF3, PIF4 and BZR1 (De Lucas et al.,

2008; Feng et al., 2008; Q. F. Li et al., 2012; T. P. Sun, 2011). Therefore, when GA levels are low, DELLAs accumulate and inhibit both PIF4 and BZR1, to suppress transcriptional activity. In this pathway, low BR and low GA act antagonistically to PHYB and CRY but positively with shade signals (Bai et al., 2012). Transcriptomic analysis of GA and BR responsive genes using BR-insensitive mutant *bri1-116* and GA-deficient mutant *ha1-3* showed that one-third of differentially expressed genes in GA mutant were also affected in the BR mutant, and 92% of those BR and GA common genes were affected by light (Bai et al., 2012). DELLA blocks both BZR1 and PIF4 individually and inhibits the PIF4/BZR1 heterodimer, and the genes commonly regulated by brassinosteroid, gibberellin and DELLA include cell-wall photosynthesis/chloroplast genes and are consistent with photomorphogenic and shade avoidance phenotypes (Bai et al., 2012).

In addition to the gibberellin-brassinosteroid-light signal integration through DELLA-PIF4-BZR1 interactions, auxin signals also integrate into this central module to control cell elongation in Arabidopsis hypocotyl. AUXIN RESPONSIVE FACTOR (ARF6) acts as a positive regulator of transcription, promoting hypocotyl elongation in part through PIF- and GA- dependent pathways (Chapman et al., 2012). Genome-wide transcriptomic analysis and biochemical assays identified a substantial overlap of auxin transcription factor ARF6 with both BZR1 and PIF4 target genes, with three transcription factor co-operatively regulating the transcription of these genes (Eunkyoo Oh et al., 2014). Furthermore, DELLA protein RGA physically interacts with ARF6, inhibiting its DNA-binding to suppress transcription of growth-promoting genes (Eunkyoo Oh et al., 2014). Together this evidence suggests that auxin signalling pathways are also integrated in a central transcriptional module including brassinosteroids, gibberellin, and light, in which DELLA acts as a master regulator of the transcription, inhibiting the expression of growth-promoting genes through the inhibition of BZR1, ARF6, and PIF4 (Eunkyoo Oh et al., 2014). This signalling pathway is illustrated in **Figure 1-4**, showing the post-translational interactions of auxin, light, gibberellin, and brassinosteroid which modulate the expression of genes associated with plant growth in Arabidopsis.

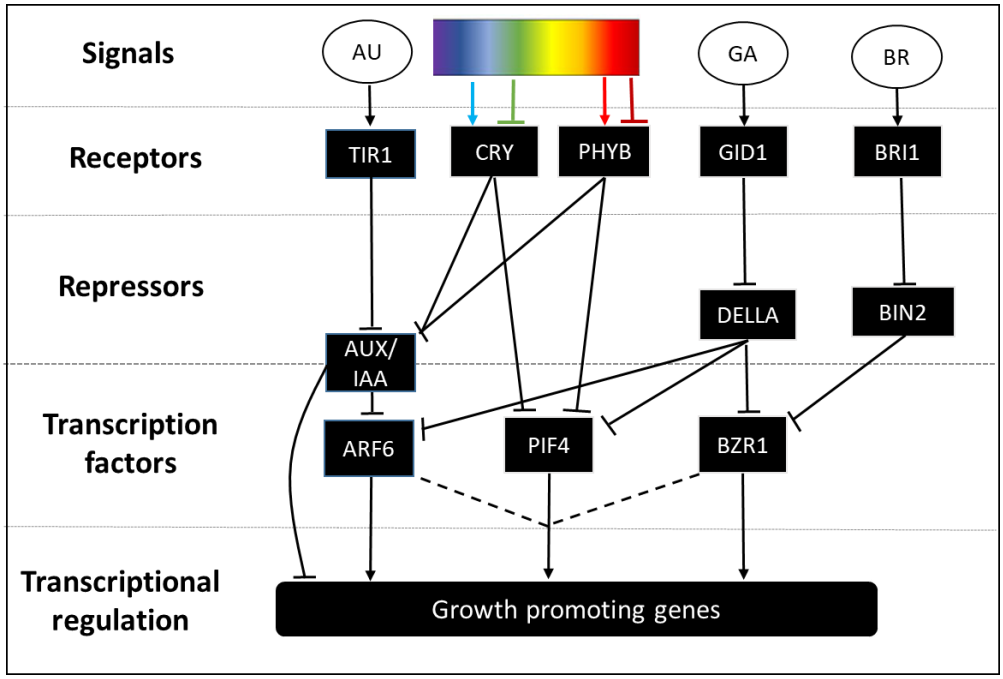


Figure 1-4 Model of light, brassinosteroid, auxin, and gibberellin signal integration through PIF4-BZR1-DELLA module. Arrows indicate positive regulation while flat-head lines indicate repression. Colored lines indicate light signals, with red (660nm), far-red (720nm), blue (450nm), and green/yellow (500-630nm). Ovals indicate hormones: auxin (AU), gibberellin (GA), and brassinosteroid (BR). Rectangles indicate proteins, while the elongated rectangle with curved corners represents growth-promoting genes. CRY- cryptochrome; PHYB- Phytochrome B.

The activity of DELLA itself has also been shown to be regulated by several hormones including auxin (Fu & Harberd, 2003), jasmonate (D.-L. Yang et al., 2012), and ethylene (Achard, 2003), identifying a central module through which light and hormone signalling can be coordinated to regulate growth-responsive gene expression (Bai et al., 2012). In addition to the integration of post-translational signalling networks, both phytochromes and cryptochromes transcriptionally regulate gibberellin biosynthesis in response to shade through promoting the expression GA20-oxidase, which catalyzes a rate-limiting step in gibberellin biosynthesis (De Lucas et al., 2008; X. Zhao et al., 2007). *pif4* deficient mutants have an altered response to gibberellin, indicative of PIF4 role in gibberellin-induced hypocotyl growth. Moreover, *pif4* over-expression in a gibberellin deficient mutant background partially overcomes the gibberellin-deficient dwarf phenotype (De Lucas et al., 2008). Another PIF family member, PHYTOCHROME-INTERACTING FACTOR-LIKE 3-5 (PIL5) regulates GA responsiveness by coordinately up-regulating the expression of gibberellin

biosynthesis genes while inhibiting gibberellin catabolic genes. Moreover, PIL5 directly promotes gibberellin responsiveness by upregulating expression of key GA-responsive transcription factors GAI and RGA (E. Oh et al., 2007). PIL5 also simultaneously activates ABA biosynthesis genes and represses ABA catabolic genes to increase ABA levels through both GA-dependent and independent pathways (E. Oh et al., 2007). DELLAs are able to bind to all PIFs, blocking transcriptional activity, and the competitive interaction of DELLA with PIF explains a great deal of DELLA-dependent GA phenotypes related to hypocotyl elongation, dwarfing and chlorophyll biosynthesis (De Lucas et al., 2008).

Photoreceptors and the plant defense response

Plants integrate light and defense signals through the phytochrome photoreceptors and the defense hormones salicylic acid (SA) and jasmonic acid (JA). Phytochromes control salicylic acid associated defense through modulating SA homeostasis and perception. Studies using light receptor mutants deficient in *phyAphyB*, *cry1cry2* and *phot1phot2* established that only phytochromes participate in the induction of systems acquired resistance in response to pathogen detection and salicylic-acid dependent defense response (Griebel & Zeier, 2008). Silencing of *phyB* increases susceptibility to necrotrophic fungus *Botrytis cinerea*. Furthermore, studies of a double mutant deficient in *phyB* and a core transcriptional repressor of jasmonic acid signalling, Jasmonate ZIM-domain transcriptional repressor *jaz10,* identified that silencing of *jaz10* in a phyB background restores defense traits. This revealed that not only does phyB regulate defense resistance, but disruption of *jaz10* in the *phyB* mutant background produced plants which have unaltered low R: FR under shade-avoidance type growth without compromising disease susceptibility (Cerrudo et al., 2017) .

1.4 Adaptive response to light

In this section I will discuss the molecular mechanisms that underpin the adaptive responses of a plant to different spectral qualities, breaking the responses down into the different developmental processes which are regulated such as

germination, de-etiolation, flowering, and fruiting and discussing the different mechanisms through which light quality and specifically photoreceptors perceive and translate these signals to affect biochemical and physiological changes in the plant.

1.4.1 Photoreceptor role in seed germination and photomorphogenesis

Phytochrome control of seed germination.

Light is an important environmental cue that regulates seed germination, as the timing of germination is crucial to maximizing successful seedling establishment. Light regulation of seed germination is exclusively controlled by the phytochrome family. Multiple members of the phytochrome family regulate seed germination: Phytochrome A photo-irreversibly triggers germination UV-A, visible and infra-red light of very low fluorescence, whilst phytochrome B and E mediates the far-red photo-reversible low fluorescence germination under red light (Hennig, Stoddart, Dieterle, Whitelam, & Schäfer, 2002; Shinomura et al., 1996). It has recently been identified that the dominance of the aforementioned photoreceptors in germination is temperature dependent, with PhyA and PhyE playing critical roles under low and high temperatures respectively, whilst PhyB is important across a broad range of temperatures (Heschel et al., 2007).

Seedling de-etiolation in response to light

Immature seedlings undergo a drastic developmental reprogramming upon their first exposure to light. Photomorphogenesis, also referred to as de-etiolation, is a light-triggered developmental switch from skotomorphic growth (dark grown) to photoautotrophic growth, and is characterized by morphological changes such as the opening of the apical hook, inhibition of hypocotyl elongation, cotyledon expansion, as well as sub-cellular changes such as the development of chloroplasts, and anthocyanin synthesis, all of which is driven by photoreceptor-mediated transcriptional reprogramming. Members of the phytochromes and cryptochromes coordinately modulate de-etiolation, and extensive research has modeled the respective roles of these photoreceptors as well as important downstream components in the process. Monogenic *phyA* and *phyB*, as well as *cry1/cry2* transgenic lines, show aberrant de-etiolation phenotypes with elongated hypocotyls, reduced cotyledon

expansion and chloroplast development, similar to dark grown skotomorphic seedlings. A major shared signalling pathway between phy and cry is their suppression of COP-mediated proteolytic degradation of HY5, an integral positive regulator of photomorphogenesis, detectably altering the expression of over 1100 genes in order to reprogram the plant development (Huiyong Zhang et al., 2011).

1.4.2 Photoreceptor regulation of plant architecture

An elegant example of how the perception of light quality can increase the fitness of a plant is through the shade-avoidance response (SAR). Under the shade of another plant's canopy, the light which passes through a leaf is enriched in far-red and green light while deficient in red and blue, as chlorophyll shows peak absorbance for blue and red light and therefore these wavelengths are absorbed for plant photosynthesis (Smith & Whitelam, 1997). *Arabidopsis* is used as a model for shade avoidance, and in response to being shaded it rapidly adjusts its genome-wide expression, inducing phenotypic changes including: adjusting its growth to promote stem and petiole elongation, arresting root and leaf expansion, and adjusting leaf angle, in an attempt to out-grow the canopy providing shade and increase light interception (de Wit et al., 2016; Tingting Zhang & Folta, 2012).

Phytochrome-mediated shade-avoidance

The R: FR ratio of the intercepted light is perceived primarily through phytochrome B and to a lesser extent phytochromes D and E. As far-red inactivates red-light photoactivated Active phytochromes, the R: FR ratio determines the photo-equilibrium of active to inactive phytochromes. When active, PhyB, PhyD and PhyE translocated to the nucleus whereby it acted to suppress shade-avoidance signalling pathways (Kircher, 2002). PIF4, PIF5, and PIF7 have been identified as integral to phy-mediated SAS, positively regulating the expression of several key shade-avoidance genes including as HFR1 and PIL1 (L. Li et al., 2012; Lorrain, Allen, Duek, Whitelam, & Fankhauser, 2008). Recently, A mechanism of PIF7 regulation of shade-avoidance has proposed because direct evidence of a pathway from photoreceptor excitation to changes in plant architecture mediated through regulates phytohormone signalling was reported by L. Li et al., (2012). In full sunlight, the increased ratio of R: FR leads to activation of phytochrome, which then translocates

to the nucleus and physically interacts with PIFs including PIF5, phosphorylating the proteins, preventing their activity (L. Li et al., 2012). In response to being shaded, the low R: FR shifts the equilibrium towards the far-red photoreversion of active Pr into inactive Pfr, dissociating with PIF7, leading to rapid de-phosphorylation of PIF7. De-phosphorylated PIF7 binds to a conserved G-box motif of several auxin biosynthesis genes, enhancing their expression and consequentially increasing the levels of indole-3 acetic acid (IAA), the most abundant active form of auxin, which then is transported into the stem and other tissues, where it promotes elongation (L. Li et al., 2012). Auxin appears to be the primary phytohormone regulating the shade-avoidance response; however, brassinosteroids, auxin, ethylene, and gibberellin have been identified as playing roles in SAS, as mutation to their biosynthetic or signalling genes reduces far-red induced etiolation response as well as suppressing the *PhyB* constitutive shade-avoidance phenotype (Stamm & Kumar, 2010). Taken together, this evidence indicates that phytochrome signalling intricately modulates the balance of phytohormones in order to adapt the plant growth and development strategy unexpected fluctuations in its environmental conditions.

Cryptochrome regulated shade avoidance by blue and green light

In addition to the phytochrome-mediated mechanisms of shade-avoidance, it has been proposed that cryptochromes function with SAS in an analogous manner. With increased density of shading, the proportion of blue within the light decreases as mentioned above. In Arabidopsis, low blue irradiance increased hypocotyl length, stem elongation, and several other phenotypes associated with R: FR mediated SAS and required both auxin and brassinosteroid signalling (Keller et al, 2007; Keuskamp et al, 2011, 2012). The low-blue light (LBL) shade-avoidance response stimulated by blue light depletion is mediated by cryptochrome photoreceptors CRY1 and CRY2, and requires PIF4 and PIF5 (Keller et al., 2011; Pedmale et al., 2016). Direct physical interaction between CRY1 and CRY2 with PIF4 and PIF5, involving direct binding of cry and pif4/5 to the same genomic loci, occurs during LBL (Pedmale et al., 2016). Phytochrome B has also been implicated in LBL SAR; physical interaction of PIF4/5 with PHYB is integral for the LBL, as mutation to the phytochrome-binding region of the PIF4/5 (APB) suppressed the LBL response (Pedmale et al., 2016). However, despite a small degree of overlap, cryptochrome and phytochrome-mediated SAS

occur by eliciting largely independent hormonal cascades, with cryptochrome and phytochromes using partially independent pathways for polar auxin transport, auxin biosynthesis and gibberellin signalling (Keller et al, 2007). Unlike in R: FR mediated shade avoidance, in Arabidopsis LBL SAR does not require changes in auxin biosynthesis. Furthermore, silencing of auxin transporter PIN3, an auxin transporter which changes its sub-cellular localisation to facilitate polar auxin transport required to induce hypocotyl elongation during low R: FR SAR (Keuschamp et al., 2010), only partially inhibited LBL hypocotyl elongation in Arabidopsis seedling stage and had no effect on LBL SAR in rosette phase (Keuschamp et al., 2011; Keller et al., 2011). However, recently a triple *pin3,4,7* mutant was found to have strongly inhibited hypocotyl elongation in response to LBL, indicating that LBL and R: FR shade avoidance recruit different enzymes to elicit similar responses (Pedmale et al., 2016). Transcriptomic analysis of the LBL response in Arabidopsis showed that it did not involve over-representation of auxin genes, unlike in low R: FR induced shade avoidance (L. Li et al., 2012; Pedmale et al., 2016; Sessa et al., 2005). However, in Arabidopsis both photo-activated PHYB and CRY1 physically interacted with AUX/IAAs mediating inhibition of auxin-induced degradation of AUX/IAA through physical interaction, thereby allowing AUX/IAA activation of growth-promoting genes (Xu et al., 2018).

Recent studies have shown that simply correlating blue-light irradiance and cry-mediated SAS does not give a strong correlation between irradiance and response, considering the ratio of blue/green rather than just B irradiance as a measurement of cryptochrome-mediated shade-avoidance improved the goodness-of-fit of the model (Sellaro et al., 2010). The current model of cryptochrome activation proposes that green light causes photo-inactivation of the activated cryptochrome through further reduction its FAD, which exists in a semi-quinone state in the activated cryptochrome (Banerjee et al., 2007; J. P. Bouly et al., 2007). However, not all responses of the plant to green light irradiance can be explained by this mechanism. Current evidence suggests that the effect of green light on growth and development is proposed to act via cryptochrome-dependent and independent mechanisms, and green light-mediated phenotypes have persisted in *cry*, *phy*, and *phot* mutants, indicating either functional redundancy that is yet fully understood or a novel green light sensor (Folta & Maruhnich, 2007).

1.4.3 Photoreceptor regulation in photosynthesis and photoprotection

Photosynthesis

As described in **Section 1.2**, absorption of light by pigments (e.g. chlorophyll *a*, chlorophyll *b*) drives photosynthetic assimilation of CO_2 into organic compounds which are used for biomass production and as the energy that fuels growth and development. The absorption of light energy by chlorophyll localized in the light-harvesting complexes of photosystems II and I within the thylakoid membranes of the chloroplast leads to the excitation of an electron from the chlorophyll transforming it into its singlet electron state. The excitation energy from the chlorophyll is transferred to the PSII and PSI reactions which provide the energy to initiate photosynthetic electron transport. The excitation energy within PSII also provides the energy for the hydrolysis water into oxygen, hydrogen ion, and an electron. The electrons derived from hydrolysis are transferred across the electron transport chain through redox reactions which provide the energy to actively transport hydrogen into the thylakoid, creating a transmembrane pH gradient which drives the production of ATP from ADP by chloroplastic ATP synthase (Murchie & Niyogi, 2010). While ultimately the electron is used to reduce NADP into NADPH by the enzyme ferredoxin-NADP reductase. In the stroma, using products of the light-dependent reaction, ATP and NADPH, the Calvin-Benson cycle reactions fix CO_2 from the environment, facilitated by the enzyme Rubisco, and build carbohydrate molecules. This fundamental process provides the carbohydrate energy which is transported to distant tissues throughout the plant and broken down to provide the energy to fuel plant growth.

In addition to photoreceptors which detects light quality and irradiance intensity, chloroplasts have an internal sensor of light intensity, redox signalling. Based on the redox state of plastoquinone, an electron carrier which involved in the electron transport chain in the light-dependent reaction of photosynthesis, the plant can sense the amount of light absorbed by the photosensory system, and this signal induces transcriptome changes within the plastid to alter the expression of photosynthesis-related genes based on the rate of photochemistry.

Light quality also influences photosynthesis, not only through differential absorption of wavelengths of light and different efficiencies with which they drive photosynthesis, but also regulates photosynthesis on a transcriptional and post-

translational level. The effect of this is seen as mentioned previously, in the photosynthetic dysfunction observed in seedlings of several species plants grown under monochromatic red light, as blue light is necessary for the development of normal photosynthesis. While the expression of photosynthesis-related genes is partially regulated through the redox state of the plastoquinone pool, the transcription of a core photosystem component, *psbD,* is regulated by the cryptochrome –mediated signalling and induction of *SIG5* transcription in the nucleus (Mochizuki, Onda, Fujiwara, Wada, & Toyoshima, 2004). In fact, studies in transgenic line with over-expressed CRY2 showed that cryptochromes extensively regulate plastid transcription, with 58% of chloroplast-related genes significantly differentially expressed in transgenic line compared to wild-type tomato (Facella, Carbone, Placido, & Perrotta, 2017). The rate of photosynthetic carbon fixation is also controlled through the stomatal opening, as this determines CO_2 availability for carbon fixation. Blue light regulates chloroplast opening to control stomatal conductance on a post-translational level predominantly through phototropin signalling, with a small effect of cryptochrome and red light signals perceived by phytochromes (H. E. Boccalandro et al., 2012; Talbott, Shmayevich, Chung, Hammad, & Zeiger, 2003). However, both cryptochromes and phytochromes control stomatal development through COP1-dependent transcriptional performance (Kang, Lian, Wang, Huang, & Yang, 2009).

Photoprotection

Light quality also regulates the photosynthetic efficiency and light absorption through photoprotection. When the irradiance levels exceed that necessary for maximum photosynthetic capacity in a plant, excess light energy is toxic to the plant, as the photoexcited electrons in the photosystem cannot be funneled into photosynthesis, they can instead be transferred to oxygen to generate extremely damaging reactive oxygen species (ROS). The irradiance level necessary to be trigger oxidative stress depends on the plants maximum photosynthetic rate, which can be reduced through a number of abiotic and biotic stresses, and through the perception of light quality. Plants have evolved photoprotective mechanisms through a protected system against excessive light. Spectral quality controls chloroplast movements (Inoue & Kinoshita, 2017), which reduce the interception of light by chloroplast thereby reducing the amount of light absorbed. Also, absorbed light energy can be

dissipated harmlessly as heat through molecular vibrations, a process termed non-photochemical quenching (NPQ). NPQ is a fundamental process which protects the plant for excess damage at the cost of reducing photosynthetic efficiency, and therefore must be finely balanced to occur at a low rate to maximize photosynthesis when light levels are ideal, and be upregulated in high light to protect the plant for light damage (Muller, 2001).

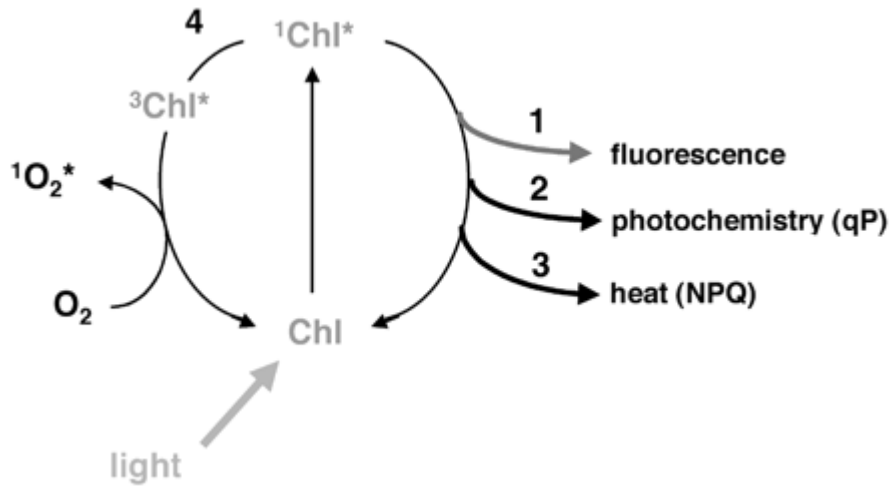


Figure 1-5 Possible fates of light energy absorbed by chloroplast (Muller, 2001). When light energy is absorbed by photosystem of chlorophyll, a chlorophyll is photo-excited, and this excitement energy is transferred to one of four sinks as the chlorophyll returns to its grounded state. 1, Photosystem II emits a small portion of chlorophyll fluorescence when reduced, prior to returning to ground state. 2, photochemistry is the main acceptor of the electron energy, and the electron is passed throughout the electron transport chain, providing energy to drive the light reaction of photosynthesis.3, Non-photochemical energy is the dissipation of the electron energy as heat. 4, chlorophyll enters triplet-state, and an electron is transferred to an oxygen molecule to produce the reactive-oxygen species singlet-oxygen.

High light acclimation and photoprotection in diatom *Phaedactylum triconutum* requires blue light, with NPQ capacity correlating with an upregulation of photoprotective proteins including zeaxanthin epoxidase (Costa et al., 2012). Recently, R/Fr shade signals have been found to regulate photoinhibition and photoprotection within canopies through PHY-A controlled transcriptional network (F. Wang et al., 2017). Low R/FR ratio leads PHYA induction of core light signalling transcription factor HY5, which upregulates abscisic acid-responsive transcription factor ABA INSENSITIVE 5 ABI-5 that subsequently triggers reactive oxygen species production in the apoplast inducing NPQ (F. Wang et al., 2017). The control

of the rate of NPQ in response to shade signals is a mechanism through which canopies can regulate the photosynthetic efficiency at different canopy levels.

1.4.4 Photoreceptor, photoperiod, and flowering

Perception of day-length and other light parameters provided the plant with an adaptive advantage to anticipate seasonal changes and coordinately regulate their developmental strategy. The interplay of the circadian clock and photoreceptor perception of photoperiod regulated flowering time in *Arabidopsis* (Valverde et al., 2004). Loss of *phyA, phyB,cry1, cry2* affects circadian rhythms and alters the plant's sense and response to photo-period (Jarillo et al., 2001). Photoreceptor ztl plays a particularly important role in the circadian clock, implied by the fact that over-expression of ztl cause arrhythmicity, and thus it is required for generating circadian rhythm (W.-Y. Kim, Geng, & Somers, 2003). CONSTANS (CO) is a zinc-finger transcription factor, whose expression is regulated by the circadian clock; suppressed during the morning, and upregulated during the evening. Under long-day conditions, CO activates the transcription of Flowering Locus T (FT), promoter of flowering. The photo-period dependent modulation of CO activity is based on light-dependent post-translation regulation of CO stability and is regulated by antagonistic interactions by multiple photoreceptors. Red-light stimulation of phyB enhances COP/SPA mediated proteolytic degradation of CO, whilst cry1, cry2, and phyA antagonize the repressive effect of phyB (Valverde et al., 2004). Diurnal timing of the expression of photoreceptor and other signalling elements leads to enhanced expression of CO in the afternoon, as phyB expression peaks in the morning while phyA and cry2 peak in the afternoon (Toth et al, 2001). Furthermore, phyB-interacting protein, Phytochrome-dependent late flowering (phl), accumulated in the nucleus during the afternoon, and directly interacted with phyB to inhibit its proteolytic degradation of CO, shifting the balance in favour of the photoreceptors promoting flowering and leading to the accumulation of CO and promotion of FT expression to promote floral initiation (Endo, Tanigawa, Murakami, Araki, & Nagatani, 2013).

The photoreceptor ZTL/ADO family photoreceptor FKF further entangles the circadian clock and photoreceptor interactions through modulating both clock-dependent regulation CO abundance and activity. FKF accumulation is regulated by

the circadian clock and accumulates during the progression to evening. As FKF levels rise, a repressor of CO expression, cdf1, declines in an FKF-dependent manner, leading to accumulation of CO in the evening (Imaizumi, Schultz, Harmon, Ho, & Kay, 2005). As well as mediating the timing of CO expression, FKF also directly interacts with CO protein during the afternoon (Song & Imaizumi, 2012). As a consequence of the integration of multiple light signals perceived by multiple photoreceptor families, exposure of light only coincides with CO expression under long-days, facilitating photoperiod-dependent flowering (Endo et al., 2013; Imaizumi et al., 2005; Valverde et al., 2004). Ztl also modulated the circadian clock through its time-of-day-dependent degradation of TIMING-OF-CAB-EXPRESSION 1 (TOC1) (W. Y. Kim et al., 2007). However, ztl-dependent degradation of TOC1 is indirectly modulated by cryptochromes and phytochromes through the COP1/SPA pathway. In the presence of blue light, photoactivated ztl interacts with GIGANTEA (GI), resulting in the stabilization of both proteins (Kim et al, 2007, 2013). In turn, the GI rhythm is determined by interaction with ELF3 and COP1, which target GI for degradation in darkness (Yu et al., 2008). CRY2 also controls the initiation of flowering through CO-independent enhancement of FT expression, as under blue-light, photoactivated CRY2 interacts with CIB1 to promote floral initiation (Liu et al., 2012). In total, the integration of red and blue light signals perceived by phytochrome, zeitlupe and cryptochrome photoreceptors and diurnal rhythms generated by circadian clock regulates flowering time through a convoluted set of pathways which use both transcriptional and post-translational mechanisms.

1.4.5 Fruit quality

Light signals perceived in the leaf have been shown to elicit transcriptional changes in distant tissue through regulation of phytohormones homeostasis and mobile transcription factors (Chen et al, 2016). However, photoreceptors are not just limited to leaves, and stable expression of phytochromes and cryptochromes have been identified in seeds, roots, stems, leaves, flowers (Sharrock and Clark, 2012) and fruit have been identified as playing a critical role in development steps in through perception and signalling within a plethora of plant tissues. In tomato fruit, phytochromes act as a ripening sensor eliciting changes in pigment composition and secondary metabolism as fruit mature (Llorente et al., 2016).

1.5 Manipulating light signalling components to improve crop yield

The term photobiotechnology has recently been coined to refer to the transgenic manipulation of gene expression with photobiological relevance (Gururani, Ganesan, & Song, 2015). This approach to crop enhancement is viewed as a promising strategy, and there are already numerous examples in which photobiotechnology has been exploited to develop crops with improved agronomical traits and yield (Gururani et al., 2015).

The pattern of resource partitioning in plants has shown that plant architecture can be modified through the manipulation of components of the photoreceptor-signalling pathways. **Table 1-1** contains a list of literature reviews about gene functional studies into cryptochrome and phytochromes in a number of crop species and the plethora of agronomically important traits. In Arabidopsis and most important crop species, decreasing R: FR ratio induces a shade-avoidance phenotype, resulting in petiole elongation, reduced leaf thickness, area, and pigment accumulation, accelerated development, reduced flowering and seed yield. Increasing investment into shade-avoidance reduces the energy available to be invested into agronomically important traits which results in reduced yield (Cagnola, Ploschuk, Benech-Arnold, Finlayson, & Casal, 2012). Ectopic overexpression of phytochromes A or B in several crop species including tobacco, rice, wheat, cotton and others, has resulted in drastic alterations in plant architectures leading to substantial increases in yield and harvestable index (H. E. Boccalandro et al., 2012; Garg et al., 2006; K.-M. Kim, Kim, & Kim, 2009; A. Q. Rao et al., 2011; Robson, McCormac, Irvine, & Smith, 1996; Thiele, Herold, Lenk, Quail, & Gatz, 1999). Ectopic PHYB over-expression alleviated the density effect on tuber yield in field potato and increased photosynthetic rates at all canopy levels compared to the wild-type through suppression of shade-avoidance (Boccalandro et al, 2003).

Despite the fact that cryptochromes have been implicated in controlling several agronomically important traits, characterization of cryptochrome activity in crop species has not been extensively explored. However, there has been studies of the effect of cryptochrome over-expression in a selection of crop species. Evidence from Arabidopsis, tomato, tobacco, sweet potato, and oil-seed rape suggests CRY1

over-expression exerts pleiotropic effects on plant growth and development at all life stages, including semi-dwarfism and an increase in pigment accumulation. Complementarily silencing of CRY1 and CRY1a in oil-seed rape and tomato, respectively, induced SAR-like phenotype (M. Chatterjee, Sharma, & Khurana, 2006). In oilseed rape, a transcriptomic study comparing the wild-type and over-expresser indicated a significant upregulation of auxin transporter PIN3-3, cytokinin dehydrogenase CKX5, and gibberellin biosynthesis gene GA1, which could underpin cryptochrome transcriptional control of phytohormones homeostasis that leads phenotypic response (Sharma, Chatterjee, Burman, & Khurana, 2014). In tomato, over-expression of CRY2 resulted in a dwarfed phenotype, increased pigment accumulation in leaf tissues, delayed flowering, as well as an increase in several fruit phytonutrient levels (Giliberto et al, 2005). Reciprocal over-expression and silencing of tomato CRY1a gene revealed antagonistic roles on fruit quality and yield (C. C. Liu et al., 2018). CRY1a expression was positively correlated with nutrient quality as soluble sugar content as well as nutrients such as β-carotene lycopene and phytoene content. However, cryptochrome expression had a negative effect on yield, as cry1a silenced plants had significantly reduced days to flower, greater yield per plant, fruit number, and individual fruit weight than wild-type plants, while the transgenic over-expresser CRY1a line exhibited significant reductions in these traits compared to the wild type (C. C. Liu et al., 2018).

Elucidation of components downstream of photoreceptor signalling pathways could allow the opportunity to improve yield and quality through targeting a subset of responses without altering important photoreceptor-mediated developmental responses (Kharshiing and Singha, 2015). In Arabidopsis, down-regulation ATHB-2, a positive regulator of phytochrome-mediated shade-avoidance, resulted in suppression of hypocotyl elongation, increased leaf number and size, and increasing root mass (Steindler et al, 1999). Recent research in Arabidopsis showed that transgenic line with silenced JAZ gene expression eliminated the negative effect that low R: FR signals have on plant immunity to necrotrophic pathogens without affecting the growth and developmental responses It showed that targeted manipulation can alter light signalling pathways to promote agronomically important traits such as disease resistance (Cerrudo et al., 2017). Tissue or developmental stage-specific targeting of light signalling pathways is another strategy that has been

employed for introducing beneficial traits. In tomato, fruit-specific RNAi mediated suppression of DET1, a negative regulator of photomorphogenic responses that acts downstream in both phytochrome and cryptochrome, resulted in an increase in tomato carotenoid and lycopene accumulation without compromising fruit yield (Davuluri et al, 2005).

The advancement of gene editing technologies allows the possibility of precise modifications of crop genomes through to elicit targeted trait improvements. This has been demonstrated in tomato, in which CRISPR/Cas9 was utilized to specifically target anthocyanin biosynthesis gene, modifying the promoter region with a strong promoter to cause constitutive over-expression (Čermák, Baltes, Čegan, Zhang, & Voytas, 2015). Specific manipulation of genes in a tissue or development-specific manner is possible and could be utilized to target light signalling genes to elicit positive effects without undermining crop yield with negative side effects. With the gene editing technology, the identification of novel gene targets becomes all the more important in realizing the goal of using photobiotechnology to improve crop yield, nutritional value or resilience.

Table 1-1 Summary of phytochrome and cryptochrome gene function studies in different crop species

Gene target	Species name	Phenotype	Reference
PHYB over-expression	*Solanum lycoperiscum*	Dwarfism, reduced anthocyanin content	(Husaineid et al., 2007)
CRY1a silencing	*Solanum lycoperiscum*	SAR phenotype; reduced photosynthesis; increased fruit number and yield; Decreased fruit quality.	(C. C. Liu et al., 2018)
CRY2 over-expression	*Solanum lycopersicum*	Dwarfism, increased pigment content, and delayed flowering.	(Giliberto et al., 2005)
CRY1a over-expression	*Solanum lycopersicum*	Dwarfism; increased pigment content; increased photosynthesis; reduced fruit number and yield; increased soluble sugar and phytonutrient content.	(C. C. Liu et al., 2018)
PHYB silencing	*Solanum tuberosum*	Increased stem length and reduced chlorophyll content.	(Jackson & Prat, 1996)
PHYB over-expression	*Solanum tuberosum*	Semi-dwarfism, reduced leaf area, increased chlorophyll content, increased photosynthesis, increased tuber yield.	(Thiele et al., 1999)
PHYB over-expression	*Solanum tuberosum*	Semi-dwarfism, increased photosynthesis; Increased yield at high densities	(Hernán E Boccalandro et al., 2003)
PHYA over-expression	Ipomoea batatas	Dwarfism, increased chlorophyll content, increased root biomass and yield	(K.-M. Kim et al., 2009).
PHYB silencing	*Oryza Sativa*	Reduced leaf area and stomatal density; increased drought tolerance.	(J. Liu et al., 2012)
PHYA over-expression	*Oryza Sativa*	Dwarfing, increased chlorophyll content, higher tiller number and yield.	(S.-G. Kong et al., 2004)
PHYA over-expression	*Oryza Sativa*	Dwarfing, increased panicles and yield.	(Garg et al., 2006)
CRY2 over-expression	*Oryza Sativa*	Delayed flowering.	Hirose et al., 2006
PHYB over-expression	*Gossypium hirsutum*	Reduced height, increased photosynthesis, increased biomass, increased fruit size, and number	(A. Q. Rao et al., 2011)
PHYA1 Silencing	*Gossypium hirsutum*	Increased yield and fiber characteristics; early flowering.	(Abdurakhmonov et al., 2014)
PHYB2 silencing	*Zea Mays*	Reduced flowering time; redundant control of plant height and stem diameter with PHYB1.	(Sheehan, Kennedy, Costich, & Brutnell, 2007)
PHYA over-expression	*Nicotiana tobaccum*	Suppressed shade avoidance, dwarfism; Increased harvest index at high densities.	(Robson et al., 1996)
CRY1 over-expression	*Nicotiana tobaccum*	Reduced hypocotyl elongation.	Lin et al., 1995
CRY1 silencing	*Brassica napus*	Increased apical growth and anthocyanin accumulation.	(M. Chatterjee et al., 2006).
CRY1 over-expression	*Brassica napus*	Dwarfism, reduced leaf expansion, and increased anthocyanin accumulation.	(Sharma et al., 2014)
CRY1 silencing	*Hordeum vulgare*	Grain dormancy and germination	(Barrero, Downie, Xu, & Gubler, 2014)

Adapted from (Mawphlang & Kharshiing, 2017).

1.6 Transcriptomic studies into light signalling

1.6.1 Transcriptomic studies of light and photoreceptor signalling

Genome-wide transcriptome studies in Arabidopsis have established the primary mechanism through which individual photoreceptors exert control over development including tight control of vast transcriptional networks and coordinating transcription based on changes in spectral quality. Early microarray studies into the effect of light on the transcriptome showed that in Arabidopsis at least 10% of the genome is coordinately regulated by light (Ma et al, 2001). Since then further studies have resolved the transcriptional responses to red and blue light coordinated by the phytochrome (J M Tepperman, Zhu, Chang, Wang, & Quail, 2001; James M. Tepperman et al., 2004) and cryptochrome (Keller et al., 2011; Pedmale et al., 2016) families, respectively. The large differences in global gene expression profile reflects alterations in plant growth and development under different light conditions, and among those differentially expressed genes, those encoding transcription factors are highly over-represented. (Lopez et al., 2012; J M Tepperman et al., 2001).

Several Microarray and RNA-Seq studies in *Arabidopsis thaliana* have revealed differentially expressed genes that are regulated in response to various spectral qualities including low R: FR (L. Li et al., 2012), LBL (Keuskamp et al., 2011; Pedmale et al., 2016) and green light (W, Dhingra, Bies, Lehner, & Folta, 2006). Despite many of the SAR responses elicited by low R: FR or LBL being similar, the transcriptome changes in response to LBL are distinct from those elicited by low R: FR, with little overlap between differentially expressed genes (Pedmale et al., 2016). Most notably, the phytochrome-mediated low R: FR shade avoidance induces the expression of auxin-responsive genes while cryptochrome-mediated LBL does not (Pedmale et al., 2016). However, the cryptochrome-mediated low blue light responses enhanced phytochrome-mediated shade avoidance, and the LBL response requires phyB (de Wit et al., 2016).

1.6.2 Transcriptomic studies of light signalling in crop species

Transcriptome studies have been conducted to understand light signalling pathways/networks in crop species. The re-construction of light signalling networks in

Arabidopsis is undertaken with the aim of translating this knowledge to crop species, comparison between light-regulated global gene expression patterns between Arabidopsis and rice identified that despite qualitatively similar expression patterns being observed, there was a high degree of divergence within the expression of transcription factors, highlighting potential limitations in discovering important regulator components in Arabidopsis (Jiao et al, 2005). Transcriptomic analysis of Norway spruce seedlings under monochromatic red or blue revealed that monochromatic red light promotes stem growth through regulation of gibberellin biosynthesis, whereas exposure to monochromatic blue light enhanced secondary metabolites including antioxidants which protect plant against oxidative stress and defense-related compounds (F. O. Yang, Mao, Wang, Zhang, & Li, 2015). A similar study of grape plants grown under white light or monochromatic red, blue, or green, revealed that growth under monochromatic red or green light elicited shade-avoidance type growth accompanied by the up-regulation of auxin-repressed proteins, and cell-wall modifying xyloglucan-endotransferases (XTHs). Meanwhile, monochromatic blue grown grape plantlets accumulated more chlorophyll and had a corresponding upregulation of pigment biosynthesis genes as well as and a down-regulation of disease-resistance genes (C.-X. Li et al., 2017).

1.6.3 Transcriptomic studies in tomato

Unlike in Arabidopsis, extensive transcriptomic analysis of phytochrome-mediated red light signalling has not been extensively carried out in tomato. Tomato contains five phytochrome genes, designated PHYA, PHYB1, PHYB2, PHYE, and PHYF (Hauser & Pratt, 1997). Mutants either impaired in specific phytochrome genes or over-expressing them have been used to study the roles of phytochromes during tomato development (Husaineid et al., 2007; Weller, Beauchamp, Kerckhoffs, Damien Platten, & Reid, 2001; Weller, Schreuder, Smith, Koornneef, & Kendrick, 2000). Tomato PHYA acts predominately at low irradiances, while PHYB1 and PHYB2 act redundantly, though PHYB1 is the stronger of the two as PHYB2 can only partially compensate for the impairment of PHYB1 (Weller, Beauchamp, et al., 2001; Weller et al., 2000). However, over-expression analysis suggested PHYB2 was the stronger of the two phytochrome B homolog as the transgenic lines showed strong inhibits of elongation, enhanced anthocyanin accumulation and strong amplification

of high-irradiance response to red light whereas over-expression of phyB had only mild phenotypic effects on elongation (Husaineid et al., 2007). Despite these genetic resources, no transcriptomic data of the phytochrome signalling has been published in tomato. However, the molecular mechanisms of red light signalling have been studied in tomato through transcriptomic analysis of the effect of low R: FR induced shade avoidance on global gene expression. The transcriptomes of both leaf and stem tissue of tomato plants grown under low R: FR shade was explored revealing induction of auxin-induced transcription factors SAUR and IAA, as well as cell-wall modifying enzymes XTHs under low R: FR shade, despite no changes in auxin biosynthesis genes of free IAA levels. Meanwhile, photosynthesis was also down-regulated in shade (Cagnola et al., 2012).

The functional roles of individual cryptochromes in light signalling have been studied in tomato using transcriptomics. Tomato contains 4 cryptochrome genes, with a duplication of Arabidopsis CRY1 leading to the presence of two CRY1 genes- CRY1a and CRY1b, as well as CRY2, and the less important CRY3. Studies using *cry* and *phy* mutant background established the contribution of PHYA, PHYB1, and PHYB2 to cry-mediated blue light sensing (Weller et al., 2001). Tomato cryptochromes were active throughout the Tomato lifecycle, regulating processes including de-etiolation, stem-elongation, apical dominance, flowering time, anthocyanin biosynthesis, and chlorophyll content of leaves and fruit (Weller et al., 2001; Giliberto et al., 2005). A recent study of cry1a over-expressing and silenced transgenic lines revealed its regulation of photosynthesis and growth-related genes, and indicated that phytohormones were actively involved in CRY1a mediated control of cell growth and plant development which influences plant architecture and plant productivity (C. C. Liu et al., 2018). Combined hormone profiling and transcriptomic analysis demonstrated GA, JA, and cytokinin content was negatively regulated by CRY1a in tomato, and that core biosynthesis genes of these hormones were transcriptionally regulated in a complementary manner, implicating phytohormone and CRY1a integration as a core component of blue-light signalling in tomato (C. C. Liu et al., 2018). Important light signalling transcription factor HY5 was positively regulated by CRY1a (C. C. Liu et al., 2018). The involvement of cryptochrome 2 in tomato light signalling has been extensively studied on a transcriptomic level using CRY2 over-expressing transgenic line. Cryptochrome 2 was found to be integral for

rhythmic oscillations of circadian-clock related genes under both fluctuating and constant light (Facella et al., 2008). Further investigation by genome-wide expression profiling using microarray in the tomato CRY2 mutant has also revealed its roles in diurnal rhythms, biotic and abiotic stress pathways, and secondary and energy metabolism (Lopez et al., 2012). Recently, transcriptomic analysis of tomato chloroplast genome in CRY2 over-expressing transgenic plants revealed that CRY2 is a master regulator of the chloroplast transcriptome, regulating the diurnal rhythm of transcription of over half the chloroplast genes and promoting photosynthesis-related gene expression (Facella et al., 2017). Not only does CRY2 control chloroplast transcription quantitatively, but some transcripts including rubisco sub-unit rbcL were found to be differentially expressed, implicating CRY-2 in the modification of transcriptional apparatus (Facella et al., 2017). The existing transcriptomic studies of cryptochrome-mediated signalling suggest the blue light has pleiotropic effects of growth and development through cryptochrome-mediated regulation of transcriptome, however in isolation of individual cryptochromes these studies do not necessarily represent the complexity of the inter-connected light signalling networks. Therefore, a complementary study of the effect of spectral quality, particularly blue light on the transcriptome, will yield insight into how individual photoreceptor signalling pathways/networks coordinate the transcription together.

1.6.4 RNA-Sequencing technology overview

Genome-wide expression studies allow the study of the expression patterns of all genes within the genome to identifying genes which are differentially expressed under different conditions or between different tissues or time-points to gain a genome-wide perspective of which genes are activated or repressed to understand the molecular mechanisms behind a cellular response.

The high-throughput sequencing of complementary DNA derived from RNA extracts is called RNA-Sequencing, and this next-generation sequencing technology provides a powerful tool for transcriptomics in which digital expression levels of all transcripts within a pool of RNA can be quantified. **Figure 1-6** is an illustration of the process of library preparation of RNA and subsequent RNA-Sequencing. To describe the process of RNA-Sequencing briefly, a population of RNA is fragmented and the

resulting short reads are converted to a library of cDNA, which is then ligated to sequencing adaptors and subjected to high-throughput sequencing whereby the nucleotide sequence of each short-reads is recorded to provide a file of millions of short read sequences. The raw read sequences are then aligned to a reference genome, or aligned together to produce a *de novo* transcriptome, and the number of short reads which align to exonic regions of a gene is counted to give a digital measure of the abundance of that transcript.

Prior to RNA-Sequencing, microarray technology was utilized to study genome-wide gene expression patterns. Microarray technology is probe-based with tens of thousands of short oligonucleotide probes designed to be complementary to the transcripts whose presence is being investigated, based on knowledge of the organism's genome being studied. Transcripts are extracted from sampled under investigation and labeled with one or two fluorescent dyes and hybridized to the microarray oligo chips, washed and then scanned with a laser, with the intensity of fluorescent signal measured to give the expression level of the transcript bound to the oligo probe.

Over the past decade, the cost of RNA-Sequencing has fallen dramatically, allowing it to become an economically viable alternative to microarrays, and also has several technical advantages. RNA-Sequencing does not rely on pre-designed probes that require existing knowledge of the genome and can, therefore, detect novel transcripts and isoforms. RNA-Sequencing is also better able to detect lowly expressed genes and a smaller difference in gene expression, as microarray suffers technical pitfalls including cross-hybridization and non-specific background signals which contributed to increased noise and limited detection range. The enhanced detection range and ability to detect novel transcripts means that RNA-Sequencing has been utilized to find new insights into old problems, finding novel genes and mechanisms involved in events previously studied with microarray.

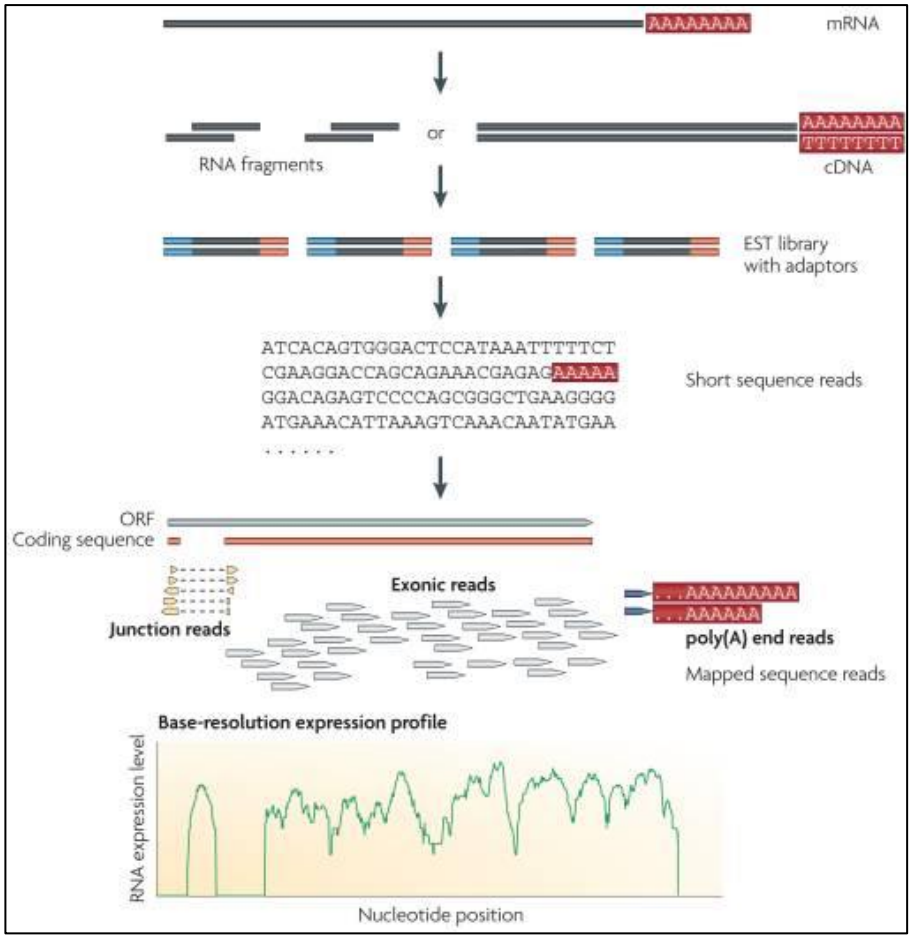


Figure 1-6 Typical RNA-Sequencing workflow from mRNA through library preparation to RNA-Sequencing generation of the expression level of genes. mRNA from the organism of interest is extracted, fragmented and converted into cDNA before being ligated to adapters and sequenced to generate millions of short reads. Short reads are then aligned to a genome and the expression at a base-resolution is calculated for each transcript present. Illustration from (Z. Wang, Gerstein, & Snyder, 2009).

1.7 Tomato is a model species and important crop

1.7.1 Tomato as an important crop

Tomato fruit is highly nutritious, providing health-promoting compounds including minerals and antioxidants including vitamins C and E, lycopene, beta-carotene and flavonoids. Numerous studies have highlighted that tomato consumption can reduce the risks of certain cancers, age-related macular degenerations, and cardiovascular disease, believed to be attributed to their rich source of nutrients (Dorais, Ehret, & Papadopoulos, 2008).

According to national statistics, the UK horticultural industry produced only 18.5% of the tomatoes marketed in the UK, with the vast majority imported from European countries, primarily Spain and the Netherlands. Tomato has been the most imported vegetable to the UK for 30 consecutive years, and in 2017, 18.2% of total vegetables imported into UK (398.8 thousand tonnes) in terms of quantity, and 21.7% of total vegetables imported to UK (£521.8 million) in terms of value, was tomato (Department for Environment Food and Rural Affairs, 2017).

In the UK, commercial tomato production is conducted under protected horticulture in glasshouses. Insufficient sunlight in winter not only affects yield but causes poor fruit setting and slower fruit growth, reducing productivity. Supplemental lighting in protected horticulture accounts for around 15% of energy consumption, and through the adoption of LED lights over less efficiency agricultural lighting, LED light can increase farmer's income and reduce electrical consumption in protected horticulture (S. Y. Lee, Kwon, Park, & Choi, 2014). Night-time supplemental LED inter-lighting increased yield of single-trust tomatoes by 24% in winter, and 12% during the summer (Tewolde et al., 2016).

1.7.2 Tomato as a model species for genetic studies

Tomato is considered a model species for genomic studies. It has a moderately sized genome, is part of the agronomically important Solanaceae family, and has been considered an excellent specimen for study of fruit development, ripening and many other processes (Matsukura et al, 2008). The tomato genome was sequenced in 2012

and is now relatively well-annotated (The Tomato Genome Consortium, 2012). Furthermore, the recent 150+ tomato sequencing project has resulted in the sequencing of over 83 tomato genotypes including 10 wild relatives (Aflitos et al, 2014). This increased understanding of natural variation provides the extraordinary potential for improvement of tomato once molecular markers conferring agronomically important traits have been identified. As mentioned earlier, light-signalling pathways have already been exploited in tomato (Giliberto et al, 2005; Davuluri et al, 2005), and further expanding knowledge genome-wide transcriptomic and network inference analysis could help identify novel regulatory components which can be targeted for improving tomato.

1.8 Aims and objectives of this project

The aim of the project was to investigate the genetic mechanisms of light signalling in tomato, utilising next-generation sequencing transcriptomic analysis and phenotypic analysis to understand the light signal transcriptomic networks which underpin the adaptive responses of tomato to varying spectral qualities, and to identify candidate hub genes in the light signalling network as targets for further gene functional analysis. The specific objectives were:

1. To analyze Micro-Tom growth, photosynthesis, physiological and morphological changes, under different LED light spectra and the effect of spectral quality in tomato.
2. To conduct RNA-Seq transcriptomic analysis in Micro-Tom tomato plants grown under different light qualities in order to identify important regulatory components and key genes involved in the adaptive responses to light and agronomically important traits
3. Investigate the effect of supplemental green light on the transcriptome of tomato to understand how green LED light to regulate tomato plant growth and development.

2 GENERAL METHODS

2.1 Plant materials and general growing conditions

For all experiments conducted in the project, *Solanum lycopersicum* c.v Micro-Tom plants were grown in a controlled environment with growth conditions maintained at a temperature of 25ºC/20ºC (day/night), and relative humidity ~60%. Within the growth room, isolated chambers were set-up containing their own light sources, either LED or fluorescent tube lighting (See **2.2** for a detailed description of light sources used) and completely covered with polyethylene sheeting to prevent light contamination between chambers. Light intensity throughout all experiments was maintained at 200µmol m^2 s^{-1} PPFD as measured at the top of the canopy using a light meter (Li-250A; Li-COR, Lincoln, Nebraska, USA) and adjusted weekly to account for growth. The photoperiod throughout all experiments was of 16h/8h (day/night). Seeds were sown in 13cm diameter 1L pots containing M3 Levington soil (Levington Horticulture Ltd, Suffolk, UK) and germinated in darkness, upon emergence seedlings were placed into the chamber and subject to the light conditions as described in the methodology in each chapter in detail.

2.2 LED lights

2.2.1 Comparison of the spectral distributions of LED and fluorescent lights

Two different models LED lights, were used in this experiment, as well as a broad-spectrum fluorescent tube lighting (UNIGRO- model: 12/634, Kent, UK). The two LED lights were Heliospectra (Heliospectra AB, Goteborg, Sweden) model RX30 and L4A, designed for research, programmable to emit nine and seven wavelength channels, respectively. Both models included wavelength channels 450nm, 530nm, and 660nm which were the only channels used throughout this project.

To understand any differences between the lighting systems, the spectral distribution of the two Heliospectra LED models in the red (660nm), blue (450nm), and green (530nm), regions, as well as the fluorescent tube lighting, were evaluated (See **Figure 2-1**). The two Heliospectra LED models RX30 (LED1) and L4A (LED2) give out virtually identical emissions within the red and blue spectrum, with peak emissions at 449nm and 661nm for LED1 compared to 444nm and 658nm for LED2, respectively. In the green spectrum, the shift is more substantial with LED1 emitting at 520nm compared to 529nm for LED2. The fluorescent tube lighting emits the highest peak is red light (45%), followed by green (36%), with a small emission in the blue (14%) region of the spectrum.

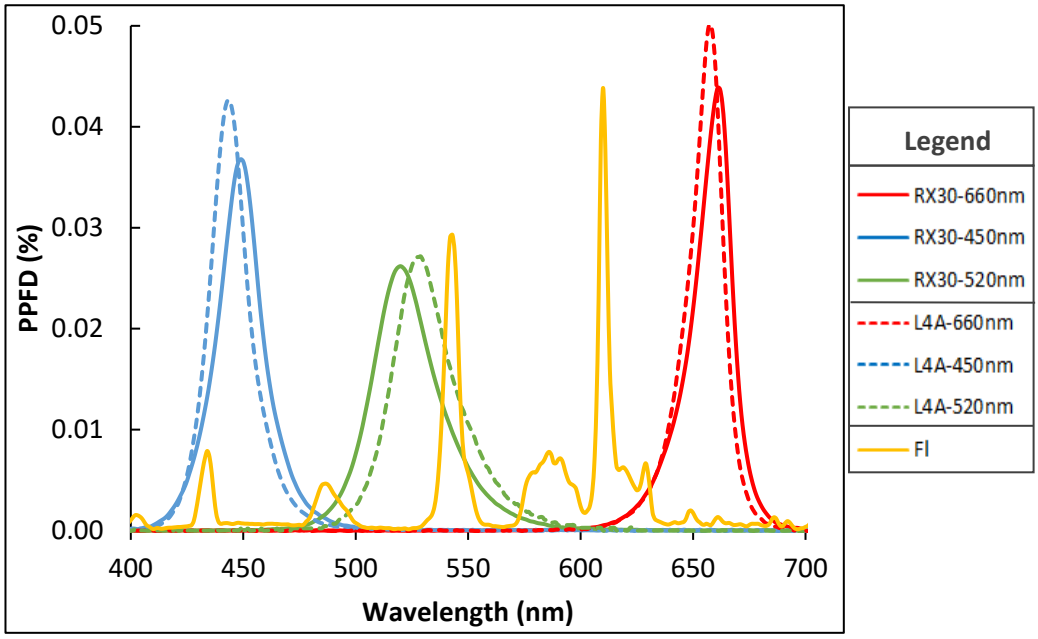


Figure 2-1 Comparison of spectral distribution of two LED light lamps and fluorescent light tube. Light intensity was measured at every nm, represented as a percentage of total light (PPFD) measured at 1nm intervals. Each LED channel was measured individually. LED lamp models are Heliospectra RX30 (solid, except yellow) and L4A (dotted). Fl, fluorescent tube lighting (solid yellow).

2.2.2 Spectral distribution of LED lights used for chapters 3,4, and 5

The spectral distribution of the LED lights used for both the phenotyping in CHAPTER 3, RNA-Seq in CHAPTER 4, and gene expression time course in CHAPTER 5 was measured using the ASD spectroradiometer (ASD FieldSpec HandHeld 2; Analytik Ltd, Cambridge, UK). The relative spectral distribution of

different wavelengths for each treatment are displayed in **Figure 2-2**. The peak emission of the red, blue and green are at 661nm, 449nm, and 520nm, respectively. The RB treatment had 7:3 distribution of red: blue (70% R and 30% B), while RBG has 7:3:1.5 distribution of red: blue: green (61% R, 26% B, and 13% G). Although the Fl light is broad spectrum, it has 3 major, peaks: the highest emission is within the red region (44%), followed by green (35%), with a relatively small portion blue (14%) and others (7%). Notable in this that the ratio of R:B:G is 5: 1.6: 4.9, with the ratio of B:G is very low at 0.39.

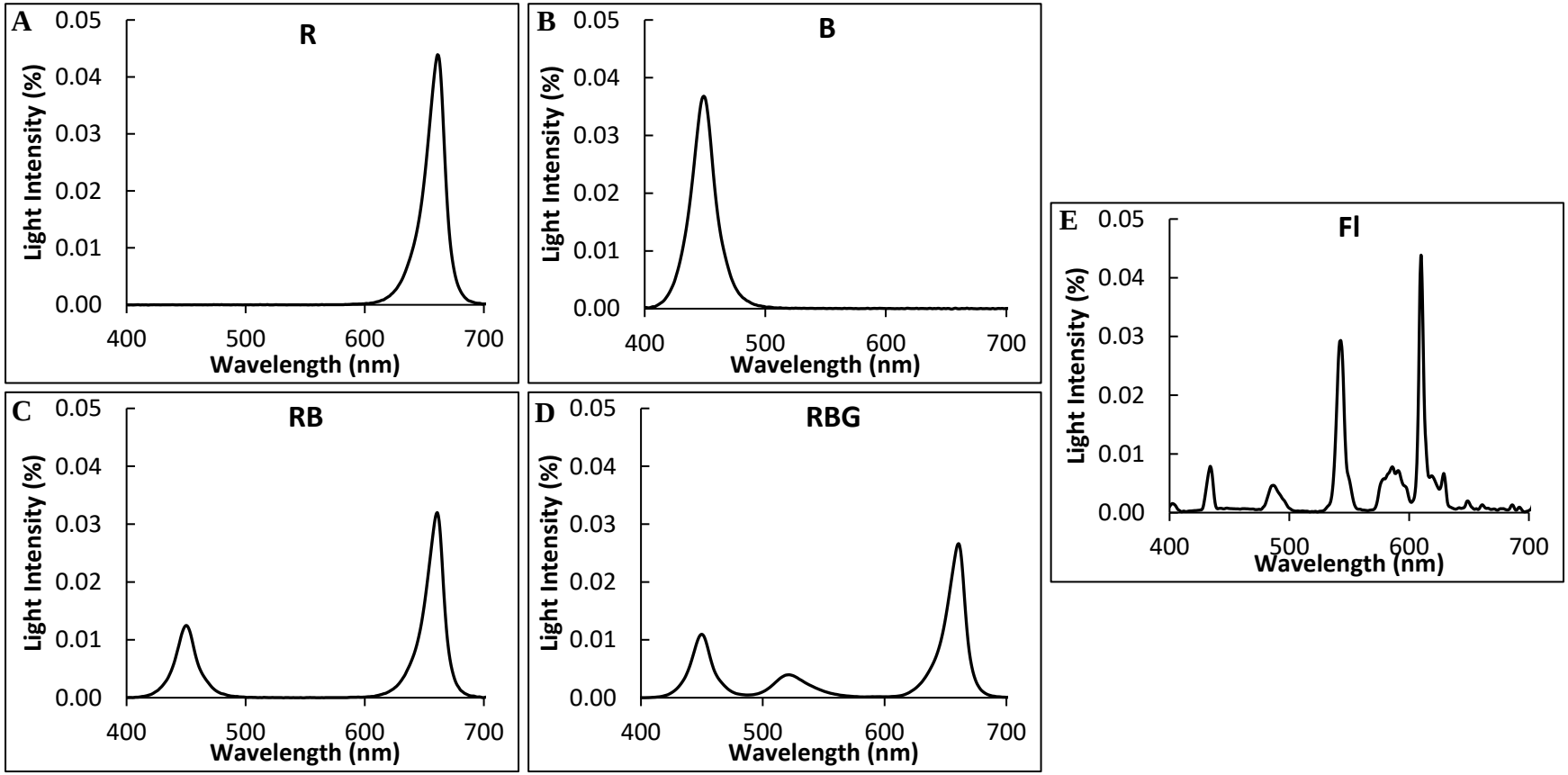


Figure 2-2 Spectral distribution of light treatments. A, Monochromatic red LED light; B, Monochromatic blue LED light; C, Mixed 7:3 red and blue LED light; D, Mixed 7:3:1 red, blue and green LED light; E, Fluorescent tube lighting. Light intensity (PPFD) was measured at every nm, represented as a % of total light measured at each nm of the total light measured between 400-700nm. Measuring spectral distribution of light sources

The spectral distribution of light source emitting all combinations of different light treatments used throughout this the project was measured using a spectroradiometer at a 1nm resolution. Irradiance measurements for each wavelength were converted into photosynthetic photon flux density (PPFD) using **Equation 2-1**. The relative proportion of light measured at each wavelength relative to the total light emitted within the photosynthetically active radiant (PAR) portion of the visible light spectrum was then calculated to normalize measurements because the light intensity was not controlled during spectral distribution measurements.

$$E_{QF}\ (\boldsymbol{umol\ m^2 s^{-1}}) = \frac{\boldsymbol{I}}{\left((\boldsymbol{\lambda} \times \boldsymbol{10^{-9}}) \div (\boldsymbol{h} \times \boldsymbol{c})\right)} \div (\boldsymbol{N_A} \times \boldsymbol{10^6})$$

Equation 2-1 Conversion of irradiance (watts/m^2) to photon flux density (µmol m^2 s^{-1}). E_{QF} is photon flux density (µmol m^{2}s^{-1}); I= irradiance (watts/m^2); λ is wavelength in nm; h= Planck's constant (J/s); c= speed of light (m/s); $N_{A=}$ Avogadro's number.

2.3 Total RNA extraction

RNA extraction was by the Phenol-chloroform method using Trizol® (Thermo Fisher Scientific, Carlsbad, CA, USA) and carried out according to manufacturer instruction. Frozen leaf tissue (treated with liquid nitrogen) was moved from -80^{o}C freezer and stored until homogenization. The frozen leaf material was homogenized into a fine powder using a pestle and mortar with liquid nitrogen, and 100mg of the leaf powder was then transferred into a 2mL Eppendorf tube. Immediately after homogenization, 1mL of cold Trizol® reagent was added to the ground sample and left to incubate for 5minutes. Following incubation, phase-separation of RNA from other cellular components was undertaken using chloroform. 0.2mL of chloroform was added to the Eppendorf tube, shaken vigorously and left to incubate for two minutes, after which it was centrifuged for 15minutes at 12,000-x g at 4^{o}C. Following centrifugation, the upper-aqueous phase (approximately ~450ul), which contains the isolated RNA, was carefully transferred by pipetting into a fresh Eppendorf tube. To improve purity, the phase-separation process was repeated again on the isolated upper-phase as described above. The RNA was precipitated by adding 0.5 mL of 100% isopropanol to the aqueous phase and incubating for 10 minutes. After incubation, the mixture was centrifuged for 10 minutes at 12,000-x g at 4^{o}C, and the

supernatant discarded. The RNA pellet was washed by adding 1mL of 75% ethanol, vortexed briefly, and centrifuged for five minutes at 7,500-x g at 4^{o}C. The supernatant was then discarded and the pellets left to air dry for five minutes, after which point the isolated total RNA was re-suspended into 50 uL of RNase-free H_20, and then re-solubilized by heating to 55^{o}C for 10minutes.

RNA-cleanup

The RNA was then further purified using the RNeasy® MiniElute™ Cleanup kit (Qiagen), according to the manufacturer's instruction. The extracted RNA was adjusted to a volume of 100ml with RNase-free water, 350 µL of Buffer RLT was added, and mixed further by pipetting. 250 µL of 100% ethanol was added to the diluted RNA, mixed thoroughly, and immediately added to an RNeasy MiniElute Spin Column (Qiagen) inside of a 2ml collection tube. The tube was centrifuged for 15 seconds at 8000xg, and the flow-through discarded. The spin column containing the bound RNA was then transferred into a fresh collection tube and 500 µL of Buffer RPE added to the spin column, after which the tube was centrifuged again for 15 seconds at 8000xg. After discarding the flow-through, the spin column was washed with 500 µL 80% ethanol and centrifuged for two minutes at 8,000xg to dry the silica membrane. The spin column was transferred into a new 2mL collection tube and air dried by centrifuging for two minutes at 8,000xg with the spin column lid open. Finally, the purified RNA was eluted by adding 20µL of RNase-free water and spinning for one minute at maximum speed.

Immediately following RNA clean-up, DNase digestion was undertaken on RNA samples to remove any DNA contamination that may be present using the 'DNase I, RNase-free' kit according to the manufacturer's instruction (Thermo Scientific, Carlsbad, CA, USA). Into an RNase-free PCR tube, 1µg of RNA, 1µL 10x reaction buffer with MgCl2, and 1 µL 'DNase I, Rnase-free' was added, and then made up to 10µL with DEPC-treated water. The RNA-DNase mixture was incubated at 37^{o}C for 30 minutes to activate DNase. Following incubation, the DNase was inactivated by adding 1 µL of 50mM EDTA to the RNA and incubating at 65^{o}C for 10 minutes. The purified DNase-free RNA samples were then stored at 80^{o}C until further use.

2.3.1 Determination of RNA concentrations

A NanoDrop spectrophotometer was used to measure RNA concentration of each total RNA extract. Before concentration was determined, the NanoDrop was calibrated against a reference of 1µL of distilled water. The distilled water was wiped away with a tissue and samples concentration and purity was determined by adding a 1µL sample onto the NanoDrop. The concentration (ng µL), A_{260}, A_{280}, A_{230} were recorded. The samples were assessed for contamination by calculating A_{260}/A_{280} and A_{260}/A_{230} with a ratio of >1.8 indicating sufficient purity. For samples to be sent for RNA-Seq quantification. The RNA integrity was quality assessed using the BioAnalyzer (Agilent Technologies, Santa Clara, California, USA), with a RIN value above 7 considered sufficiently high-quality to be used as RNA samples for RNA-Sequencing or qRT-PCR determination of gene expression levels..

2.4 RNA-Sequencing processing and bioinformatics

2.4.1 RNA extraction and libraries prep for RNA-Sequencing

For both RNA-Seq experiments in **Chapter 4** and **Chapter 6**, the same general procedure was followed. For each of the treatment condition, three replicate RNA samples were prepared, each containing the pooled RNA of two leaves taken from two independent plants. Total RNA extraction was performed using TRIzol® and according to manufacturer's instructions (Life Technologies, Carlsbad, California, USA), followed by RNA clean-up using Qiagen RNA plant mini-kit (Qiagen, Hilden, Germany). 3µg of total RNA from each sample was sent to the Wellcome Trust genomics centre (Oxford, UK) where RNA samples underwent mRNA enrichment by polyA selection, and barcoded libraries prepared using Illumina's TruSeq Stranded Total RNA Library Prep Kit (Illumina, San Diego, California, USA). The libraries were then pooled and sequenced at 75bp paired-end on 1 lane on the HiSeq4000 (Illumina, San Diego, California, USA).

2.4.2 Mapping of Illumina reads

Following sequencing, raw fast-QC files were quality-assessed using, and then reads trimmed using Sickle and Scythe (Joshi and Nash, 2011). Reads were aligned to *Solanum lycopersicum* SL2.5 reference genome using HISAT2 (D. Kim, Langmead, & Salzberg, 2015). The technical replicates were merged using SAMtools (H. Li et al., 2009), and gene level counts were generated using HTseq (Simon Anders et al, 2014). The pipeline itself was provided by Tom Giles (ADAC, University of Nottingham).

2.4.3 Quality assessment and unsupervised analysis

For quality assessments of transcriptomic data, library normalized count data for each sample was processed using R package Noiseq. Gene length, GC content, and gene biotype information for *Solanum lycopersicum SL2.5* was downloaded from BiomaRt Plant. Sensitivity plots were generated comparing the distribution of read counts among different biotypes. CPM distribution was compared against GC content and length to assess the transcriptome data for bias.

2.4.4 PCA + Hierarchical clustering

Log-normalized count-per-million (CPM) data for all expressed genes were used to conduct PCA and hierarchical clustering. The R package *limma* (Phipson, Lee, Majewski, Alexander, & Smyth, 2015) function prcomp() for Principal Component Analysis (PCA). A distance matrix was calculated using Euclidean distance and hierarchical clustering of samples computed using the hclust() function Hierarchical clustering.

2.4.5 Differential expression analysis (EdgeR)

The EdgeR Bioconductor package v3.14 (Robinson, McCarthy, & Smyth, 2009) was used to call differentially expressed genes (DEGs) and was run using R v3.3.0 (R core team, 2016). Count data was first normalized to account for differences

in library size, and then filtered to remove genes in which the counts per million (CPM) was below one, in at least 3 samples. To test for between-samples variations, Principal component analysis (PCA) was conducted on all samples, based on the regularised-log transformed count filtered and normalized count data, followed by hierarchical clustering performed based on the Euclidean distance between samples. Gene-wise dispersion estimates were calculated and a negative binomial (NB) general linear model (GLM) was used to fit a log-linear model for each gene. Likelihood ratio testing was used in a pair-wise manner to test for differential expression between all treatments combinations.

2.4.6 Gene-Set Enrichment Analysis (GSEA)

Both GO and KEGG enrichment analyses were conducted using GOStats package in R. Genes were annotated with GO terms using Ensembl biomaRt R package (Durinck et al., 2005), and KEGG annotations with the KEGG.db (Carlson, 2016) R package. The Hyper-geometric test for significant enrichment in terms relating to Biological process, Molecular Function and Cellular Compartment were investigated for differentially expressed gene sets identified by EdgeR pair-wise comparisons and compared against the background list of all genes found to be expressed in our experiment. Pathview R package (Luo & Brouwer, 2013) was then used to visualize KEGG metabolic maps and overlay expression data to visualize pathways of interest.

2.5 qRT-PCR

2.5.1 cDNA synthesis

The DNA-free RNA samples were diluted to a concentration of 200ng/uL^{-1} using DEPC-treated water. The SuperScript™ IV First-Strand Synthesis kit was used for cDNA synthesis according to the manufacturer's instructions. Briefly, for annealing of primer to RNA a mixture containing: 1µL 10mM dNTP mix, 1µL random hexamer primer (50ng/µL), 6µL of DEPC-treated water was made, to which 5µL of sample RNA (200ng/µL) was added and mixed gently pipetting up the mixture

and down several times. The RNA-primer mix was heated at 65ºC for five minutes, and then immediately incubated on ice for two minutes. The reverse transcription reaction mix containing: 4µL SSIV Buffer (Invitrogen), 1µL 100 mM DTT, 1µL Ribonuclease Inhibitor (40U/µL), and 1µL SuperScript™ IV Reverse Transcriptase (200 U/µL) was then added to the annealed RNA, and the combined reaction mixture was incubated at 55ºC for 10 minutes. The stock cDNA produced was stored at -20ºC and working concentrations were 1/10 diluted with RNase-free H_2O and also stored at -20ºC.

2.5.2 qRT-PCR analysis

SYBR green qPCR was run on a LightCycler480™ system (Roche, Applied Science, West Sussex, UK). The PCR reaction contained 2 µL cDNA, 5µL 2x SyBR Green PCR Master Mix (Life Technologies), 0.1µL of 10mM forward primer, 0.1 µL of 10mM reverse primer, and 2.8 µL of RNase-free water to give a final volume of 10 uL. Two technical replicates were used per cDNA sample, and three biological replicates per treatment. Standard curves for each gene were run concurrently. The PCR conditions consisted of initial denaturation step at 95ºC for 5 minutes, followed by 40 cycles of: denaturation at 95ºC for 10 seconds, annealing at 60ºC for 15 seconds, and extension for 20 seconds. Standard curves were used to calculate relative mRNA concentrations, and the normalized Ct (cycle threshold) value was generated using the "Abs. Quant Analysis" LightCycler480 software (v1.5). Relative gene expression was calculated using the $2^{-\Delta\Delta CT}$ method corrected for actual primer efficiencies, with target gene expression normalized against house-keeping gene (X. Rao, Huang, Zhou, & Lin, 2013).

$$2^{-\Delta\Delta CT} = Pe^{-(\Delta CT(target\ sample)-\Delta CT(reference\ sample))}$$

Equation 2-2.Relative quantification of expression from qPCR Ct thresholds. Where CT= is threshold cycle; ΔCT is the difference in threshold cycle between target gene-reference gene; and Pe is the primer efficiency (X. Rao et al., 2013).

2.6 Primer design and efficiency

Oligonucleotide primers were designed specifically for each gene using Primer-BLAST program (NCBI), ensuring that each primer was specific only to the target gene, and synthesized by Sigma. Upon arrival, primers were diluted according to the manufacturer's instructions and stored at -20^{o}C. Stock concentrations were diluted 1/10 with sterile H_20 to give working concentrations, and stored at -20^{o}C.

The amplification efficiency of each primer set was determined by calculating the standard curve of Ct against cDNA input. cDNA from multiple samples was pooled together and serial diluted 5-fold four times, to generate 1,5,25,125,625 times diluted cDNA. For each dilution of cDNA, two technical replicates were made and qPCR was carried out as described above to determine the Ct value. Individual primer efficiency was then calculated as by plotting the Ct value versus the dilution factor to a straight line in a base-10 semi-logarithmic graph and determining the slope and correlation efficiency (R^2) of the straight line. The R^2 was used as a quality check, with >0.99 required before primer efficiency was calculated. Primer efficiency was then calculated using **Equation 2-3** as described by Ramakers and colleagues (Ramakers, Ruijter, Lekanne Deprez, & Moorman, 2003). Primer efficiencies below 80% or above 120% were not tolerated, and new primer sets were generated instead.

$$Pe = 10^{\left(\frac{-1}{slope}\right)}$$

Equation 2-3 Primer efficiency calculation. Pe is primer efficiency; the slope is the slope of the linear regression of Ct vs log10 cDNA input. (Ramakers et al., 2003)

3 PHENOTYPING MICRO-TOM GROWN UNDER VARYING LED SPECTRA QUALITIES

3.1 Introduction

Light is the most important parameter for plant growth and development. In addition to light intensity, spectral quality is a strong determinant of crop yield, as plant photoreceptors regulate agronomically important traits including plant architecture and resource allocation, pigment metabolism, photosynthesis, and phototropism. The advent of narrow-waveband LED lighting technology has enabled the possibility of using precise control of spectral quality to manipulate plant growth in a way that is not possible with standard horticultural light sources. In controlled environment agriculture, where the sole-source of light is from artificial lighting, spectral quality of light can be precisely controlled and optimized to influence time to harvest, maximize yield and improve nutrient quality. Through understanding the traits regulated by light quality, not only the potential to optimize the spectral distribution of light supplied to plants at varying stages of development to maximize yield but also could permit the identification of molecular markers associated with beneficial traits which could be targeted for crop breeding.

Previous studies on agronomically important traits have identified that photoreceptors and light signalling influence productivity-related traits such as biomass production, growth, development, and metabolism. Phytochromes not only regulate photomorphogenic responses but also pigment accumulation, photosynthesis, biomass accumulation, and resource allocation through altering primary and secondary metabolism (D. Yang, Seaton, Krahmer, & Halliday, 2016). Exposure to a low irradiance of blue light leads to dwarfism through inhibition of internode elongation in petunia, rose (Terfa et al., 2012), cucumber (Cosgrove., 1981), lettuce (Hoenecke et al., 1992), and tomato (Giliberto et al., 2005). Blue light also controls leaf hyponastic movements and phototropism which allows the plant to optimize light interceptions, as well as regulating stomatal opening which controls transpiration and CO_2 uptake. Moreover, in tomato, both *CRY1a* and *CRY2* over-expressing plants exhibit dwarfism, increased pigment accumulation, while the latter plants also have

delayed flowering (Giliberto et al., 2005; C. C. Liu et al., 2018). Together these cryptochrome-mediated blue light signals are able to control plant morphology and physiology, altering fundamental plant processes which could be considered important for maximizing plant yield.

The effects of varying spectral qualities of supplemental light supplied by LEDs in a greenhouse on tomato has been previously studied. Combinations of red, blue, and green light and white LED lights did not influence tomato yield, biomass accumulation or photosynthesis in tomato variety Bonny Best, although water use efficiency was reduced under red-blue LED lighting compared to HPS (Lanoue, Leonardos, Ma, & Grodzinski, 2017). While greenhouse studies using LEDs as supplementary lighting are informative, using LEDs as sole-source lighting allows precise control of the light environment enabling the photobiological study of the adaptive response of plants to spectral quality.

In controlled environment conditions using LEDs as sole-source lighting, the study of effects of spectral quality on tomato has been limited to young plants. A study of growth and photosynthesis of young cherry tomato plants (var. *cerasiforme*) under monochromatic and mixed combinations of monochromatic and mixed wavelengths of LED lighting compared to a fluorescent tube control (Liu Xiaoying, 2012). Liu and colleagues (2012) reported that after tomato seedlings grown under monochromatic red, green or orange LEDs exhibited shade avoidance related phenotypes including substantially increased height and specific leaf area compared to those grown under mixed LED lighting. Despite having reduced maximum photosynthetic rate and no difference in photosynthetic efficiency, Liu (2012) also reports the monochromatic blue grown cherry tomato seedlings to have a significantly increased quantum yield of photosynthesis and correspondingly an increased biomass compared to mixed LED grown seedlings despite having significantly reduced maximum rate of photosynthesis.

While the study of tomato seedlings enables the identification of traits regulated by light, whether these effects are transient, whether other developmental traits emerge later in plant development, and to what extent spectral quality influences fruit yield and quality are not currently understood. This is likely due to the large size of mature tomato plants making the growth of tomato under sole-source lighting

impractical. The Micro-Tom tomato cultivar is a dwarf variety that has been identified as a model system for genetic studies. Introgression of disruptive hormonal and light signalling mutations including those auxin (*diageotropica, dgt*), ethylene (*never-ripe, nr*), gibberellin (*gib1-3; pro*) and brassinosteroid *(curl 3; cur3*) and light (*Aurea; high-pigment2*) induce comparable phenotype between Micro-Tom to commercial tomato varieties, meaning Micro-Tom can be used for plant developmental research which can then be applied to commercial varieties (Carvalho et al., 2011). In addition to this, owing to its compact size, it is ideal for the study of the effects of spectral quality on tomato, as it can be grown within small compartments.

The aim of this chapter is to characterize the effects of spectral quality on Micro-Tom growth, development, yield and agronomically important traits. In the controlled environment growth room, isolated compartments completely covered to prevent light contamination have been set-up with Heliospectra LED lights (Heliospectra AB, Goteborg, Sweden) programmable to emit desired proportions of 11 different wavelengths of light. Micro-Tom plants will be grown under monochromatic red, monochromatic blue, a mixture of red/blue, red/blue/green, and compared fluorescent tube lighting from germination to harvest, revealing the effect of spectral quality on yield in tomato, while physiological and photosynthetic measurements characterize the adaptive responses of tomato to light.

3.2 Methods

3.2.1 Plant materials and growth conditions

Solanum lycopersicum c.v Micro-Tom plants were grown in a Phytotron controlled environment growth room under artificial light, at a fixed light intensity of 200µmol m^2 s^{-1} PPFD with a photoperiod of 16h/8h (day/night), the temperature was maintained at 25ºC/20ºC (day/night), relative humidity at ~60%, and water bi-weekly. Seeds were sown in pots containing M3 Levington soil (Levington Horticulture Ltd, Suffolk, UK) and germinated in darkness, upon emergence seedlings were placed under treatment conditions. Thirty plants were divided into five treatment groups, which differed in spectral quality output by artificial light. The first four treatment groups were grown under Heliospectra^{TM} LED lights (Heliospectra AB, Goteborg, Sweden) emitting either: monochromic red light (R) (R 100%); monochromic blue (B) (B 100%); dichromic red and blue (RB) (R 70 %: B30%); or the fourth LED group was an adjustment to the RB group to include a small portion of green light (RBG) (R= 63 %: B= 27 %: G= 10%). Peak wavelengths emitted from Heliospectra LED lights were blue (450nm), green (550nm) and red (660nm). The fifth treatment group was a broad-spectrum fluorescent tube light source.

3.2.2 Morphological measurements

Micro-Tom plants were grown for 93 days post-emergence. Light levels were adjusted according to growth every week to ensure a fixed light intensity of 200 µmol m^2 s^{-1} PPFD at canopy level for each treatment. Plant height, leaf number, flower number, and fruit number, were measured/counted weekly. At harvest, height and petiole length measurements were taken with a ruler and measured from the soil to the top of the canopy, and from the stem along the petiole until terminal leaflet, respectively. Leaf number, flower number, and fruit number were counted every week. For biomass measurements, all fruits were harvested, leaves were separated from petioles, and fresh weight of fruit, leaves, and combined stem and petiole (considered as a stem) materials were measured separately. Fresh leaves were then immediately taken for leaf area measurements using the LI-3000C area meter (LI-COR, Lincoln, Nebraska, USA), with every leaf from each plant processed in the

machine and the total leaf area per plant calculated. Fruit, stem, and leaf material were then dried in an oven for 72 hours at 70°C and weighed to measure the dry weight of each portion of the plant. Specific leaf area (SLA) which is the ratio of leaf area to dry mass of leaf material was calculated for each plant.

$$SLA\ (cm^2/g) = total\ leaf\ area\ (cm^2) \div total\ leaf\ dry\ weight\ (g)$$

Individual fruit weight and number were measured. Five fruits per plant were taken and total soluble sugar content was measured using a refractometer, with the tomatoes crushed and juices collected and filtered, before being measured.

3.2.3 Photosynthesis analysis and chlorophyll measurements

LI-COR gas exchange and chlorophyll fluorescence

Gas exchange and chlorophyll fluorescence of leaves were measured with a portable gas exchange system head (LI-6400xt, LI-COR, Lincoln, NE, USA) with leaf chamber fluorimeter (LCF 67400-40, LI-COR, USA). Measurements were taken on one leaf per plant and five biological replicates were carried out. A single leaflet from the third mature leaf was inserted into the chamber and allowed to acclimate at 1000µmol $m^{-2}s^{-1}$ until both A and stomatal conductance (Gs) stabilized. Then, a light curve was then performed, measuring photosynthetic assimilation of CO_2 (A) and chlorophyll fluorescence at 11 light intensities (0, 50, 100, 200, 300, 500, 750, 1000, 1300, 1600, 2000 µmol *photon* m^{-2} s^{-1}; 90% 620nm: 10% 450nm)), from high to low with up to 2 minutes acclimatisation time. LI-COR system temperature was maintained at 25°C, with a flow rate of 400µmol m^2, and CO_2 concentration of 400µmol m^{-1}. Minimal fluorescence yield (F'_o), maximal fluorescence yield (F'_m), and fluorescence yield (F_t) were recorded at the same point, and used to calculate: Photochemical quenching (qP), quantum yield of PSII (Φ_{PSII}), the maximum efficiency of PSII photochemistry in the light, if all centers were open (F_v'/F_m'), and electron transport rate (J), adjusted using absorption measurements taken using integrating sphere, were calculated as described by Murchie and Lawson (Murchie & Lawson, 2013).

Fluorcam chlorophyll fluorescence measurements

The chlorophyll fluorescence induction kinetics of whole plants dark-adapter for 40minutes was measured using the kinetic imaging fluorimeter (Fluorcam, Photon System instruments Ltd., Brno, Czech Republic). Briefly, the plants were placed inside the chamber, and chlorophyll fluorescence measurements were recorded every two minutes. Inside the chamber, red LED lights were set to a light curve program, increasing from 0-100% intensity (100% intensity was recorded to be 1380 µmol m^2s^{-1} at top of canopy). The program was set to increase in 6 light intensities: 0%, 10%, 20%, 40%, 80%, 100%, with light intensity increasing every two minutes, and chlorophyll fluorescence measurements record at each interval. After the collection of the chlorophyll fluorescence measurements, the analysis was conducted using the Fluorcam7 software, with measurements from 5 flat leaves per plant used to determine average per plants, with 5 biological replicates per treatment used to get a within treatment average. Measurements of qP, NPQ,Fv'.Fm', and ETR was automatically computed by the Fluorcam7 software from raw fluorescence values.

3.2.4 Measurement of leaf optical properties

Fresh leaf tissue samples were harvested and immediately placed on ice. Leaf transmittance and reflectance of the adaxial surface of each leaf were measured throughout the 350-1050nm spectrum using spectroradiometer (model: ASD handheld 2) attached via fiber optic cable to an integrating sphere (model: Li1800, LI-COR) according to the Li-1800 manual ((LI-COR, 1989)). Leaf absorption was then calculated at a 1nm resolution from reflectance and transmittance data **Equation 4**. Absorption over different portions of the visible light spectrum were calculated by averaging the absorption across the wavelengths, including: Photosynthetically Active Radiation (PAR) = 400-700nm; violet = 400-454nm; blue = 445-492nm; green = 493-577nm; yellow = 578-597nm; orange = 597-620nm; red = 621-700nm. 5 biological replicates were taken for each treatment, leaf absorption within each other the aforementioned spectral ranges were analyzed by one-way ANOVA and Tukey-post-hoc test for significance ($p<0.05$).

$$Absorptance = 1 - (reflectance + transmittance).$$

Equation 4 Calculation of absorptance from reflectance and transmittance measurements.

3.2.5 Pigment content analysis

Leaf chlorophyll and carotenoid extraction

Leaf chlorophyll and carotenoid pigment content were quantified through pigment extraction and spectrophotometric quantification. 300mg of fresh leaf tissue was weighed. , The leaf tissue with liquid nitrogen was homogenized with a pestle and mortar and then directly transferred into cold 15mL falcon tube, which was immediately frozen in liquid nitrogen. 5mL of 80% acetone was added to the Falcon tube and left to shake in the dark for 30minutes. Following the extraction, the falcon tube was centrifuged at 3,000 x g for 15 minutes at 4^{o}C. The supernatant was collected in a fresh Falcon tube and the extraction in acetone and centrifugation steps were repeated another two times, pooling the supernatants. The collected supernatant was mixed thoroughly and analyzed spectrophotometrically by measuring the absorbance (A) of the solution at an optical density (OD) 480nm, 663nm, and 645nm, blanked against 80% acetone reference. Chlorophyll-a, chlorophyll-b, total chlorophylls, and carotenoid and xanthophyll contents were then estimated using Equation 5 as established by Ni and colleagues (Z. Ni, Kim, & Chen, 2009).

$$Chla\left(\frac{mg}{g}\right) = [12.7 \times A663 - 2.69 \times A645] \times \left[\frac{V}{1000}\right] \times W \qquad (A)$$

$$Chlb\left(\frac{mg}{g}\right) = [22.9 \times A645 - 4.86 \times A663] \times \left[\frac{V}{1000}\right] \times W \qquad (B)$$

$$Chlab\left(\frac{mg}{g}\right) = [8.02 \times A663 + 20.20 \times A645] \times \left[\frac{V}{1000}\right] \times W \qquad (C)$$

$$Car + Xan\left(\frac{mg}{g}\right) = [5.02 \times A480] \times \left[\frac{V}{1000}\right] \times W \qquad (D)$$

Equation 5. Equations for spectrophotometric estimation of chlorophyll-a, chlorophyll-b, chlorophylls-a+b, and carotenoid and xanthophyll content from leaf tissue samples. Equation (A) is for chlorophyll-a, equation, equation (B) for chlorphyll-b, equation (C) for total chlorophylls-a+b, equation (D) for total carotenoids and xanthophyll content. Chla =chlorophyll-a; Chlb = chlorophyll-b; Chlab= Chlorophyll a+b; Car+Xan= combined carotenoid and xanthophyll; V= volume (mL); W= weight (mg). Ax= Absorbance at ODx.

Anthocyanin pigment extraction

Anthocyanin contents were estimated spectrophotometrically. 1000mg of fresh leaf material accurately weighed and immediately frozen with liquid nitrogen, homogenized using a pestle and mortar, and transferred into a 2ml cold Eppendorf tube. 0.5mL of acidified methanol (w/ 1% HCl) was added and the Eppendorf tubes were left overnight to extract at 4^{o}C shaking at in darkness. The following morning (approximately 16 hours), 0.35mL of distilled H_20 and 0.5mL of chloroform was added to the Eppendorf tubes, which were then vortexed and left for 2 minutes for phase separation to occur. The mixture was then centrifuged at 13,000x g for 5 minutes. The upper phase was extracted, being careful not to remove any of the lower phase, and placed into a fresh Eppendorf tube. The upper phase was then analyzed spectrophotometrically, by measuring A at OD 530nm and 657nm. Relative anthocyanin contents were then calculated using the following equation, with A_{657} compensating for any possible chlorophyll contamination, using. Equation 6 also used by Gilberto and colleagues (Giliberto et al., 2005).

$$Anth\left(\frac{mg}{g}\right) = [A530 - A657] \times 1000$$

Equation 6 Equations for spectrophotometric estimation of anthocyanin content from leaf tissue samples. Anth= Anthocyanin; Ax= Absorbance at ODx.

3.3 Results

3.3.1 Plant growth analysis at vegetative stage

To characterize the effect of spectral quality on Micro-Tom plant growth during the vegetative stage, Micro-Tom plants were grown under varying spectra from emergence throughout vegetative phase until 25 days after emergence (DAE), at which point and physiological and destructive measurements were carried (See **Figure 3-1**). Significant differences in plant height were observed between the light treatments (See **Figure 3-1A**). Shade avoidance responses typified by increased apical dominance are characteristic responses to spectral quality. Micro-Tom grown under R light were significantly taller than plants grown under any other light quality, 76%, 78%, 60%, and 30% taller than B, RB, RBG, and Fl, respectively. Plants grown under Fl were significantly taller than all other groups except R, which was 30% taller. The difference in plant height between B, RB, and RBG was minimal although significant between RB and RBG grown plants. Leaf number did also vary Micro-Tom under different light qualities during the vegetative stage (See **Figure 3-1B**), indicating different development rate between treatments. Micro-Tom plant grown under Fl had significantly more leaves than all groups except R, while of the different LED treatments RB had the least leaves, found to be significant compared to R, RBG, and Fl. Total leaf area was also measured destructively (See **Figure 3-1C**), and while Fl had the largest average leaf area, it was similar to that of R and RBG, while B and RB were significantly less than the former treatments. Specific leaf area, which is the ratio of leaf area to leaf dry material, and a function of leaf thickness and leaf density, and plants have been shown to increase in SLA in response to shade (Y. Liu et al., 2016). Total specific leaf area calculations (See **Figure 3-1D**) identified Fl grown Micro-Tom had significantly lower SLA than any of the LED groups at 25 DAE. No significant differences in SLA were observed between LED treatments, although R and B had a higher average but exhibited large variation within the group.

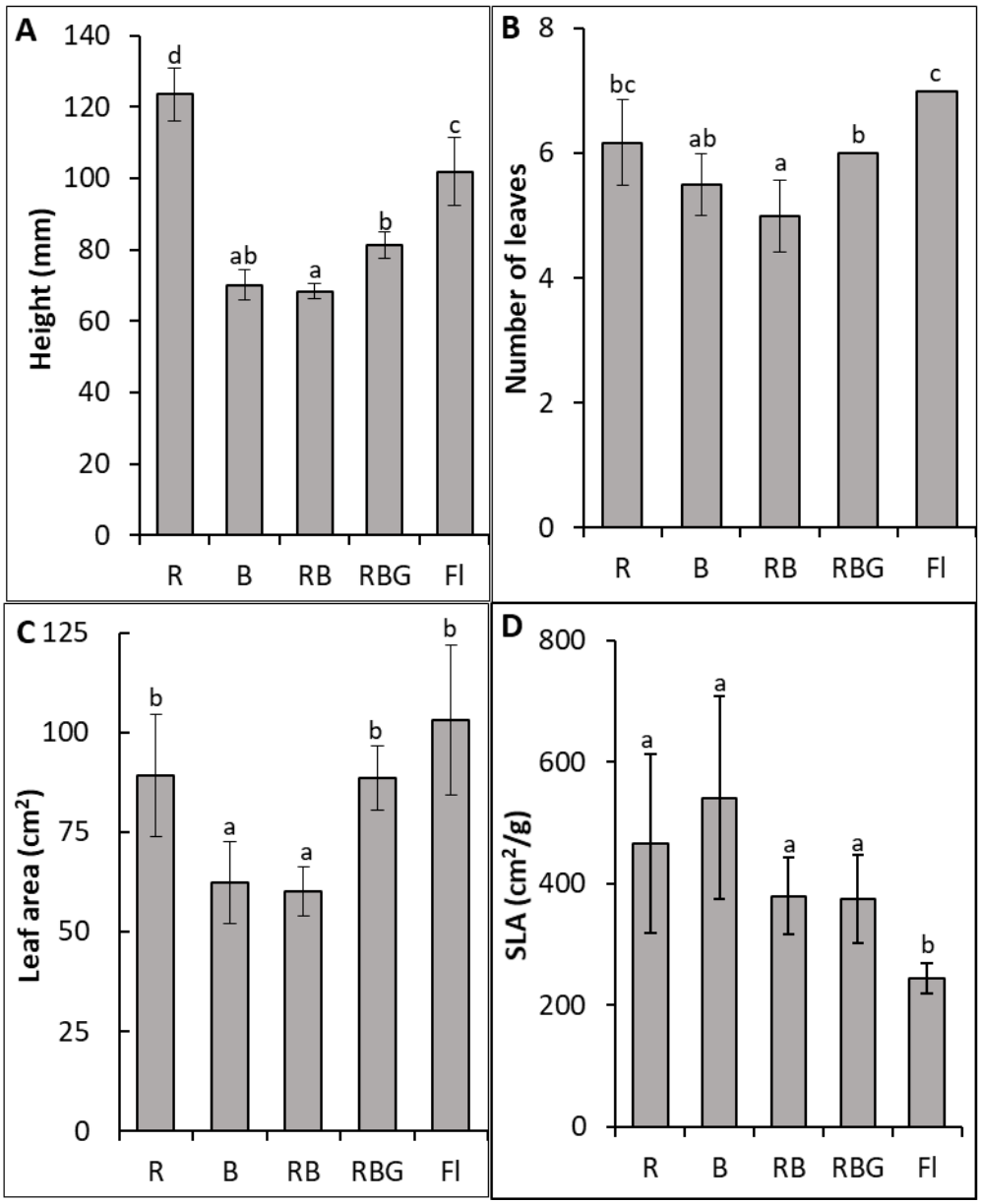


Figure 3-1 Morphological and physiology changes of Micro-Tom plants grown under different spectral qualities at vegetative stage. A. height above ground, measured in mm. B. The average number of leaves. C. Total leaf area of plants, measured in cm2. D. Specific leaf area, calculated from total leaf area measurements and total leaf dry weight. Micro-Tom plants were grown under LED lights emitting R= 100% red; B= 100% blue; RB= 70% red/ 30% blue; RBG= 63% red/ 27% blue/ 10% green; or Fl= fluorescent tube lighting. Error bars = ±SD (n=6). Letters indicate statistical significance, One-way ANOVA and Tukey post-hoc test ($p=<0.05$), where different letters indicates a statistic significant difference between groups.

Destructive measurements of both fresh and dry weight were taken to understand biomass accumulation and partitioning of the Micro-Tom plants after 25 days being grown under varying spectral qualities. Above ground materials were separated into leaf and stem tissues, with petioles included in stem material.

Figure 3-2A and **Figure 3-I2B** shows fresh and dry weight measurements, respectively. Significant differences were observed in both fresh and dry weight of leaf and stem material individually and combined light spectra between treatments. Fl grown Micro-Tom had a significantly higher leaf, stem, and total above ground fresh and dry weight than any of the LED treatments. Fl grown plants had a ~100% increase in total dry weight compared to R and RBG grown plants, which had the highest dry weight of the LED treatments. Comparison of fresh and dry weight between the different LED spectral qualities revealed significant differences in both fresh and dry weight, while no significant differences were observed in stem fresh or dry weight between treatments. R and RBG had similar total fresh weight, with B and RB having substantial reductions in fresh weight compared to both. B had significantly less leaf fresh weight than RBG, while R and RB had slight reductions relative to RBG these were not significant. Of the LED treatments, RBG and R had the highest average total dry weight accumulation, with a 33% reduction in total dry weight in RB compared to RBG. However, within the LED treatments the only significant difference in total dry weight was in B compared to RBG,

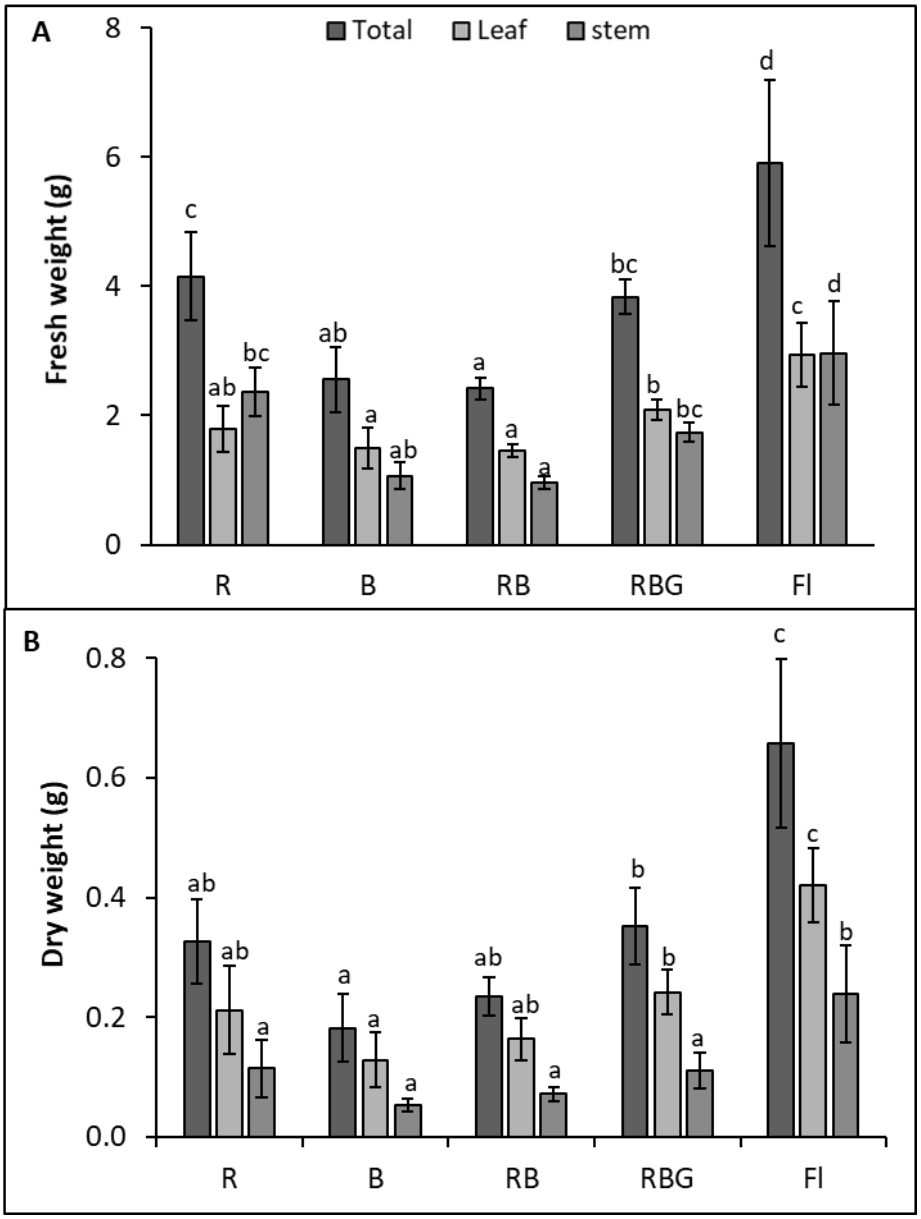


Figure 3-2 Fresh and dry weight of Micro-Tom grown under different light spectra at vegetative stage. A. Fresh weight; B. Dry weight of Micro-Tom plants above ground material. Coloured bars, as indicated on the legend at top, represent total above ground material= Dark grey; Leaf= light grey; stem= grey. Plants were grown under LED lights emitting R= 100% red; B= 100% blue; RB= 70% red/ 30% blue; RBG= 63% red/ 27% blue/ 10% green; or Fl= fluorescent tube lighting. Error bars = ±SD (n=6). Letter indicates statistical significance, according to One-way ANOVA and Tukey post-hoc test ($p=<0.05$), where different letters indicates a statistic significant difference between groups.

3.3.2 Plant growth analysis at harvest

The light and environmental conditions were then replicated for a second experiment, this time growing Micro-Tom plants until harvest to evaluate the effect of spectral quality on physiological traits over the entire life-cycle and to see the effect of light quality on yield. Micro-Tom plants were grown for 91 days after seedling emergence, at which point some fruit from all treatments had ripened. Light intensity was maintained at 200µmol m2s-1 to the top of canopy throughout development.

Weekly physiological measurements throughout development

Figure 3-3 shows the physiological traits which were measured weekly. As it was seen at the vegetative stage, height measurements of Micro-Tom plants (See **Figure 3-3A**) grown under monochromatic red light were significantly taller than those under any other condition, assessed by one-way ANOVA of growth at different time-points throughout development. When all treatments reaching maximum plant height at approximately DAE 36, at which point R grown plants were ~60-70% taller ($p<0.05$) compared to Micro-Tom plants grown under any other spectral quality. B grown plants were observed to be significantly smaller ($p<0.05$) than RB, RBG, and Fl grown plants at DAE 9 and15, with the difference reducing until DAE 29 at which point B, RBG and RBG and DAE 36 when Fl is no longer significantly taller. The mixed light treatments, RB, RBG, and Fl, are similar height throughout development. Leaf number was counted weekly (See **Figure 3-3B**) and apart from at one point at DAE36 when R treatment was significantly less ($p<0.05$) than all other treatments and no significant difference was observed between any treatment throughout development [$F (15.3, 95.8) = .55$, $p= .908$], although within-treatment variation was large at harvest.

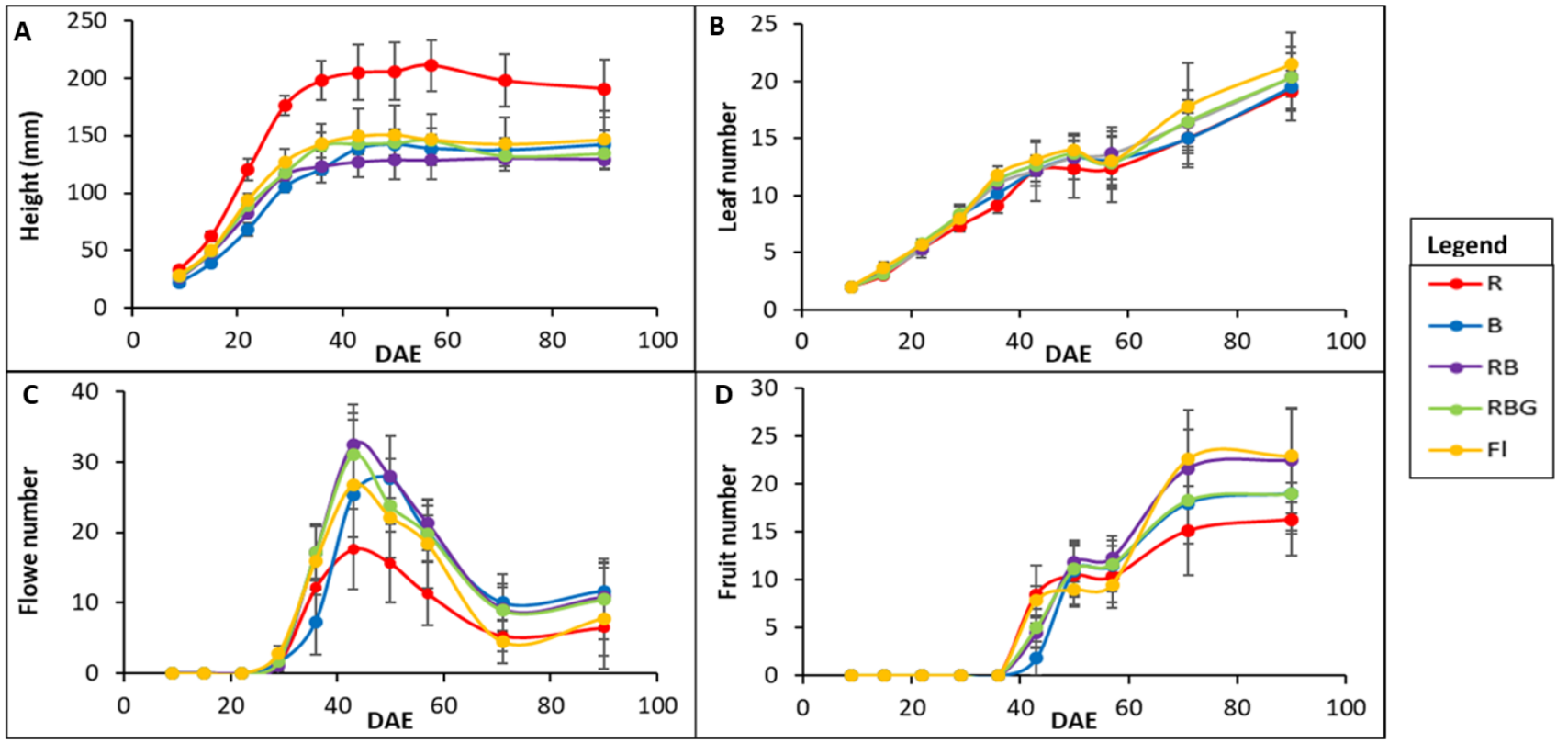


Figure 3-3 Plant growth analysis during different developmental stages when grown under different spectral qualities. A. Plant height measurements; B. Leaf number counts; C. Flower number counts; D. Fruit number counts. Measurements were taken weekly, up until day 56, and bi-weekly until harvest at DAE 91. The legend indicates the colour of each treatment, where: Error bars = ±SD (n=6). Significant differences ($p<0.05$) between groups were assessed using One-way ANOVA with Tukey post-hoc follow-up, and descriptive analysis of statistics is presented below.

Figure 3-3C shows the weekly measurements of flower number taken throughout the experiment, and statistical assessment of flower number throughout development identified significant differences [F= (14, 87.8) = 2.84, p= .000]. The average flower number observed in R grown plant is consistently lower than any other treatment between DAE 36 and 57, and across all time-points, R treatment has significantly fewer flowers than all groups except Fl. When flower number peaks for all groups between DAE 43 and 50, RB and RBG treatments had significantly more flowers than R (46% greater). At DAE36, B treatment has significantly less ($p<0.05$) flowers than all other treatments except R. The difference likely to be due to a delay in flowering time (See supplementary table flowering time). However, despite the slight shift to right in the curve of flower number, B treatment maintains a similar average flower number as RB and RBG treatments from DAE 42 to harvest.

Fruit number was also counted weekly to assess the timing and a total number of fruit throughout development (See **Figure 3-3D**). No significant differences were found with fruit number at harvest, although average fruit number deviated substantially between groups, with R, less fruit on average than RBG and Fl at harvest. B and RB had identical averages fruit number, which was ~15% less than R and RBG. Assessment of early stage of first fruit emergence revealed significant difference, at DAE43, R grown plants had significantly more fruit than RB and B grown plants. R and Fl and RB and RBG had similar fruit number at this time point, with the latter two having ~40% less than former. After this time point, there were no more significant difference observed, as within-group variation increases substantially.

Harvest morphological measurements

Micro-Tom were grown under R, B, RB, RBG, or Fl lights for 93 days from seedling emergence until harvest, at which point morphological measurements were recorded and are presented in **Figure 3 4**. The height of each plant at time of harvest was measured, from soil to top of canopy **(Figure 3 4A**). Micro-Tom grown under R light were significantly taller than those grown under any other light quality, with no significant difference observed

between any of the remaining treatments. Petiole length (**Figure 3 4B**) was also measured, and the average petiole length calculated from petioles of leaves 3-5. Micro-Tom plants grown under monochromatic R had significantly longer petioles than those grown under any other spectral quality. The RBG and Fl plants were also significantly longer petioles than those grown under B or RBG. Total leaf area (**Figure 3 4C**) was highly variable within plants grown under the same spectral qualities, especially Fl, and although R had larger average leaf area than all other treatments, it was only significantly different from Fl which had much smaller leaf area. Although there was not a significant difference in leaf area, specific leaf area, which is the ratio of leaf area to leaf dry material, revealed large significant variations between treatments. Plants grown under monochromatic R had significantly higher specific leaf area (SLA) than all other treatments, which was approximately ~40% higher than that of the 3 LED treatments, which all had similar average SLA. Fl grown plants had the lowest SLA, which was significant to both B and RBG, and R.

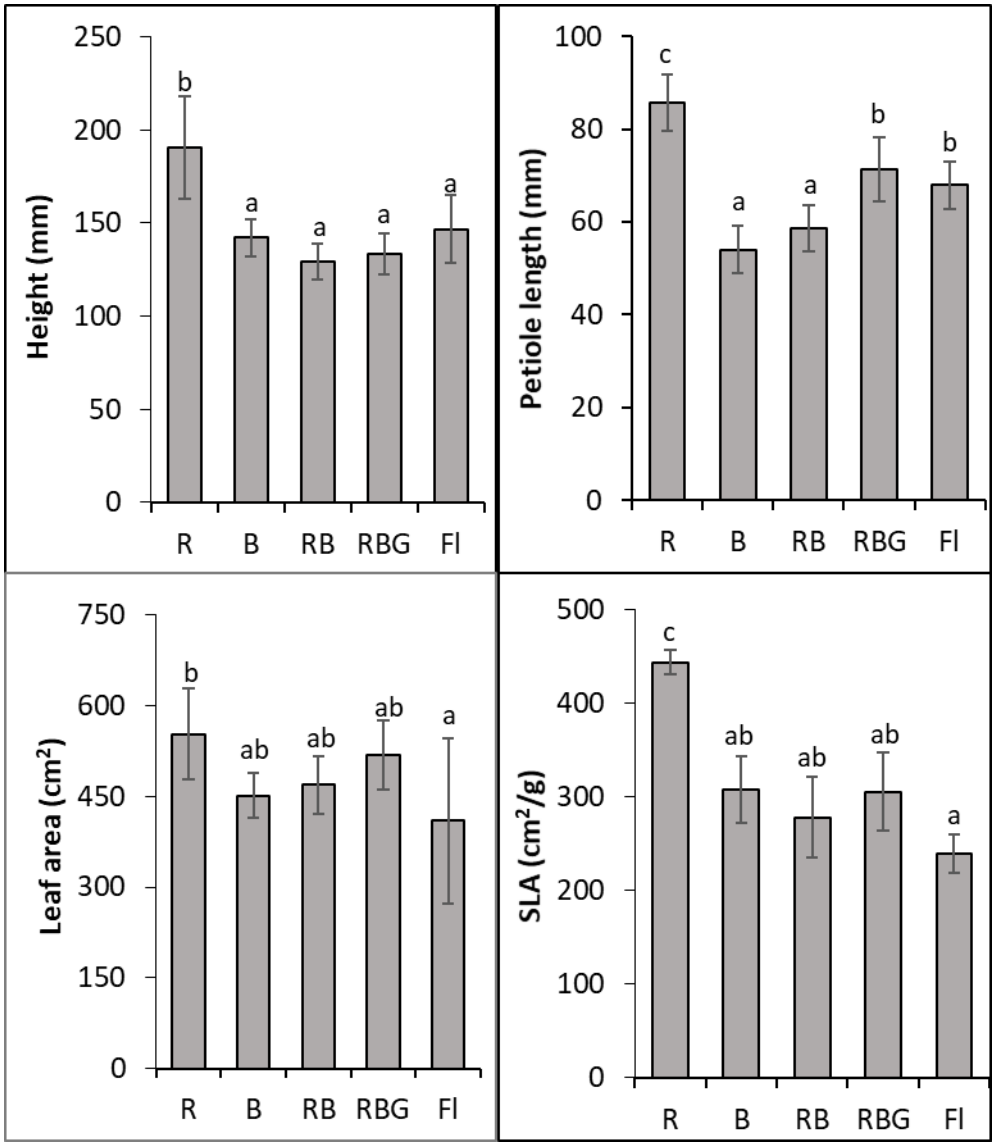


Figure 3-4 Leaf morphological analysis of plants grown under varying spectral qualities at harvest DAE93. A. height above ground, measured in mm. B. Average petiole length of 3-5 oldest leaves, measured in mm. C. Total leaf area of plants, measured in cm2. D. Specific leaf area, calculated from total leaf area measurements and total leaf dry weight. Micro-Tom plants were grown under LED lights emitting R= 100% red; B= 100% blue; RB= 70% red/ 30% blue; RBG= 63% red/ 27% blue/ 10% green; or Fl= fluorescent tube lighting. Measurements were taken at harvest, 93 days after emergence. Total PAR was maintained at 200µmol m^2s^{-1} measured at the top of the canopy. Statistical significance calculated by one-way ANOVA ($p<0.05$) and Tukey HSD post-hoc test ($p<0.05$), with statistical significance indicated by a letter, where comparisons with the same letter are not significantly different. Error bars indicate ±1 SD; n=6.

Biomass accumulation at harvest

Next, we looked at biomass accumulation, measured as the total dry weight of above-ground materials. Leaf, stem, and fruit dry weight were measured from plant materials harvested at 93 DAE (See **Figure 3-5**). Total biomass accumulation was calculated from the combined dry weight of above-ground material including leaves, stem, and fruit (See **Figure 3-5A**). Fl grown plants had significantly higher total biomass accumulation compared to all LED treatments. RB and RBG had identical biomass accumulation, while B was slightly but not significantly reduced. R grown plants had significantly lower total biomass accumulation compared to all groups except B, with a 20%, 30%, 31%, and 47% average reduction in total above ground dry weight compared to B, RB, RBG, and FL, respectively. The biomass accumulation in individual materials collected was then evaluated. No significant difference was observed in leaf dry weight materials between Micro-Tom grown any of the light qualities including Fl, although the Micro-Tom plants grown under R had the lowest average biomass, followed by B, while RB, RBG, and FL all had similar average leaf dry weight. For stem materials including both petioles and the main stem, we saw significant difference dry (B) weight, despite the increased plant height and average petiole length of R compared to all LED groups, its stem dry weight was not significantly different. Fl grown plants had the highest stem dry weight, however, this was only significantly higher stem dry weight than both R and B groups. Significant differences were also observed in fruit dry weight, as monochromatic R had the lowest average dry weight, which was significantly lower than RB, RBG, and Fl. B. RB and RBG had similar average fruit dry weight, whilst Fl grown plants had significantly greater fresh and dry weight than those grown under any of the LED spectral treatments.

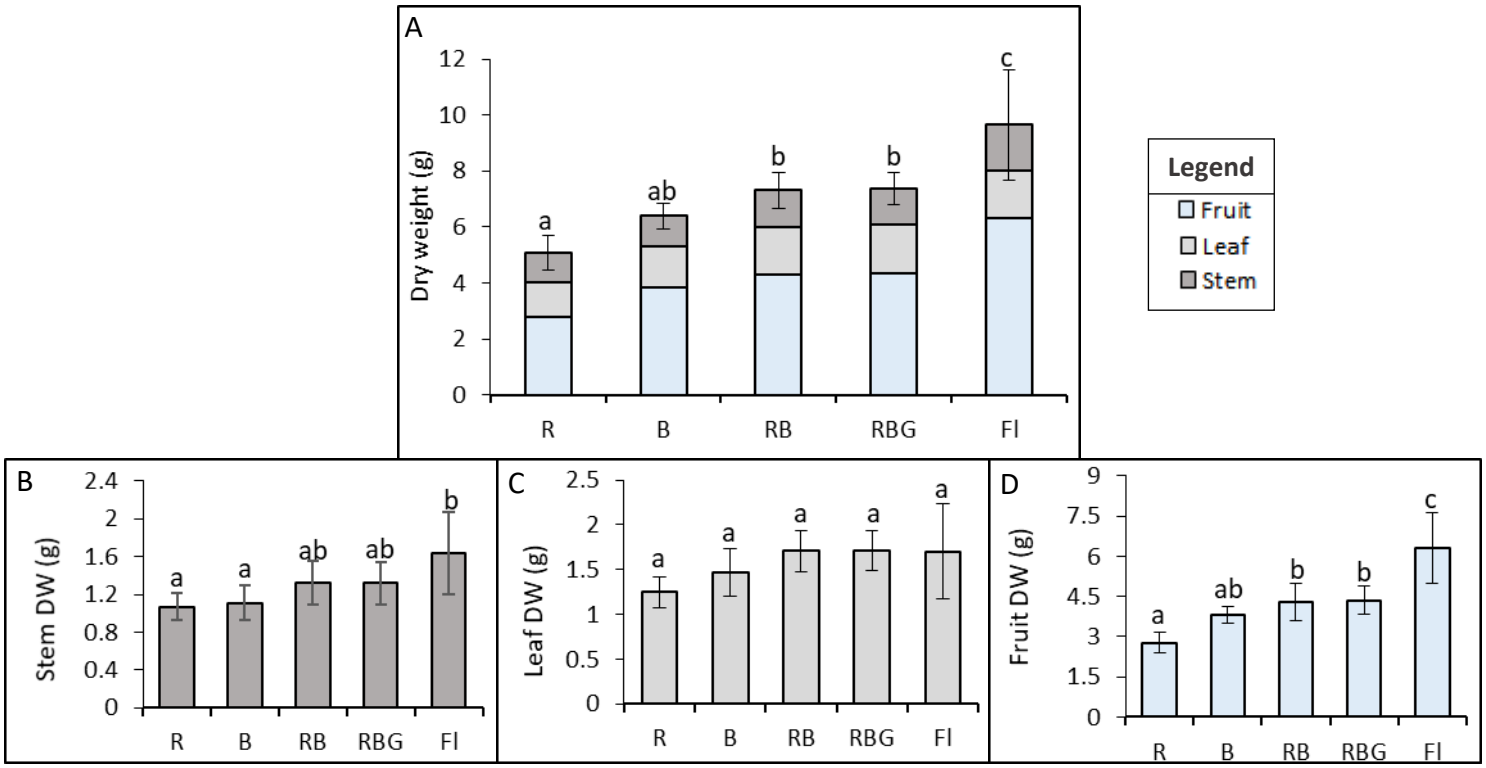


Figure 3-5 Biomass accumulation and partitioning of Micro-Tom plants grown under different light spectral conditions. at 93 DAE A. Combined total dry weight of above-ground material; B, dry weight of stem material; C, Dry weight of leaf materials; D, Total dry weight of fruit. Micro-Tom plants were grown under LED lights emitting. R= 100% red; B= 100% blue; RB= 70% red/ 30% blue; RBG= 63% red/ 27% blue/ 10% green; or Fl= fluorescent tube lighting. Measurements were taken at 93 days after emergence. Statistical significance calculated by one-way ANOVA ($p<0.05$) and Tukey HSD post-hoc test ($p<0.05$), and different letters indicate significant differences between groups. Error bars indicate ±1 SD; n=6.

Yield and fruit quality measurements

Yield and fruit quality of Micro-Tom plants were assessed at harvest after 93 days after emergence under light sources emitting different spectral qualities (See **Figure 3-6**)**.** The total number of fruit was measured per plant, excluding immature fruit (See **Figure 3-6A**). Micro-Tom grown under R light had the lowest fruit number, however this was only significantly lower than Fl, which had the highest fruit number, while no other significant differences were observed. Micro-Tom grown under both RB and RBG had similar fruit number, with average fruit number reduced in B and to a greater extent in R. **Figure 3 6B** shows the total fresh fruit weight per plant, including unripe and immature fruit, with R grown Micro-Tom producing a significantly lower yield of fruit compared to the other LED treatments B, RB, and RBG, while Fl produced significantly more than all of the other treatments. **Figure 3-6C** shows the average weight of individual ripe fruit between the light treatments.Fluorescent grown plants had the highest average individual fresh fruit weight at least 1g heavier than those of RBG which had the heaviest of any of the LED group, although only B was significantly smaller than Fl, which on average weighed 27% less. In fact between, different LED treatments, no significant difference was observed and average fruit weight differed marginally. Finally, we assessed the total soluble sugar content of individual ripe fruit from each plant using a refractometer (See **Figure 3-6D**), and R grown plant was found to produce tomatoes with significantly reduced total soluble sugars (TSS) compared to all other groups. The average TSS of R grown plants measured 4^{o}B, which was substantially reduced compared to tomatoes from B which had 5.3 ^{o}B, and RB, RBG, and Fl had almost identical TSS content of ~4.9^{o}B.B.

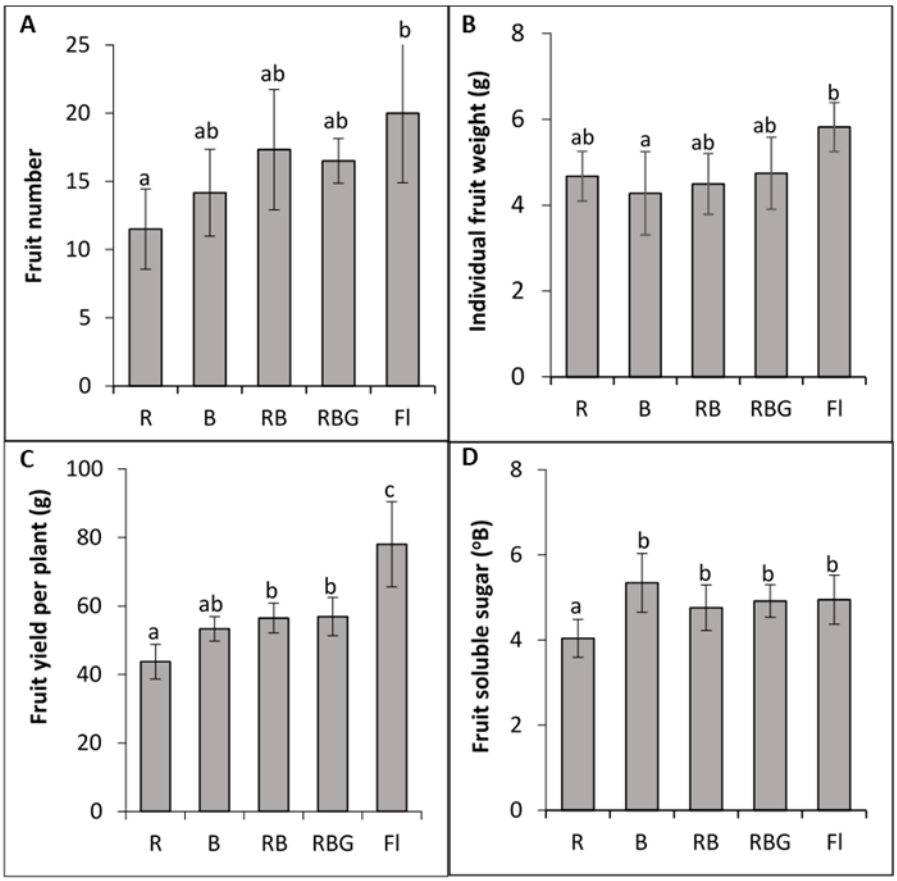


Figure 3-6 Fruit quality analysis of Micro-Tom grown under varying light spectral conditions. A. Fruit number; B. Average individual fruit weight; C. Yield of fruit per plant; D. Fruit total soluble sugar content; Micro-Tom plants were grown under LED lights emitting R= 100% red; B= 100% blue; RB= 70% red/ 30% blue; RBG= 63% red/ 27% blue/ 10% green; or Fl= fluorescent tube lighting. Measurements were taken at 93 days after emergence. Statistical significance calculated by one-way ANOVA ($p<0.05$) and Tukey HSD post-hoc test ($p<0.05$), and is indicated by letters. Error bars indicate ±1 SD (n=6). Each fruit total soluble sugar measurement: 4 fruits per plant, 6 biological replicates.

3.3.3 Photosynthesis and chlorophyll fluorescence analysis

Using the LICOR, IRGA, and chlorophyll fluorescence measurements were performed on leaves of Micro-Tom plants acclimated to different light conditions under LED or fluorescent lights. Light curves were conducted measuring stomatal conductance and chlorophyll fluorescence at increasing light intensities under an RB LED light (90% 620nm: 10% 450nm).

Infra-red gas analysis

The light curve comparison of photosynthesis against light intensity (See **Figure 3 7A**) revealed that R acclimated leaves had a significantly reduced maximum rate of photosynthesis compared to all other treatments. Analysis of individual light levels revealed that from 0-200µmol$m^{-2}s^{-1}$ PAR there are no significant differences in Pn between any of the treatments, despite R averaging lower than the other 4 treatments. The reduction in the net photosynthetic rate of R compared to all other treatments increases with increasing light intensity, becoming significant above 300 µmol $m^{-2}s^{-1}$. B, RB, RBG, and Fl show no significant difference in Pn at any light intensity. To identify what the difference in absorption would have on photosynthesis, given we calculated absorbed PAR (See **Figure 3 7B**), to estimate the amount of PAR that is absorbed for photosynthesis. The Pn vs light intensity plot shows similar trends in comparison to uncorrected Pn, identifying that a difference in absorption is not responsible for the reduction in photosynthetic rate.

Quantum yield (QY), which is molecules of CO2 fixed per mole of the photon absorbed, is a measurement that explains the efficiency with which light is converted into fixed carbon (See **Figure 3 8**). QY is calculated from the linear portion of the light-responsive curve and based on absorbed light, and is the gradient (y) of the linear regression. Using the 4 points between 0-200µmol m-2s-1, and correcting PAR for absorbance, the quantum yield was calculated for each biological replicate and assessed for significance using a one-way ANOVA between treatments. Leaves of R acclimated plants had a significantly lower QY (delta ~0.05; 14%) than the B, RB, RBG. Fl acclimated plants had an intermediate average QY to R and B, RB, RBG which was not significantly different to any treatment.

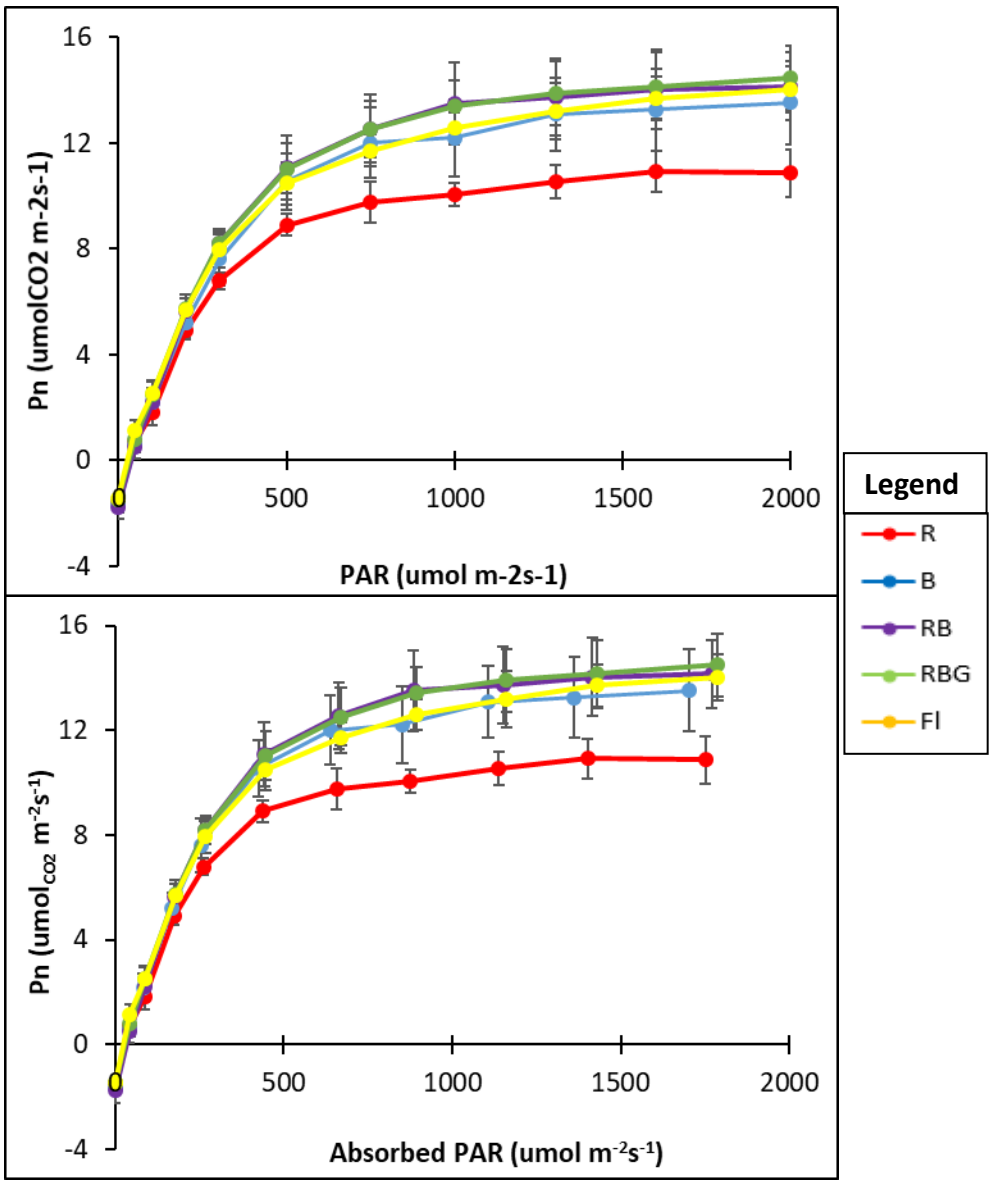


Figure 3-7 Photosynthetic light curve of Micro-Tom plants grown under varying light spectra. A. Net photosynthesis (Pn) against light intensity (PAR) B. Net photosynthesis against light intensity (Absorbed PAR). Micro-Tom plants were grown under LED lights emitting R= 100% red; B= 100% blue; RB= 70% red/ 30% blue; RBG= 63% red/ 27% blue/ 10% green; or Fl= fluorescent tube lighting. PAR is measured as irradiance at leaf surface level. Absorbed PAR calculated by adjusting PAR based on leaf absorption measurements are taken, accounting for fact actinic light emitted 90% 620nm; 10% 450nm. Error bars indicate ±1SD (n=5).

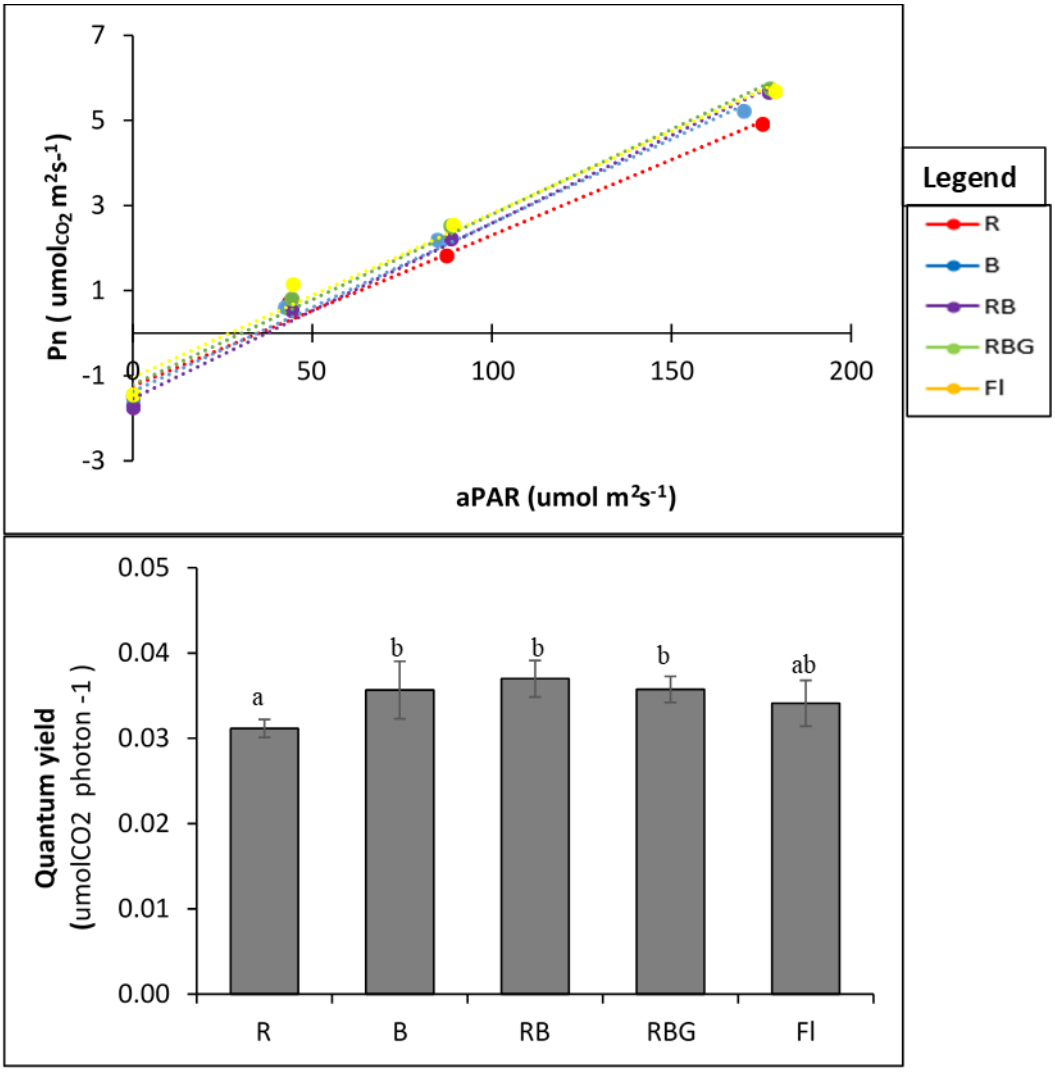


Figure 3-8 Quantum yield of photosynthesis of Micro-Tom plants leaves grown under different light spectra. A is net photosynthesis (Pn) measured at light-limiting PAR and corrected for absorption efficiency (aPAR). B shows the quantum yield of photosynthesis from plants grown under different light spectra. Dotted lines in A represent linear regression for each treatment of Pn vs aPAR across 5 light levels. R: $y = 0.031x - 1.25$, $R^2 = 0.99$; B: $y= 0.034x -1.371$, $R^2 = 0.99$; RB: $y = 0.037x - 1.54$, $R^2 = 0.99$; RBG: $y = 0.036x - 1.2$, $R^2 = 0.99$; Fl: $y = 0.035x - 1.04$, $R^2 = 0.98$. Quantum yield estimation derived directly from linear regression in A. Pn is net photosynthesis; aPAR is photosynthetically absorbed radiation at leaf level adjusted for leaf absorption. 5 biological replicates per treatment and error bars indicate ±1SD. Tukey post-hoc test $p<0.05$ represented where different letters indicate significant differences.

Chlorophyll fluorescence measurements

Chlorophyll fluorescence was measured during LICOR light curves and was used to examine the photosynthetic performance of plants acclimated to different light spectral qualities at varying light intensities (**Figure 3 9A-D**). Quantum efficiency of PSII, (Φ_{PSII}) expresses the proportion of absorbed light used in PSII photochemistry (Murchie & Lawson, 2013). Φ_{PSII} typically drops as light intensity increases due to increases in non-photochemical quenching (NPQ), which can be indirectly estimated from reductions in PSII maximum efficiency (Fv'Fm') and the level of photochemical quenching (qP; Fq'/Fv') (Murchie & Lawson, 2013). **Figure 3 9A** shows the comparison of Φ_{PSII} against light intensity during the light curve and reveals that plants grown under R light has significantly lower Φ_{PSII} than those grown under B, RB, RBG, and Fl across all light intensities. At saturating light intensities, Fl had significantly greater Φ_{PSII} than B although B did not significantly deviate from either RB or RBG.

We then looked at the maximum quantum efficiency of PSII (Fv'/Fm'), which estimates the maximum quantum efficiency of PSII photochemistry at a given PPFD, and is the PSII operating efficiency (Φ_{PSII}) if all reaction centers were open (Baker, 2008). Fv'/Fm' drops with increasing light intensities, and indicates increases in non-photochemical quenching (NPQ) (Murchie & Lawson, 2013). **Figure 3 9B** shows Fv'Fm' during the light curve as a function of light intensity**.** R grown plants had a lower Fv'Fm when compared to all other treatments. At low light intensities and up to 750µmol $m^{-2}s^{-1}$ light level R had significantly lower Fv'Fm' than all other treatments. However, as light intensity continued to increase towards saturation point, both mixed LED light treatments RB and RBG dropped towards R Fv'/Fm' levels, indicating a larger increase in NPQ than in the B or Fl acclimated leaves. The Fv'/Fm' of RB and RBG became significantly lower than Fl at 1300µmol $m^{-2}s^{-1}$ and this difference increased with increasing light intensity. The Fv'/Fm' did not differ significantly between B, RB, and RBG at any light intensity.

We then assessed photochemical quenching (qP), which relates maximum PSII efficiency to operating efficiency (See **Figure 3 9C**). As light

levels increase, qP decreases, yet between treatments R and B averaged consistently lower than qP than RB, RBG, and Fl at all light intensities, although only the difference between B and RB was only significant from 200µmol$m^{-2}s^{-1}$ and increasing light intensities. R had significantly reduced qP to the mixed light treatments at all light intensities.

The final fluorescence parameter we were interested in was electron transport rate, which is estimated from information on the proportion of light used in PSII photochemistry and corrected for absorption efficiency**. Figure 3 9D** shows the light dependence of PSII electron transport rates (ETR), measured for the leaves of Micro-Tom plants grown under varying spectral qualities, and comparing ETR across all light intensities found R and B to have lower ETR then RB, RBG, and Fl. Although the differences are small at limiting light intensities, as PAR increases the differences between the ETR of the mixed light treatments (RB, RBG, and Fl) and the monochromatic treatments (R and B) becomes significantly larger, and at saturating light levels ETR of R and B is ~24% and ~15% lower in the mixed light treatments, respectively.

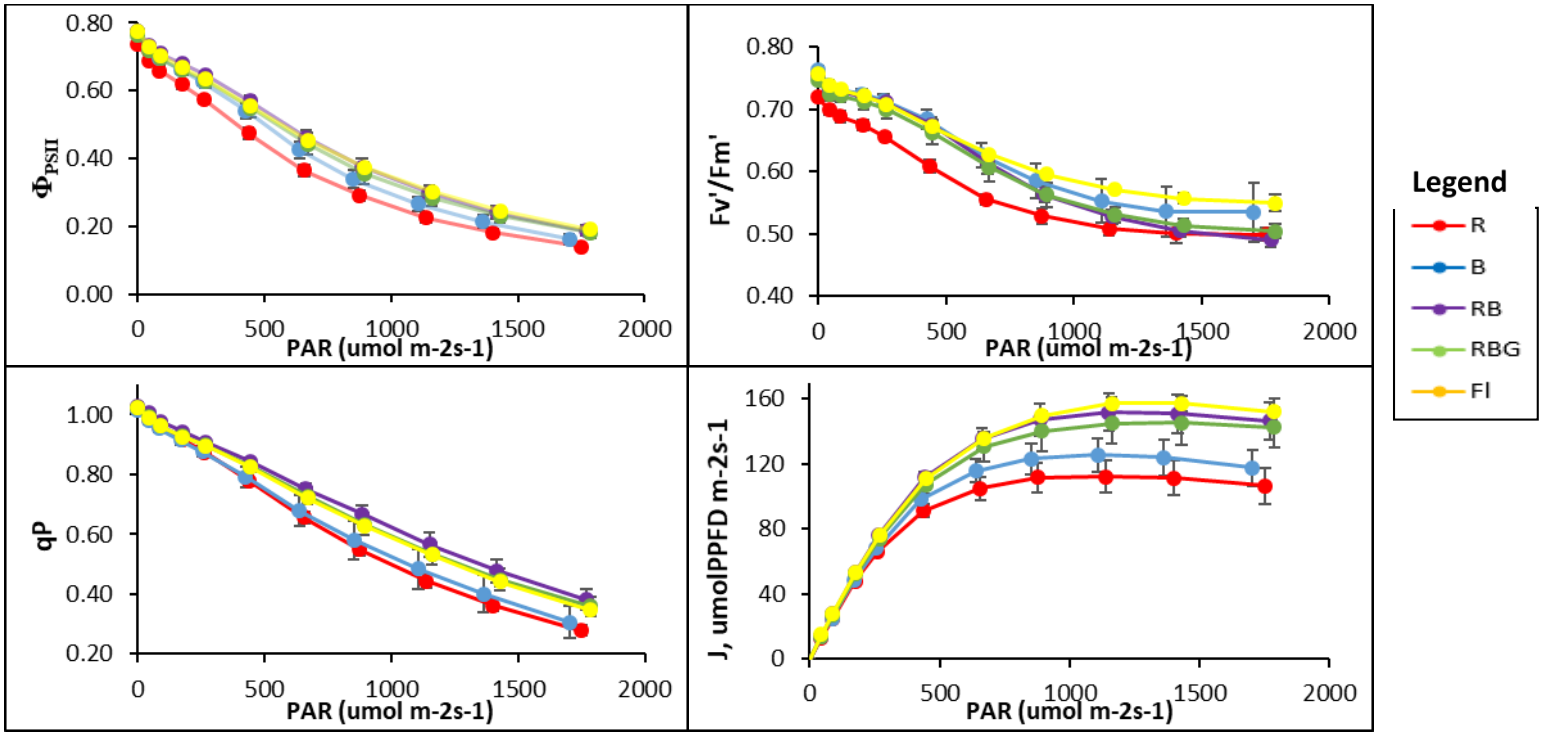


Figure 3-9 Photosynthesis and Chlorophyll fluorescence analysis of Micro-Tom leaves at different irradiances. A. Quantum efficiency of PSII (phiPSII); B, Maximum efficiency of PSII photochemistry in the light, if all centers were open (Fv'/Fm'); C, Photochemical quenching (qP); D, Electron transport rate (J). Micro-Tom plants were grown under LED lights emitting R= 100% red; B= 100% blue; RB= 70% red/ 30% blue; RBG= 63% red/ 27% blue/ 10% green; or Fl= fluorescent tube lighting. PAR is measured as irradiance at leaf surface level and is adjusted for absorption. Error bars are ±1 standard error (n=5). One-way ANOVA test for the significant difference was used α=0.05, with significance described in results.

3.3.4 Whole plant chlorophyll fluorescence analysis

In addition to the single leaf chlorophyll fluorescence measurements taken using the Li-COR during the light curves, whole plant chlorophyll fluorescence was assessed using the FLUORCAM fluorescence imager. Micro-Tom plants were X DAE, were dark adapted for 2 hours before being placed inside FLUORCAM chamber where a light curve was taken at 0%, 10% 20% 40%, 80%, 100% light intensity, and chlorophyll fluorescence parameters were measured at the end of each light level and are presented in figure .

Quantum yield of photosystem II (Φ_{PSII}) was measured during light curve (See **Figure 3-10A**) with the profiles of both red and blue grown plants significantly deviating from RB, RBG, and Fl during the light curve. B grown plants exhibited a sharp drop in Φ_{PSII} at a low light intensity, but then recover to the level as RB, RBG, and Fl did when light intensity increased to 20% to 100%. In contrast, the difference between R and RB, RBG, and Fl increased with increasing light intensity as the Φ_{PSII} of R dropped substantially between 40% - 100% light intensity compared to the other light treatments, with Φ_{PSII} at maximum light intensity of 20% lower than all other groups, which was significantly different ($p<0.05$).

Non-photochemical quenching (NPQ), which is a measure of the proportion of absorbed photon energy dissipated as heat, was also calculated (See **Figure 3-10B**). As light intensity increases the rate of NPQ to a greater in R compared other treatments, however, this was only significant between Fl and RBG ($p<005$) which had the lowest NPQ. The Fv'Fm' profile of R relative to all other light treatments showed a significant reduction at all light intensities when assessed by one-way ANOVA of Fv/Fm' at each light level (See **Figure 3-10**C). As plants were dark-adapted prior to light curve, measurements at 0% light intensity of Fv/Fm, which represents the maximum quantum efficiency of PSII, is generally taken as an indicator of plant stress. R light-grown plants had a moderately reduced dark-adapted Fv/Fm of 0.8 compared to all other groups which had an Fv/Fm of 0.82-0.83 in all other treatments, which is universally considered the expected value for healthy unstressed plants, although this

difference was only significant ($p<0.05$) between R with B. RB, and RBG. The significant difference in qP (See **Figure 3-10D**), which is related to the amount of absorbed photon energy using in photochemistry, were also observed between light treatments across all light intensities. The profiles of qP show a similar trend to that observed in Fv'/Fm'/, in that as light intensity increases, the qP of R drop significantly compared to all other treatments, while qP of B dips at 10% then recovers to the higher level of qP from 20%-100% light intensity. At 100% light intensity the qP of R is ~14% significantly ($p<0.05$) reduced compared to all other light treatments.

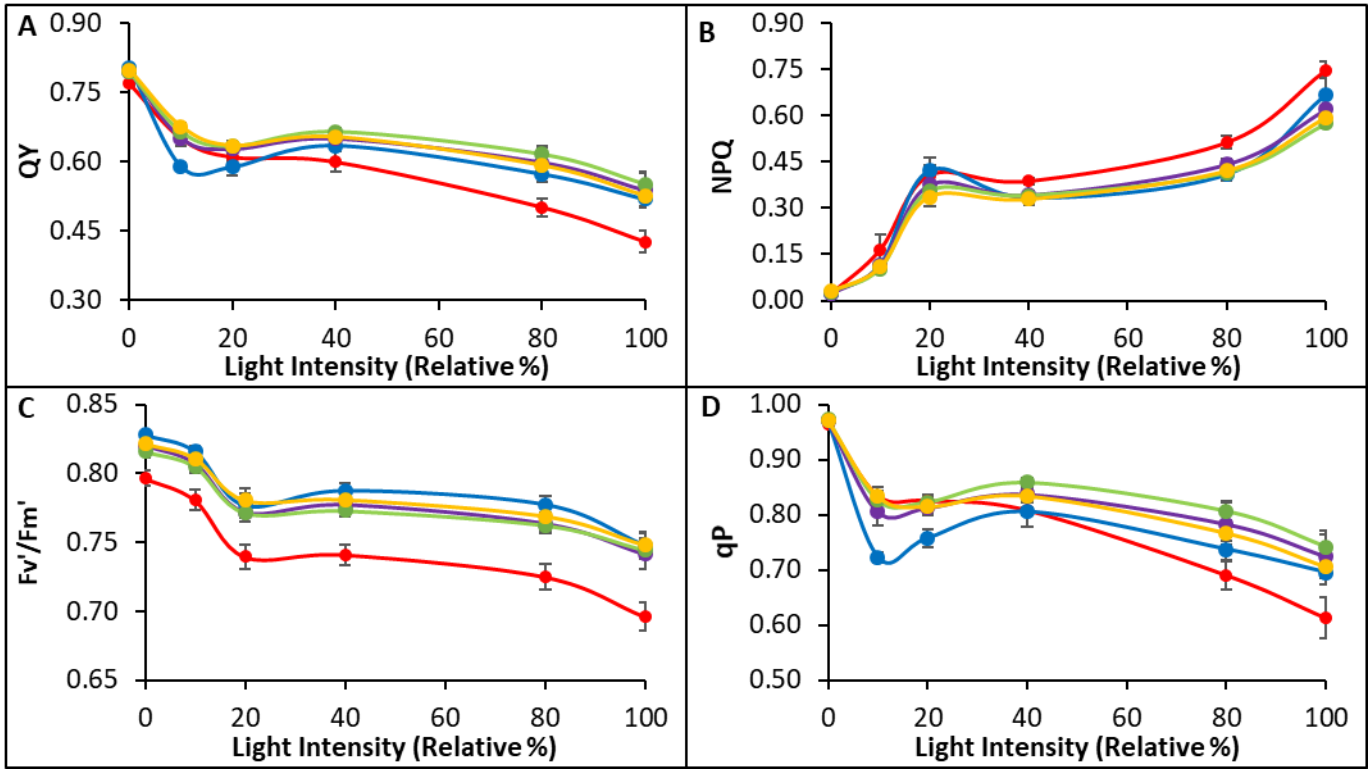


Figure 3-10 Whole plant chlorophyll fluorescence light curve of dark-adapted Micro-Tom plants grown under varying light spectra. A. Quantum efficiency of PSII (phiPSII); B; Non-photochemical quenching C, Maximum efficiency of PSII photochemistry in the light, if all centers were open (Fv'/Fm'; D, Photochemical quenching (qP). Micro-Tom plants were grown under LED lights emitting R= 100% red; B= 100% blue; RB= 70% red/ 30% blue; RBG= 63% red/ 27% blue/ 10% green; or Fl= fluorescent tube lighting. PAR is measured as irradiance at the leaf level and is adjusted for absorption. Error bars are ±1 standard error (n=5).

3.3.5 Analysis of leaf optical properties

Leaf absorption was calculated reflectance and transmittance measurements taken of the adaxial leaf surface using integrating sphere and ASD spectrometer. **Figure 3-11** shows the overall light absorption spectrum of Micro-Tom leaves grown under different spectra. The absorption profile reveals there are substantial differences in the absorption profile of leaves grown under all spectral qualities. While there are small differences in the blue spectrum, the largest differences in the absorption profile are characterized by the size of the drop in absorption within the green portion of the spectrum, and also the within the orange/red spectrum. To quantify the absorption profile, the average absorption within different regions of the spectrum was analyzed (See **Table 3-1)**. Over the entire PAR spectrum (400-700nm), B had a significantly reduced absorption, ~4% compared to all other treatments. Looking more closely at different regions of the spectrum, R leaves had significantly higher absorption with the violet (400-454nm) spectrum than all other treatments, though the difference was relatively small (~3%). Between the two mixed LED treatments, though RBG leaves had a higher absorption than RB within the green, yellow, orange and spectrums, this was not significant. B had significantly reduced absorption between the green-red wavelengths, while Fl leaves have considerably higher absorption at these wavelengths compared to leaves grown under other spectral qualities. R leaves have significantly reduced absorption than Fl and RBG across the green, orange, portion of the spectrum, though only the former was significant in at red wavelengths.

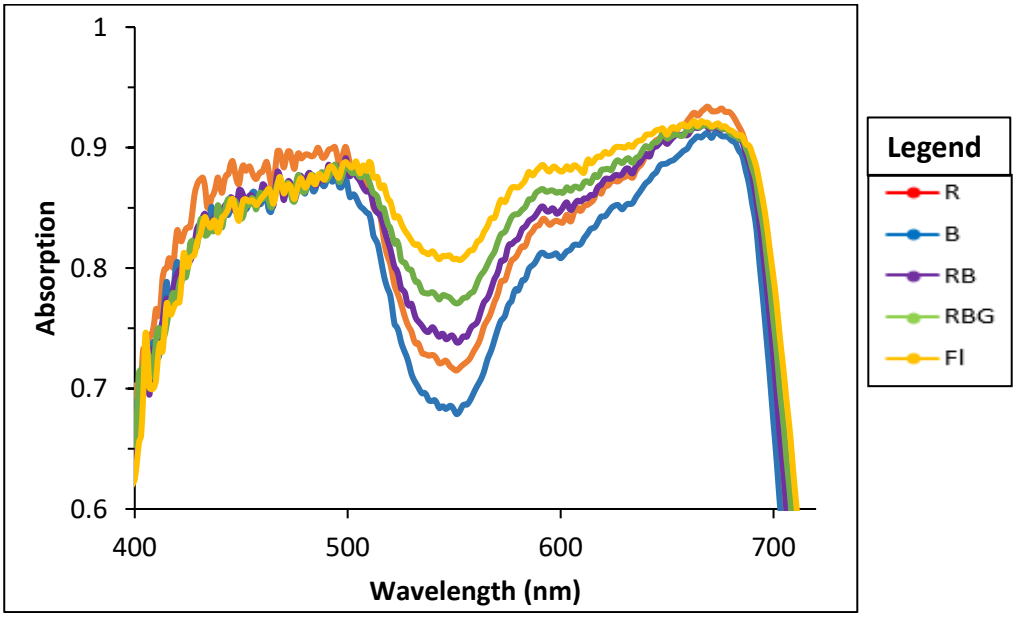


Figure 3-11Absorption spectrum of tomato leaves grown under different light spectra. Absorption profile was measured using an integrating sphere with ASD spectrometer. A mature leaf with 6 biological replicates was tested per treatment. Measurements were taken every 1nm from 400-700nm. Legend above graph indicates which treatment is represented by each line; R= Red; B= Blue; RBG= purple; RBG= green=; Fl= yellow.

Table 3-1 Leaf absorption within different regions of the visible light spectrum

Wavelength	Region	R	B	RB	RBG	Fl
400-454nm	**Violet**	0.83 ^{c}	0.80 ^{ab}	0.81 ^{b}	0.80 ^{ab}	0.79 ^{a}
445-492nm	**Blue**	0.89 ^{b}	0.87 ^{b}	0.88 ^{ab}	0.87 ^{ab}	0.87 ^{a}
493-577nm	**Green**	0.78 ^{b}	0.75 ^{a}	0.80 ^{bc}	0.82 ^{c}	0.84 ^{cd}
578-597nm	**Yellow**	0.83 ^{b}	0.80 ^{a}	0.85 ^{bc}	0.86 ^{cd}	0.88 ^{d}
597-620nm	**Orange**	0.86 ^{b}	0.83 ^{a}	0.87 ^{bc}	0.87 ^{cd}	0.88 ^{d}
621-700nm	**Red**	0.87 ^{b}	0.85 ^{a}	0.88 ^{bc}	0.88 ^{bc}	0.89 ^{c}
400-700nm	**PAR**	0.84 ^{a}	0.81 ^{b}	0.84 ^{a}	0.85 ^{a}	0.85 ^{a}

Averages taken from 6 biological replicates according to the method. Statistical significance calculated using one-way ANOVA with Tukey HSD post-hoc test for significance ($p<0.05$) with different letters indicate significant difference between groups.

3.3.6 Pigment content analysis

Given the differences observed in leaf optical qualities, we next analyzed pigment content of leaf tissue spectrophotometrically (See **Figure 3-12)**. Leaves of Micro-Tom grown under either monochromatic R or B had significantly less chlorophyll-a, chlorophyll-b, total chlorophyll (See **Figure 3-12a)**, and carotenoids and xanthophyll (See **Figure 3-12b)** than those leaves grown under either RB, RBG or Fl. Anthocyanin content was also estimated (See **Figure 3-12c**). No anthocyanin was detectable in B grown Micro-Tom leaves. Anthocyanin content in R grown leaves was significantly less anthocyanin than in any of the mixed light treatments; approximately half of that presented in the two mixed LED treatments RB, and RBG and three times less than in Fluorescent tube lit Micro-Tom leaves. The difference in anthocyanin content between RB and RBG compared to Fl was also significant.

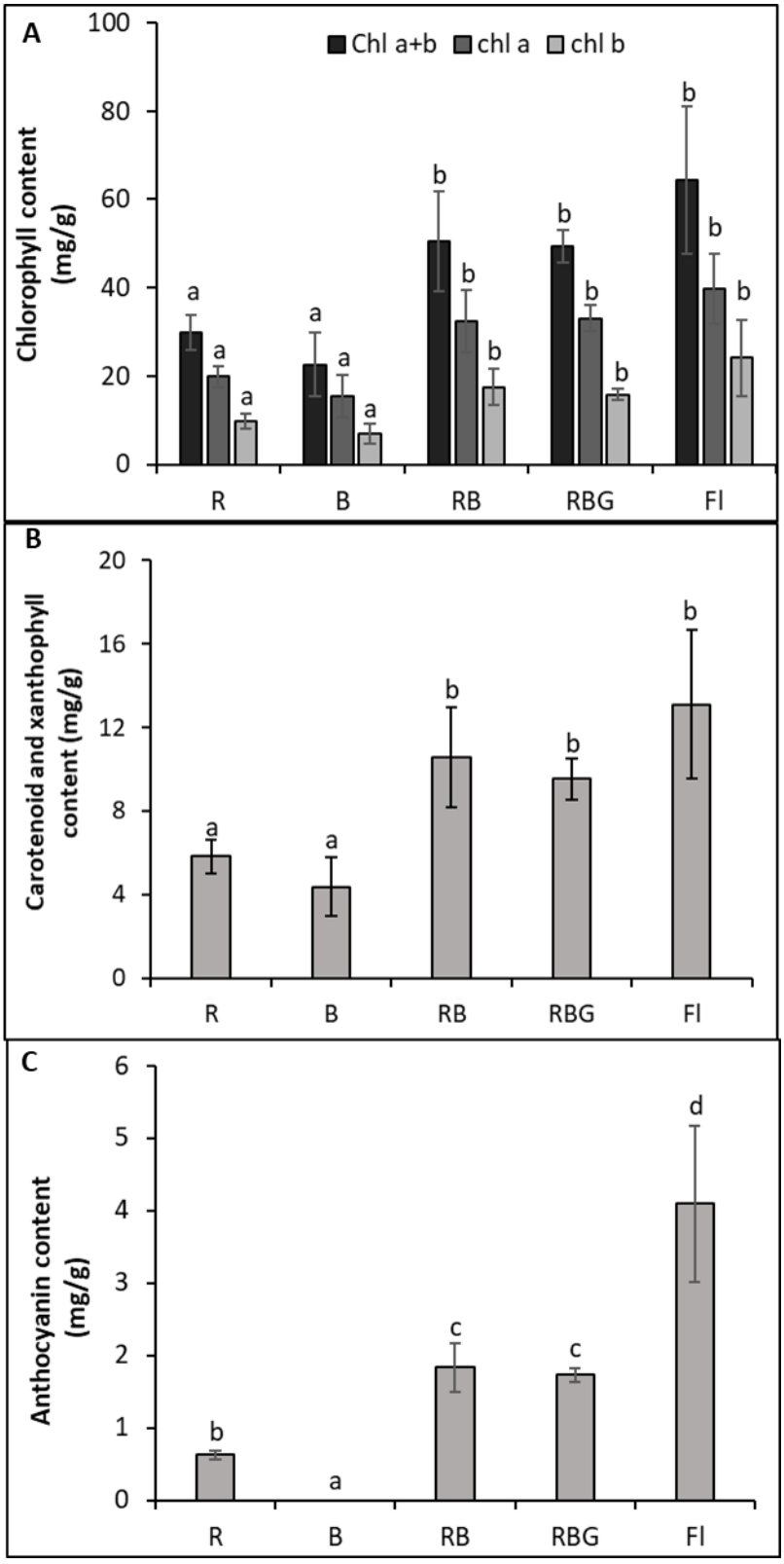


Figure 3-12 Pigment content analysis of Micro-Tom grown under different light spectra. A. Chlorophyll content, B. Carotenoid content, C. Anthocyanin content. Micro-Tom plants were grown under LED lights emitting R= 100% red; B= 100% blue; RB= 70% red/ 30% blue; RBG= 63% red/ 27% blue/ 10% green; or Fl= fluorescent tube lighting. Error bars indicate ±1SD (n=3). Tukey post-hoc test $p<0.05$ represented where different letters indicate significant differences between groups.

3.4 Discussion

Plant yield and quality is determined by environmental factors, of which light is critical. In controlled environment agriculture, optimization of light spectral quality is integral to maximizing plant yield and improving food quality. Through the use of LED lights to tailor spectral quality, it is possible to maximize yield and reduce energy-use efficiency, by providing only the optimal wavelengths. In the present study, we examined the effect of spectral quality on physiological traits, pigment content and optical properties, photosynthesis, and yield in the tomato variety Micro-Tom. While the effect of LED spectral quality on yield has been studied in other crop species (Hogewoning et al., 2010; Matsuda, Ohashi-Kaneko, Fujiwara, & Kurata, 2008; Ohashi-Kaneko, Matsuda, Goto, Fujiwara, & Kurata, 2006; X. Y. Wang, Xu, & Cui, 2015), in tomato studies using LED as sole-source lighting have been in young plants (Liu Xiaoying, 2012), or using LEDs as supplemental lighting in glasshouse (Lanoue et al., 2017).

3.4.1 Photosynthesis, biomass accumulation, and yield

The reduction in photosynthetic efficiency observed under R conditions appeared to contribute to the reduction in biomass and fruit yield. The chlorophyll fluorescence data supported the reduction in quantum yield of photosynthesis, with R grown plants having reduced PhiPSII, electron transport rate and increased NPQ. The chlorophyll fluorescence and photosynthesis showed the same overall trends. Monochromatic R acclimated plants had significantly reduced the quantum yield of photosynthesis and a substantially reduced maximum rate of photosynthesis under saturating light. At 200µmol m^2s^{-1}, the light intensity at which plants were grown, Micro-Tom acclimated to R light had significantly reduced net photosynthesis. Chlorophyll fluorescence revealed R light grown Micro-Tom also had reduced electron transport rate, photochemical quenching, and quantum efficiency of photosystem II, and increased NPQ at high light intensity compared to the mixed LED and fluorescent tube grown plants. It should be noted that for Li-COR photosynthesis measurements, inside the chamber all leaves were subjected to identical spectral qualities, 90% R 10% B, and so measurements

of photosynthesis reflect the photosynthetic capacity of Micro-Tom plant acclimated to different spectral qualities and not directly the actual rate of photosynthesis under different spectral qualities. Lanoue and colleagues showed the tomato acclimated to white light have altered photosynthetic traits when subjected to varying LED monochromatic and mixed light (Lanoue et al., 2017), although the rate of photosynthesis of plants acclimated to different spectral qualities under those light qualities was not studied.

In a similar study by Liu and colleagues (2012) in tomato seedlings cv. cerasiforme, both monochromatic R and B grown tomato had reduced maximum photosynthetic capacity compared to mixed RB and RBG LED treatments (Liu Xiaoying, 2012). Although led to increased biomass accumulation in B compared to RBG and R, albeit this was only in young plants (<30 days) (Liu Xiaoying, 2012). In spinach, B deficiency reduced CO_2 assimilation and quantum efficiency of PSII at high light intensity (500µmol m2s-1) (Matsuda et al., 2008). In rice, supplementing red light with a small proportion of blue drastically improved photosynthesis, biomass accumulation and yield (Ohashi-Kaneko et al., 2006)). Similarly, in cucumber monochromatic R grown plants had reduced photosynthesis compared to B or white grown plants (Hogewoning et al., 2010; X. Y. Wang et al., 2015), and a blue-light dose-response experiment revealed that the addition of 7% B to red treatment was sufficient to alleviate photosynthetic dysfunction observed in monochromatic red light (Hogewoning et al., 2010). The general agreement between our data and research in several other species shows the importance of blue light in for promoting improved photosynthetic efficiency and capacity, which is required for biomass accumulation and subsequently maximizing yield.

3.4.2 Relationship between optical properties of plant and pigment metabolism

The optical properties of leaves and pigment content were evaluated to determine the effect of spectral quality on pigment metabolism and how this effect light absorption across the spectrum of PAR. Both the chlorophyll and carotenoid content of Micro-Tom grown under either monochromatic R or B was significantly reduced relative to the 3 mixed light treatments, with RB, RBG, and Fl grown leaves containing approximately doubled the content on these photosynthetic pigments. Neither red nor blue light alone was sufficient to increase pigment content, whereas the presence of both red and blue light together stimulated increased chlorophyll and carotenoid biosynthesis. Studies of tomato combinatorial knockout mutants deficient in multiple photoreceptors; *phyA, phyB1, phyB2,* and *cry1* revealed that silencing of cryptochrome *cry1a* in addition to phytochromes (*phyA, phyB1, phyB2*) reduced chlorophyll content further compared to phytochrome silencing alone, implicating the red and blue photoreceptors in the co-regulating chlorophyll biosynthesis (Weller, Perrotta, et al., 2001). In Barley, chlorophyll synthesis requires the co-action of both red and blue light to induce chlorophyll biosynthesis (Bukhov, Drozdova, Bondar, & Mokronosov, 1992). In *Arabidopsis*, coordinated activation of both red-light activated phytochrome and blue-light activated cryptochrome is necessary for some phytochrome signals, as inactivation of one photoreceptor attenuates the others signal (de Wit et al., 2016). Our findings suggest that rather than acting additively, red and blue light are both required together for stimulation of pigment synthesis. However, there did not seem to be a relationship between chlorophyll content and absorption within the red- and blue- portions of the visible light spectrum, as chlorophyll metabolism was significantly up-regulated under RB and RBG compared to both R and B, yet no R, RB, and RBG had similar absorption values in both the red and blue region of the absorption spectrum. R grown Micro-Tom had a similar absorption in the blue region of the spectrum to RB, RBG, and Fl despite having half the chlorophyll and carotenoid content. The only significant reduction in absorption across PAR was in the B treatment, which due to substantially reduced absorption within the green spectrum. As

for anthocyanin, a non-photosynthetic pigment which absorbs light within absorb light in the green portion of the visible light spectrum and is involved in photoprotection and has been implicated in defense, the pigment content measured correlated well with absorption profile of leaves under different light qualities. Monochromatic B grown Micro-Tom had the lowest absorption within the green portion of the spectrum, and no anthocyanin was detected in B grown Micro-Tom. While the anthocyanin content in RB and RBG was double that present in R. As suggested with chlorophyll metabolism, this is indicative of co-activation of both red and blue wavelengths, as blue alone was insufficient to stimulate anthocyanin production and red only to a small degree while the combination of both drastically increased anthocyanin accumulation.

3.4.3 Monochromatic R grown plants exhibit LBL induced shade avoidance phenotype

Micro-Tom plants grown under monochromatic red light exhibited drastic morphological differences, reduced photosynthetic efficiency and capacity and decreased biomass accumulation and fruit yield compared to Micro-Tom grown under monochromatic blue, mixed red and blue LED, mixed red, blue and green LED and fluorescent tube lighting. Collectively, the increased plant height, petiole length, leaf area and specific leaf area observed at plant maturity under monochromatic red light are all traits associated with shade-avoidance response (SAR). The absence of substantial difference in morphology between B, RB and RBG grown plants which have 0%, 63% (126 µmol m^2s^-1), and 70% (140µmol m^2s^{-1}), respectively, indicated that red light is not responsible for the SAR morphology in monochromatic red light grown Micro-Tom tomato plant. The major difference is the absence of blue light in R compared to all other groups, with RBG, RB, and B groups emitted with 27%, 30% and 100% blue light, respectively. While shade-avoidance is typically described in terms of red: far-red ratio, far-red was absent in the monochromatic red-light treatment. However, phytochrome-mediated R: FR shade avoidance is not the only mechanism through which shade avoidance response can be triggered. In true shade, both red and blue light are depleted, and cryptochrome-mediated SAR has been reported. When cryptochromes are

inactive in response to persistent low-blue light (LBL) the resulting attenuation of CRY signal results in PIF mediated SAR (Keller et al., 2011). Silencing of tomato *cry1a* results in SAR phenotype, while over-expression caused dwarfing (Y. Liu et al., 2016), while both over-expression and silencing of *CRY2* causes dwarfing and internode elongation, respectively (Giliberto et al., 2005).

3.4.4 Fluorescent tube lighting vs LEDs

Micro-Tom plants grown under fluorescent tube lighting had increased biomass accumulation and total fruit yield compared to mixed LED treatments, in spite of not having any differences in photosynthetic properties. It is worth noting that the fluorescent tube lighting emits a substantial amount of heat compared to LED lights, and while we used airflow to dissipate some of this the average temperature inside the fluorescent tube chamber was 2^{o}C higher than in any of the LED light compartments. It is, therefore, possible that increased heat improved plant biomass accumulation. Secondly, whereas LED the light intensity could be precisely controlled, this was more difficult to achieve with the fluorescent chamber and so light intensity was likely higher compared to the LED chambers, which may have also improved photosynthesis. No differences in quantum yield or photosynthesis at 200µmol m^2s^{-1} between Fl and mixed LED plants, which would explain the significantly increased biomass.

3.4.5 Addition of green light to mixed red and blue LED seems to not be improving agronomically important traits

We characterized the effect of supplementing a small proportion of green light into mixed red and blue LEDs to observe if green light could improve plant yield. Traditionally, red and blue light has been considered the most physiologically important wavelengths for maximizing plant growth and productivity, as they are absorbed most efficiently by photosynthetically pigment. The optimal ratio of R: B for growth and biomass production in tomato seedlings is 7:3 (R. Hernández & Kubota, 2016), which was adopted

for this experiment. Recent research suggests the importance of green light is under-estimated, and supported the inclusion of a small portion of green light improves carbon fixation and yield (H. Kim et al., 2004; J. Sun, Nishio, & Vogelmann, 1998; Terashima, Fujita, Inoue, Chow, & Oguchi, 2009). In this experiment, the physiology and biomass of the RB plants were significantly different from the RBG during the vegetative stage, with RBG plants being taller, having more leaves and increased biomass. Despite this, no difference was observed in the photosynthesis and chlorophyll fluorescence light profiles of leaves acclimated to either mixed red and blue LEDs or mixed red and blue with the supplementation of 13% green light (7:3:1.5). The only difference at harvest was significantly increased petiole length in RBG. An accumulating body of evidence suggests that green light is able to penetrate deeper into the leaves, driving photosynthesis in the mid and lower levels of the leaf where photosystems are less saturated and quantum efficiency yield of photosynthesis is higher (J. Sun et al., 1998; Terashima et al., 2009). However, under our conditions no difference in above ground biomass accumulation or yield at harvest were observed at harvest between RB and RBG, suggesting that there was no benefit of using green light supplementation under these conditions. However, more extensive research on the effects of green light proportion under different photoperiods, light intensities, and with increasing proportions of green light would need to be conducted to establish the importance of green light. Green light has a beneficial effect on yield under continuous light growing systems, alleviating photoinhibition and increasing photosynthesis (Bian, Cheng, Wang, Yang, & Lu, 2018).

3.5 Conclusion

Spectral quality influences series of agronomically important traits in Micro-Tom including plant architecture, pigment synthesis, fruit soluble sugar content, transpiration, and photosynthetic capacity. The addition of green light to mixed red and blue LED did lead to altered morphology during the vegetative stage but as development progressed the differences diminished and

it did not have any effect on photosynthesis, pigment metabolism, biomass accumulation or yield. Under monochromatic R light, tomato exhibit shade avoidance phenotypes, have reduced quantum yield of photosynthesis and maximum photosynthesis, and have reduced biomass accumulation and total yield of tomato, and reduced fruit soluble sugar content. This is the first work phenotyping tomato to harvest in a controlled environment using LEDs as the sole-light source. The stark phenotypic difference in monochromatic red light grown tomato indicate the importance of blue light wavelengths for tomato growth and implicate the cryptochrome photoreceptor and specifically low-blue light responses in the control of agronomically important traits. As cryptochromes primarily control development in response to blue light through regulation of transcription, focused research of the effect of LBL on the transcriptome may reveal the mechanisms through which the difference photosynthesis, morphology, and ultimately yield.

4 TRANSCRIPTOMIC ANALYSIS OF MICRO-TOM GROWN UNDER DIFFERENT LIGHT SPECTRA

4.1 INTRODUCTION

4.1.1 Overview of the previous chapter

In the previous chapter, we identified morphological and physiological traits affected by spectral quality. In particular, Micro-Tom plants grown under monochromatic red light (R) exhibited shade-avoidance phenotype associated with stem growth and elongated petioles, photosynthetic dysfunction which ultimately resulted in reduced biomass accumulation and reduced fruit yield compared to Micro-Tom grown under monochromatic blue (B), mixed red/blue/green LED or fluorescent tube lighting. These were consistent with the cryptochrome-mediated low-blue light shade avoidance response which has been characterized on a phenotypic and molecular level in *Arabidopsis*. Micro-Tom grown under monochromatic blue light had a slight but insignificant decrease in average biomass and yield compared to the mixed light-grown plants, and in general, exhibited a normal development. The only abnormality observed was in the reduction of pigment content, with chlorophyll and carotenoid content reduced in both monochromatic R and B compared to the mixed light treatment, and zero detectable anthocyanins in the B plant which correlated with a reduction of absorption in the leaf absorption profiles. It is clear that spectral quality drastically alters development in Micro-Tom and that our controlled environment set-up with an isolated compartment enables the study of the effects of specific wavelengths and combination of wavelengths on Micro-Tom growth and development. In the following chapter, we will investigate the molecular response of Micro-Tom to varying spectral qualities using RNA-Seq transcriptomic analysis.

4.1.2 Light re-programs transcriptome

Light induces extensive re-programming of the plant transcriptome, which has been described in **Chapter 1.3**. Transcriptomic studies in *Arabidopsis thaliana* identified that approximately 25-30% of its transcriptome is coordinately regulated by light (Ma et al., 2001). This transcriptional response to spectral quality is controlled primarily by two photoreceptor families; the phytochrome and cryptochrome receptors, which perceive red/far-red and blue/green signals, respectively. Cryptochrome and phytochrome signals operate through a partially overlapping signalling cascade, which are integrated to determine plant growth and development in response to shade (de Wit et al., 2016; Keller et al., 2011). Key regulators of phytochrome and cryptochrome status are the phytochrome-interacting factors, as red light-activated phyB mediates the proteolytic degradation PIF4 and PIF5 and the inactivation of PIF7 (Hornitschek et al., 2012; L. Li et al., 2012), while blue light-activated cry1 inactivates both PIF4 and PIF5 (de Wit et al., 2016). Over 60% of genes differentially expressed in responses to low R: FR inhibition of phytochromes or low-blue light (LBL) inactivation of cryptochromes are targets of PIF4/PIF5 (de Wit et al., 2016; Pedmale et al., 2016). Another core light transcription module is transcription factor HY5, which is modulated post-translationally by light as photo-active cryptochrome and phytochromes inhibit its degradation by the 26S proteasome degradation system. HY5 binds to over 9000 genes and differentially regulates the expression of 1100 genes (Huiyong Zhang et al., 2011).

Plant responses to light spectra are also regulated by the endogenous hormonal status of the plant, with the levels of gibberellins, auxins (Eunkyoo Oh et al., 2014), cytokines and abscisic acid affecting the responsiveness of plants growth responses to shade (Lau & Deng, 2010). Both phytochromes and cryptochromes have been shown to not only regulate development through regulation of hormone abundance but direct interaction of the photoreceptors themselves and PIFs with core hormone signalling elements to modulate sensitivity to hormones and hormone transcriptional networks (de Lucas & Prat, 2014; F. Xu et al., 2018). Furthermore, light regulates the abundance and sensitivity of gibberellins (Bai et al., 2012), auxin (Eunkyoo Oh et al., 2014), cytokinin (Kurepin, Emery, Pharis, & Reid, 2007), abscisic acid, and jasmonate (Cerrudo et al., 2017). This central module integrates a diverse range of cue allowing the plant to coordinate growth, development, and metabolism according

to its environment. Phytochrome regulation of JA metabolism and sensitivity regulates the growth-defense balance of plants (Cerrudo et al., 2017).

Transcriptomic studies of photoreceptor mutants have been conducted on various crop species with the aim to elucidate the genetic mechanisms underpinning light signalling. In Sorghum, CRY1a mediates the expression of phytohormone and stress-responsive gene expression, significantly up-regulating HY5 and abscisic acid signalling transcription factor ABI5, altering sensitivity to ABA (T. Zhou et al., 2018). Functional characterization of CRY1a in tomato through gene over-expression and silencing identified significant phenotypic abnormalities, with altered plant architecture, hormone content and pigment metabolism that correlated with extensive transcriptional miss-regulation of photosynthesis, hormone metabolism and cell growth encoding genes (C. C. Liu et al., 2018). Transcriptomic analysis of the effect of low R: FR ratio on both stem and leaf transcriptome of tomato has previously shown that phytochrome-perceived shade induces the expression of growth-promoting auxin signalling related genes and cell-wall modifying enzymes, while photosynthesis-related gene expression is repressed (Cagnola et al., 2012).

In addition to the study of individual photoreceptors, the effect of LED spectra on the transcriptome has been conducted in several plant species. In Norway Spruce, gene expression analysis identified red light regulates gibberellin biosynthesis to promote stem elongation, while blue light promotes secondary metabolism including the production of plant defense compounds (F. O. Yang et al., 2015). In grape plantlets, monochromatic red light grown plantlets exhibit shade avoidance-type growth and chlorophyll levels, accompanied by an up-regulation in the cell-wall modifying endotransglucosylase/hydrolases, and a concomitant decrease in auxin-repressed protein- and chlorophyll a/b binding protein-encoding genes (C.-X. Li et al., 2017).

4.1.3 Gene regulatory networks

Large-scale gene expression studies by transcriptomic analysis have identified many genes that are associated with light-induced response to plants growth and development. However, expression data alone can’t effectively distinguish among genes that have similar expression patterns but are under the control of different

regulatory networks. Gene interaction studies can give critical insight into the regulation of light response and induction. Gene regulatory networks (GRN) are a method for computational modeling from expression data since they are able to represent the network both graphically and quantitatively and to predict answers to particular questions in complex data (Friedman N et al. 2000). These models can display reliable dynamics and help to understand parts of cellular regulation mechanisms, for example, gene co-expression network (GCN) which is an integrative system biology approach for describing the correlation patterns among genes (De Smet & Marchal, 2010; Stuart, Segal, Koller, & Kim, 2003). If there is a significant co-expression relationship between pairs of genes it shows a similar expression pattern across samples. Gene co-expression network relies on the behaviours of biological features since co-expressed genes are controlled by the same transcriptional regulation (activation and inhibition), and functionally related to the same pathway or phenotype. In this study, we explored gene co-expression networks containing differentiation of expression patterns and highlight specific genes or gene clusters which are thought to facilitate responses to different light spectra.

4.1.4 Aims and objectives

Light spectra can effectively control the growth, photosynthetic capacity, and pigment metabolism of tomato plants. The aim of this chapter is to increase the understanding of the effect of LED spectra on tomato plant growth and development at the transcriptomic level. Particularly, it focuses on the identification of target genes associated with hormone homeostasis, growth, high photosynthesis efficiency, and metabolism through RNA Seq analysis and the photoreceptor-mediated light signalling pathway. We conducted the work along with tomato genome data to identify both differentially expressed genes and novel genes in Micro-Tom tomato plants grown under different LED light spectra. These genes are potentially extremely valuable molecular markers for breeding new varieties which will be suitable to grow under LED light for the protected horticulture. The specific objectives are:

1. Generate and analyze a comprehensive transcriptomic dataset from plants grown under varying spectral qualities of Micro-Tom.

2. Identify differentially expressed genes from transcriptomic data and key genes from gene co-expression network. These candidate genes will be implemented to test by gene silencing and further transgenic plant's phenotypes.

3. Confirm candidate genes by qRT-PCR analysis

4. The gene co-expression networks and pathway analysis will be developed to quantitatively describe the effects of multifactorial interactions between light spectral quality, including light shade avoidance response, light signal transduction.

4.2 METHODS

4.2.1 Sample collection and Illumina sequencing

Micro-Tom plants were grown in isolated compartments under Heliospectra LED lights emitting either R (red= 660nm), B (blue= 450nm), RB (red= 660nm, blue 450nm; 7:3 ratio), RBG (red= 660nm, blue 450nm, green= 520nm; 7:3:1 ratio), or under fluorescent tube lighting. Whole leaf tissue samples were harvested from mature leaves during the vegetative stage, prior to anthesis, at 25 days after seed emergence. For each of the five light treatments, we used three biological replicates and the pooled RNA from two individual plants for each replicate. Total RNA extraction was performed using TRIzol® and according to manufacturer's instructions (Life Technologies, Carlsbad, California, USA), followed by RNA clean-up using Qiagen RNA plant mini-kit (Qiagen, Hilden, Germany). The RNA concentration and quality were assessed using the BioAnalyzer (Agilent Technologies, Santa Clara, California, USA), with a RIN value above 7 considered high-quality. 3µg total RNA from each sample was sent to the Wellcome Trust genomics center (Oxford, UK) where RNA samples underwent mRNA enrichment by polyA selection, and barcoded libraries prepared using Illumina's TruSeq Stranded Total RNA Library Prep Kit (Illumina, San Diego, California, USA). The 15 libraries were then pooled and sequenced at 75bp PE on 1 lane on the HiSeq4000 (Illumina, San Diego, California, USA).

4.2.2 Mapping of Illumina reads

Raw fast-QC files were quality-assessed, with those reads passing threshold then were adapter timed using Sickle and Scythe (Joshi and Nash, 2011). The trimmed and filtered read were then aligned to *Solanum lycopersicum* SL2.5 reference genome using HISAT2 (Kim, Langmead and Salzburg, 2015). Technical replicates from different lanes were merged using SAMtools (Heng Li et al, 2009), and gene level counts were generated using HTseq (Simon Anders et al, 2014).

4.2.3 Quality assessment and unsupervised analysis

For quality assessments of transcriptomic data, library normalized count data for each sample was processed using R package Noiseq. Gene length, GC content, and gene biotype information for *Solanum lycopersicum SL2.5* was downloaded from BiomaRt Plant. Sensitivity plots were generated comparing the distribution of read counts among different biotypes. CPM distributions were compared against GC content and length to assess the transcriptome data for bias.

4.2.4 PCA + Hierarchical clustering

The count data were log-normalized against gene length to generate count-per-million (CPM) count data for all expressed genes. Principal Component Analysis (PCA) was conducted using the R package *limma* (Smyth, 2005) function ‘prcomp’ for PCA. A distance matrix was calculated using Euclidean distance and hierarchical clustering of samples computed using the ‘hclust’ function.

4.2.5 Differential expression analysis (EdgeR)

The ‘Empirical Analysis of Digital Gene Expression data’ Bioconductor package better known as EdgeR, version 3.14 (Robinson et al, 2010) was used to identify differentially expressed genes (DEGs) and was run by using R (version 3.3.0) (R core team, 2016). Count data were first normalized to account for differences in library size and then filtered to remove genes in which the counts per million (CPM) was below one, in at least 3 samples. To test for between-sample variation, PCA was conducted on all samples, based on the regularised-log transformed count filtered and

normalized count data, followed by hierarchical clustering performed based on the Euclidean distance between samples. The following procedure for computing differential expression was conducted following the EdgeR user manual (Robinson, McCarthy, Chen, & Smyth, 2013). Gene-wise dispersion estimates were calculated and a negative binomial (NB) general linear model (GLM) was used to fit curve. Likelihood ratio testing was for determining differential expression of each gene between treatments in pair-wise comparisons, with false discovery rate correction (FDR) applied and the significance threshold set to 0.05<FDR. Pair-wise manner all treatments combinations, with the FDR threshold for calling significant differential expression set to 0.05 <FDR. Differential expression tables of all expressed genes were generated for each pair-wise comparison between R, B, RB, RBG, and Fl transcriptomes.

4.2.6 *Gene-Set Enrichment Analysis (GSEA)*

GO enrichment analysis was conducted using GOStats package in R (Falcon & Gentleman, 2007). Genes were annotated with GO terms using Ensembl BiomaRt R package. The Hyper-geometric test for significant enrichment in terms of Biological process, Molecular Function and Cellular Compartment were investigated for differentially expressed gene sets identified by EdgeR pair-wise comparisons and compared against the background list of all genes found to be expressed in our experiment.

KEGG is an integrated database compendium of molecular pathways that have been manually curated and drawn mapping current knowledge on molecular interactions, reaction and relation networks (Carlson, 2016). Gene to KEGG annotation was obtained from UNIPROT database. KEGG enrichment analysis was conducted using GOStats package in R, against the KEGG Solanum lycopersicum specific pathway maps (Falcon & Gentleman, 2007). Pathview was then used to visualize KEGG metabolic maps and overlay expression data to visualize pathways of interest (Luo & Brouwer, 2013).

4.2.7 *Gene co-expression Network modeling*

Gene co-expression network analysis was conducted using the DeGNServer (Jun Li, Wei, & Zhao, 2013). RPKM expression data from R, B, RBG, and Fl samples were log-transformed, and genes filtered to keep only those differentially expressed in at least one pair-wise comparison between R, B, and RBG treatments. Value-based co-expression networks were used to assess co-expression similarity and association for all gene pairs calculated using Spearman's ranked correlation method. A high-stringency association cut-off of 0.9 was set to keep only high-confidence interactions. The co-expression network was then imported into Cytoscape. Condition-specific networks were investigated by filtering for genes differentially expressed in a particular pair-wise comparison, and filtered to remove lowly differentially expressed genes set at a threshold of Log FC >0.5 or Log FC < -0.5. NetworkAnalyzer was used to calculate statistics on co-expression networks of differentially expressed genes, and analyzer the importance of each node to the overall network topology.

4.2.8 qRT-PCR validation of RNA-Sequencing results

To validate the gene expression results of the RNA-Sequencing, the

Table 4-1 Primer sequences for qRT-PCR validation of RNA-Seq

Gene ID	Description	Forward primer 5' - 3'	Reverse primer 5' - 3'
Solyc08g006960.2	CAC (Housekeeping)	CCTCCGTTGTGATGTAACTGG	TTGGTGGAAAGTAACATCATCG
Solyc05g053550.2	CHS2; chalcone synthase	GGTCACCGTTGAGGAGGTTC	TCGATTTATCACACATGCGCT
Solyc05g053410.2	PHYB2; phytochrome B2	AGGATGGTTCCCTGGAGCTT	AGCGAAAACCTGTTGAATTCTG
Solyc06g060830.2	HAT4-MYB	TCCTCATTCCTCGTCAGATCG	TCTCCTCAGTACAGTTCCCTTCT
Solyc08g080040.2	Anthocyanidin synthase	GAACTAGCACTTGGCGTCGAA	TTGCAAGCCAGGCACCATA

4.3 RESULTS

4.3.1 Summary of RNA-Seq Libraries and Alignment to Genome

Approximately 354 million Illumina sequencing reads were generated from 15 libraries with an average sequencing depth of 24million clean paired-end reads (See **Table 4-2**). Raw reads were aligned against the Solanum lycopersicum SL2.5 genome (Aflitos S., Schijlen E., de Jong H., de Ridder D., Smit S., Finkers R., Wang J., Zhang G., Li N., Mao L., Bakker F., Dirks R., Breit T., Gravendeel et al., 2014) using HiSat2 (D. Kim et al., 2015), with all samples showing consistent alignment above 97%. The uniquely mapped clean reads were counted using HTSeq (Anders, Pyl, & Huber, 2015), with an average of 19.36 million read counts unambiguously assigned to 21,928 genes. After filtering to remove lowly expressed genes, 19,072 genes were found to be expressed in at least one treatment.

Table 4-2 Summary statistics for RNA-Sequencing

Library	Raw reads		Total reads mapped in pairs		Total read counts	
	(millions)	(%)	(millions)	(%)	(millions)	(%)
R1	22.25	100	21.73	97.7	18.62	83.70
R2	22.37	100	21.81	97.5	18.45	82.50
R3	20.34	100	19.83	97.5	16.62	81.69
B1	22.45	100	21.89	97.5	18.45	82.17
B2	24.68	100	24.05	97.4	20.15	81.64
B3	25.14	100	23.36	92.9	20.74	82.50
RB1	22.31	100	21.65	97.1	17.90	80.25
RB2	24.94	100	24.22	97.1	20.09	80.54
RB3	26.71	100	26.02	97.4	21.78	81.53
RBG1	24.04	100	23.41	97.4	19.64	81.72
RBG2	21.73	100	21.22	97.6	17.86	82.18
RBG3	28.19	100	27.51	97.6	23.18	82.22
FL1	23.31	100	22.76	97.6	19.42	83.30
FL2	22.91	100	22.28	97.3	18.39	80.27
FL3	23.34	100	22.76	97.5	19.14	82.01

*Mapped to tomato genome. R= Red; B= Blue; RB= Red/Blue; RBG= Red/Blue/Green; Fl= Fluorescent.

4.3.2 Quality assessment of transcriptome data

Samples (gene-level counts) were normalized to eliminate differences in sequencing using EdgeR, and the library-normalized counts-per-million (CPM) data qualitative assessed in Noiseq (See **Figure 8-5**; **Figure 8-6**; **Figure 8-7**). The Sensitivity plot (See **Figure 8-5**) identifies that half of the genome (49%; 19,072 genes) is expressed within tomato leaves regardless of light quality above a threshold of 1 CPM. A large proportion of genes, approximately 20% genome in each treatment, were found to be expressed below 1 CPM. As the interpretation of lowly expressed genes is impaired as there is not a sufficient number of counts for statistical vigour`, a CPM minimum threshold of 1 (in at least 3 of 15 samples) was set, filtering out lowly expressed genes from the down-stream analysis. Comparison of the distribution of reads between treatments shows that prior to filtering (**Figure 8-6a**) the data exhibited a bimodal distribution pattern, with a peak around -6 logCPM and a second more evenly distributed peak around 5logCPM. Normal distribution of count data was attained after applying the cut-off to remove genes with CPM <1 (**Figure 8-6b**).

Detecting read-mapping biases in transcriptomic data is essential as RNA-Seq data can suffer from sample-specific biases which result from technical artifacts from RNA extraction and library preparation. Comparison of gene length (**Figure 8-7b**) and GC content (**Figure 8-7a**) against read count distribution revealed a normal distribution with expected peaks in GC content at the expected 40-60% range and there is no sample-specific bias in the transcriptomic data which will affect differential expression analysis, and therefore no bias correction is needed. Biotype composition was also assessed (**Figure 8-8**) – the proportion of different RNA types – which can be altered during the preparation for sequencing. The Qiagen RNA clean-up kit used post-extraction filters out RNA below 200 nucleotides in length, whilst we elected to use poly-A enrichment to enhances the proportion of mRNA in each sample as we are primarily interested in protein-coding genes. The most abundant biotype detected in all treatments is protein-coding genes, with over 90% of counts assigned to protein-coding genes across all treatments.

4.3.3 Unsupervised analysis of Transcriptomic data

To assess the transcriptome similarity between samples, principal component analysis (PCA) and hierarchical clustering were performed on the log-normalized CPM for each sample (Figure 4-1). Both analyses revealed discrete clustering of samples according to different treatments and biological replicates, indicating high-similarity between the transcriptomes of tomato leaves grown under the same LED spectra.

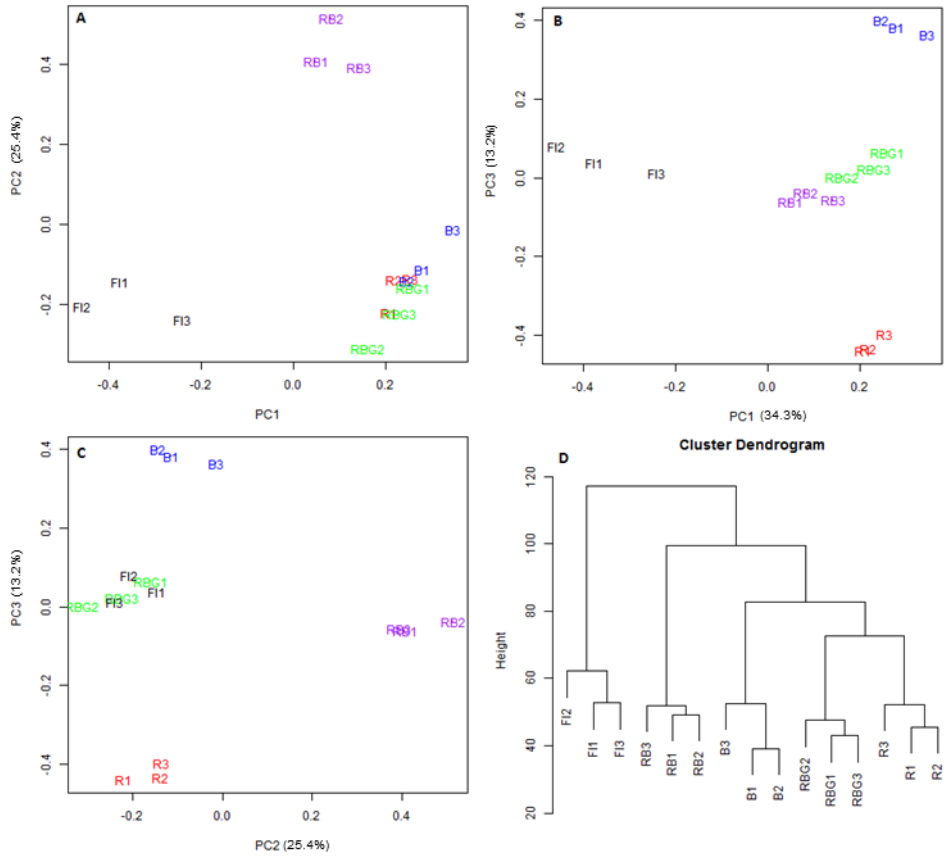


Figure 4-1 PCA and Hierarchical clustering of RNA-Seq data. A-C is a PCA analysis of variant normalized read count data in which input samples treated with different light condition. A) Principal components 1:2; B) Principal components 1:3; C) principal components 2:3. D) Hierarchical clustering based on Euclidean distances. Genetic distance between samples was calculated from the Euclidean distance between log-normalized count data, filtered to remove genes in which cpm <1 with biological replicates per treatment. Treatment groups: Monochromic red light= R; Monochromic Blue= B, Dichromic Red/Blue= RB; Tri-chromic Red/Blue/Green= RBG; Fluorescent tube lighting= Fl.

Principal component analysis of transcriptomic data reduces the dimensionality of the dataset, finding the underlying variables (principal components) which best differentiate the data. The first 3 principal components, those that best

explain the variance, are compared in against each other in Figure 4-1 A-C. Principal component 1 (PC1), the PC which explains the largest proportion of variances (45%) is compared against PC2 and PC3 in Figure 4-1 A-B. Along the PC1 axis, the three Fl samples are clearly separate from the other samples. This suggests that primarily, FL samples are different from all LED treatments, regardless of wavelength. Along the PC2 axis, RB separates from all other treatment groups (Figure 4-1; B-C). It is concerning that RB shows such a high degree of variation along the PC2 from the other LED treatments, especially considering the difference between treatment RB and RBG is 10% green, and so our expectation would be a subtle degree of variation between these two treatments. As for PC3, the RB, RBG, and Fl samples clearly group in the center of the axis, with R and B samples separating to opposite ends of the axis. The 3rd PC expresses the difference between the two monochromatic light treatments R and B from both each other and the three mixed light treatments RB, RBG, and FL, and may express the effect of LED spectra on the transcriptome, and this will be further explored through differential expression analysis. The dendrogram of the hierarchical clustered samples also identifies the same trend that within each treatment group samples are tightly clustered, and that between treatment groups, Fl followed by RB are more dissimilar to other samples, whereas R, B and RBG show the least variation.

4.3.4 Transcriptomic analysis of MT grown under different spectral qualities.

To identify differentially expressed genes (DEGs), we used R package EdgeR to evaluate the significance of the difference in expression and to control for multiple testing. Normalized and filtered RNA-Seq data were fitted to a negative binomial log-linear model and gene-wise dispersion estimates were calculated. Likelihood-ratio testing was conducted making a pair-wise comparison between all possible treatment combinations, with a false discovery threshold set at 0.05 (McCarthy, 2012). As RB exhibited substantial unexplainable variance, these samples were excluded from the differential expression analysis. We first investigated the effect of LED spectra on Micro-Tom leaf transcriptome through pair-wise comparisons of differential expression between R, B, and RBG in pair-wise comparisons. After this, we

conducted a second differential expression analysis comparing the three LED transcriptomes R, B and RBG to the Fl samples.

Differential expression analysis

Differentially expressed genes (DEGs) were identified in pair-wise comparisons between R, B, and RBG light conditions, and are summarised and compared in **Figure 4-2**, while the volcano plots of significance and size of differential expression between treatments is presented in **Figure 4-3**. There are 5206 genes in total were significantly DE between the three treatments R, B, and RBG. In the comparison between the two monochromatic light treatments R and B (RvB), 3348 genes were differentially expressed, of which 1653 were significantly up-regulated and 1795 were significantly down-regulated. In the comparison between R and RBG (RvRBG), there were 2846 genes differentially expressed; with 1361 up- and 1485 down- regulated. Finally, in the comparison between BvRBG, there were 2232 genes significantly differentially expressed; 1086 up-regulated and 1147 down-regulated. The volcano plots (See **Figure 4-3**) of RvB and RvRBG showed a relatively equal distribution between up and down-regulated genes. However, in the BvRBG, there is a far greater proportion of up- than down-regulated genes, as log2fold change increases above 1.

The relationship between DEG sets from each comparison was compared for common and unique elements, which is visualized in the Venn (See **Figure 4-2B**). There were 5506 genes differentially expressed in at least one pair-wise comparison between R, B, and RBG. Only 385 genes (7%) were commonly DE between RvB, RvRBG, and RvRBG differentially expressed gene sets. Of the 5506 genes DE in at least one comparison, 1174 genes (23%) were commonly differentially expressed between both RvB and RvRBG, indicating that these genes significantly differ in expression in R compared to both B and RBG.

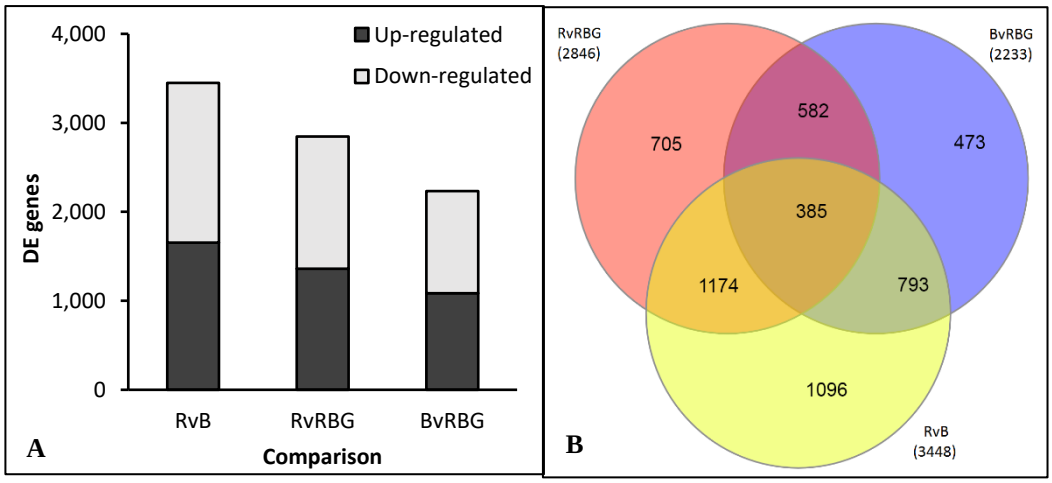


Figure 4-2 RvBvRBG differential expression analysis summary and comparison of overlap in DE gene sets. A, Differentially expressed genes between RvBvRBG in pair-wise comparisons. B, Venn overlap of differentially expressed genes between RvBvRBG in pair-wise comparisons. Significance called at FDR <0.05. n=3.

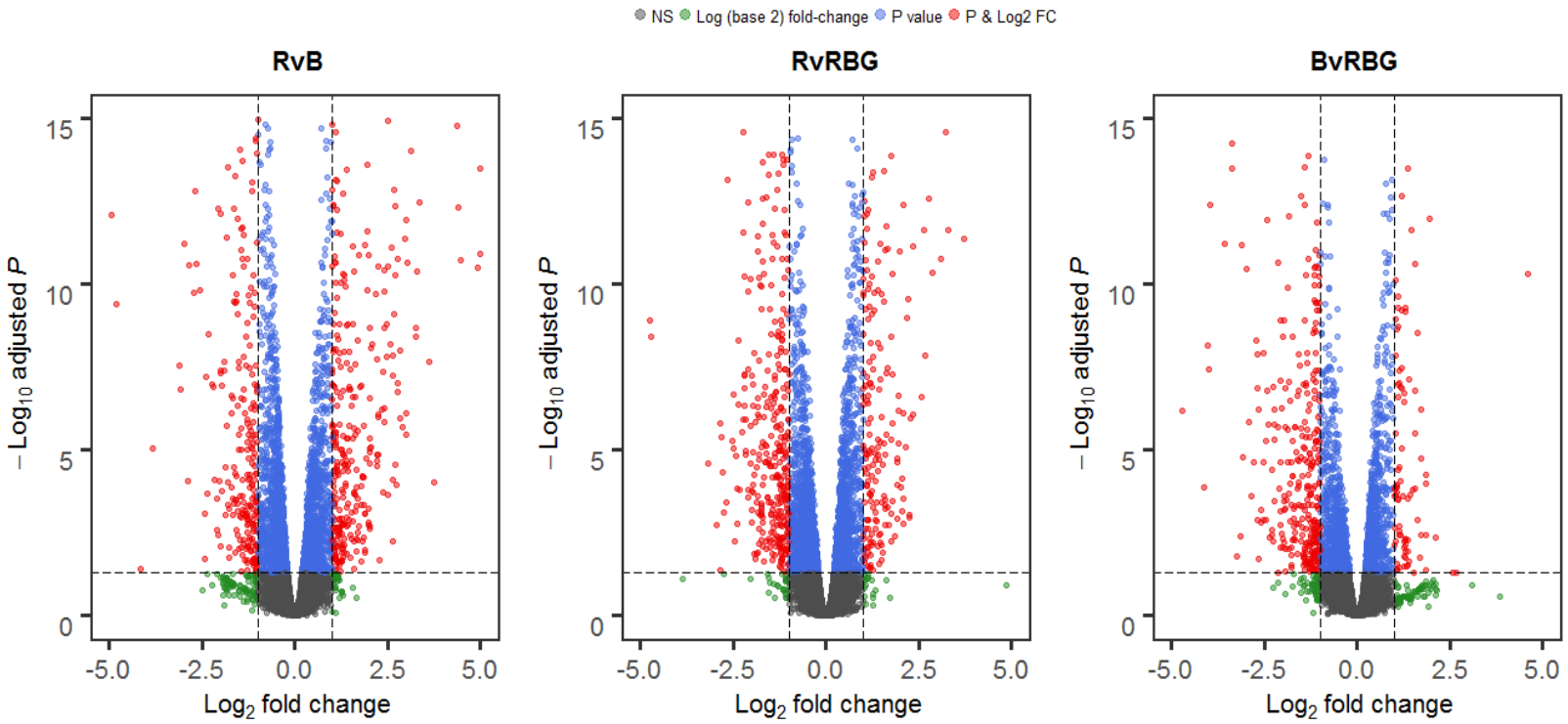


Figure 4-3 Volcano plot of differentially expressed genes in RvBvRBG pair-wise comparisons. The colour key identifies genes which are: Not significantly DE (NS; FDR>0.05)= grey; significantly differentially expressed (FDR<0.05) = blue; NS but with two-fold change in expression (log_2fold change difference in mean expression of >1 or <-1) = green; Both significantly DE and two0fold change in expression= red.

Top DEGS between R, B, and RBG

The top differentially expressed genes in terms of fold-change were evaluated between RvB, RvRBG, and BvRBG (See **Table 4-3**). Every single gene in the top 10 ranked RvB up-regulated list is significantly differentially expressed in RvRBG and significantly down-regulated in BvRBG. The top-ranked differentially expressed gene in both RvB up-regulated (log2FC=9.7) and BvRBG down-regulated (log2FC=-7.2) sets is Solyc07g054980.1, an MYB family transcription factor. Solyc07g054980.1 is homologous to *Arabidopsis* MYB-15, an R232 MYB TF which is responsive to several hormones and positively regulates cold tolerance. Two other of the highly ranked genes in RvB up-regulated are Soly12g00890.1 and Solyc09g010000.2, both of which are important enzymes involved in hormone homeostasis. Soly12g00890.1 encodes a cytokinin oxidase/dehydrogenase 2 which is involved in the degradation of growth hormone cytokinin. Solyc09g010000.2 encodes an ethylene biosynthesis gene, 1-aminocyclopropane-1-carboxylase oxidase (ACO; Solyc09g010000.2) involved in a rate-limiting step of ethylene biosynthesis. Four of the top 10 RvB up-regulated genes are involved in isoprenoid biosynthesis. Solyc11g011240.1 encodes Geranylgeranyl pyrophosphate synthase I (GGPS1), which is an enzyme that catalyzes the formation of geranylgeranyl pyrophosphate and serves as the branch-point compound to several isoprenoids, including carotenoids, chlorophylls, and several phytohormones including gibberellin, abscisic acid, and jasmonic acid (Ruppel et al., 2013). The other three isoprenoid metabolism genes in the top 10 RvB upregulated genes are also ranked in the top 10 BvRBG down-regulated genes. Solyc09g082660.2, Solyc02g085020.2, Solyc08g080040.2 encode a caffeoyl-CoA O-methyltransferase, dihydroflavonol 4-reductase, anthocyanidin synthase, respectively, all of which are involved in the biosynthesis of anthocyanin.

The most highly down-regulated gene in RvB comparison encoded an ‘unknown protein’. Solyc06g060830.2 is on both the RvB down-regulated and BvRBG up-regulated to DE gene lists, exhibiting expression pattern of being up-regulated in B only compared to R and RBG. Solyc06g060830.2 encodes a Homeobox-leucine zipper protein, homologous to *Arabidopsis* ATHB2, which is a transcription factor involved in regulating photoperiodic control of plant growth and shade avoidance responses (Kunihiro et al., 2011). An auxin-responsive GH3-like (Solyc12g084490.1) was 9th most down-regulated in RvB, and also significantly

down-regulated in R compared to RBG. GH3 family proteins are auxin signalling genes which negatively regulate auxin homeostasis by conjugating free auxin to an amino acid. An early-light induced protein (ELIP7; Solyc09g082690.1), was -4.7 and -3.1 log2fold down-regulated in R compared to B and RBG. ELIPs are chlorophyll a/b binding proteins which promote tolerance to high light stress and in Arabidopsis have been identified as being regulated by transcription factor HY5 in response to red and blue light signals (Harari-Steinberg, Ohad, & Chamovitz, 2007; Kleine et al., 2007). Several of the remaining RvB down-regulated genes encode defense responsive genes, proteinase inhibitors which are involved in pathogen defense; both Kunitz trypsin inhibitors Solyc09g089530.2 and Solyc11g022590.1), and proteinase inhibitor I (Solyc09g089530.2, Solyc09g084470.2, Solyc09g084480.2).

The most highly up-regulated gene in RvRBG up-regulated differential expression analysis is a beta-galactosidase (Solyc10g055470.1), which is 4.5- and 5-log_2fold up-regulated in R compared to B and RBG, respectively. Beta-galactosidase in tomato function in cell wall expansion and remodeling, and plays an important role in fruit ripening (Eda, Matsumoto, Ishimaru, & Tada, 2016). In addition to cytokinin dehydrogenase and GGPS1 already discussed above as being RvRBG up-regulated, several of the remaining top RvRBG up-regulated genes are related to defense response. Solyc02g089620.1 encodes a Proline dehydrogenase, is involved in Pro-P5C cycle which can generate reactive oxygen species and has been associated with both pathogen resistance and abiotic stress tolerance (Cecchini, Monteoliva, & Alvarez, 2011). Of the RvRBG most highly down-regulated RvRBG, ELIPs, gibberellin 2-beta-dioxygenase 7 is involved in the gibberellin metabolism pathway, inhibiting bio-active gibberellin production through catalyzing the 2beta-hydroxylation of gibberellins (GA) precursors, rendering them unable to be converted to active GA.

The top 10 most highly differentially expressed between BvRBG are: a xyloglucan endotransglucosylase/hydrolase 9 (XTH9; Solyc09g092520.2) was both highly up-regulated in BvRBG and RvRBG indicating a down-regulation in RBG compared to R and B. XTHs are cell wall re-modeling proteins involved which is involved in cell elongation and growth (Shin et al., 2006). Solyc04g080820.2 a second Cytokinin oxidase/dehydrogenase is both significantly up-regulated in BvRBG

(log2FC= 2.6) and down in RvRBG (log2FC=-2.1) meaning it is only up-regulated in B transcriptome.

Six of the top 10 most highly down-regulated genes in BvRBG relate to flavanoid and more specifically anthocyanin biosynthesis. In addition to the previously mention flavonoid biosynthesis genes mentioned along as being both RvB down-regulated as well as BvRBG down-regulated, three more flavonoid biosynthesis genes, glutathione S-transferase (Solyc02g081340.2) and UDP-glucosyltransferase-1 (Solyc12g098590.1), and Cytochrome P450 (Solyc11g066580.1) – a putative flavonoid 3’5’-hydroxylase – all exhibit high down-regulation in B compared to RBG (<-4 log2fold) and R (<-3.8 log2fold), while being generally being significantly higher in RBG compared to R. A Gibberellin 2-oxidase (Solyc10g007560.1), which are involved in inactivation of bio-active gibberellin, is ~5 log2fold in both BvRBG and up RvRBG, identifying a B-specific down-regulation.

Table 4-3 Top 10 most highly up- and down- regulated genes in RvBvRBG comparisons

#	Gene_ID	Description	RvB		RvRBG		BvRBG	
			LogFC	FDR	Log FC	FDR	Log FC	FDR
RvB up-regulated								
1	Solyc07g054980.1	Myb-related transcription factor	**9.7**	**1.2E-54**	2.5	7.5E-20	-7.2	1.8E-13
2	Solyc12g008900.1	Cytokinin oxidase/dehydrogenase 2	**7.0**	**6.9E-42**	2.9	4.2E-11	-4.1	5.6E-17
3	Solyc03g031870.1	Acyl-CoA synthetase/AMP-acid ligase	**6.7**	**3.5E-42**	2.8	2.6E-13	-4.0	4.1E-13
4	Solyc11g011240.1	GGPS1; Geranylgeranyl pyrophosphate synthase 1	**5.3**	**5.2E-49**	2.9	6.2E-23	-2.4	1.6E-07
5	Solyc08g080040.2	Anthocyanidin synthase	**5.2**	**1.5E-31**	-1.4	2.2E-07	-6.7	1.3E-58
6	Solyc05g012430.1	LRR receptor-like serine/threonine-protein kinase, RLP	**5.2**	**2.3E-37**	1.8	5.1E-08	-3.4	3.2E-14
7	Solyc09g010000.2	1-aminocyclopropane-1-carboxylate oxidase-like protein	**4.9**	**3.1E-11**	2.3	1.1E-03	-2.7	1.3E-03
8	Solyc08g016270.1	LRR receptor-like serine/threonine-protein kinase, RLP	**4.8**	**6.8E-54**	2.4	1.6E-16	-2.4	7.2E-16
9	Solyc09g082660.2	Caffeoyl-CoA O-methyltransferase	**4.8**	**3.6E-32**	-1.2	1.1E-04	-6.0	1.8E-51
10	Solyc02g085020.2	Dihydroflavonol 4-reductase	**4.7**	**1.3E-35**	-1.3	6.1E-06	-6.0	2.6E-59
RvB down-regulated								
1	Solyc05g008240.2	Unknown Protein	**-7.6**	**2.7E-32**	-2.9	4.4E-02	4.7	6.6E-24
2	Solyc03g098790.1	Kunitz-type protease inhibitor	**-6.1**	**5.1E-14**	-4.7	3.9E-09	NS	NS
3	Solyc09g008670.2	Threonine ammonia-lyase biosynthetic	**-5.0**	**8.3E-13**	NS	NS	4.6	4.7E-11
4	Solyc09g082690.2	Early light-induced protein 7	**-4.7**	**1.9E-52**	-3.1	2.0E-22	1.6	2.9E-09
5	Solyc09g089530.2	Proteinase inhibitor I	**-3.8**	**9.2E-06**	-3.0	1.8E-03	NS	NS
6	Solyc09g084470.2	Proteinase inhibitor I	**-3.1**	**1.5E-07**	-2.0	1.5E-03	NS	NS
7	Solyc11g022590.1	Kunitz trypsin inhibitor 4	**-3.0**	**5.9E-12**	-2.2	1.2E-06	NS	NS
8	Solyc06g060830.2	Homeobox-leucine zipper protein	**-2.9**	**5.8E-91**	-0.5	4.9E-03	2.4	7.5E-66
9	Solyc12g005310.1	Auxin-responsive GH3-like	**-2.9**	**2.2E-18**	-1.9	1.5E-06	1.0	9.2E-04
10	Solyc09g084480.2	Proteinase inhibitor I	**-2.9**	**8.4E-05**	NS	NS	2.1	4.5E-03
RvRBG up-regulated								
1	Solyc10g055470.1	Beta-galactosidase	4.5	1.8E-11	**5.0**	**1.7E-12**	NS	NS
2	Solyc06g083130.2	MazG nucleotide pyrophosphohydrolase	4.4	2.4E-21	**3.8**	**2.3E-18**	NS	NS
3	Solyc10g048020.1	Pathogenesis-related protein-1	7.0	2.3E-20	**3.7**	**4.1E-12**	-3.2	1.7E-02
4	Solyc02g089620.2	Proline dehydrogenase	2.2	2.9E-11	**3.6**	**6.5E-25**	1.4	2.9E-04
5	Solyc06g071700.1	Primary amine oxidase	5.3	6.3E-35	**3.4**	**1.2E-24**	-1.9	4.6E-02
6	Solyc09g098420.1	Receptor like kinase, RLK	5.6	3.2E-23	**3.3**	**2.4E-12**	-2.3	3.8E-03
7	Solyc06g084190.2	Non-specific lipid-transfer protein	3.7	9.3E-18	**3.2**	**2.5E-15**	NS	NS

#	Gene_ID	Description	RvB		RvRBG		BvRBG	
			LogFC	FDR	Log FC	FDR	Log FC	FDR
8	Solyc02g093960.2	Genomic DNA chromosome 5 P1 clone MAC12	4.8	3.7E-19	**3.1**	**1.7E-11**	NS	NS
9	Solyc12g008900.1	Cytokinin oxidase/dehydrogenase 2	7.0	6.9E-42	**2.9**	**4.2E-11**	-4.1	5.6E-17
10	Solyc11g011240.1	Geranylgeranyl pyrophosphate synthase 1	5.3	5.2E-49	**2.9**	**6.2E-23**	-2.4	1.6E-07
		RvRBG down-regulated						
1	Solyc09g082700.2	Early light-induced protein 7	-4.8	3.8E-10	**-4.7**	**1.2E-09**	NS	NS
2	Solyc03g098790.1	Kunitz-type protease inhibitor	-6.1	5.1E-14	**-4.7**	**3.9E-09**	NS	NS
3	Solyc03g036470.1	Phenylalanine ammonia-lyase	NS	NS	**-3.2**	**2.6E-05**	-2.5	1.3E-03
4	Solyc09g082690.2	Early light-induced protein 7	-4.7	1.9E-52	**-3.1**	**2.0E-22**	1.6	2.9E-09
5	Solyc09g089530.2	Proteinase inhibitor I	-3.8	9.2E-06	**-3.0**	**1.8E-03**	NS	NS
6	Solyc05g008240.2	Unknown Protein	-7.6	2.7E-32	**-2.9**	**4.4E-02**	4.7	6.6E-24
7	Solyc07g052070.1	Cytochrome P450	-3.1	2.8E-08	**-2.8**	**1.5E-06**	NS	NS
8	Solyc02g080120.1	Gibberellin 2-beta-dioxygenase7	-2.4	2.1E-04	**-2.8**	**4.2E-06**	NS	NS
9	Solyc02g091180.1	cDNA clone J100026I16 full insert sequence	-2.1	2.5E-03	**-2.8**	**4.6E-05**	NS	NS
10	Solyc07g040960.1	Os07g0175100 protein	NS	NS	**-2.7**	**7.4E-04**	NS	NS
		BvRBG up-regulated						
1	Solyc05g008240.2	Unknown Protein	-7.6	2.7E-32	-2.9	4.4E-02	**4.7**	**6.6E-24**
2	Solyc09g008670.2	Threonine ammonia-lyase biosynthetic	-5.0	8.3E-13	NS	NS	**4.6**	**4.7E-11**
3	Solyc06g024340.1	Unknown Protein	NS	NS	NS	NS	**2.7**	**4.9E-02**
4	Solyc04g080820.2	Cytokinin oxidase/dehydrogenase	-2.1	4.3E-19	NS	NS	**2.6**	**1.3E-26**
5	NCRNA_9_2	Plant signal recognition particle RNA	NS	NS	NS	NS	**2.6**	**4.9E-02**
6	Solyc06g060830.2	Homeobox-leucine zipper protein	-2.9	5.8E-91	-0.5	4.9E-03	**2.4**	**7.5E-66**
7	Solyc12g008600.1	Unknown Protein	NS	NS	1.8	4.8E-11	**2.2**	**1.5E-16**
8	Solyc05g054750.2	Plant-specific domain TIGR01589 family protein	-2.4	1.8E-40	NS	NS	**2.1**	**1.0E-33**
9	Solyc09g084480.2	Proteinase inhibitor I	-2.9	8.4E-05	NS	NS	**2.1**	**4.5E-03**
10	Solyc09g092520.2	Xyloglucan endotransglucosylase/hydrolase8	0.6	4.4E-02	2.6	4.7E-26	**2.0**	**5.1E-16**
		BvRBG down-regulated						
1	Solyc07g054980.1	Myb-related transcription factor	9.7	1.2E-54	2.5	7.5E-20	**-7.2**	**1.8E-13**
2	Solyc08g080040.2	Anthocyanidin synthase	5.2	1.5E-31	-1.4	2.2E-07	**-6.7**	**1.3E-58**
3	Solyc09g082660.2	Caffeoyl-CoA O-methyltransferase	4.8	3.6E-32	-1.2	1.1E-04	**-6.0**	**1.8E-51**
4	Solyc02g085020.2	Dihydroflavonol 4-reductase	4.7	1.3E-35	-1.3	6.1E-06	**-6.0**	**2.6E-59**
5	Solyc02g081340.2	Glutathione S-transferase	4.2	1.4E-23	-1.2	1.6E-04	**-5.4**	**5.2E-41**

#	Gene_ID	Description	RvB		RvRBG		BvRBG	
			LogFC	FDR	Log FC	FDR	Log FC	FDR
6	Solyc12g098590.1	UDP-glucosyltransferase family 1 protein	3.8	3.3E-30	-1.5	1.3E-08	**-5.3**	**2.6E-59**
7	Solyc11g066580.1	Cytochrome P450	4.0	1.0E-18	-1.2	2.7E-04	**-5.3**	**2.0E-34**
8	Solyc10g007560.1	Gibberellin 2-oxidase 3	5.0	1.2E-11	NS	NS	**-5.1**	**6.0E-12**
9	Solyc02g092890.1	Unknown Protein	6.7	2.7E-21	2.0	6.1E-06	**-4.7**	**6.5E-07**
10	Solyc02g067730.1	RNA exonuclease 4	6.3	3.7E-17	2.1	8.0E-06	**-4.1**	**1.3E-04**

NS= not significantly differentially expressed (FDR>0.05)

Functional enrichment of differentially expressed gene sets

To gain biological insight into the biological processes and pathways that were differentially regulated under varying spectral qualities, functional enrichment analysis was performed on the DEG sets generated from the pair-wise comparisons as well as unique and common genes identified from Venn overlap. Bioconductor-based enrichment analysis was conducted using Gene Ontology (GO) and KEGG databases, and REVIGO was used to reduce overlapping terms within the enriched lists. A separate analysis of up- and down-regulated genes for GO enrichment was conducted as it is more powerful for detecting biologically significant differences (Hong et al, 2014).

RvB differentially expressed genes

The 3448 DEGs were separated into 1653 up- and 1795 down-regulated genes. The RvB up-regulated DEGs were enriched for 22 biological processes, 17 molecular functions, 4 cellular compartment terms and 4 KEGG pathways (See Full gene enrichment tables

Table 8-7). Genes up-regulated in red-light compared to blue were related to biotic stress and defense, with several terms including ‘systemic acquired resistance’ (*p*=1.4e-06), ‘jasmonic acid-mediated signalling’ (*p*=3.88e-04) and ‘salicylic acid-mediated signalling’ (*p*=5.36e-04) enriched. This was further supported by enrichment of KEGG pathways relating to ‘Plant-pathogen interaction’ (*p*=1.493e-09) and ‘MAPK signalling pathway – Plant’ (*p*=1.58e-08), while enrichment of ‘plant hormone signal transduction’ (*p*=4.66e-10) pathway potentially implicating phytohormones involvement.

The 1795 genes significantly down-regulated between RvB were significantly over-represented for 121 biological processes, 26 molecular functions, 26 cellular compartment terms, and 8 KEGG pathways. Notably, significant enrichment of genes annotated to response to light quality, both the 'response to red light' (p=2.23e-09) and 'response to blue light' (p=7.88e-09) were enriched. The most significantly enriched terms up in B relative to R surrounded photosynthesis and chloroplasts; with 'chloroplasts' (p=3.16e-77), 'thylakoid membrane organization' (p=1.87e-40), 'photosynthesis' (p=1.57e-06), 'photosystem II assembly' (p=1.53e-18), as well as 'carbon fixation in photosynthetic organisms' (p=3.67e-07) KEGG pathway and GO terms relating to control of gene expression from chloroplast and protein-targeting to chloroplast as 'transcription from plasmid promoter' (p=1.19e-17) and 'protein targeting to chlorophyll' (p=1.25e-07). Pigment synthesis was also enriched with 'pigment metabolic process' (p=2.22e-29) as well as specific photosynthetic pigments chlorophyll 'chlorophyll biosynthesis' (p=6.73e-13) and 'carotenoid metabolism', leaf and shoot development (leaf morphogenesis, stomatal complex morphogenesis; shoot system development), transcription (positive regulation of transcription, ncRNA metabolism, mRNA modification) and secondary metabolism (cellular aromatic compound metabolic process ; cellular aldehyde metabolic process ; isopentenyl diphosphate biosynthetic process, glycosinolate biosynthetic process). Biosynthesis of secondary metabolites (p=1.98e-14) was the most enriched KEGG pathway, with carbon fixation in photosynthetic organisms and carbon metabolism also significantly over-represented.

RvRBG differentially expressed genes

In the RvRBG pair-wise comparison, 1361 and 1485 genes were significantly up-regulated and down-regulated, respectively. The significantly up-regulated genes were enriched for 11 BP, 11 MF, 7 CC terms and 2 KEGG pathways (See **Table 8-9**). The most significantly enriched terms in the BP and MF terms related to 'protein phosphorylation' (p=9.71e-20), 'protein kinase activity' (p=4.62e-11), and the KEGG category 'MAPK signalling pathway – Plant' (p=8.26e-04). The RvRBG up-regulated genes were also significantly over-represented with terms related to cell growth, such as 'unidimensional growth' (p=4.85e-04), 'developmental growth' (p=5.47e-04), and cell-wall metabolism terms such as 'xyloglucan metabolic process' (p=3.57e-04) and 'xyloglucan: xyloglucosyl transferase activity' (p=8.26e-04) all enriched. Terms

related to hormone signalling were also enriched with both the BP term ‘Hormone-mediated signalling pathway’ (*p*=2.02e-04) and ‘Plant hormone signal transduction’ (*p*=7.05e-06) both over-represented.

The 1485 down-regulated genes between R compared RBG were significantly enriched for 26 BP, 20 MF, 12 CC and 6 KEGG terms (See **Table 8-10**). Blue-light signalling was implicated in the up-regulation of genes in RBG relative to R from over-representation of genes annotated to ‘Response to Blue light’ (*p*=2.62e-04) and ‘Response to UV-B’ (*p*=6.69e-05). There was also over-representation of genes related to ‘Transcription factor activity, sequence-specific DNA binding’, indicating a coordinated transcriptional control by a large group of transcription factors. A substantial amount of the enriched terms related to photosynthesis; including BP terms “Photosynthesis- light harvesting’ (*p*=3.49e-09), and ‘Photosynthesis, light reaction’ (*p*=5.11e-04), as well as the KEGG category ‘photosynthesis – Antennae proteins’ (*p*=8.75e-08), while all of 12 enriched CC terms were components of the chloroplast (*p*=2.40e-08). Photosynthetic pigment metabolism was also enriched in genes significantly up-regulated in B relative to RBG, with ‘pigment metabolism’ (*p*=2.40e-07) ‘carotenoid biosynthesis’ (*p*=1.14e-04), and ‘chlorophyll biosynthesis’ (3.60e-04) enriched. Di-terpenoid biosynthesis, which contains growth hormone gibberellin was also over-represented.

BvRBG

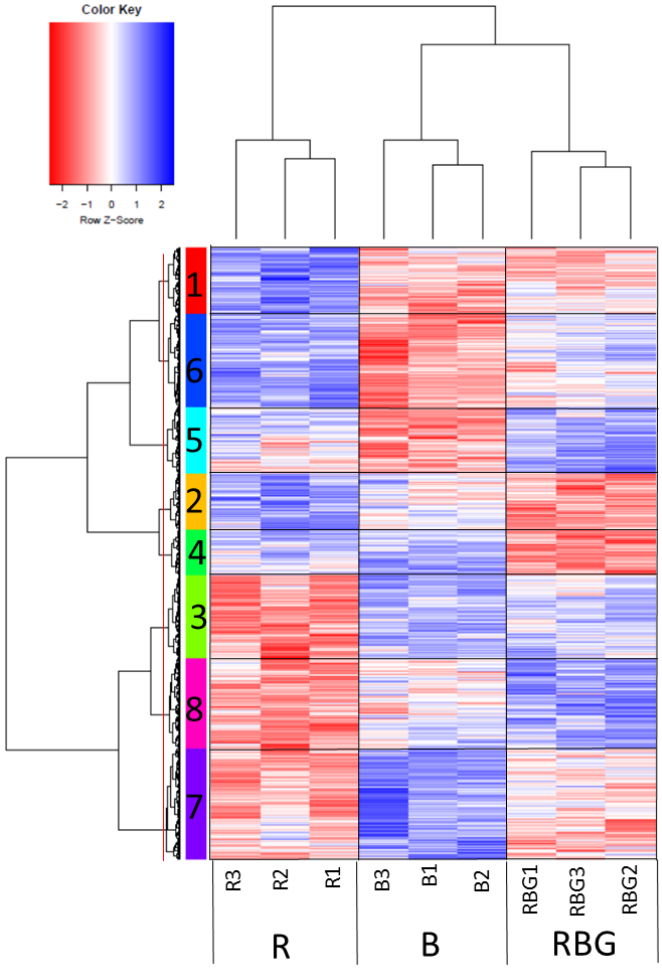
The 1147 genes significantly down-regulated in the BvRBG comparison genes were significantly enriched for BP, MF, CC, and KEGG (See **Table 8-12**). A substantial number of enriched terms related to defense including biological processes terms regulation of defense response, regulation of plant-type hypersensitive response, and the KEGG pathways MAPK signal transduction (and protein serine/threonine kinase in MF) and plant-pathogen interaction. The ‘Plant hormone signal transduction’ pathway was over-represented, while so was the response to abscisic acid stimulus, and the alpha-linolenic acid pathway containing the biosynthesis pathway for defense hormone JA. Transcription factor activity (‘Transcription’ ‘factor activity, sequence-specific binding’) and protein-targeted modification involved in protein degradation (ubiquitin-protein transferase activity) were enriched. To further complement the association with disease, cellular component enriched for an integral

component of membrane, a category highly associated with MAPK pathways, and photosystem II was also over-represented.

Far greater enrichment was observed in the 1086 genes up-regulated in B relative to RBG, with significant enrichment in response to light (‘Red, far-red light phototransduction’, ‘cellular response to radiation’), transcription (‘positive regulation of transcription, DNA-templated’) and RNA processing ‘rRNA processing’, ‘mRNA modification’, ‘ncRNA metabolism’, ‘mRNA modification’),’photosynthesis’, ‘chloroplast organisation and chlorophyll metabolism’, as well as other primary metabolic processes (‘starch metabolism’, ‘maltose metabolism’, ‘oligosaccharide metabolic process’). Enrichment for cellular compartment identified the DE genes were over-represented as being chloroplast localized (‘Chloroplast’), cell-wall localized (‘plant-type cell wall’), and ‘cytoplasm’. KEGG enrichment found enrichment relating to ‘circadian rhythm’ and ‘biosynthesis of secondary metabolites’, this correlates with the photoreceptor activity enrichment in MF category, and other categories were ‘plastid sigma factor activity’ and ‘core DNA-dependent RNA polymerase binding promoter specific activity’.

4.3.5 Hierarchical clustering of RvBvRBG DEGs

To further analyze the gene differentially expressed between RvBvRBG transcriptome pair-wise comparisons, the 5209 genes identified to be differentially expressed in at least one comparison were analyzed by hierarchical clustering (See **Figure 4-4**). Genes were clustered in 8 discrete clusters based on the similarities of their expression profiles across the 9 samples of the R, B, and RBG treatments, with the table in showing a number of genes assigned to each cluster. Below the size, expression trends and GO and pathway enrichment of each cluster is examined.



#	Colour	Genes
1	Red	564
2	Orange	477
3	Light green	705
4	Dark green	385
5	Light blue	567
6	Dark blue	789
7	Purple	945
8	Pink	776

Figure 4-4 Hierarchical clustering with a heatmap of RvBvRBG differentially expressed genes. Hierarchical clustering was performed on the 5209 genes differentially expressed in at least one pairwise comparison between R, B, and RBG transcriptomes based on hierarchical clustering of genetic distance (z-score) using Euclidean distance method. Heatmap of expression is 3-colour with red indicating down-regulated genes and blue indicating up-regulated based on X-axis dendrogram cluster samples. Y-axis dendrogram clusters genes, with the red line indicating cur-off for cluster membership. Cluster membership indicated by colour and number on Y-axis, with a table (right) indicating the number of genes in each cluster.

Cluster 1 genes exhibit up-regulation of genes expression in R, compared to both B and RBG genes. These genes were over-represented for involvement in ‘MAPK signalling’ (*p*=3.9E-07) and ‘plant-pathogen interaction’ (*p*=0.00011) KEGG pathways. GO terms over-represented included localization to membrane ‘integral component of membrane’ as well as the biological process involved in ‘signal transduction’ (*p*=0.000743)and ‘protein phosphorylation’ (*p*=3.25E-07).

Cluster 6 Genes were highly up-regulated in R and down in B with RBG exhibiting a general trend of moderate up- or down-regulation (z-score). Similarly to cluster 1 these genes were enriched for genes membrane-associated genes, with enrichment of CC terms ‘Integral component of membrane’ (*p*= 4.10E-08) and ‘membrane part’ (*p*=1.66E-06), while ‘protein phosphorylation’ (*p*= 1.60E-14) was again the most significantly over-represented term. This cluster was enriched for genes assigned to KEGG pathways ‘alpha-linoleic acid metabolism’ (*p*= 1.25E-05) which is the jasmonic acid biosynthesis pathway, as well as the ‘Plant hormone signal transduction’ (*p*= 6.38E-05).

The 477 genes assigned to cluster 2 exhibit relatively high expression levels in R, moderate in B and are down in RBG. Significant over-representation of genes involved in ‘xyloglucan metabolic process’ (*p*= 8.42E-05), ‘developmental growth involved in morphogenesis’ (*p*= 1.49E-04), and ‘cell growth’ (*p*= 1.70E-04) all of which are associated with growth, while enrichment in cellular compartment identified these genes to be ‘integral components of membrane’ (*p*= 1.66E-06) and ‘cell wall’ (*p*= 2.11E-05). Xyloglucan endotransglucosylase hydrolase 6 (XTH16; Solyc07g052980.1). Cytokinin oxidase (CKX6; Solyc12g008900.1) which catalyzes the catabolism of growth hormone cytokinin was highly differentially expressed. Notably, C2H2 transcription factor (Solyc05g009170.1) was 3.4 and 2.3 log2fold up-regulated in RvB and RvRBG respectively.

Cluster 3 contains 705 genes which exhibit a consistent down-regulation R compared to B and RBG. GEA identified massive enrichment with 56 BP, 16 MF, 17CC, and 9 KEGG pathways over-represented. The most highly enriched term was the CC term ‘plastid part’ (*p*= 2.64E-21) with several related terms localizing enriched genes to the chloroplast. Additionally, photosynthesis-related terms, ‘photosynthesis, light harvesting’ (*p*= 4.10E-04), and KEGG pathways ‘carbon

fixation in photosynthetic organisms' (*p*= 1.14E-05) and 'carbon metabolism' (*p*= 4.20E-06) were enriched further implicating genes down in R with the association to photosynthesis. Additionally, light signalling pathways, both responses to red light (*p*= 2.73E-05) and response to blue light (*p*= 4.96E-04) were enriched. Additionally, secondary metabolism-related genes were enriched, with the KEGG pathway 'biosynthesis of secondary metabolism' (*p*=3.20E-06) itself significantly over-represented, as well genes related to 'pigment metabolism' (*p*= 1.00E-10) and 'carotenoid biosynthesis' (*p*= 2.90E-08). Phytochrome B encoding gene

Cluster 7 genes were exclusively upregulated in B light, with R and RBG expression both downregulated. This cluster exhibited substantial over-representation of GO terms with 115Bp, 9MF, and 19 CC terms enriched. Primary enrichment of this category related to chloroplast and photosynthesis, with the CC chloroplast the most significantly enriched term (*p*= 9.80E-67), with BP terms including 'transcription from plastid promoter' (*p*= 3.29E-20) and 'photosynthesis' (*p*= 1.29E-19) also enriched. 'Response to blue light' (*p*= 5.67E-04) was also amongst enriched terms. While development related BP terms were enriched including 'leaf morphogenesis' (*p*= 3.33E-09) and 'shoot system development' (*p*= 3.59E-06). Finally, significant enrichment in the KEGG pathway 'biosynthesis of secondary metabolites' (*p*= 3.15E-05) and 'pigment metabolic process' (*p*= 1.08E-13) genes was observed. Two important light signalling transcription factors, bHLH transcription factors HY5 (Solyc08g061130) and HAT4 (Solyc06g060830) were significantly up-regulated in B compared to both R and RBG. In Arabidopsis, HY5 binds to over 9000 genes and transcriptionally regulates over 1100 in response to light (Huiyong Zhang et al., 2011). Meanwhile, HAT4 homolog AtHB2 is transcriptionally up-regulated by B light in *Arabidopsis* (Iannacone et al., 2008).

4.3.6 Transcription factor analysis

Analysis of differentially expressed transcription factors

In the tomato genome, there are 1845 transcription factors, of which 954 were found to be expressed in the leaf transcriptome (CPM >1 in at least 3 samples). 350 unique transcription factors were differentially expressed in at least one comparison between RvB, RvRBG, and RvRBG, with the total number of differentially expressed

transcription factors 216, 200, and 177, respectively. The most highly differentially expressed, ranked by log_2FC (FDR <0.05), transcription factors in each comparison are presented in **Table 4-2**. In both RvB and RvRBG, the most highly up-regulated transcription factor is Solyc07g054980.1 an MYB family transcription factor which is almost exclusively expressed in R, is homologous to Arabidopsis MYB-15, anR232 MYB TF which is responsive to several hormones and positively regulates cold tolerance. Solyc07g054980.1 is also the most down-regulated in BvRBG. The most highly down-regulated transcription factor in both RvB and BvRBG is Solyc06g060830.2, an HD-ZIP TF encoding a homolog of Arabidopsis thaliana ATHB2/HAT4, a phytochrome-regulated mediator of R/Fr light effects negatively regulating gene expression in response to shading (Ohgishi, Oka, Morelli, Ruberti, & Aoyama, 2001; Schena, Lloyd, & Davis, 1993; Steindler et al., 1999). In BvRBG there are two more HD-ZIP transcription factors occupying the most highly differentially expressed transcription factor spots as these genes show significant up-regulation in B relative to all other treatment conditions. The three most highly down-regulated in the RvRBG comparison were all ERF transcription factor genes, including Solyc10g076370.1, an ERF transcription factor with high homology (E-value= $1e^{-32}$) to Arabidopsis transcription factor DREB2C, an abscisic acid (ABA) -responsive stress genes involved in promoting tolerance to abiotic stresses ABA sensitivity (K. Lee et al., 2009).

Table 4-4 Top 5 most highly differentially up- and down- regulated transcription factors RvBvRBG

Rank	Gene_ID	TF Family	RvB DEA		RvRBG DEA		BvRBG DEA	
			LogFC	FDR	LogFC	FDR	LogFC	FDR
RvB up-regulated								
1	Solyc07g054980.1	MYB	9.7	1.2E-54	2.5	7.5E-20	-7.2	1.8E-13
2	Solyc05g007110.2	WRKY	6.4	8.2E-35	2.4	7.1E-12	-4	6.9E-09
3	Solyc05g009170.1	C2H2	3.4	5.4E-19	2.2	1.0E-09	-1.2	2.1E-02
4	Solyc04g009440.2	NAC	2.6	9.1E-24	1.6	3.3E-10	-1.1	1.5E-03
5	Solyc07g055710.2	HSF	2.6	6.3E-09	NS	NS	-3	3.3E-11
RvB down-regulated								
1	Solyc06g060830.2	HD-ZIP	-2.9	5.8E-91	-0.5	4.9E-03	2.4	7.5E-66
2	Solyc12g049350.1	MYB	-2	1.8E-04	NS	NS	1.4	1.2E-02
3	Solyc04g005600.1	MYB	-1.7	8.9E-04	NS	NS	1.3	1.6E-02
4	Solyc10g008160.2	G2-like	-1.6	3.7E-10	-0.9	3.2E-03	0.7	1.1E-02
5	Solyc10g076370.1	ERF	-1.6	2.5E-03	-2.3	2.8E-06	NS	NS
RvRBG up-regulated								
1	Solyc07g054980.1	MYB	9.7	1.2E-54	2.5	7.5E-20	-7.2	1.8E-13
2	Solyc05g007110.2	WRKY	6.4	8.2E-35	2.4	7.1E-12	-4	6.9E-09
3	Solyc05g009170.1	C2H2	3.4	5.4E-19	2.2	1.0E-09	-1.2	2.1E-02
4	Solyc07g045180.2	CO-like	1.6	3.9E-34	2.1	4.9E-56	0.6	2.6E-03
5	Solyc03g119530.2	LBD	1.2	2.5E-07	1.6	8.9E-12	NS	NS
RvRBG down-regulated								
1	Solyc12g009240.1	ERF	NS	NS	-2.5	5.4E-03	NS	NS
2	Solyc03g026280.2	ERF	NS	NS	-2.4	1.7E-03	-1.8	3.6E-02
3	Solyc10g076370.1	ERF	-1.6	2.5E-03	-2.3	2.8E-06	NS	NS
4	Solyc08g083130.2	HD-ZIP	NS	NS	-1.9	1.9E-02	-2.4	4.2E-03
5	Solyc09g010960.2	WRKY	-1.4	2.1E-02	-1.9	3.8E-04	NS	NS
BvRBG up-regulated								
1	Solyc06g060830.2	HD-ZIP	-2.9	5.8E-91	-0.5	4.9E-03	2.4	7.5E-66
2	Solyc02g077590.1	HD-ZIP	-1.3	9.1E-04	NS	NS	1.7	1.8E-05
3	Solyc08g078300.2	HD-ZIP	-1	1.5E-07	0.6	2.4E-02	1.6	9.2E-16
4	Solyc10g054010.1	bZIP	-0.6	4.7E-02	0.8	4.4E-03	1.4	7.5E-08
5	Solyc12g049350.1	MYB	-2	1.8E-04	NS	NS	1.4	1.2E-02
BvRBG down-regulated								
1	Solyc07g054980.1	MYB	9.7	1.2E-54	2.5	7.5E-20	-7.2	1.8E-13
2	Solyc05g007110.2	WRKY	6.4	8.2E-35	2.4	7.1E-12	-4	6.9E-09
3	Solyc09g065100.1	bHLH	1.9	8.3E-04	-1.5	3.1E-05	-3.4	5.6E-15
4	Solyc08g008280.2	WRKY	1.8	6.6E-05	-1.3	6.7E-03	-3.1	6.3E-12
5	Solyc07g055710.2	HSF	2.6	6.3E-09	NS	NS	-3	3.3E-11

To better understand the patterns of expression of transcription factors in RvBvRBG pair-wise comparisons, TFs which were SSTF (absolute log_2FC >1) in at least one comparison had log2FC painted on heatmap (**Figure 4-5).** 20 TF families were in the heatmap represented, with the most highly represented families being the 'WRKY', 'ERFs', and 'MYB_related', which had 28.6 %, 57.7%, and 56.3% of expressed TFs SSTF regulated in at least one comparison. ERF and WRKY transcription factor families associated with the promotion of defense and stress-related gene expression showed differential expression. A notable trend in the heatmap expression is within the ERFs (Ethylene Regulated Factors), with both RvB and RvRBG showing down-regulation implicating ERFs as being significantly down-regulated in R compared to both B and RBG. Another family which stands out based on the heatmap expression profile is the WRKY family, which is can be split into two groups based on patterns observed in gene expression. The first group is the upper-half of the WRKY category which shows down-regulation in the RvRBG and BvRBG, with no significantly DE genes in RvB, suggesting these genes are significantly up-regulated in RBG compared to both R and B. The second group is up-regulated in RvB and down in BvRBG with minimal colour in the RvRBG, suggesting these WRKY genes are significantly down-regulated in B compared to R and RBG, with are expressed similarly.

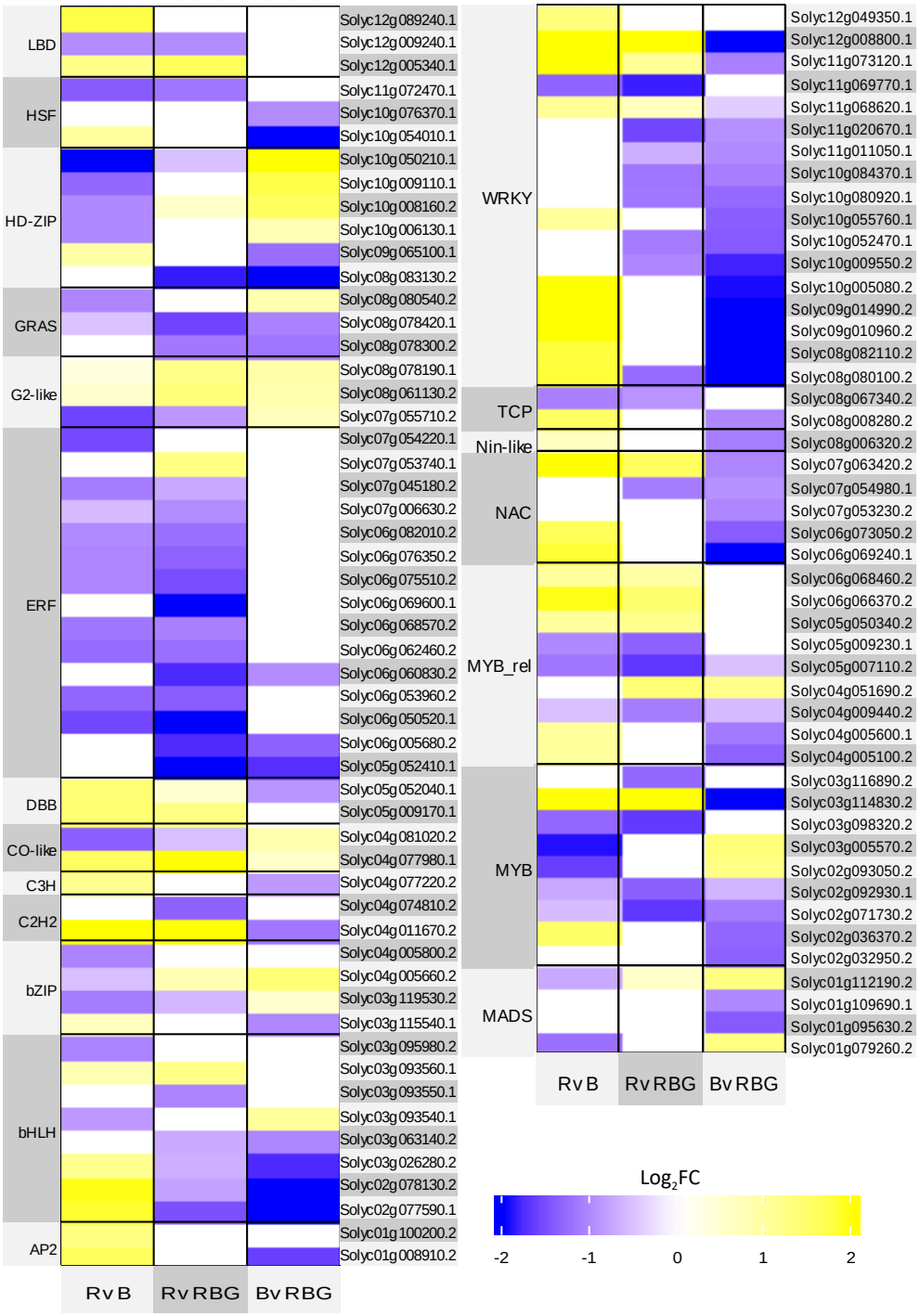


Figure 4-5 Gene expression of differentially expressed transcription factors between RvBvRBG in pair-wise comparisons. 101 TF organized by transcription factor family. DE TFs were filtered to keep only those where log_2FC >1 between at least one comparison. Min and maximum log_2FC values were set at -2, and 2, respectively, with extreme values, painted as the minimum or maximum. Nonsignficiantly expressed genes (FDR<0.05) were assigned a given a log_2FC value of 0.

Transcription factor target enrichment

Transcription factor target enrichment analysis was conducted on genes differentially expressed between RvB leaves. A database of regulatory interactions from PlantRegMap (associated with TFDB) provides a list of curated and predicted TF-target gene interactions.62 transcription factors were identified as having significant over-represented (FDR<0.01) for target genes within the differentially expressed genes compared against a background population of the tomato genome. Genome-wide enrichment comparison, as conducted by PlantRegMap can be misleading, as many of the genes within the tomato genome are only transcribed in certain tissues, and others are not expressed at all, while some non-coding genes were filtered out in sample preparation for sequencing. To reduce bias within the enrichment analysis, we manually conducted TF enrichment against a background population of the 19072 genes identified as being expressed from our experiment using the database of TF-gene interactions from the TFDB 4.0 database (PlantRegMap), and calculated enrichment as using Fisher's exact test with Benjamini Hochberg correction for false discovery. The enriched transcription factors were not filtered to remove those which were not differentially expressed, as it is well established the many transcription factors can be modulated by post-translational modification, including many transcription factors involved in light signalling.

Transcription factor target enrichment analysis of RvB differentially expressed genes was conducted on both RvB significantly up- and down- regulated genes separately (**Table 4-5**). The 1653 RvB significantly up-regulated genes were significantly enriched for seven transcription factors; two bHLH and five WRKY transcription factor family genes. As for the 1795 down-regulated RvB genes, there was 18 transcription factor significantly enriched in RvB down-regulated genes, of which only four were differentially expressed in the RvB set. Of the 18 transcription factors enriched in RvB down-regulated genes, 5 were bHLH and 7 bZIP family transcription factors. Notably, the two most highly enriched transcription factors were bHLH transcription factors, respectively (Rosado et al., 2016). In Arabidopsis, PIF1is Solyc06g008030.2 and Solyc09g063010.2, which encode PIF1a and PIF1b an integral component of the light signal transduction systems and has been implicated in both phytochrome- and cryptochrome- signalling, and regulating photomorphogenesis and light quality dependent regulation of development. PIF1 interacts with both RGA and

GAI promoters to alter gibberellin sensitivity, as well as promoting expression of ABA metabolism genes (E. Oh et al., 2007). In addition to these, a PIF3 encoding gene Solyc01g102300.2 is also significantly enriched in RvB down-regulated genes. While none of the enriched PIF family transcription factors are differentially expressed, they are known to be regulated post-translational in response to red- and blue- light signals (Pablo Leivar & Quail, 2011). Other genes of interest in the list include Solyc08g005290.2 a g-box transcription factor which shows high homology to Arabidopsis AtBZIP16, which is involved in negative regulation of red-light photomorphogenesis and integrates light and hormone signalling through interaction with DELLA protein RGA (Hsieh, Hsieh, & Wu, 2012). Expression of bZIP16 is not significantly altered by abiotic or biotic stresses including light and phytohormones, and ChIP analysis revealed it directly targets ABA-responsive genes (Hsieh et al., 2012). Other G-box b-zip genes enriched in the RvB down-regulated genes are Solyc01g095460.2, Solyc01g095460.2 both of which are significantly up-regulated in R compared to B. Another TF enriched in the RvB down-regulated gene set is Solyc08g005780.2 which encodes a BES1 family transcription factor, a group of E-box binding cis-elements involved in Brassinosteroid signalling (Yin et al., 2005). Solyc03g098320.2 is significantly enriched and highly differentially expressed and is homologous to Arabidopsis EPR1 (Early-phytochrome Responsive 1), a reveille family transcription factor. EPR1 is transiently up-regulated by R light and involved in circadian clock regulation (Kuno, 2003), and other REV genes have been identified as integrating auxin and circadian clock signals to affect growth (Rawat et al., 2009). AtEPR1 mutagenesis experiment revealed aberrant photoresponsiveness in AtEPR1 silenced plants which also had retarded growth (R. Khanna, 2006).

In RvRBG differentially expressed gene sets, 18 transcription factors were over-represented in the RvRBG significantly down-regulated gene set, and 14 in the RvRBG significantly up-regulated gene set (See **Table 4-6**). There was substantial overlap between the transcription factors enriched between the down-regulated genes in both RvB and RvRBG comparisons, with 13 overlapping transcription factors, all bHLH or BZIP TFs, and including the PIF family genes. Only 5 of the 18 enriched transcription factors were differentially expressed in RvRBG.Solyc09g009490.2 encodes transcription factor abscisic acid insensitive 5 (ABI5) and is significantly over-represented in both RvB and RvRBG down-regulated genes. Although not

differentially expressed under any conditions, this transcription factor has been shown to be regulated by HY5 and involved in light quality mediated photoprotection (F. Wang et al., 2017).

Finally, the transcription factor enrichment of BvRBG differentially expressed genes was also conducted. No enrichment was found in the BvRBG up-regulated genes. There were nine transcription factors enriched for target genes in the 1147 genes significantly down-regulated in BvRBG, of which 7 transcription factors were WRKY family members. Three of the WRKY TFs were significantly down-regulated around ~-1 log_2FC. Neither of the two remaining transcription factors were significantly DE in BvRBG; Solyc06g070900.2 a TCP family transcription factor, which was also significantly enriched in the RvRBG down-regulated gene set, and Solyc12g036480.1 a NAC family TF.

Table 4-5 Transcription factor target enrichment analysis of genes up or down-regulated in RvB DEGs

TF Gene_ID	Family	Enrichment		RvB DEA	
		FDR	O/R	LogFC	FDR
RvB up-regulated genes					
Solyc10g079050.1	bHLH	1.09E-03	1.92	NS	NS
Solyc02g071130.2	WRKY	1.09E-03	2.15	NS	NS
Solyc09g014990.2	WRKY	1.09E-03	2.15	NS	NS
Solyc06g065040.2	bHLH	1.69E-03	1.89	NS	NS
Solyc09g066010.2	WRKY	1.96E-03	2.13	NS	NS
Solyc04g078550.2	WRKY	2.45E-03	2.04	-0.55	8.49E-03
Solyc08g081610.2	WRKY	2.59E-03	2.04	NS	NS
RvB down-regulated genes					
Solyc06g008030.2	bHLH	8.94E-06	1.83	NS	NS
Solyc09g063010.2	bHLH	8.94E-06	1.83	NS	NS
Solyc08g005290.2	bZIP	1.06E-04	1.68	NS	NS
Solyc09g009490.2	bZIP	1.06E-04	1.69	NS	NS
Solyc10g081350.1	bZIP	1.06E-04	1.69	NS	NS
Solyc02g062950.2	bZIP	1.65E-04	1.69	0.40	9.05E-03
Solyc04g078840.2	bZIP	4.19E-04	1.61	-1.00	1.80E-05
Solyc01g095460.2	bZIP	5.88E-04	1.61	0.71	1.13E-07
Solyc05g006650.2	bHLH	5.96E-04	1.65	0.36	4.79E-04
Solyc08g005780.2	BES1	6.09E-04	1.80	NS	NS
Solyc04g005280.2	bHLH	1.65E-03	1.70	NS	NS
Solyc03g098320.2	MYB_related	3.33E-03	1.79	-1.72	2.02E-14
Solyc03g096350.2	MYB	3.33E-03	1.82	0.54	1.87E-02
Solyc01g102300.2	bHLH	3.33E-03	1.62	NS	NS
Solyc09g089870.2	bHLH	3.33E-03	1.89	NS	NS
Solyc01g097330.2	bZIP	5.19E-03	1.61	NS	NS
Solyc02g036370.2	MYB_related	5.23E-03	1.76	0.94	6.35E-03
Solyc09g057710.2	bHLH	6.84E-03	1.90	NS	NS

Table 4-6 Transcription factor target enrichment analysis of genes up or down-regulated in RvRBG DEGs

TF Gene_ID	Family	Enrich		RvRBG DEA	
		FDR	O/R	LogFC	FDR
RvRBG up-regulated genes					
Solyc04g008380.2	BBR-BPC	7.24E-05	1.38	NS	NS
Solyc10g079050.1	bHLH	7.24E-05	2.21	NS	NS
Solyc03g112930.2	Dof	1.42E-04	1.40	NS	NS
Solyc06g071480.2	Dof	1.42E-04	1.40	NS	NS
Solyc11g008560.1	AP2	4.91E-04	1.30	NS	NS
Solyc03g115940.2	Dof	6.18E-04	1.47	-0.64	8.85E-10
Solyc06g076030.2	Dof	1.13E-03	1.31	NS	NS
Solyc03g111590.2	C2H2	1.13E-03	1.59	NS	NS
Solyc04g081170.2	BBR-BPC	1.31E-03	1.33	NS	NS
Solyc06g065040.2	bHLH	2.60E-03	1.89	NS	NS
Solyc04g071160.2	bZIP	2.60E-03	2.23	NS	NS
Solyc06g060490.2	bZIP	2.60E-03	2.23	NS	NS
Solyc02g090220.2	Dof	3.04E-03	1.30	NS	NS
Solyc11g011260.1	GRAS	9.85E-03	1.26	0.27	2.37E-03
RvRBG down-regulated genes					
Solyc08g005290.2	bZIP	2.86E-07	1.99	NS	NS
Solyc09g009490.2	bZIP	3.53E-07	1.99	NS	NS
Solyc10g081350.1	bZIP	3.53E-07	1.97	NS	NS
Solyc04g078840.2	bZIP	2.34E-06	1.88	-1.00	1.80E-05
Solyc01g095460.2	bZIP	2.60E-06	1.90	0.71	1.13E-07
Solyc02g062950.2	bZIP	2.60E-06	1.91	0.40	9.05E-03
Solyc06g008030.2	bHLH	2.60E-06	1.91	NS	NS
Solyc09g063010.2	bHLH	2.60E-06	1.91	NS	NS
Solyc05g006650.2	bHLH	1.43E-05	1.87	0.36	4.79E-04
Solyc08g005780.2	BES1	2.99E-05	2.04	NS	NS
Solyc02g036430.1	NAC	7.46E-05	2.21	NS	NS
Solyc01g102300.2	bHLH	1.29E-04	1.86	NS	NS
Solyc01g097330.2	bZIP	1.58E-04	1.87	NS	NS
Solyc02g093280.2	bHLH	8.06E-04	1.85	NS	NS
Solyc01g109880.2	bZIP	1.92E-03	1.73	0.76	3.95E-05
Solyc06g070900.2	TCP	2.06E-03	1.67	NS	NS
Solyc09g057710.2	bHLH	2.99E-03	2.07	NS	NS
Solyc04g009180.1	TCP	7.41E-03	1.57	NS	NS

Table 4-7 Transcription factor target enrichment analysis of genes up or down-regulated in BvRBG DEGs

TF Gene_ID	Family	Enrichment		BvRBG	
		FDR	O/R	LogFC	FDR
BvRBG up-regulated genes					
No Significantly enriched transcription factors					
BvRBG down-regulated genes					
Solyc02g071130.2	WRKY	1.87E-03	2.42	NS	NS
Solyc01g095100.2	WRKY	2.08E-03	2.36	NS	NS
Solyc06g070900.2	TCP	2.08E-03	1.87	NS	NS
Solyc12g036480.1	NAC	2.08E-03	2.57	NS	NS
Solyc04g078550.2	WRKY	3.02E-03	2.25	-0.96	6.23E-07
Solyc08g081610.2	WRKY	3.76E-03	2.23	NS	NS
Solyc06g068460.2	WRKY	4.94E-03	2.07	-0.96	6.23E-03
Solyc08g006320.2	WRKY	6.40E-03	2.17	-1.01	1.74E-05
Solyc08g062490.2	WRKY	6.40E-03	1.87	NS	NS

4.3.7 Investigation of Pathways of Interest

Photoreceptor signalling and circadian rhythm expression

The expression of photoreceptor signalling genes and circadian rhythm gene expression were investigated. Heatmap of the average expression of differentially expressed genes annotated to the 'circadian rhythm' KEGG pathway between R, B, and RBG is overlayed onto the map (See **Figure 4-6**). Further to this, selected photoreceptor signalling and circadian clock genes are reported in **Table 4-8**. Photoreceptors PHYB2 (Solyc05g053410.2) was 4-fold significantly down-regulated in R compared to B and RBG, while PHYA (Solyc10g044670.1) and CRY1B (Solyc12g057040.1) photoreceptor genes were only very moderate down-regulated in BvRBG. E3 ubiquitin ligase COP1 (Solyc11g005190.1) and COP1-like (Solyc11g005190.1), which negatively regulates light signalling by targeting proteins for proteasomal degradation, was significantly down-regulated in RvB and RvRBG. Light signalling transcription factor HY5 (Solyc08g061130.2), was also significantly down-regulated in RvB and RvRBG and up-regulated in BvRBG. Although not annotated to the circadian rhythm pathway, phytochrome-interacting factors (PIFs), integral negative regulators of both phytochrome-mediated red light signalling and cryptochrome-mediated blue light signalling. Five phytochrome-interacting factors were found to be expressed in tomato leaf tissue: PIF1a (Solyc06g008030.2), PIF1b (Solyc01g102300.2), PIF3 (Solyc01g102300.2). PIF7a (Solyc03g115540.1) and PIF7b (Solyc06g069600.1). PIF1b was significantly down-regulated in B compared to R and RBG, PIF1a was not differentially expressed in any comparison, and PIF3b was only significantly down-regulated in RvB. Two other PIF genes were significantly differentially regulated by light, PIF7a and PIF7b were highly differentially expressed in all comparisons between B, R, and RBG, with expression of both genes being lowest in two-fold higher in R than B, and then ~2-fold and ~4-fold higher in RBG than R and B, respectively. Several genes encoding integral circadian clock components were differentially expressed. Two-component response regulator APPR5 (Solyc10g005030.2) was significantly down-regulated in both RvB and RvRBG, while Late hypocotyl (LHY; Solyc10g005080.2) was also down-regulated in RvB and RvRBG, and up-regulated in BvRBG.

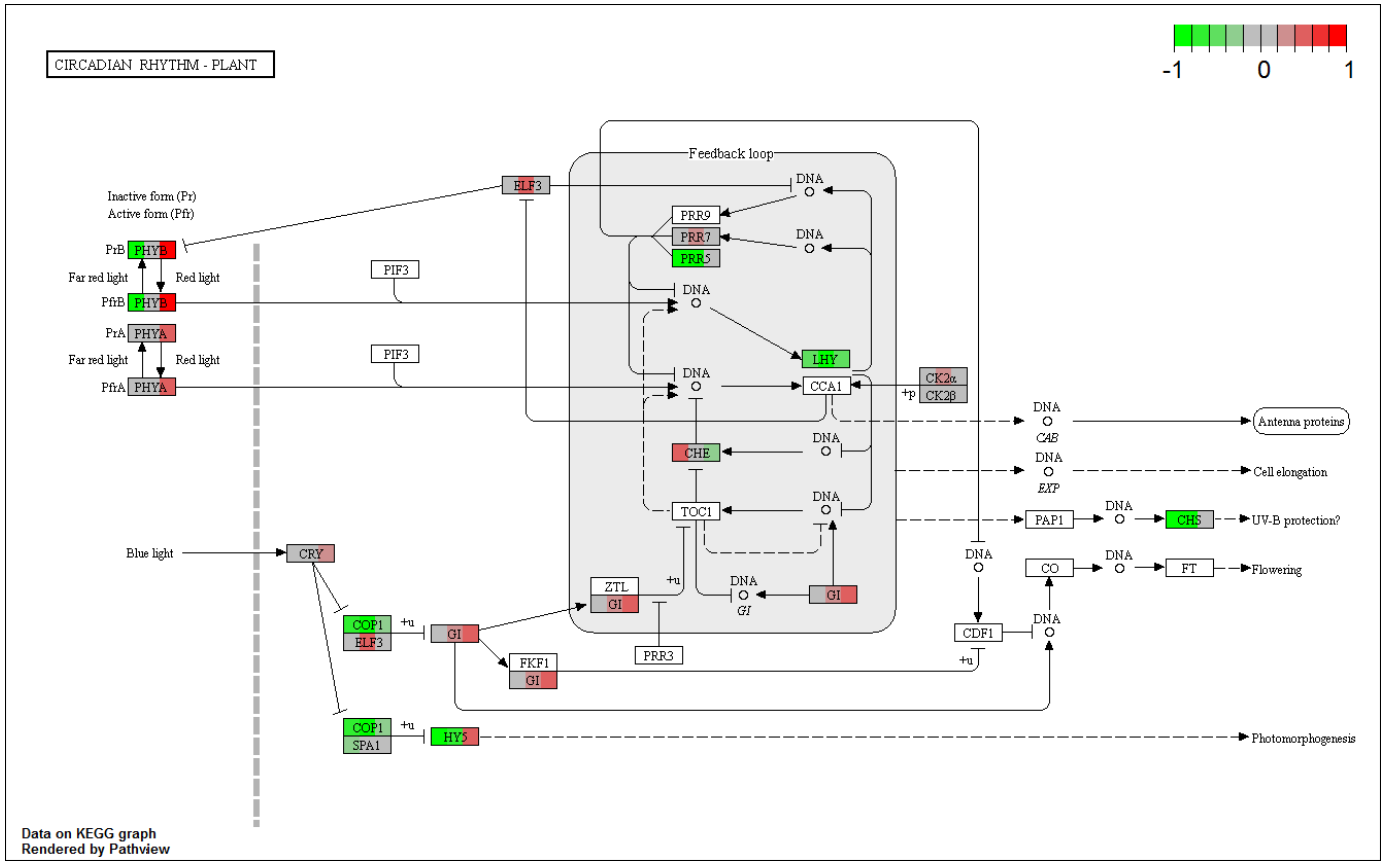


Figure 4-6 RvBvRBG heatmap of differential expression overlayed onto 'Circadian Rhythm' KEGG pathway. Each circle represents a compound and each rectangle box represents an enzyme. The expression of each gene in multiple comparisons between RvBvRBG is represented in each gene as it is split into three sections, where: left= RvB; center = RvRBG; right= BvRBG. Expression is shown on 3-colour 'green-grey-red' scale, limits: -1 to 1 log2FC. Enzymes filled in white were not expressed in the experiment.

Table 4-8 light signalling and circadian clock gene expression

Gene_ID	Description	RvB		RvRBG		BvRBG		Average FPKM			
		Log2FC	FDR	Log2FC	FDR	Log2FC	FDR	R	B	RBG	Fl
Solyc05g053410.2	PHYB2; phytochrome B2	-2.2	2.3E-56	NS	NS	1.9	1.5E-44	2.3	10.5	2.8	2.3
Solyc09g091510.2	CHS1; chalcone synthase	-2.1	5.1E-13	-2.1	3.4E-13	NS	NS	3.5	14.5	14.8	12.4
Solyc10g005030.2	two-component response regulator-like APRR5	-1.2	1.8E-35	-1.7	4.9E-79	-0.5	3.8E-09	8.6	19.2	28.0	22.5
Solyc08g061130.2	Transcription factor HY5	-1.1	4.0E-07	-0.6	2.3E-02	0.5	4.5E-02	2.0	4.4	3.1	1.9
Solyc11g005190.1	COP1-like protein	-1.1	1.0E-03	-1.0	2.2E-03	NS	NS	1.5	3.2	3.1	1.9
Solyc05g053550.2	CHS2; chalcone synthase	-1.0	4.9E-05	-1.5	5.4E-10	NS	NS	6.9	14.1	19.7	20.4
Solyc10g005080.2	protein LHY	-0.6	1.5E-03	-1.1	1.7E-14	-0.6	1.8E-04	1.9	2.8	4.2	1.8
Solyc01g102300.2	PIF3; Phytochrome-interacting factor 3	-0.5	1.8E-02	NS	NS	NS	NS	3.7	5.2	4.5	4.0
Solyc12g005950.1	COP1; COP1 homolog	-0.3	2.7E-03	-0.3	6.9E-03	NS	NS	13.7	17.4	17.1	13.8
Solyc08g081990.2	protein SPA1-RELATED 2	-0.3	3.6E-02	NS	NS	NS	NS	13.2	15.7	14.6	11.9
Solyc09g063010.2	PIF1b; Phytochrome-interacting factor 1b	0.7	1.3E-06	NS	NS	-0.5	6.4E-04	13.4	8.3	12.0	12.9
Solyc03g115540.1	PIF7A; Phytochrome-interacting factor 7a	1.1	1.8E-07	-0.7	1.1E-03	-1.8	2.5E-19	5.5	2.5	8.9	8.8
Solyc06g069600.1	PIF7B; Phytochrome-interacting factor 7b	2.0	1.5E-10	-0.8	1.1E-02	-2.8	2.6E-20	6.0	1.5	10.5	9.6
Solyc10g086000.1	two-component response regulator-like PRR73	NS	NS	0.2	3.6E-02	NS	NS	33.2	30.3	28.3	30.5
Solyc04g071990.2	protein GIGANTEA	NS	NS	0.2	4.0E-02	0.3	1.3E-02	83.0	85.6	70.4	85.5
Solyc08g065870.2	protein EARLY FLOWERING 3-like	NS	NS	0.4	9.5E-04	NS	NS	10.3	9.3	7.8	7.8
Solyc06g008030.2	PIF1a; Phytochrome-interacting factor 1a	NS	NS	NS	NS	-0.8	8.1E-03	33.6	22.4	39.6	34.8
Solyc10g044670.1	phyA; Phytochrome A	NS	NS	NS	NS	0.2	1.8E-02	20.7	21.3	18.1	18.2
Solyc12g057040.1	Cry1b; cryptochrome 1b	NS	NS	NS	NS	0.3	2.8E-02	57.8	64.5	53.0	63.0

NS= Not significant

Photosynthesis

Photosynthesis-related terms were enriched in multiple comparisons between RvBvRBG in both GO and KEGG databases. To further understand the differences in gene expression of photosynthesis pathways, we visualized the expression of genes annotated to two photosynthesis related pathways which were DE in at least one RvBvRBG comparison: 'photosynthesis, light harvesting' and 'photosystem II' (See **Figure 4-7**). For photosynthesis, light harvesting (See **Figure 4-7A**) related genes are substantially up-regulated in RBG compared to both R and B, with few exceptions in which expression is highest in B. Photosystem II-related genes that were differentially expressed in at least pair-wise comparison (See **Figure 4-7A**), had lowest expression in R grown plants, as the heatmap shows a trend of substantial down-regulation relative to RBG and B. Several chloroplast a-binding proteins (CABs) were significantly down-regulated in both RvB and BvRBG including CAB1-A (Solyc02g070980.1), CAB12 (Solyc06g069730.2), CAB8 (Solyc12g011280.1). while others were differentially expressed only in RvRBG including CAB4 (Solyc07g047850.2) and CAB13 (Solyc07g063600.2). One of the few genes up-regulated in R compared to B and RBG was ferredoxin-NADP reductase, involved in regulating cyclic electron flow (FNR; Solyc02g062130.2) (Mulo, 2011).

KEGG pathway for 'Carbon fixation in photosynthetic organisms' (See **Figure 4-8**) showed that a substantial amount of genes were differentially expressed. Generally, significantly down-regulated in comparisons between RvB a BvRBG revealing a down-regulation of the expression of genes in this pathway. The most highly expressed gene in not only the carbon fixation pathway but the entire transcriptome (average RPKM in B=47574), Ribulose bisphosphate carboxylase small chain (), was significantly up-regulated in B compared to R (RvB log2FC= -0.42). Two fructose-1,6-bisphosphate aldolase, (FBA) key enzymes a chloroplast localized enzyme involved in energy metabolism, FBA1 (Solyc01g110360.2) and FBA3 (Solyc02g084440.2) were similarly significantly up-regulated in RvB and RvRBG. While SlFBA3 (Solyc09g009260.2) relatively lowly expressed at FPKM <35 and not

differentially expressed compared to SlFBA7 over FPKM <1812 at log2FC down-regulated -0.38 and -0.54 in RvB, and RvRBG, respectively. Another key sedoheptulose-1,7-bisphosphatase (SBPase; Solyc05g052600.2) was significantly down-regulated in RvB. Additionally, four RNA-polymerase sigma factors were significantly up-regulated in B compared both R and RBG. These sigma factors included sigB(Solyc01g081490.2), sigC(Solyc08g065970.2), sig5(Solyc01g087690.1), and sigF(Solyc09g008040.2). Sigma factors are initiation factors that promote the attachment of plastid-encoded RNA polymerase (PEPs)

A subset of photosynthesis genes integral for photoprotection were differentially expressed. Zeaxanthin epoxidase (Solyc02g090890.2), violaxanthin de-epoxidase (Solyc04g050930.2) and PsbS (Solyc06g060340.2). Both Zeaxanthin epoxidase and PsbS were significantly down-regulated in RvB and RvRBG comparisons, while violaxanthin epoxidase was significantly down-regulated in RvB and BvRBG.

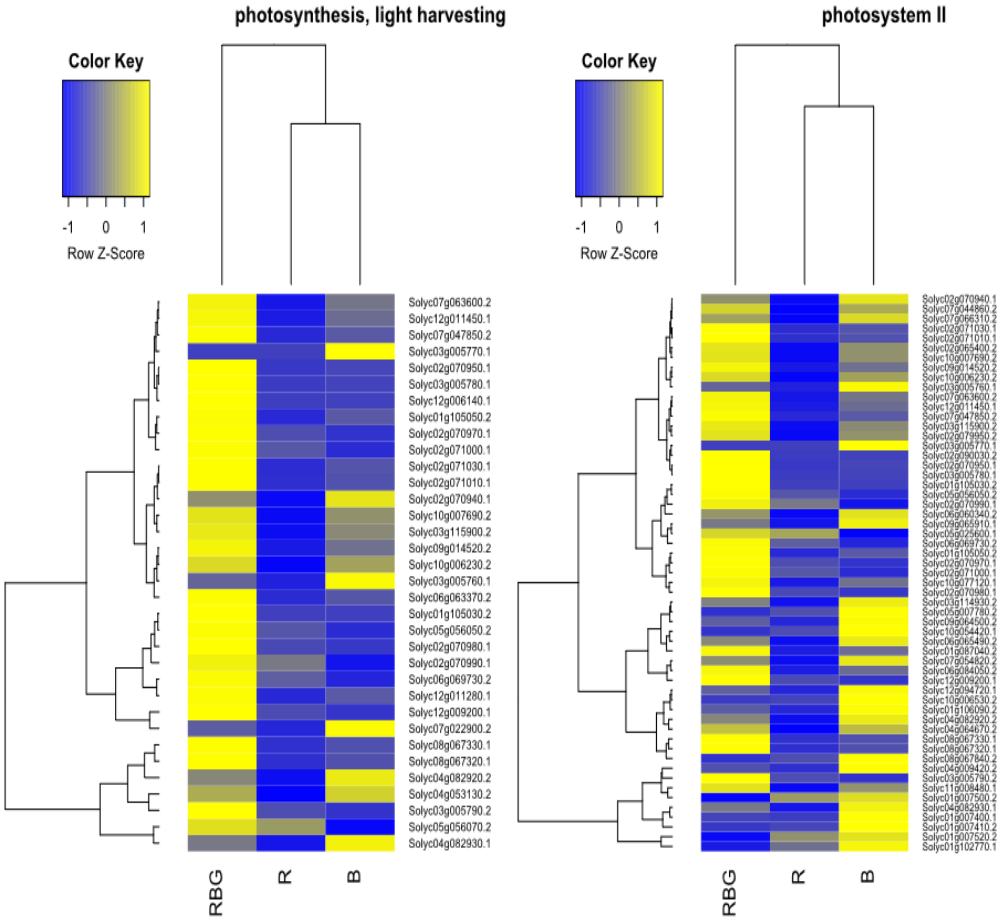


Figure 4-7 Heatmap of DEGs between RvBvRBG in photosynthesis-related GO terms. Heatmap of log normalized count data for genes differentially expressed in at least one pair-wise comparison between RvBvRBG that are annotated to GO:BP terms ‘photosynthesis, light harvesting’ (GO:0009765) and ‘photosystem II’(GO:0009523).

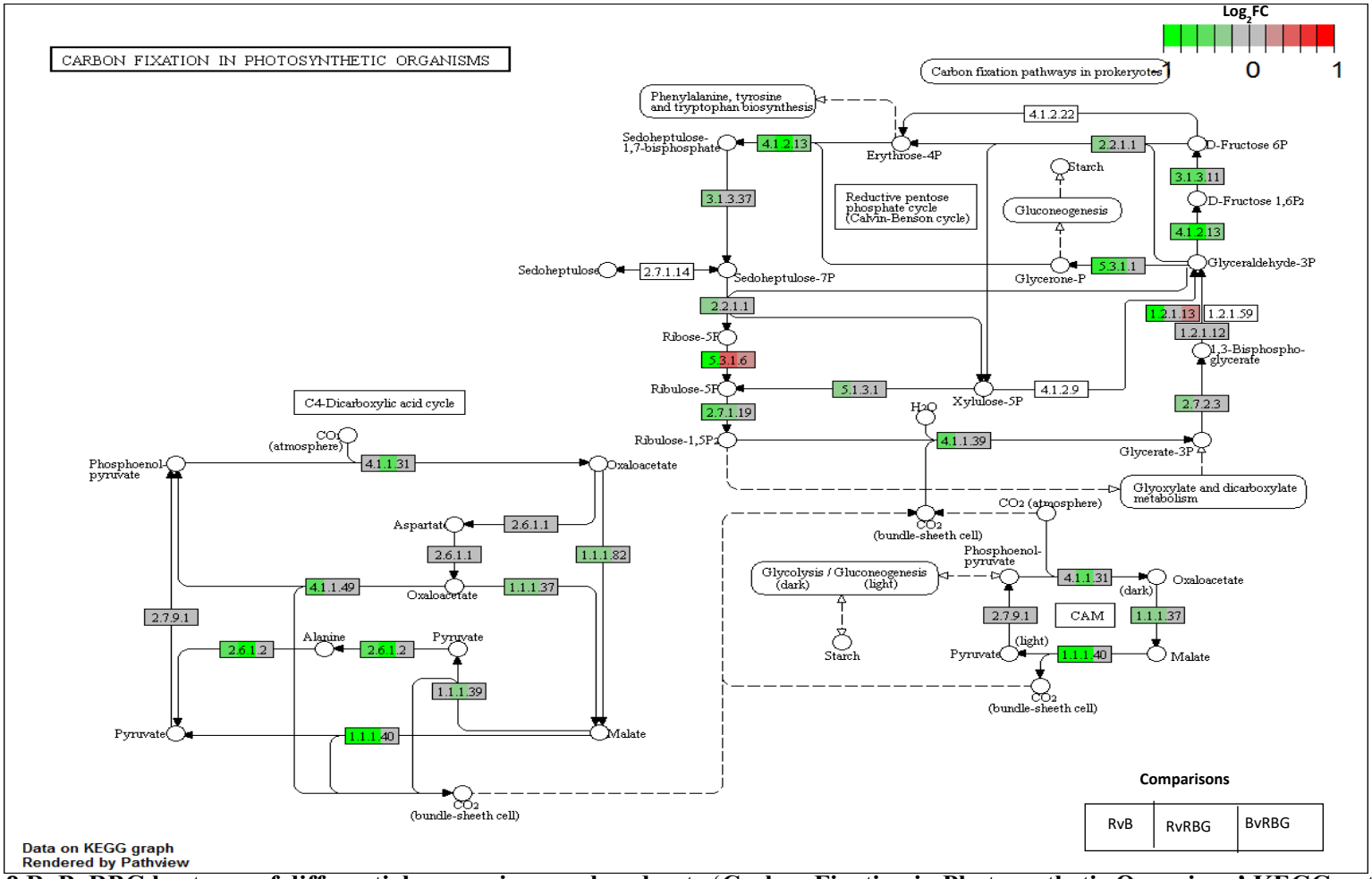


Figure 4-8 RvBvRBG heatmap of differential expression overlayed onto 'Carbon Fixation in Photosynthetic Organisms' KEGG pathway. Each circle represents a compound and each rectangle box represents an enzyme. The expression of each enzyme in multiple comparisons between RvBvRBG is represented in each enzyme as it is split into three sections, where: left= RvB; centre= RvRBG; right= B vRBG. Expression is shown on 3-colour 'green-grey-red' scale, limits: -1 to 1 $\log_2$FC. Enzymes filled in white were not expressed in experiment.

Table 4-9 Photosynthesis and photoprotection DEA between RvBvRBG

		RvB		RvRBG		BvRBG		Average FPKM			
Gene_ID	Description	Log2FC	FDR	Log2FC	FDR	Log2FC	FDR	R	B	RBG	Fl
					Carbon fixation						
Solyc02g085950.2	Ribulose bisphosphate carboxylase small chain	-0.42	0.017	NS	NS	NS	NS	35547.1	47574.2	40141.3	25843.2
Solyc01g110360.2	SlFBA1; fructose 1,6-bisphosphate aldolase 1	-0.51	0.019	-0.65	0.002	NS	NS	1286.6	1836.5	2015.0	857.7
Solyc02g084440.2	SlFBA3; fructose-bisphosphate aldolase	-0.38	6E-04	-0.54	4E-07	NS	NS	1248.7	1629.2	1811.8	1516.1
Solyc09g009260.2	SlFBA7; fructose-1,6-bisphosphate aldolase	NS	NS	NS	NS	NS	NS	35.1	33.5	37.5	38.8
					RNA-polymerase sigma factors						
Solyc01g081490.2	RNA polymerase sigma factor sigB	-0.39	0.003	NS	NS	0.29	0.047	70.8	92.7	75.6	47.2
Solyc08g065970.2	RNA polymerase sigma factor sigC	-0.23	0.023	NS	NS	0.25	0.023	27.3	32.2	27.2	21.5
Solyc01g087690.1	RNA polymerase sigma factor	-0.26	0.026	NS	NS	0.47	1E-05	22.9	27.4	19.8	17.5
Solyc09g008040.2	RNA polymerase sigma factor sigF, chloroplastic	-0.23	0.018	NS	NS	0.28	0.004	37.9	44.3	36.5	30.0
					Xanthophyll cycle						
Solyc02g090890.2	zeaxanthin epoxidase, chloroplastic	-0.76	1E-07	-0.98	7E-12	NS	NS	145.0	246.0	285.4	266.3
Solyc04g050930.2	VDE; violaxanthin de-epoxidase	-0.54	3E-08	NS	NS	0.51	4E-07	52.5	76.3	53.5	41.1
Solyc06g060340.2	PsbS	-0.72	1E-08	-0.47	7E-04	NS	NS	905.9	1495.9	1253.0	715.2

Pigment metabolism

Chlorophyll and carotenoids

The expression pattern of chlorophyll metabolism genes was evaluated, with the expression RvB, RvRBG, and BvRBG differentially expressed genes involved in chlorophyll biosynthesis and catabolic genes (**Table 4-10)**. Several essential chlorophyll biosynthesis genes (A. Chatterjee & Kundu, 2015) were significant up-regulation in RBG compared to both R and B. The most highly down-regulated gene in the chlorophyll biosynthesis process (GO: 0016995) in R compared to B (log2FC=-0.9) and RvRBG (log2FC=-1.1) was magnesium chelatase H subunit (CHLH; Solyc04g015750.2). Magnesium chelatase has also been shown to play a critical role in ABA signal perception and signal transduction with transgenic *Arabidopsis* seedling constitutively expressing CHLH c- and n- terminal units resulted in ABA hypersensitivity and exhibited typical ABA physiological responses (Wu et al., 2009). Glutamyl-tRNA reductase (Solyc01g106390.2), was the most significantly down-regulated genes in both RvRBG and RvRBG. glutamyl-tRNA reductase (GluTR) catalyzes the NADPH-dependent reduction of glutamyl-tRNA which is a rate-limiting step in tetrapyrrole biosynthesis which produces chlorophyll (A. Zhao et al., 2014). Other chlorophyll biosynthesis genes significantly upregulated in RBG included: Chlorophyllide a oxygenase (Solyc11g012850.1), Chlorophyllide a oxygenase (Solyc06g060310.2), geranylgeranyl diphosphate reductase (Solyc03g115980.1), Magnesium-protoporphyrin IX monomethyl ester (Solyc10g077040.1). Conversely, chlorophyll catabolic genes chlorophyllase-2 (Solyc06g053980.2) and Chlorophyllide b reductase (Solyc07g024000.2) were significantly up-regulated in both R and B compared RBG.

Table 4-10 Differential expression of chlorophyll metabolism genes between R, B, and RBG

Gene_ID	Description	RvB DEA		RvRBG DEA		BvRBG DEA		Average FPKM			
		Log2FC	FDR	Log2FC	FDR	Log2FC	FDR	R	B	RBG	Fl
Chlorophyll metabolism											
Solyc01g106390.2	glutamyl-tRNA reductase 1, chloroplastic-like	NS	NS	-1.55	6E-16	-1.31	2E-11	6.3	7.4	18.5	7.8
Solyc11g012850.1	chlorophyllide a oxygenase, chloroplastic-like	-0.69	6E-18	-1.14	2E-49	-0.46	4E-08	42.9	69.1	94.8	76.1
Solyc04g015750.2	magnesium-chelatase subunit ChlH, chloroplastic	-0.87	2E-19	-1.07	5E-28	NS	NS	381.6	698.7	798.9	636.0
Solyc06g060310.2	chlorophyllide a oxygenase, chloroplastic	NS	NS	-0.95	1E-14	-0.71	4E-08	44.2	52.3	85.2	66.2
Solyc10g077040.1	Magnesium-protoporphyrin IX monomethyl ester	NS	NS	-0.44	9E-07	-0.33	0.0007	1606.7	1734.1	2178.3	2085.4
Solyc03g115980.1	geranylgeranyl diphosphate reductase, chloroplastic	NS	NS	-0.39	7E-06	-0.22	0.0315	1480.2	1664.0	1940.9	1881.8
Solyc07g054210.2	POR2; protochlorophyllide reductase	-0.23	0.0376	-0.33	0.0012	NS	NS	577.9	676.8	725.2	779.6
Solyc03g044470.2	rccr; red chlorophyll catabolite reductase, chloroplastic	NS	NS	0.23	0.0432	NS	NS	55.2	51.4	47.2	53.2
Solyc06g053980.2	chlorophyllase-2, chloroplastic-like	NS	NS	0.36	0.0194	0.39	0.0121	72.4	73.9	56.6	71.0
Solyc07g024000.2	probable chlorophyll(ide) b reductase NYC1, chloroplastic	NS	NS	0.40	0.0001	0.56	2E-08	110.8	124.1	84.1	67.6

Hormone biosynthesis and signalling

Perception of light quality by photoreceptors has been shown to not only affect hormone metabolism but also to modulate hormone sensitivity and directly control the expression of hormone-responsive genes. Plant hormone signal transduction was repeatedly over-represented within sets of differentially expressed genes between R, B, and RBG. W, therefore, looked at the expression of genes involved in hormone signal perception, transduction and known genes which regulate hormone-based transcriptomic response. To identify genes involved in phytohormones metabolism, both the Solanaceae Genomics Network's (SGN) LycoCyc database and KEGG Solanum lycopersicum pathway maps of known/predicted metabolic pathways were utilized.

By examining plant hormone signal transduction and metabolism-related gene expression we found extensive differential regulation of both metabolism and signalling genes. The expression of genes KEGG plant hormone signal transduction pathway was overlayed onto the pathway to visualize patterns in gene expression (See **Figure 4-9**), with the average log_2FC of significantly differentially expressed genes annotated to each protein on the map displayed as a heatmap of pair-wise comparisons between RvBvRBG comparisons. Additionally, **Table 4-11** shows the significance and fold change of a selection of genes differentially expressed in RvBvRBG pair-wise comparisons encoding proteins involved in hormone metabolism and signalling.

Gibberellins, auxins, brassinosteroids, are major growth hormones which been implicated in the photoreceptor-mediated shade avoidance response establishing them as core components of the plant response to spectral quality. Gibberellin receptor GID1B-like was also significantly down-regulated in B compared to both R and RBG. Several Gibberellin metabolism genes were found to be differentially expressed including those involved in both syntheses of bio-activate gibberellin an enzyme involved in its inactivation. GA-20 oxidase encoding gene (GA20ox-1; Solyc03g006880), which is involved in biosynthesis of bioactive gibberellin, is significantly down-regulated in R compared to both B (log_2FC= -1.8) and RBG (log_2FC= -1.4). Gibberellin 2-oxidase (Solyc10g007560.1), which are involved in the inactivation of bio-active gibberellin (Chen et al., 2016), is ~5 log2fold in both BvRBG and up RvRBG, identifying a B-specific down-regulation. Meanwhile, GA

biosynthesis inhibitor GA2-beta-dioxygenase-7 (Solyc03g006880) was over log_2fold down-regulated in R compared to B and RBG. Tomato GIBBERELLIN STIMULATED TRANSCRIPT 1(GAST1; Solyc02g089350.2), a GA-reporter gene which is positively transcriptionally regulated by GA (Chen et al., 2016), was significantly up-regulated in R compared to B (log2FC=0.6) and RBG (log2FC=1.1), while also significantly higher in B to RBG (log2FC=0.5). The coordinated up- and down-regulation of GA biosynthesis (Gibberellin 2-oxidase (Solyc10g007560.1) and inhibitor (GA2-beta-dioxygenase-7; Solyc03g006880) genes, respectively, with up-regulation of GA-report gene GAST1 (GAST1; Solyc02g089350.2), suggests GA is transcriptionally suppressed by blue light.

Auxin biosynthesis gene FLOOZY6 (Solyc06g008050.2) was significantly up-regulated in B relative to both R and RBG. There are three major classes of auxin-signalling genes, SAURs, GH3s, and AUX/IAAs, all of which have been demonstrated to regulate photomorphogenesis via either direct and indirect interactions with photoreceptors their signalling components in a light and auxin-dependent manner (Park et al., 2007; N. Sun et al., 2016; F. Xu et al., 2018). In the KEGG pathway heatmap of Plant hormone signal transduction (See **Figure 4-9**), the mean expression of AUX/IAA and GH3 family genes revealed were down-regulated in RvB and RvRBG and up-regulated in BvRBG, whereas SAUR expression is up-regulated in RvB and down-regulated in both RvRBG and BvRBG comparisons. While the KEGG pathway gives an overview of the mean expression of different gene families involved in response to auxin, to get a more detailed picture of the expression patterns of individual genes, the expression of all genes within the SAUR, AUX/IAA, GH3 and PIN families which were differentially expressed and with at least a 50% change in expression in at least one comparison between RvBvRBG were visualized in a heatmap (**Figure 4-10**). The general trend among all the families observed in the heatmap was a down-regulation in both the RvB and RvRBG comparisons. Selected highly differentially expressed genes from auxin signalling and biosynthesis pathways are presented in **Table 4-11.** IAA8 (Solyc03g120390) was significantly down-regulated in R compared to B and RBG. SAUR59 (Solyc06g053290) was the most highly expressed SAUR gene and found to be down-regulated in both RvB and RvRBG in both comparisons. Auxin influx carrier encoding gene LAX3

(Solyc11g013310) was also significantly up-regulated in both RvB and RvRBG comparisons.

Abscisic acid biosynthesis related gene expression as also found to be differentially regulated. One integral ABA biosynthesis gene was found to be significantly down-regulated in monochromatic red grown plants. 9-cis-epoxycarotenoid dioxygenase (NCED) catalyzes the first committed and rate-limiting step in abscisic acid biosynthesis, converting 9-cis-epoxyxanthophylls to ABA biosynthesis intermediate xanthin by oxidatively cleavage in the plastid. The expression of five NCED genes present in *Solanum* genome were evaluated, three were found to be expressed in the transcriptome data, and NCED1 (Solyc07g056570.1) and NCED4 (Solyc08g075490.2) were expressed at equal levels in monochromatic red grown plants. However, NCED4 was significantly down-regulated up-regulated log2FC >2 in B, RBG, and Fl compared to R. Additionally, PYRL/PYL an ABA receptor, is significantly upregulated in both RvB and RvRBG comparisons (See **Figure 4-9**). Several ABA signalling genes exhibited no differential expression between RvB but were significantly up-regulated RBG compared to both R and B, including ABA transcription factor AREB (Solyc04g078840), and two PP2C encoding genes (Solyc03g096670 and Solyc06g076400) (See **Table 4-11**).

Three ethylene biosynthesis genes; 1-aminocyclopropane-1-carboxylate oxidase (ACO; Solyc07g049530.2 and Solyc12g005940.1) and an ACO1-like (Solyc09g010000.2), were significantly up-regulated in both RvB and RvRBG, and significantly down-regulated in BvRBG. Ethylene signalling gene, E3 ubiquitin ligase EIN3-binding F-box protein 1(Solyc12g009560.1) wassignificantly up-regulated in R compared to both B and RBG. Jasmonic acid biosynthetic genes were significantly differentially expressed in this dataset. Both allene oxidase synthase (AOS; Solyc04g079730.1) and allene oxide cyclase (AOC1; Solyc02g085730.2) were differentially expressed in all comparisons between RvB, RvRBG, and BvRBG being most significantly up-regulated under R light and lowest expression B. Core jasmonic acid signalling transcription factor jasmonate ZIM-domain protein 1(JAZ1; Solyc12g009220.1) was also significantly differentially expressed in a similar manner. Ninja-family protein 3 (Solyc02g088910.2) is a JA responsive transcription factor that interacts with ABI5, AREB2, and AREB3. AFP expression is 3-times

higher in dark-grown *Arabidopsis* seedlings than etiolated seedlings (Garcia et al., 2008; Jiao et al., 2005).

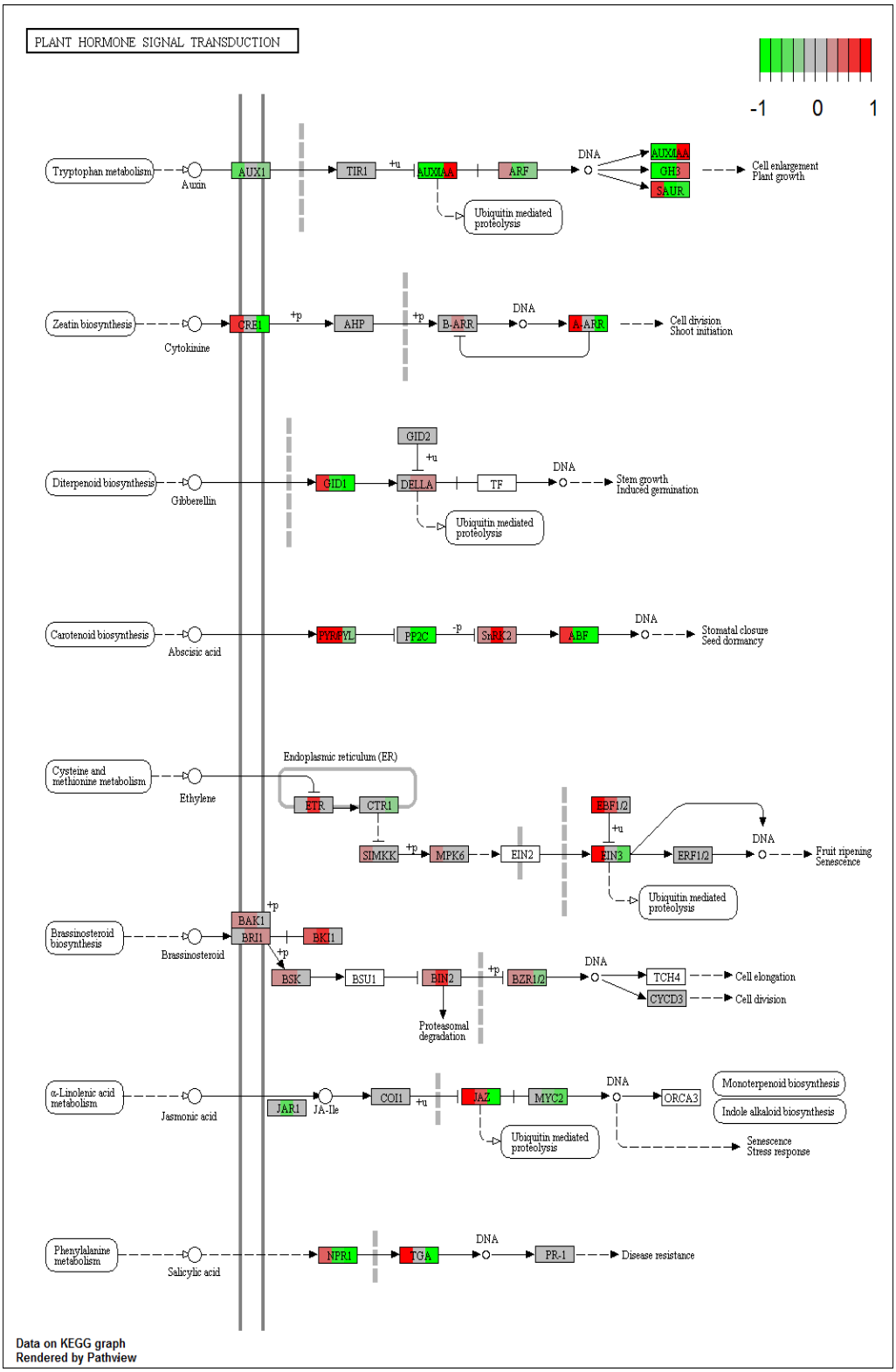


Figure 4-9 Plant hormone signal transduction gene expression pathway overlay. Each circle represents a compound and each rectangle box represents a gene. The expression of each gene in multiple comparisons between RvBvRBG is represented in each enzyme as it is split into three sections, where: left= RvB; center = RvRBG; right= B vRBG. Expression is shown on 3-colour 'green-grey-red' scale, limits: -1 to 1 $\log_2$FC. Gene filled in white were not expressed in the experiment.

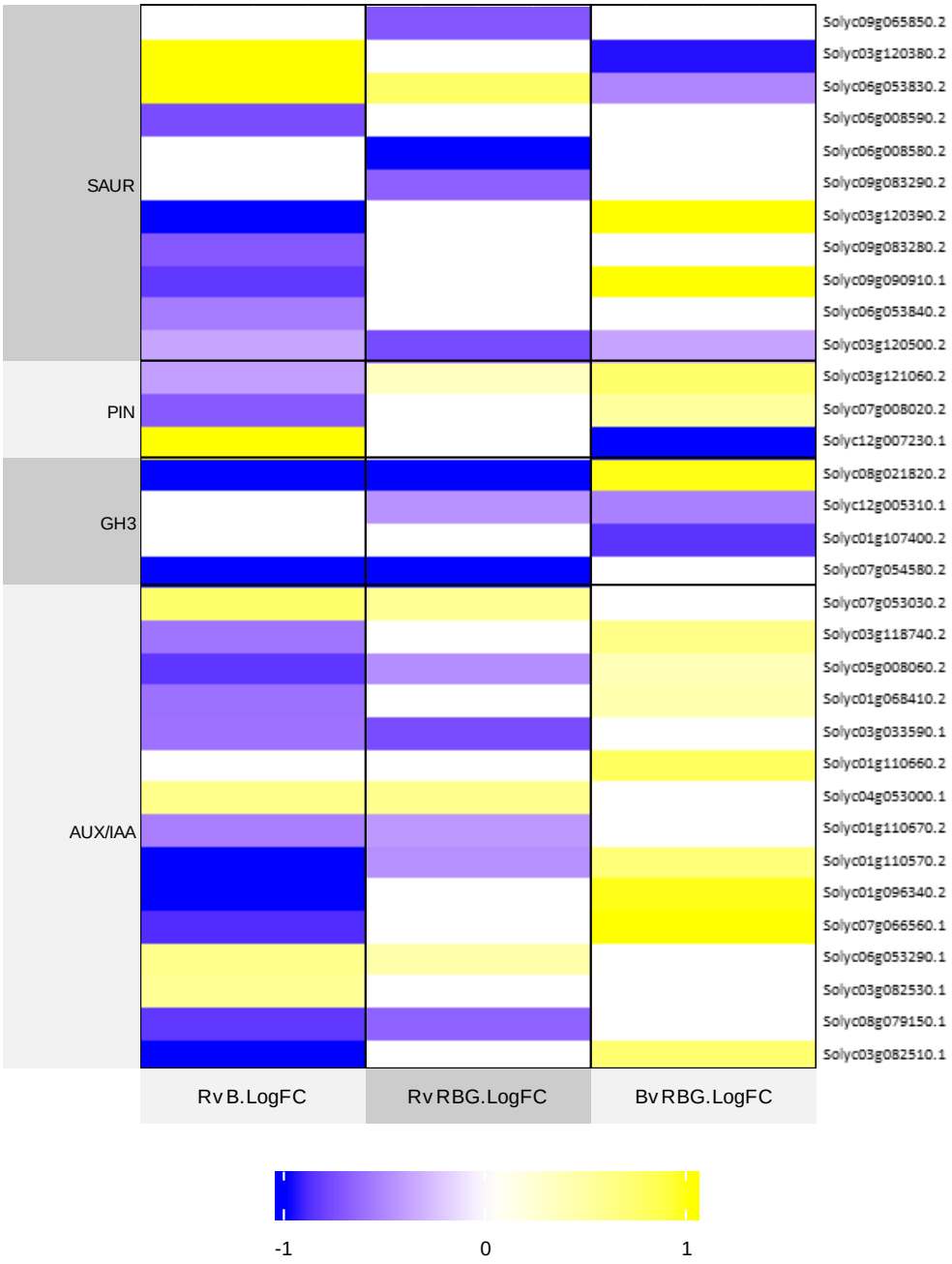


Figure 4-10 Log-Fold change of auxin-responsive genes in RvBvRBG comparison. Heatmap of log2 gene expression of R, B, and RBG differentially expressed genes from SAUR, PIN, GH3, and AUX/IAA families of auxin-responsive genes which are differentially expressed in at least one pair-wise comparison between RvBvRBG. If the gene was not differentially expressed (FDR >0.05) then log_2FC was adjusted to 0 for the pair-wise comparison of that gene.

Table 4-11 Hormone biosynthesis and signalling genes differentially expressed in response to spectral quality

Gene_info				RvB		RvRBG		BvRBG		Average FPKM			
Hormone	Gene_ID	Description	Action	LogFC	FDR	LogFC	FDR	LogFC	FDR	R	B	RBG	Fl
AUX	Solyc09g074430.2	FZY6; probable indole-3-pyruvate monooxygenase YUCCA10	Biosynthesis	1.21	0.002	0.96	0.02	NS	NS	1.1	0.5	0.6	0.8
AUX	Solyc06g053290.1	SAUR59; auxin-induced protein X15	Signalling	1.28	2E-20	0.76	7E-08	-0.52	0.002	57.6	23.7	34.3	40.3
AUX	Solyc03g120390.2	IAA8; protein IAA8	Signalling	-0.86	7E-10	-0.68	4E-06	NS	NS	6.9	12.5	11.0	8.3
AUX	Solyc11g013310.1	LAX3 protein	Signalling	1.09	4E-24	0.79	2E-13	-0.30	0.05	17.5	8.2	10.1	9.2
GA	Solyc03g006880.2	20ox-1; gibberellin 20-oxidase-1	Biosynthesis	-1.76	3E-50	-1.42	4E-32	0.33	0.016	8.1	27.4	21.7	22.8
GA	Solyc06g008870.2	gibberellin receptor GID1B-like	Signalling	0.65	0.002	NS	NS	-0.99	2E-07	4.0	2.5	5.0	9.4
CK	Solyc12g008900.1	SlCKX6; cytokinin dehydrogenase 3	Catabolism	6.99	7E-42	2.87	4E-11	-4.12	6E-17	56.6	0.4	7.8	4.6
JA	Solyc04g079730.1	aos; allene oxide synthase	Biosynthesis	3.38	3E-18	1.79	2E-06	-1.59	4E-04	6.4	0.6	1.8	0.9
JA	Solyc02g085730.2	AOC; allene oxide cyclase	Biosynthesis	1.17	1E-28	0.57	4E-07	-0.60	2E-07	146.4	64.9	98.7	121.1
JA	Solyc12g009220.1	ZIM1; jasmonate ZIM-domain protein 1	Signalling	1.56	2E-22	0.48	0.007	-1.08	4E-10	23.4	8.0	16.9	9.9
ABA	Solyc08g075490.2	NCED4; carotenoid cleavage dioxygenase 4, chloroplastic	Biosynthesis	-2.00	5E-08	-1.97	1E-07	NS	NS	45.8	183.3	179.6	199.0
ABA	Solyc07g056570.1	NCED1; nine-cis-epoxycarotenoid dioxygenase	Biosynthesis	NS	NS	NS	NS	NS	NS	42.9	44.3	52.9	16.3
ABA	Solyc10g076410.1	abscisic acid receptor PYL4-like	Signalling	1.41	4E-06	1.41	5E-06	NS	NS	6.3	2.4	2.4	3.0
BR	Solyc02g063010.2	BES1/BZR1 homolog protein 2-like	Signalling	0.27	0.015	0.31	0.006	NS	NS	66.7	55.1	53.9	67.1
ETH	Solyc07g049530.2	ACO1	Biosynthesis	2.78	9E-08	1.48	0.007	-1.29	0.039	11.8	1.7	4.2	3.6
ETH	Solyc09g010000.2	1-aminocyclopropane-1-carboxylate oxidase 1- like	Biosynthesis	4.93	3E-11	2.25	0.001	-2.68	0.001	5.3	0.2	1.1	0.6
ETH	Solyc12g009560.1	EBF1; EIN3-binding F-box protein 1	Signalling	0.65	7E-05	0.58	6E-04	NS	NS	26.3	16.7	17.6	24.2
ABA	Solyc03g096670.2	PP2C-2; protein phosphatase 2C AHG3	Signalling	NS	NS	-1.03	9E-05	-1.39	1E-07	2.3	1.8	4.8	4.7
ABA	Solyc04g078840.2	AREB; AREB-like protein	Signalling	NS	NS	-1.00	2E-05	-0.74	0.003	2.5	3.0	5.0	4.4
ABA	Solyc06g076400.2	probable protein phosphatase 2C	Signalling	NS	NS	-0.75	2E-07	-0.52	0.001	20.0	23.5	33.8	34.3

Defense related to gene expression

Given that defense related gene expression was observed in RvB and BvRBG down-regulated genes, including enrichment of genes annotated to the plant-pathogen interaction KEGG pathway, we further investigated the expression of defense related gene expression. An overview of the RvB, RvRBG, and BvRBG expression of genes annotated to the plant-pathogen interaction KEGG pathway is visualized in **Figure 4-11** and the differential expression of several gene in this pathway reported in **Table 4-12**. Calcium and reactive oxygen species are crucial for plant biotic and abiotic stress responses.

Several defense related genes were significantly up-regulated in RvB and down in BvRBG.Defense and heat stress transcription factor WRKY33B (Solyc09g014990.2) was also significantly down-regulated in B compared to both R and RBG, -1.8 and -2.7 log_2fold, respectively. Other defense related genes including RPM1-interacting protein 4 (Solyc06g083390.2), cysteine protease (Solyc02g076980.2), calcium-binding protein CML30 (Solyc06g069740.1) exhibited the same expression pattern. The second subset of defense genes was up in R compared to both B and RBG. RESPIRATORY BURST OXIDASE HOMOLOG1 (RBOH1; Solyc06g068680.2), a gene encoding an enzyme that catalyzes the production of ROS (F. Wang et al., 2017), and is 0.7 log_2fold significantly up-regulated in pair-wise comparisons between R with B and RBG, respectively. LRR receptor-like serine/threonine-protein kinase EFR (Solyc02g068820.1), which is a pathogen-recognition receptor involved in innate immunity and resistance to *p.syringae* (J. Li et al., 2009) was 1.4 log_2fold up-regulated in R compared to both B and RBG.

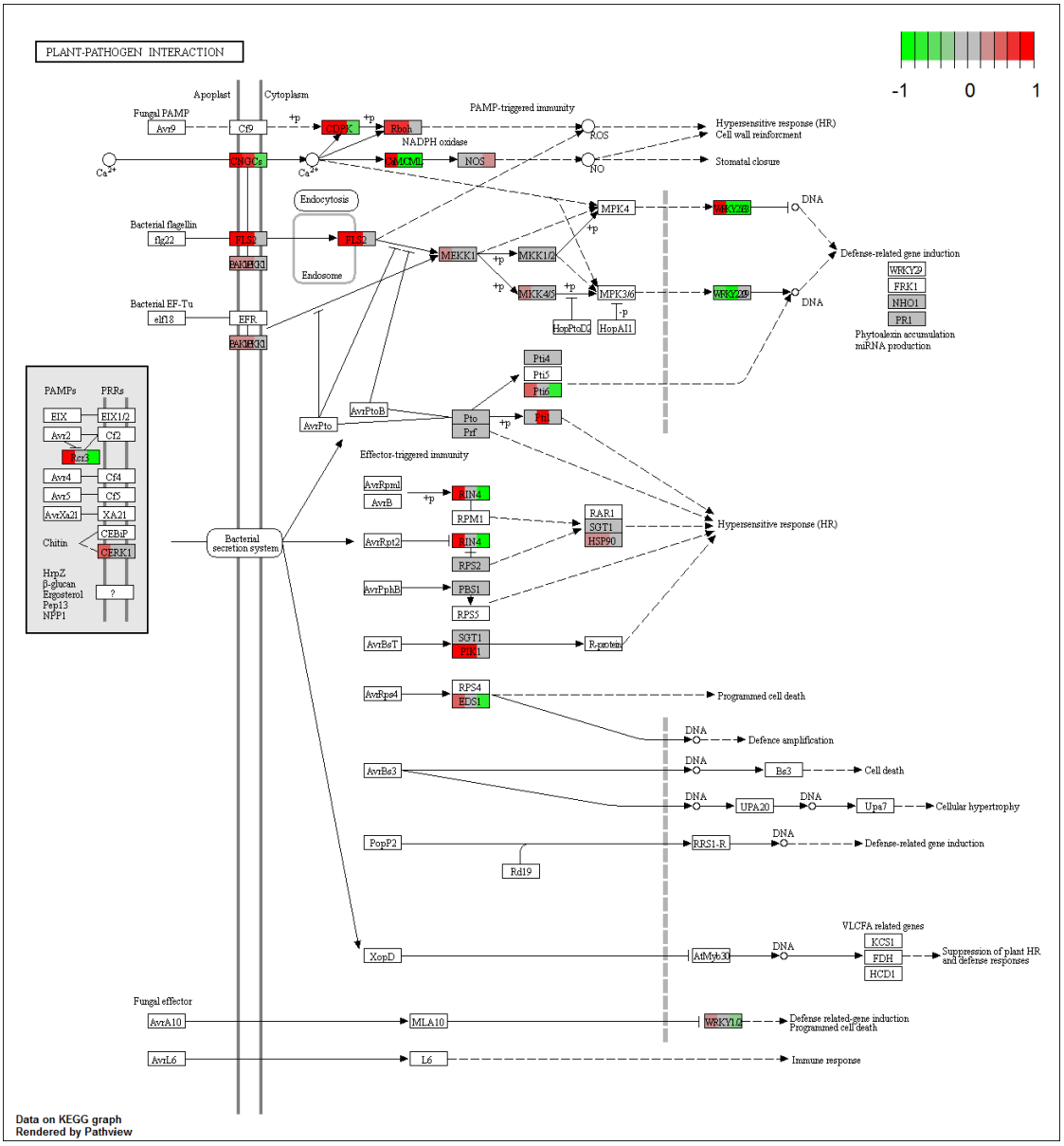


Figure 4-11 Plant-pathogen interaction gene expression pathway overlay. Each circle represents a compound and each rectangle box represents a gene. The expression of each gene in multiple comparisons between RvBvRBG is represented in each enzyme as it is split into three sections, where: left= RvB; center = RvRBG; right= B vRBG. Expression is shown on 3-colour 'green-grey-red' scale, limits: -1 to 1 log2FC. Enzymes filled in white were not expressed in the experiment.

Table 4-12 DEA of plant-pathogen interaction keg pathway genes between R, B, and RBG

Gene_ID	Description	RvB		RvRBG		BvRBG		Average FPKM			
		Log2FC	FDR	Log2FC	FDR	Log2FC	FDR	R	B	RBG	Fl
Solyc02g091500.1	calcium-binding protein CML24	-1.1	2.5E-04	-1.8	1.0E-10	-0.7	3.2E-02	14.1	29.6	48.2	22.4
Solyc02g088090.1	probable calcium-binding protein CML30	-0.9	2.0E-02	-1.5	3.0E-05	NS	NS	6.5	12.3	18.2	22.2
Solyc03g123800.1	MKK2; MAPKK	0.3	5.1E-03	NS	NS	NS	NS	40.1	32.5	35.8	43.4
Solyc03g033540.2	calcium-dependent protein kinase	0.4	1.3E-02	NS	NS	NS	NS	21.1	16.6	19.3	23.8
Solyc02g088560.2	cyclic nucleotide-gated ion channel 2	0.4	1.2E-03	0.6	1.9E-08	NS	NS	88.6	67.6	57.2	79.3
Solyc04g058160.1	probable calcium-binding protein CML44	0.5	1.2E-02	0.5	2.6E-03	NS	NS	11.3	8.1	7.8	10.8
Solyc06g071280.2	EDS1; protein EDS1	0.5	1.2E-03	NS	NS	-0.8	7.6E-08	22.4	15.8	27.3	33.8
Solyc10g081170.1	SlCaM2; calmodulin 2	0.5	1.5E-05	NS	NS	-0.6	4.4E-07	675.6	475.4	717.4	734.7
Solyc06g068680.2	respiratory burst oxidase homolog protein D	0.7	2.0E-03	0.7	9.5E-04	NS	NS	8.4	5.2	5.1	7.8
Solyc04g015980.2	probable LRR receptor-like serine/threonine-protein kinase At3g47570	0.7	8.0E-04	NS	NS	NS	NS	1.2	0.7	0.9	0.8
Solyc03g113390.2	Hop-interacting protein THI080	0.8	2.6E-06	NS	NS	-0.5	1.1E-02	6.1	3.6	5.0	5.8
Solyc06g083390.2	RPM1-interacting protein 4	1.2	8.8E-11	NS	NS	-1.1	1.2E-08	29.9	12.7	27.8	18.7
Solyc02g068820.1	LRR receptor-like serine/threonine-protein kinase EFR	1.4	3.2E-05	1.4	4.2E-05	NS	NS	1.7	0.6	0.6	1.1
Solyc09g014990.2	SlWRKY33B; WRKY transcription factor 33B	1.8	1.3E-04	NS	NS	-2.7	4.9E-09	6.0	1.7	11.2	2.1
Solyc06g069740.1	probable calcium-binding protein CML30	2.2	8.8E-07	NS	NS	-1.7	1.2E-03	2.6	0.5	1.8	0.9
Solyc02g076980.2	Rcr3; cysteine protease	2.5	1.5E-09	NS	NS	-1.9	2.2E-05	5.2	0.9	3.5	2.6

NS= Not significant

4.3.8 Differential gene expression analysis between Micro-Tom grown under Fluorescent light compared to LED lighting.

During the experimental design of this experiment, fluorescent tube lighting was included to serve as a broad spectrum light source which would be a control, and serve as a technological comparison between narrow-band LED lights. The principle-component analysis revealed substantial variance between the transcriptome of leaves grown under LED lightings compared to fluorescent tubing (**Figure 4-1**). To further understand the transcriptome differences, differentially expressed genes (DEGs) were identified in pair-wise comparisons between Fl transcriptome and those of the 3 LED treatments using EdgeR (**Figure 4-12**; A, D).

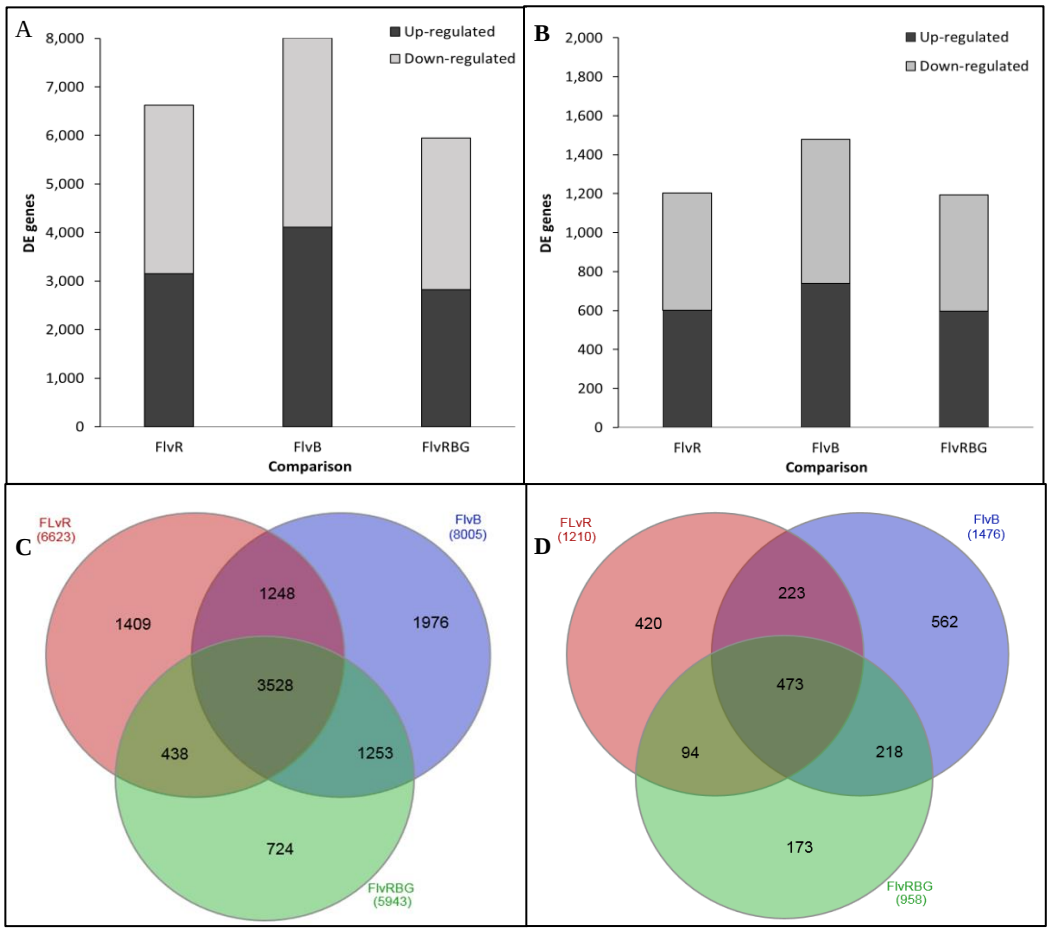


Figure 4-12 Differential expression analysis of Micro-Tom grown under Fluorescent tube lighting in comparison to LEDs. A) Differentially expressed genes between Fl v LED treatments in pair-wise comparisons B) Statistically significantly two-fold regulated (logFC >1 or <-1) genes between Fl and LED treatments in pair-wise comparisons. C) Venn overlap of differentially expressed genes differentially expressed in Fl v different LED spectral qualities. D) Venn overlap of statistically significantly two-fold differentially expressed genes in Fl v different LED spectral qualities. Significance called at FDR <0.05. n=3.

Fluorescent tube lighting had a profound effect on transcriptome profile compared to monochromic red, monochromic blue, or combined red, blue and green LEDs with over 6623, 8005, and 5942 DEGs, respectively. Comparison of overlap between the sets of differentially expressed genes (**Figure 4-12**; C) identified substantial variation in the differential expression of each LED group to fluorescent light, with a total of 10,576 unique DEGs in at least one treatment. FlvB has the greatest number of DEGs, with a large number of these are only differentially expressed in this comparison (1976). Evaluation of overlapping genes between FL and the LED transcriptomes revealed that a large proportion of genes 3528 were differentially expressed between Fl and all LED conditions (See **Figure 4-12**). Hierarchical clustering of these commonly differentially expressed genes showed that that R, B, and RBG have a very similar expression of these genes while they are antagonistically regulated in Fl (See **Figure 4-13**). GO and KEGG enrichment analysis of these commonly DE genes identified 35 BP, 9 MF, 11 CC terms as well as 5 KEGG pathways (See **Table 8-13**). The statistically enriched terms, related to ribosome and translation, photosynthesis, pigment metabolism ('tetrapyrrole biosynthetic process', 'pigment metabolic process'), and development ('stomatal complex morphogenesis', 'shoot system development').

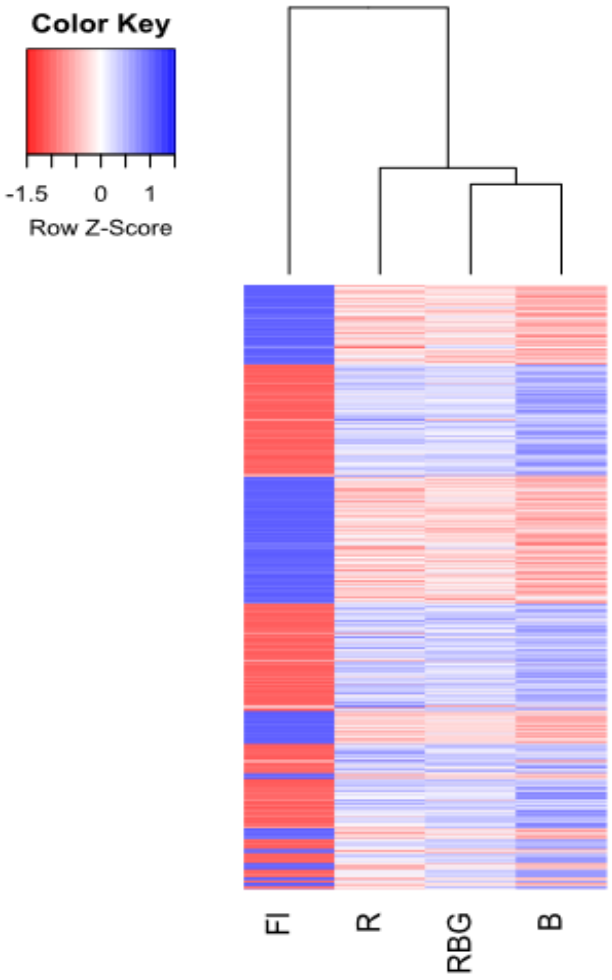


Figure 4-13 Hierarchical clustering of genes commonly differentially expressed between Fl and LED transcriptomes. Hierarchical clustering of the 3528 genes that were differentially expressed in pairwise comparison between Fl with R, B, and RBG. Hierarchical clustering based on row-wise scores of Euclidean distance of each genes log-CPM.

4.3.9 Co-Expression network modeling

Co-expression networks are gene expression networks in which interactions between individual genes are assigned based on the correlation in gene expression across samples. Expression-based networks have been shown to resemble biological networks, and as such is a powerful tool for the discovery of novel regulatory interactions, in which genes of unknown function can be associated with known biological processes based on similarities in gene expression patterns. Although all samples and gene expression across R, B, RBG, and Fl samples was used to generate co-expression network, it was then filtered to keep only genes which were significantly differentially expressed between RvBvRBG and with a log2fold change of at least 0.5 up or down. In total, the network contained 1662 genes (nodes) with 11439 interaction (edges). Nodes are coloured based on the log_2fold change between RvB, and to reduce the network a minimum fold change in expression of 50% was introduced.

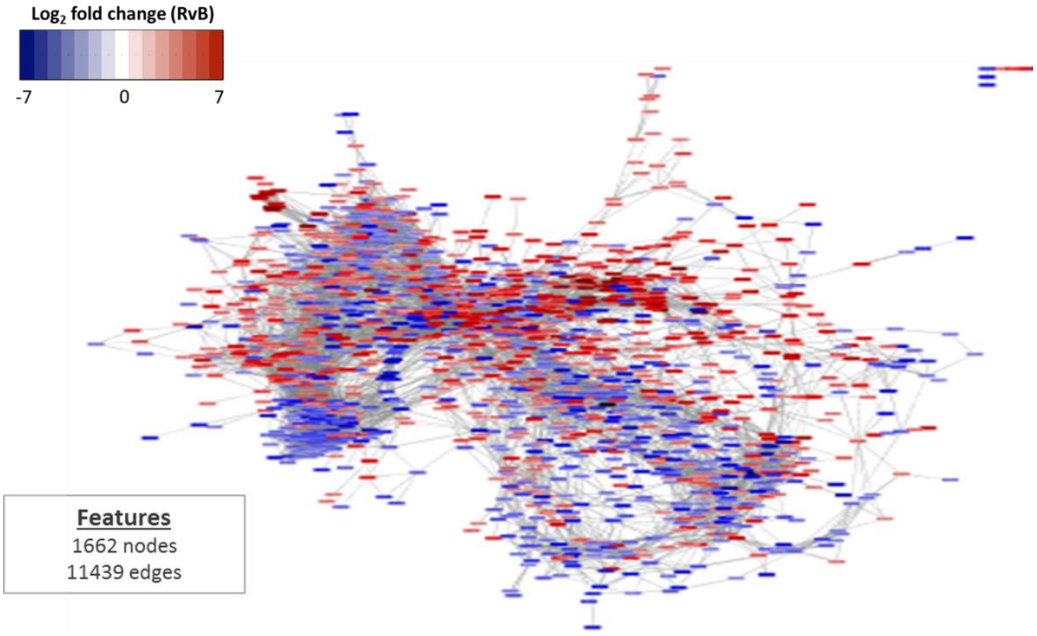


Figure 4-14 Global view of co-expression network built from gene expression of Micro-Tom leaves grown under varying spectral qualities. Co-expression network from log2 normalized RPKM of samples from R, B, RB, RBG, and Fl transcriptomes**.** Interactions were filtered to include only those significantly differentially expressed (q<=0.05) in at least one pair-wise comparison between RvBvRBG with a log2 fold change of above >0.5 or <-0.5. Correlation co-efficient cut-off R^2=0.9.

As the network was so dense with interactions, biological interpretation was challenging. The network was constructed with 12 samples, and this is at the minimum threshold necessary for co-expression network analysis. Increased sample size teases apart similarly expressed genes reducing the number of interactions and complexity of the network and improving its accuracy.

Anthocyanin metabolism

Anthocyanins, a class of flavonoid compounds, are plant pigments which have a diverse range of functions including photoprotection against light oxidative stress, as well as salicylic-acid mediated defense. A sub-module of the co-expression network gene network involving anthocyanin metabolic genes was identified (**Figure 4-15**), with the differential expression of these genes between R, B, and RBG presented in **Table 4-10.** The expression of these genes was then correlated against the anthocyanin content of leaf tissue of Micro-Tom plants grown under the same spectral qualities as used in this experiment (See data presented in chapter **Figure 3-12**). The expression of several anthocyanin metabolism genes correlated with anthocyanin content (See **Figure 4-16** and **Table 4-13** Expression of anthocyanin metabolism genes and correlation coefficient of expression of genes compared to anthocyanin content**.** Both anthocyanidin synthase (ANS) and dihydroflavanol reductase (DFR) are involved in a 2-step conversion of dihydroflavanol to anthocyanidin, and not only are these genes highly differentially expressed between light treatments they show a high correlation between expression level (R^2 = 1 and 0.93, respectively) to anthocyanin content measured from the leaf tissue. In addition to these, phenyl ammonia lyase (PAL) the first committed enzyme in phenylpropanoid metabolism through catalyzes of phenylalanine to cinnamic acid, are also strongly positively correlated with anthocyanin accumulation. In addition to anthocyanin metabolism genes, a key bHLH transcription factor regulating anthocyanin content in tomato is Hoffman's Anthocyaninless (AH; Qui et al, 2016) which has identified as regulating the expression of several of the aforementioned flavonoid biosynthesis genes, is co-expressed with the anthocyanin metabolic genes and is strongly positively correlated with anthocyanin content (R^2 =0.96). Furthermore, at the top of the network is AP2e, an APETALA2/ERF transcription factor homologous to the AP2a

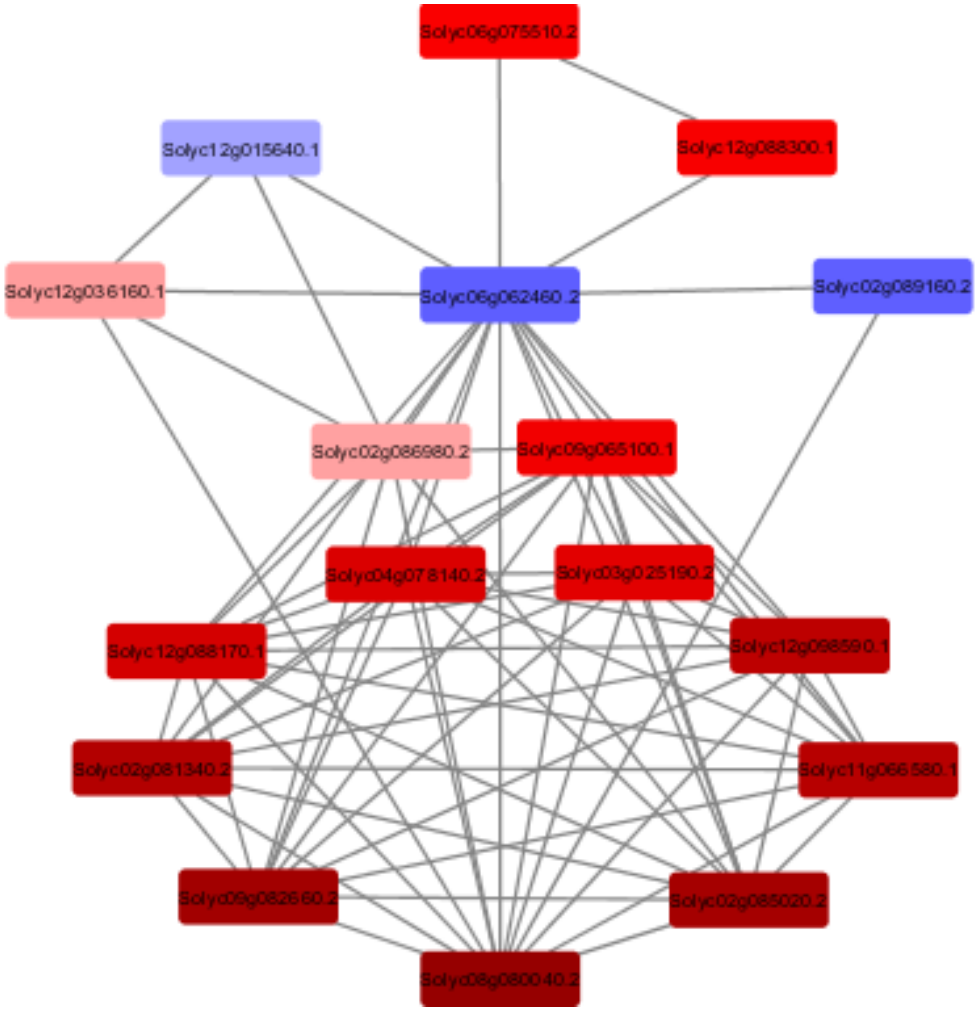


Figure 4-15Co-expression network of anthocyanin biosynthesis genes. Co-expression network from log2 normalized RPKM of samples from R, B, RB, RBG, and Fl transcriptomes**.** Interactions were filtered to include only those significantly differentially expressed (*q*<=0.05) in at least one pair-wise comparison between RvBvRBG with a log2 fold change of above >0.5 or <-0.5. Correlation co-efficient cut-off R^2=0.9. Genes colour is heatmap of log2fold change in expression between RvB, which is reported in Table **4-10**, Blue is down-regulated while red is up-regulated.

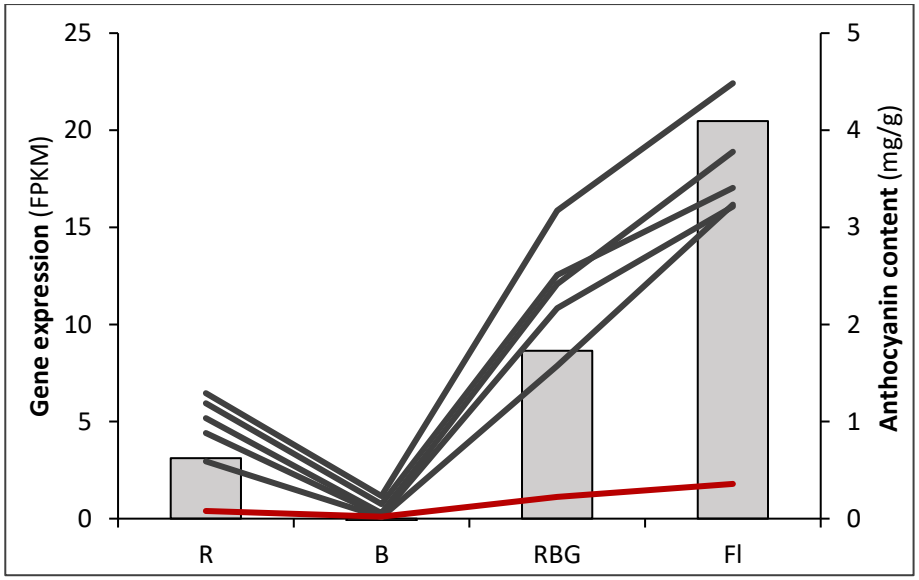


Figure 4-16 Gene expression of anthocyanin metabolism genes and transcription factor Anthocyanin-less as well as anthocyanin content on leaf tissue of Micro-Tom plants grown under varying spectral qualities. Gene expression is in FPKM from RNA-Seq transcriptomic data. Anthocyanin content mg anthocyanin per gram of fresh weight. Grey lines indicate anthocyanin metabolic gene expression. Red line indicates the expression of transcription factor Anthocyaninless (AH). Bars indicate the anthocyanin content of leaves grown under varying spectral qualities.

Table 4-13 Expression of anthocyanin metabolism genes and correlation coefficient of expression of genes compared to anthocyanin content

Gene ID		Log_2FC			FPKM				R^2
		RvB	RvRBG	BvRBG	R	B	RBG	Fl	
Solyc08g080040.2	ANS	5.2	-1.4	-6.7	3.0	0.1	7.9	16.2	**1.00**
Solyc02g085020.2	DFR	4.7	-1.3	-6.0	4.4	0.2	10.8	16.1	**0.93**
Solyc02g081340.2	GST	4.2	-1.2	-5.4	5.2	0.3	12.1	18.9	**0.95**
Solyc12g088170.1	AAC	3.0	-1.1	-4.1	5.9	0.7	12.5	17.0	**0.90**
Solyc03g025190.2	PAL	2.5	-1.3	-3.8	6.5	1.2	15.9	22.4	**0.92**
Solyc10g083440.1	3GT	NS	-1.2	-1.0	3.1	3.7	7.2	8.6	**0.83**
Solyc09g092500.1	5GT	-0.5	-0.8	NS	9.5	13.2	16.1	23.6	**0.85**
Solyc09g065100.1	AH	1.9	-1.5	-3.4	0.4	0.1	1.1	1.8	**0.96**
Solyc06g075510.2	AP2e	1.6	NS	01.7	15.2	5.1	16.1	29.1	**0.92**

R2 is correlation co-efficienct of expression of the genes in transcriptomic data (FPKM) to anthocyanin pigment content both extracted from leaf tissue of plants grown under varying spectral qualities (See **Figure 3-12** and **Figure 4-16**).

4.3.10 qRT-PCR confirmation of RNA-Seq data

In order to prove the reliability of the RNA-Seq data, real-time RT-PCR (qRT-PCR) was performed on the same pools of RNA used for sequencing. We first sought to select a reference gene for qRT-PCR normalization. To do this, a list of potential reference genes was compiled from a literature search of experimentally validated reference genes in Solanum lycopersicum. The normalized expression values of these candidate reference genes across all samples within the RNA-Seq data was assessed and the coefficient of variation was calculated to determine which gene was most stable within our dataset (Table 4-14). The best reference gene was identified to be CAC (Solyc08g006960.2), which had a co-efficient of variation of 4.6% between all 15 RNA-Seq samples. Actin-B (Solyc11g005330.1), a popular reference gene, was the second stably expressed gene. CAC, which encodes a Clarthrin adapter complex sub-unit protein, and CAC was also evaluated as being the ideal reference gene for Solanum lycopersicum in several studies (Expósito-Rodríguez, Borges, Borges-Pérez, & Pérez, 2008; Wieczorek, Wrzesińska, & Obrepalska-Steplowska, 2013).

Table 4-14 Assessment of the variation in expression of candidate reference genes within RNA-Seq dataset.

Gene_ID	Name	Average expression (CPM)	CV	Reference*
Solyc08g006960.2	CAC	42.3	4.6%	Expósito-Rodríguez et al, 2008; Wieczorek et al, 2013; González-Aguilera et al, 2016.
Solyc10g049850.1	TIP41	35.8	7.2%	Expósito-Rodríguez et al, 2008.
Solyc07g025390.2	"*Expressed*"	10.2	8.3%	Expósito-Rodríguez et al, 2008; González-Aguilera, 2016.
Solyc03g115810.2	SAND	45.2	8.4%	Expósito-Rodríguez et al, 2008
Solyc11g005330.1	Actin-B	324.8	5.5%	Wieczorek et al, 2013; González-Aguilera, 2016.
Solyc06g009970.2	EF1-a	525.4	17.4%	Wieczorek et al, 2013.

References are published assessments of reference gene expression stability in Solanum lycopersicum.*

In addition to reference gene CAC, 6 genes were selected for qRT-PCR confirmation of the RNA-Seq results: Phytochrome B-2 (Solyc05g053410.2), Chalcone synthase 2 (Solyc05g053550.2), MYB transcription factor HAT4 (Solyc06g060830.2), Anthocyanidin synthase (Solyc08g080040.2), Cytokinin oxidase/dehydrogenase 7 (Solyc12G00890.1), MYB transcription factor MYB4-like (Solyc07g054980.1). Gene-specific primers were constructed for target genes using Pri-BLAST (**Table 4-1**). To compare the expression of selected genes, the log_2FC difference in expression between R against B, RB, RBG and Fl for each gene was correlated between the qRT-PCR and RNA-Seq and the coefficient of determination (R^2) was calculated to evaluate the strength of correlation (**Figure 4-17**). Comparison of the expression of these 6 genes, using CAC as a reference gene, identified a strong correlation between the RNA-Seq dataset and the qRT-PCR. Overall, the R^2 of 0.85, a strong correlation between the qRT-PCR and RNA-Seq across all treatment comparison and all genes, validating the reliability of the RNA-Seq data.

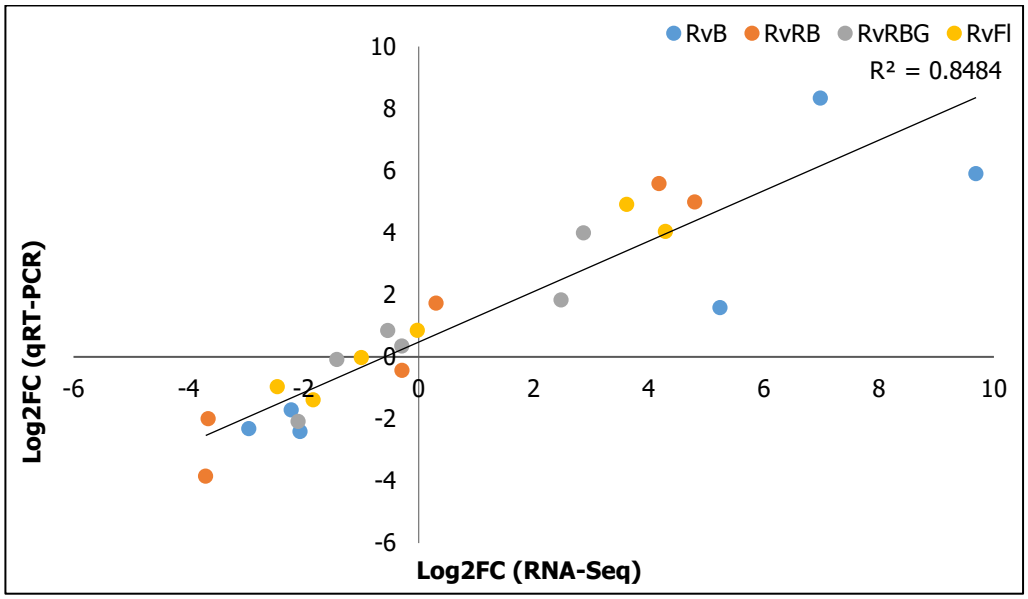


Figure 4-17 qRT-PCR validation of RNA-Seq data. Comparison of average log2 fold ratios of RNA-Seq samples compared to qRT-PCR. Between R v B, RB, G or Fl treatments. APX used as a reference gene for qRT-PCR.

4.4 Discussion

4.4.1 Effect of LED spectra on Micro-Tom leaf transcriptome

We principally investigated the effect of light spectra on the tomato transcriptome through comparisons between plants exposed to a monochromatic red, blue or mixed red, blue, and green light environment. As the light intensity was maintained at 200µmol $m^{-2}s^{-1}$, the only variable was the spectral distribution emitted by the LED lights. The plants were grown continuously from germination under these light environments from germination until 25 days after emergence, and so the difference observed in the transcriptomes are those of the plants long-term acclimated response to shade. In response to changes in spectral quality, there are many early-responsive, short-term signalling events which are attenuated in response to prolonged light signals, allowing plants to respond differently to short-term and sustained signals (L. Li et al., 2014).

Blue light-dependent regulation of gene expression

When R, B, and RBG differentially expressed gene sets were compared for overlap, the largest portion of genes were those in common between RvB and RvRBG, but not differentially expressed in BvRBG. As discussed in the chapter 3 discussion, the common difference in both of this comparison is the absence of blue light in R compared to both RBG and B groups, which emitted with 27% and 100% blue light, respectively. Low-blue light (LBL) regulated shade avoidance is mediated by cryptochrome photoreceptor and occurs when limiting blue light results in low pool of active cryptochrome photoreceptor, as cryptochrome negatively regulates PIF and COP genes, and when inactivated these genes facilitate SAR (de Wit et al., 2016; Keuskamp et al., 2011; Pedmale et al., 2016). In our dataset, PIF1a, PIF1b, and PIF3 were found to be significantly enriched for target genes in both the low RvB and RvRBG differentially expressed gene sets, although the importance tomato PIFs remains largely unknown.

The phenotypes observed in Micro-Tom grown under monochromatic red light compared to those under blue or mixed red, blue, and green LEDs, was consistent with LBL mediated SAR (See **Chapter 3**). LBL is typified by shade-avoidance type apical dominance and petiole elongation as well as photosynthetic

dysfunction in Arabidopsis (Pedmale, 2016). The low-blue light (LBL) shade-avoidance response is a cryptochrome mediated transcriptional response (de Wit et al., 2016; Keller et al., 2011; Keuskamp et al., 2011; Pedmale et al., 2016). In Arabidopsis, the LBL transcriptomic response does not involve enrichment of auxin-responsive genes, despite auxin transport genes being responsible for full induction of LBL mediated shade avoidance (Keuskamp et al., 2011; Pedmale et al., 2016). LBL transcriptome does promote differential expression and over-representation of genes related to cell wall re-modeling and expansion genes (Pedmale et al., 2016), and several members of the XTH family are differentially regulated by PIFs in response to LBL (Keuskamp et al., 2011). Response to blue light was enriched in genes significantly down-regulated in RvRBG while in those genes significantly up-regulated were over-represented for terms related to cell growth, hormone signalling, and xyloglucan metabolism. However, in RvB, there was an absence of growth-related enrichment in genes significantly up-regulated, with enrichment focusing around defense regulated terms (See **Table 8-7**), although as B grown plants are likely to experience induced B absence of low red light, it could be that these genes are being hidden amongst the genes differentially regulated due to the effect of no red on transcriptome. A recent study by Liu on transgenic cry1a identified that cry1a silencing results in increased apical dominance, reduced chlorophyll content and photosynthesis at saturating light, similar to those in monochromatic red light and which we have asserted to be caused by low-blue light (C. C. Liu et al., 2018). However, comparison of transcriptomes of *cry1a* silenced and over-expresser lines to wild-type tomato and our low-blue light dataset of genes commonly differentially expressed in monochromatic red light to blue or mixed red blue and green light showed little overlap in differentially expressed genes (See **Figure 4-18**). Comparison of datasets reveals 77% of genes (905/1174) observed to be differentially expressed under LBL in our dataset are not differentially expressed with manipulation of CRY1a gene. Given the similar phenotypes observed between monochromatic R grown Micro-Tom plants (See Chapter 3) and *cry1a* silenced tomato (C.C. Liu et al., 2018), it is surprising to see the lack of overlap in differentially expressed genes. This suggests the possibility of either a redundant or independent transcriptomic effect of other blue light photoreceptors, most likely cryptochrome homolog CRY1b or CRY2, or that this response is not mediated by cryptochromes.

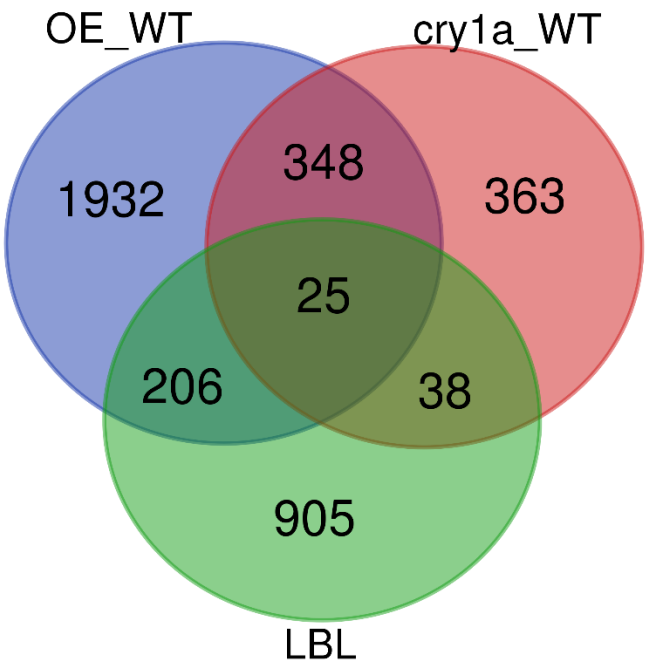


Figure 4-18 Overlap between genes differentially expressed in low-blue light compared to genes differentially expressed in cry1a silenced and over-expression transgenic tomato lines. Venn overlap comparison of low blue light (LBL) differentially expressed genes identified from shared DE genes between RvB and RvRBG from our dataset compared to (C. C. Liu et al., 2018) transcriptomic study of DE genes between wild-type (WT) tomato and transgenic lines cry1a silenced (cry1a) and over-expresser (OE).

Hormone metabolism and signalling are coordinately regulated by LED spectra

The largest overlap in differentially expressed genes between R, B, and RBG transcriptomes was in genes commonly differentially expressed genes in both RvB and RvRBG comparisons. The expression patterns of several hormone-metabolic and signalling genes was significantly altered in R compared to both B and RBG, including growth regulating transcription factors gibberellins, cytokines, auxin, and abscisic acid. The role of light spectra in the control of hormone homeostasis and signalling is well established in model plant *Arabidopsis thaliana*, indicating an integration of photoreceptor-mediated light signals and hormone signals to coordinately regulate gene expression. Phytohormones gibberellin, auxin and brassinosteroids have been found to be integral secondary messengers to photoreceptor-mediated light signalling, integrating light and hormone signals effect

on growth and development (Bai et al., 2012; E. Oh et al., 2007; Eunkyoo Oh et al., 2012; F. Xu et al., 2018) (Oh et al., 2007; Oh et al., 2012). Plant hormone signal transduction was strongly enriched in RvB up-regulated, RvRBG up-regulated and BvRBG down-regulated gene sets, indicative of a transcriptional re-programming of the gene responsible for inducing hormone-mediated light responses.

Gibberellins play an important role in promoting stem growth. Gibberellin biosynthesis genes were up-regulated in R compared to B and RBG (GA20ox-1; Solyc03g006880), while catabolic gene expression (GA2ox7; Solyc02g080120.1) was coordinately down-regulated. Similarly, in rice, blue light triggers a reduction in GA level through simultaneous repression of GA20-oxidases and induction GA2-oxidases involving the cryptochrome1a and cryptochrome 1b (Hirose et al., 2012). Constitutive suppression of GA20ox-1 in tomato resulted in dwarf phenotype and darker leaves (Olimpieri et al., 2011). Conversely, over-expression of GA2ox7 homolog in Arabidopsis *AtGA2ox7* also create dwarf plants through reducing the active GA levels (Schomburg, Bizzell, Lee, Zeevart, & Amasino, 2003). The GA-reporter gene SlGAST1 (Solyc02g089350.2) was significantly up-regulated in R compared to B and RBG, significantly down- and up-regulated in *cry1a*. Together this suggests, that blue light suppresses GA biosynthesis and signalling. Both GA levels and expression of GA metabolic genes were positively regulated by cryptochrome 1a differentially regulated in *cry1a* tomato over-expressers and knockouts (C. C. Liu et al., 2018), suggesting that cryptochrome 1a regulates blue light suppression of GA biosynthesis and signalling.

In addition to gibberellins, auxins play a significant role in photoreceptor-mediated growth regulation. In contrast to R, the transcription of negative regulators of auxin signalling was enhanced in B and RBG light, suggesting that auxin levels are high in monochromatic red grown plants. Gene enrichment did not find any significant over-representation of genes related to auxin biosynthesis or signalling. However, the plant hormone signal transduction KEGG path showed strong differential expression of auxin signalling genes (See **Figure 4-9**
Figure 4-9). Further heatmap analysis of the patterns in gene expression showed substantial down-regulation of auxin-regulated genes (SAUR, AUX/IAA, PIN, GH3) in R compared to B and RBG (See **Figure 4-10**). Light modulates auxin sensitivity through PIF4/PIF5 (Hornitesch et al., 2012) and direct interaction between

phytochrome and cryptochromes with AUX/IAA (Xu et al., 2018). Furthermore, photoreceptor signalling components PIFs directly promote/repress 32 SAUR gene expression (N. Sun et al., 2016), as well as a transcription of auxin biosynthesis, conjugation, transport, perception and signalling genes (Iglesias, Sellaro, Zurbriggen, & Casal, 2018). Several SAURS, AUX/IAAs, and GH3 were significantly differentially expressed in our dataset. SAUR59 (Solyc06g053290.2) the most highly expressed SAUR family gene in leaf tissue, was significantly up-regulated in RvB and RvRBG, 1.3 and 0.7 log_2fold, respectively. Several SAUR family genes are rapidly induced by shade in Arabidopsis hypocotyls, and the pattern of expression of SAUR59 is consistent with the blue-light suppression of shade avoidance response (Spartz et al., 2012). A link between photoreceptors signalling and SAURs has been made, as in Arabidopsis, SAUR genes have been shown to be induced by shade and photoreceptor signalling components, transcription factors PIF4 and PIF5, as they directly bind to several SAUR gene (Hornitschek et al., 2012). Notably, a GH3-like encoding gene (Solyc12g084490.1) significantly down-regulated in R compared to B and RBG. GH-3 negatively regulating auxin homeostasis through reducing free auxin levels, and over-expression of an *OsGH3* in rice resulted in reduced free-IAA causing shade avoidance responses including dwarfing increased leaf size (Du, Wu, Fu, & Lizhong, 2012). Moreover, the hierarchical clustering identified that in a cluster of R up-regulated genes (cluster 2), xyloglucan endotransglucosylase/ hydrolase 16 was significantly up-regulated in R grown plants, and the family was enriched in this cluster. XTHs are integral enzymes involved in the loosening of cell walls associated with cell elongation and growth, and in Arabidopsis, facilitate shade-avoidance induced growth in response to both red and blue light (Keuskamp et al., 2011). Additionally, auxin signals regulate the levels of growth hormone cytokinin to control cell expansion and growth (Carabelli et al., 2007). Cytokinin oxidases are induced by auxin signals which degrade cytokinin resulting in the arrest of leaf growth and development (Carabelli et al., 2007). Promotion of cytokinin catabolic gene, cytokinin dehydrogenase/ oxidase (CKX6; Solyc12g008900.1) in R compared to B and RBG implicates the B light in the suppression of cytokinin catabolism. Tomato cryptochrom1a negatively regulates cytokinin levels and expression of CKX genes to control cell growth (C. C. Liu et al., 2018).

Abscisic acid plays an antagonistic role to gibberellin in plant growth. In wheat, over-expression of wheat abscisic acid and gibberellin metabolism are antagonistically regulated, with blue light promoting NCED expression and ABA accumulation (Gubler, Hughes, Waterhouse, & Jacobsen, 2008). Similarly, the highly expressed ABA biosynthesis gene NCED4 (Solyc07g056570.1) was 4-fold down-regulated in both RvB and RvRBG differential expression analysis. Consistent with increased ABA in B and RBG compared to R, ABA signalling transcription factor ABI-5, AREB and PP2C were not significantly differentially expressed but were significantly enriched for target genes from down-regulated RvB and RvRBG gene sets. In Arabidopsis blue-light dependent. Interestingly, silencing *OsGH3* not only reduced free-IAA but also ABA levels and expression of ABA biosynthesis genes (Du et al., 2012). The role of abscisic is antagonistic to that of both auxin and gibberellin, repressing growth. In fact, *OsGH3-2* over-expression in ABA in rice transgenic lines decreased ABA biosynthesis and increased stress tolerance (Du et al., 2012).

Photosynthesis expression was also suppressed under monochromatic red LED light

The expression pattern of Calvin-Benson cycle genes involved in carbon-fixation and starch metabolism were significantly down-regulated in Micro-Tom plants grown under R compared to B and RBG, evident in the enrichment of photosynthesis-related terms in the down-regulated genes in RvB and RvRBG, as well as in the heatmap of expression photosynthesis-related genes (See **Figure 4-7**, **Figure 4-8).** Targeted improvement of crop species has through increasing expression of photosynthesis-related gene expression, as several mutants deficient in components of photosynthesis pathways exhibit decreases in CO_2 assimilation. Rubisco sub-unit rbcS, (Solyc02g085950.2), the most highly expressed gene in the leaf transcriptome, was significantly down-regulated in R compared to B (-0.42 log2fold) and RBG (-0.18 log2fold). ABA positively regulates rbcS transcription in tomato leaves (Bartholomew, Bartley, & Scolnik, 1991), and since ABA biosynthesis gene NCED4 was down-regulated in R compare to B and RBG, it is possible ABA down-regulation in R is responsible for reduced rbcS expression. Two highly expressed fructose 1,6-bisphosphate aldolase 1, FBA1 (Solyc01g110360.2) and FBA3 (Solyc02g084440.2), which are integral enzymes to the Calvin-Benson cycle where it generates enzymes metabolites for starch metabolism. Repression of FBA in potato drastically reduced

photosynthesis and plant growth (Kossmann & Sonnewald, 1991). SlFBA7 over-expression increased the not only expression and activity of other enzymes within the Calvin cycle but also net photosynthetic rate, which increased stem diameter, seed size, and resistance to abiotic stress (Cai et al., 2016). In Arabidopsis, phytochrome inactivation by sustained low R: FR inhibits photosynthesis in Arabidopsis through inactivation of phytochromes causing down-regulation of photosynthesis-related genes (Cagnola et al., 2012), However, as photosynthesis was down-regulated in monochromatic R plants, in which phytochrome activation status will be high, it is unlikely phytochromes regulate photosynthesis in tomato. Multiple tomato cryptochrome receptors have been identified to extensively positively regulate transcription of photosynthesis-related genes (Facella et al., 2017; C. C. Liu et al., 2018). In fact, several sigma factors were found to be promoted by blue light, as the expression was significantly higher in B compared to both R and RBG (See **Table 4-9**). Sigma factors facilitate PEP promotion of plastid transcription and promote the expression of photosynthesis-related gene expression including rbcS and light-harvesting components (Puthiyaveetil et al., 2010). In Arabidopsis, cryptochromes regulate sigma factor transcription in response to blue light (Onda, Yagi, Saito, Takenaka, & Toyoshima, 2008). The promotion of PEP transcription in response to blue light could be a module through which blue light promotes photosynthesis in tomato. Given this, we propose that the absence of blue light in the monochromatic R treatment resulted in inactive cryptochrome pool and therefore no CRY-mediated promotion of photosynthesis gene expression.

Defense and jasmonic acid biosynthesis was down-regulated under monochromatic blue light

The expression of defense related hormones and defense signalling genes were significantly altered in response to spectral quality. Red light is strongly associated with positive regulating defense, as a strong body of evidence generated in Arabidopsis shows phyB inactivation increasing plant susceptibility to pathogens and herbivores (Ballaré, 2014; De Wit et al., 2013). The genes upregulated in R compared to B and RBG in the hierarchical clustering (cluster 1) were enriched for association to two defense related pathways ‘plant-pathogen interaction’ and ‘MAPK signalling pathway – Plant’, as were RvB up-regulated genes. Jasmonic acid biosynthesis, jasmonic acid signalling, and defense related genes were significantly enriched in

RvB up-regulated genes, and to a lesser extent defense related terms enriched in BvRBG down-regulated genes, implicating B as having reduced defense related gene expression. Jasmonic acid biosynthesis genes encoding Allene oxidase cyclase (AOC; Solyc02g085730.2), allene oxidase synthase (AOS1; Solyc04g079730.1), were significantly up-regulated in RvB and RvRBG, and significantly down-regulated in BvRBG. This pattern of expression is consistent with either red light promotion of JA biosynthesis, or blue light inhibition of it. Both AOS1 and AOC were negatively regulated by tomato cry1a, as was JA content (C. C. Liu et al., 2018). R: FR induced shade avoidance in tomato reduces jasmonate sensitivity, and induced of defense related ERF transcription factor (Cagnola et al., 2012), a family which was down-regulated in B grown plants in this experiment (See **Figure 4-5**). Core JA positive signalling transcription factor Jasmonate ZIM-domain 1 (ZIM1; Solyc12g009220.1), was also transcriptionally up-regulated under monochromatic red light (See **Table 4-11**). ZIM is a transcriptional repressor which is regulated phytochrome B and red light and has been shown to not only control defense-related gene expression but also regulates growth and photosynthesis (Campos et al., 2016). *phyB* and *pif4* transgenic lines have reduced defense and photosynthetic efficiency, however, this is rescued by crossing with *jazQ*, a quintuple Jasmonate ZIM-domain transcription factor silenced plants (Campos et al., 2016). The expression of defense related transcription factors was also affected by spectral quality, as substantial down-regulation of ERF family, transcription factors occurred in R, while WRKY genes showed a trend of up-regulation in both R and RBG compared to B (See **Figure 4-5**). Finally, ROS biosynthesis gene RESPIRATORY BURST OXIDASE HOMOLOG1 (RBOH1) was also significantly up-regulated in R compared to B and RBG. RBOH-dependent is integral for ROS mediated promotion of abiotic and biotic stress resistance (Baxter, Mittler, & Suzuki, 2014).

4.4.2 Co-action of red and blue light up-regulates pigment metabolism

The GO term ‘pigment metabolism’ was significantly enriched in both RvRBG down-regulated and BvRBG up-regulated gene sets (See**; Table 8-10; Table 8-11**). Chlorophyll synthesis in the present experiment was increased in Micro-Tom grown under the mixed LED light treatment RBG in comparison to both monochromatic R and monochromatic B grown plants. Blue light regulates some of

the enzymes involved in chlorophyll biosynthesis. In rice, blue light regulates several chlorophyll biosynthetic genes including. Cryptochromes regulate the expression of chlorophyll biosynthetic genes, and over-expression of SlCRY2 in tomato resulted in the over-production of chlorophyll biosynthesis (Giliberto et al., 2005). However, in this experiment Neither B or R alone was sufficient to stimulate the expression of chlorophyll biosynthesis genes (See **Table 4-10**). A synergism between red and blue light in the regulation of both gene expression and subsequent development has been described in Arabidopsis. In this model, co-action of both red and blue light signals perceived by the phytochrome and cryptochrome photoreceptors, respectively, is required for effective signalling and involves several key light signalling components such as HY5, COP1, and DET1 (Sellaro, Hoecker, Yanovsky, Chory, & Casal, 2009; Usami, Mochizuki, Kondo, Nishimura, & Nagatani, 2004). Given the expression of chlorophyll biosynthesis genes is up-regulated in RBG, it is plausible that pigment metabolism in *Solanum lycopersicum* requires co-activation of both red and blue light signals.

The expression of several anthocyanin biosynthesis genes exhibited a pattern whereby expression was non-detectable or lowly expressed in B, moderately expressed in R and highly upregulated in RBG. This suggests again of a co-action model which necessitates both red and blue light signals together to stimulate anthocyanin gene expression. Through co-expression network analysis, we identified a module of co-expressed anthocyanin biosynthesis genes (See **Figure 4-15**), in which nine highly differentially expressed anthocyanin biosynthesis genes were co-expressed, including phenylpropanoid biosynthesis gene phenyl ammonia lyase and downstream genes in the anthocyanin biosynthesis pathway anthocyanidin synthase, dihydroflavanol reductase. Additionally, a known anthocyanin regulating transcription factor was also co-expressed with these genes (Qiu et al., 2016), suggesting that light regulates anthocyanin biosynthesis through transcriptional regulation of the AH transcription factor. AP2e was linked indirectly to the anthocyanin metabolic genes and showed strong correlation ($R^{2=}0.92$) with the anthocyanin content of Micro-Tom leaves grown under the same spectral qualities used in the transcriptomic experiment. AP2e tomato homolog AP2a is a core regulator of fruit ripening, and positively regulates phenylpropanoid pathway gene expression, of which anthocyanin is a part of, as well as and carotenoid biosynthesis (Karlova et

al., 2011). Phenyl ammonia lyase, the phenylpropanoid biosynthesis genes, was also part of our co-expression module. Given this evidence, the expression pattern and co-expression network AP2a in the regulation of anthocyanin biosynthesis through regulation of AH transcription.

4.4.3 Fluorescent tube lighting elicited vastly different transcriptome to LEDs

The transcriptomic comparison of Micro-Tom plants grown under fluorescent tube lighting and various LED spectral qualities revealed that the greatest difference was the technology, with the first principle component of variation separating Fl from the LED transcriptomes. If spectral quality was the only variable, then we would expect the Fl transcriptome to be somewhat similar to that of the mix LED lighting, as the integral wavelengths red and blue, as well as green, are all there. However, one benefit of LED lights and an important uncontrolled variable in this experiment was the while LEDs are cool and do not generate a lot of waste heat energy, fluorescent tube lighting produce significantly more heat. The fluorescent tube lighting operated ~2^{o}C hotter than the LEDs, and this could be the cause of the subtle (generally low log2FC) but substantial (several thousand genes) shifts in the transcriptome of Fl compared to all the LED wavelengths. If it were the effect of the spectral quality that acted as the main factor causing the difference, we would not expect to see such a large degree of overlap between DE genes of FlvR, FlvB, and FlvRBG.

Nevertheless, the fluorescent tube lighting had a substantial effect on the transcriptome and the gene enrichment analysis of the overlapping genes revealed that the technological differences impacted on development, photosynthesis, pigment metabolism. Relatively small changes in temperature have been shown to extensively reprogram the transcriptome of Arabidopsis, and changes in temperature which do not elicit heat stress but cause a change are collectively known as themormorphogenesis (Quint et al., 2016). Several core components of the light signal transduction have recently been discovered to be integral to temperature perception. In fact, red light photoreceptor phytochrome B perceives temperature through it its temperature-dependent reversion of active phytochrome to an inactive form, and this is physiologically relevant, integrating growth responses to both temperature and light

(Legris et al., 2016). Core light signal transduction transcription factor PIF4, as well as the circadian clock, have recently been identified as being regulated in response to temperature and as important hub elements in the transcriptional reprogramming (Jung et al., 2016; Quint et al., 2016). The integration of temperature and light signals through shared networks may explain why many of the enriched terms present in FlvLED overlapping genes as those seen enriched in comparisons between RvBvRBG, relating to photostynthesis, development, and pigment metabolism. While fluorescent tube lighting has been traditionally used for a broad spectrum control in experiments investigating the effects of LED spectra, the effect of

4.4.4 The unexplained variance between RB and RBG transcriptome

The PCA plot revealed an unexpected variance in the RB grown plants compared to all other treatments, including RBG, with it being the second leading cause of variance between all samples. Due to the similarity in the wavelengths emitted in the RB and RBG treatment, with the difference being only 15% green light, compared to the drastically different spectral qualities in the R and B monochromatic treatments. Investigation of the particular LED light revealed a malfunction in one of the four panels, in which it overheated and intermittently switched off, meaning at times these plants were receiving approximately 25% less light intensity than the other treatments. Future transcriptomic investigation of the effect of supplemental green light in addition to RB revealed the difference in the transcriptome is not substantial, and therefore we feel it necessary to remove this data from further analysis.

4.4.5 Limitations of this experiment

As this study involved transcriptomic analysis of RNA samples taken at a single time-point there are inherent limitations to the interpretation of the results, as this transcriptomic study only determines the expression of genes between treatments in a single tissues, at a specific developmental stage. The RNA samples were extracted from leaf tissue after 25 days grown under different LED spectra, and so the plants would have adapted to the different spectral qualities, and those genes differentially expressed will either be those directly persistently differentially

regulated by light or those indirectly regulated by the effect of light spectra on the developmental speed of the plant. Further analysis of a time-course throughout different stages of growth would reveal the effect spectral quality has on tomato throughout its lifecycle, while the study of other tissue such as the stem could reveal how spectral quality differentially regulated gene expression in different plant tissues. Furthermore, as light interacts with other environmental signals, such as temperature, which has been shown to be perceived through the phytochrome and cryptochrome photosensors (Legris et al., 2016; Toledo-Ortiz et al., 2014), the effect of spectral quality on the transcriptome observed in this experiment may vary as other environmental conditions fluctuate. As well as environmental conditions, the properties of the light given itself, such as light intensities and photoperiod may also influence the effect of spectral quality on the transcriptome. This study is a step towards understanding the effect of light spectra on tomato transcriptome, and future experiments studying the contribution of other developmental and environmental factors are necessary to fully resolve the complex transcriptional networks which underpin the adaptive responses to light.

4.4.6 Conclusions

In summary, the use of RNA-Sequencing allowed us to identify thousands of genes that were differentially regulated by spectral quality in tomato, providing insight into the response of tomato plant to various wavelengths of LED light. Compared to plants grown under monochromatic blue or a mixed spectra of red, blue and green LED light, plants grown under monochromatic red light were associated with the expression of growth-promoting hormones gibberellin, cell-wall modifying enzymes, pigment metabolism, and photosynthesis. Secondly, a large number of defense genes, including jasmonic acid biosynthesis and signalling, and ROS biosynthesis genes, and WRKY transcription factors were significantly down-regulated in monochromatic blue grown plants. Chlorophyll and anthocyanin metabolic genes were up-regulated in plants grown under mixed RBG light compared to R and B, suggesting the necessity for both red and blue wavelengths for transcriptional promotion of pigment metabolism. Furthermore, we identified a co-expression module involving nine anthocyanin biosynthesis genes, a known transcription factor ANTHOCYANINLESS which is responsible for transcriptionally

regulating the expression of anthocyanin biosynthesis genes, and an APETELA/ERF transcription factor. Finally, the profound effect of fluorescent tube lighting on the transcriptome compared to various LED light wavelengths highlighted the influence of even moderate temperature fluctuations on gene expression. These findings contribute to a better understanding of the molecular basis of the responses of S. Lycopersicum to light spectra and could provide new insight into mechanisms through which spectral quality coordinates plant development through regulation transcriptional control, and be helpful in identifying new molecular markers for genetic improvement of tomato growth in response to light quality.

5 Investigating Genes of Interest and Candidate Gene Selection

5.1 Introduction

In our previous work, we have conducted phenotyping of Micro-Tom grown under varying spectral qualities and then complemented this with a transcriptomic study to understand the genetic mechanisms which underpin the phenotypic plasticity of plants depending on its light environment. In this chapter, we will report research on several genes which meet selection criteria for consideration as candidate genes for investigation of function by transformation:

(i) Transcriptomic criteria: Gene must be highly differentially expressed, be moderate-to-highly expressed (CPM >5), and exhibit a considerable change in fold expression (significantly DE).

(ii) Literature/bioinformatics evidence: Evidence from previous literature/bioinformatics must associate this gene, or orthology from another species with either/both an important role in photomorphogenic response to light or a role in a specific phenotype observed.

(iii) Gene must not have been previously studied in tomato.

(iv) Gene must be constitutively differently regulated by light as shown by time-course analysis

5.1.1 Review of Candidate Genes of Interest

Table 5-1 reports the differential expression statistics between R, B, and RBG in pair-wise comparisons for 10 candidate genes of interest, identified from RNA-Seq transcriptomic analysis of Micro-tom leaves grown under varying spectral qualities. Their description according to UNIPROT and $\log_2$ fold change (LFC) and significance (FDR) is reported.

Table 5-1 RNAseq differential expression analysis results for genes of interest in RvBvRBG leaf samples

ID	Gene_ID	Description	RvB		RvRBG		BvRBG	
			LFC	FDR	LFC	FDR	LFC	FDR
XTH16	Solyc07g052980	XTH16; xyloglucan endotransglucosylase/hydrolase	0.8	5.8E-10	1.7	5.2E-44	0.9	5.7E-13
MYB-D	Solyc07g054980	Myb-related transcription factor	9.7	1.2E-54	2.5	7.5E-20	-7.2	1.8E-13
HAT4	Solyc06g060830	homeobox-leucine zipper protein HAT4	-2.9	5.8E-91	-0.5	4.9E-03	2.4	7.5E-66
CKX	Solyc12g008900	SlCKX6; cytokinin dehydrogenase 3	7.0	6.9E-42	2.9	4.2E-11	-4.1	5.6E-17
C2H2	Solyc05g009170	zinc finger protein 6	3.4	5.4E-19	2.2	1.0E-09	-1.2	2.1E-02
FSM1	Solyc10g052470	fsm1; SANT/MYB domain protein	2.0	2.3E-14	1.5	8.7E-09	NS	NS
SAUR59	Solyc06g053290	SAUR59; auxin-induced protein X15	1.3	1.8E-20	0.8	7.3E-08	-0.5	2.3E-03
FLZ6	Solyc09g074430	FZY6; probable indole-3-pyruvate monooxygenase	1.2	2.4E-03	1.0	2.0E-02	NS	NS
DOT3	Solyc05g051580	putative BTB/POZ domain-containing protein DOT3	-2.6	1.9E-26	-2.1	1.7E-16	NS	NS
LBD	Solyc03g119530	LOB domain-containing protein 40-like	1.2	2.5E-07	1.6	8.9E-12	NS	NS

R= monochromatic red; B=- monochromatic blue, RBG= Red, blue and green light; NS= Not significantly DE.

XTH16- Solyc07g052980

XTH16 (Solyc07g052980.2) encodes a xyloglucan-endotransglucosylase transferase/ hydrolase, which is a family of enzymes that are involved in the modification of cell wall structure by cleaving and re-joining the xyloglucan molecules that in primary cell walls. XTH16 was significantly up-regulated in R compared to B and RBG (See **Table 5-1**). The cleavage and re-assembling of xyloglucan chains functions in the loosening and rearrangement of the cell wall, which promotes elongation response. In Arabidopsis, several XTH family genes are positively upregulated in response to both low red: far-red and green simulated shade (Sasidharan et al., 2010). Knockout mutants of two XTH genes (XTH15 and XTH17) in Arabidopsis had reduced or absent shade avoidance response to both low red: far-red and green shade, measured by petiole elongation rate (Sasidharan et al., 2010). The tomato XTH Solyc07g052980.2 shares one-to-one homology with Arabidopsis AT4G03210 (79/68% identity) which encodes XTH9. XTH9 in Arabidopsis has been shown to be transcriptionally regulated in a developmental manner, and is expressed in leaves, petioles, and internodes, and associated with cell elongation and growth (Hyodo et al., 2003). An AtXTH9 homolog in *Brassica campestris* (Field mustard), BcXTH1, was over-expressed in Arabidopsis producing distinct cell expansion

phenotype, with the protein almost exclusively located at cell wall (Shin et al., 2006). In a transcriptomic study of tomato *cryptochrome-1a* silenced plants, GO terms ‘xyloglucan: xyloglucosyl transferase activity’ and ‘hydrolase activity, acting on glycosyl bonds’ were significantly enriched in genes differentially expressed in the mutant relative to the wild-type transcriptome, and this was complemented with mutant plants exhibiting a SAR related elongation phenotype, increased cell expansion, and up-regulation of genes involved in cell cycle control (C. C. Liu et al., 2018).

HAT4- Solyc06g060830

HAT4 (Solyc06g060830.2) encodes a member of the Homeodomain, Leucine-zipper (HD-ZIP) family of transcription factor. HAT4 was significantly up-regulated in monochromatic B transcriptome (See **Table 5-1**). Member of this family have been identified in Arabidopsis to function in roles including response to environmental conditions, meristem regulation, organ, and vascular development, and mediation of hormone action (Ariel, Manavella, Dezar, & Chan, 2007). The best reciprocal BLAST hit against the Arabidopsis genome is Arabidopsis AT4G16780 (ATHB2 | AtHAT4). Arabidopsis transcription factor AtHB2 is rapidly induced by upon encountering low R: FR simulated shade (Carabelli, Morellit, Whitelamt, & Ruberti, 1996). Several Arabidopsis HD-ZIP family members (HAT2, HAT3, HAT4/AtHB2)) are all strongly and rapidly decrease in mRNA levels under blue light (Jiao et al., 2003). Evidence suggests AtHB2 functions down-stream of phytochrome photoreceptors in light signal transduction and is modulated through interaction with PIF4 and PIF5 (De Lucas et al., 2008; Hornitschek et al., 2012). AtHB2 is proposed to be involved in an external coincidence model involving the circadian clock regulated PIF4/PIF5 in the regulation of photoperiodic control of plant growth and development (Kunihiro et al., 2011). AtHB2 is a negative regulator of gene expression, and a positive regulator for hypocotyl elongation, however, the over-expression of AtHB2 resulted in only modest increases in elongation (Steindler et al., 1999). AtHB2 is involved in leaf development as well as regulating activity in the shoot apical meristem (Turchi et al, 2011). There is no evidence this gene has been characterized in tomato.

CKX- Solyc12g008900

CKX (Solyc12g008900) is a putative cytokinin dehydrogenase/kinase which shares many-to-many homology with two Arabidopsis Cytokinin dehydrogenases CKX2 and CKX4. Cytokinins are a class of phytohormones that promote cell division, though often having opposing effects on roots and shoots. They are key regulators of cell growth and differentiation but also have been shown to regulate processes such as apical dominance, axillary bud growth, and leaf senescence. Cytokinin dehydrogenases (CKX) are catabolic enzymes which play a principal role in controlling cytokinin levels in plant tissues (Werner, Motyka, Strnad, & Schmülling, 2001). CKX6 was significantly upregulated by R light compared to both B and RBG, whilst also significantly down in B compared to RBG. Low R: FR shade signals have been shown to inhibit leaf growth through auxin-induced up-regulation of CKX activity resulting in a reduction of cytokinin levels (Carabelli et al., 2007). CKXs have been characterized in several species. Arabidopsis CKX was over-expressed in tobacco leading to drastically improved root mass as well as shoot dwarfing (Werner et al., 2001). Similarly, Barley HvCKX2 was over-expressed in tobacco, with mutant plants exhibiting elevated CKX activity, a dwarf phenotype caused by internode shortening and substantially increased root mass (Galuszka et al., 2004).In rice, reduced expression of OsCKX2 in rice led to cytokinin accumulation in inflorescence meristems and increases the number of reproductive organs, resulting in enhanced grain yield (Ashikari, 2005). Tomato Cytokinin dehydrogenases have not been characterized by mutant analysis. Gene expression studies have shown tomato a CKX was shown to be upregulated during drought stress, and was associated with hydrogen peroxide accumulation by the author, although based on data this was speculative (Cueno et al, 2012). An Arabidopsis CKX gene has been over-expressed in tomato: Tomato plants transformed to over-express Arabidopsis CKX3 enzyme showed improved drought resistance due to reduced leaf area and stomatal density caused by reduced Cytokinin levels, therefore positive associating Cytokinin levels with transpiration rate (Farber, Attia, & Weiss, 2016). Several CKX genes were differentially regulated in complementary silencing and over-expression of CRY1a gene in tomato, including CKX (our gene of interest) which is highly down-regulated in *cry1a* overexpressing lines.

MYB-D –Solyc07g054980.1

MYB-D (Solyc07g054980.1) is an MYB transcription factor uncharacterized on gene/protein level. MYB gene containing EAR motif, a highly conserved domain involved in transcriptional repression (Li et al, 2016). This transcription factor was differentially expressed in all comparisons between R, B and RBG (See **Table 5-1**). In fact, MYB-D was the most highly differentially expressed gene between in both RvB and BvRBG comparisons, substantially light regulated. MYB-D is an R2R3 type MYB transcription factor homologous to Arabidopsis AtMyb15 (1e151). *AtMyb15* overexpression confers hypersensitivity to abscisic acid and improved drought and salt stress tolerance through promoting the expression of ABA biosynthesis and signalling genes (Ding et al., 2009).

SAUR59 – Solyc06g053290.1

SAUR59 (Solyc06g053290.1) encodes a member of the SAUR (Small Auxin up RNA) family, which are well established as auxin signalling genes. Several SAUR genes have been found to positively regulate apical growth in response to auxin. Several SAUR proteins are rapidly induced by shade in elongating hypocotyls (Spartz et al., 2012). A link between photoreceptors signalling and SAURs has been made, as in Arabidopsis, SAUR genes have been shown to be induced by shade and photoreceptor signalling components, transcription factors PIF4 and PIF5, as they directly bind to several SAUR gene promoters (SAUR19 subfamily genes) (Hornitschek et al., 2012). **Figure 5-1** shows the expression profile of this gene across from RNA-Seq of Micro-Tom leaf tissue grown under varying spectral qualities. Solyc06g053290 is a highly expressed SAUR, with expression under R light of 56 FPKM. In addition to this, it is significantly differently expressed between R and all other light treatments, and correlation of average height of plants and gene expression shows a high correlation (R^2=0.95). **Table 6-1** shows the differential expression of SAUR gene in pairwise comparisons between RvBvRBG.

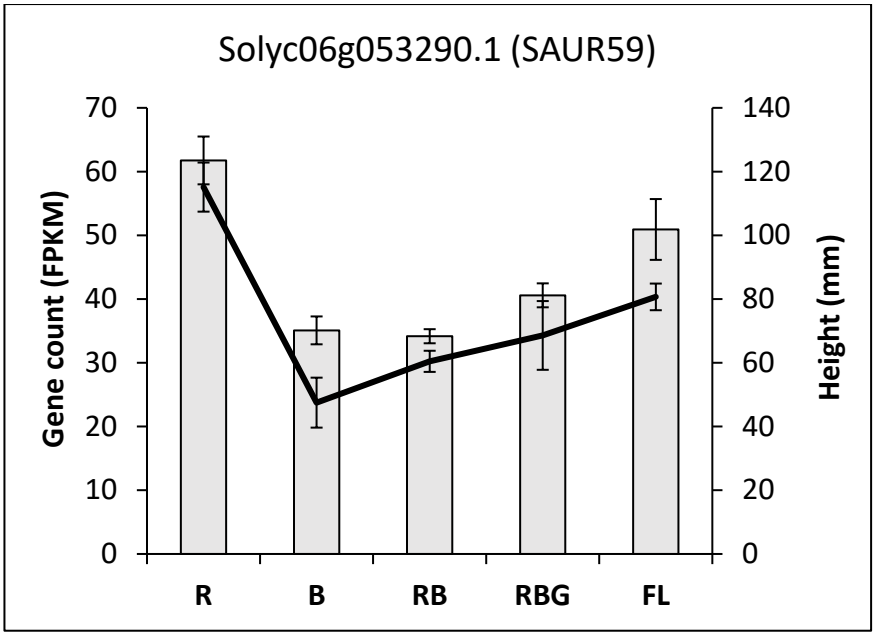


Figure 5-1 Expression of gene Solyc06g053290.1 and height of plants grown under varying spectral qualities. Both leaf tissue samples and height measurements are taken from Micro-Tom 25 days after emergence. The line is the height (right axis), columns are the gene count (left axis). Correlation coefficient between the expression of leaf tissue and height (R^2) = 0.95.

C2H2- Solyc05g009170.1

C2H2 (Solyc05g009170.1) encodes a zinc-finger protein transcription factor. C2H2 Zinc finger proteins have been implicated as light responsive, as they are switched on during photomorphogenesis, as well as being regulated by phytohormones gibberellin and cytokinin (Chrispeels, Oettinger, Janvier, & Tague, 2000; L. Sun et al., 2015). C2H2s have been shown to regulate plant development including trichrome formation, shoot maturation, and flowering. In addition to this, C2H2s have also been implicated in stress tolerance, while genetic engineering of a C2H2 gene, ZaT12, resulted in enhanced drought tolerance (Rai, Singh, & Shah, 2013). There is no evidence that this gene has been studied in tomato according to several databases included PlantTFDB, UNIPROT and NCBI annotation of the gene or protein.

DOT3 - Soly05g051580.2

Soly05g051580.2 (DOT3) is a BTB/POZ domain-containing protein which shares one-to-one homology (65% ID, coverage 79%, E= 2e-82) with Arabidopsis gene encoding DOT3. DOT3 contains an NPH3 domain, which interacts with phot1

photoreceptor, functioning as a substrate adapter targeting phot1 for proteolytic degradation by E3 ligase CULLIN3. Silencing of *Atdot3* in *Arabidopsis* resulted in plants with dwarf phenotype, stunted root development, and reduced fertility (Petricka, Clay, & Nelson, 2008). Solyc05g051580 is significantly down-regulated in RvB and RvRBG (See **Table 5 1**). No evidence that this gene has been studied in tomato according to several databases included PlantTFDB, UNIPROT and NCBI annotation of the gene or protein.

LBD- Solyc03g119530

Solyc03g119530 encodes a lob-domain containing protein (LBD). Silencing of an LBD homolog in Arabidopsis altered anthocyanin metabolism and nitrogen uptake assimilation and nitrogen-use efficiency, resulting in retarded growth (Rubin, Tohge, Matsuda, Saito, & Scheible, 2009). The LBD homolog in Arabidopsis (3e-79), AtASL2, is expressed in an ARF-dependent manner, that partially complements ARF function in promoting lateral root formation (Okushima, Fukaki, Onoda, Theologis, & Tasaka, 2007), and is also involved in leaf development (Iwakawa et al., 2002). This gene is significantly up-regulated in R light and the expression of this gene also strongly correlates with height profiles observed at the time of tissue harvest (R^2= 0.96). This expression range of this gene is good, with its minimum expression observed 4FPKM.

FLZ6 - Solyc09g074430

FLOOZY6 (FLZ6; Solyc09g074430) is a flavin mono-oxygenase enzymes involved in a rate-limiting step in auxin biosynthesis in plants. *flz* is homologous to Arabidopsis *yucca* gene, over-expression of these genes in Arabidopsis results in auxin overproduction (Cheng, Dai, & Zhao, 2006) and are required for shade avoidance (C.-X. Li et al., 2017; Sellaro et al., 2010). In Arabidopsis and other diverse species including rice and petunia, FLOOZY/YUCCA genes are involved in auxin biosynthesis which regulates plant development and leaf and flower architecture (Tobeña-Santamaria et al., 2002; Yamamoto, Kamiya, Morinaka, Matsuoka, & Sazuka, 2007). ToFLZ6 is preferentially expressed in the roots (Expósito-Rodríguez, Borges, Borges-Pérez, & Pérez, 2011), however, in our experiment not only was it differentially up-regulated in red light but also the most highly expressed tomato FLZ

gene in our experiment. Given the importance of auxin to shade avoidance, and the differential up-regulation of R in conjunction with shade-avoidance type growth, flz6 was selected for quantification of expression by time-course series.

FSM1- Solyc10g052470

Solyc10g052470 encodes an MYB-related transcription factor (FSM1) which is a known negative regulator of cell expansion and morphogenesis-regulating transcription factor (MacHemer et al., 2011). Fsm1 was 4-fold up-regulated in RvB and 3-fold up-regulated in RvRBG (See **Table 5-1**). This gene has a previously been characterized in *Solanum lycopersicum*, yet was included anyways

5.1.2 Aims

To further validate the differential expression of the candidate genes of interest, we not only validate the expression of the genes in the RNA samples sent for RNA sequencing but also ran an independent gene expression time-course experiment. A second independent experiment replicated the conditions used for both Chapter 3 and Chapter 4 was conducted, growing Micro-Tom under R, B, RB, and RBG LED lights. In this experiment, leaf RNA will be harvested at three different time-points weekly during the vegetative stage of plant growth. qRT-PCR analysis of gene expression was conducted on the genes of interest across the time-series, as well as the RNA samples used for RNA-Seq. This identified which of the candidate genes identified from chapter 4 are consistently differently regulated by varying spectral quality.

5.2 Methods

5.2.1 Plant materials and growing conditions

Solanum lycopersicum c.v Micro-Tom plants were grown in a Phytotron controlled environment growth room under artificial light, at a fixed light intensity of 200µmol m^2 s^{-1} PPFD with a photoperiod of 16h/8h (day/night), the temperature was maintained at 25ºC/20ºC (day/night), and relative humidity ~60%, and water bi-

weekly. Seeds were sown in pots containing M3 Levington soil (Levington Horticulture Ltd, Suffolk, UK) and germinated in darkness, upon emergence seedlings were placed under treatment conditions. Twenty-five plants were divided into four treatment groups, which differed in spectral quality output by artificial light. The treatment groups were grown under Heliospectra^{TM} LED lights (Heliospectra AB, Goteborg, Sweden) emitting either: monochromic red light (R) (R= 100%); monochromic blue (B) (B 100%); dichromic red and blue (RB) (Red= 70 %: Blue= 30%); or the fourth LED group was an adjustment to the RB group to include a small portion of green light (RBG) (R= 63 %: B= 27 %: G= 10%). Peak wavelengths emitted from Heliospectra LED lights were blue (450nm), green (550nm) and red (660nm). Time points for the harvesting of leaf material were 14, 21, 28 days after emergence, with material harvested at 3 pm each time. One leaf from three individual plants was taken per treatment at each time-point and immediately frozen in liquid nitrogen.

5.2.2 qRT-PCR gene expression analysis

RNA extraction, reverse transcription, and qRT-PCR were conducted as described in sections Chapter 2 (**2.3-2.5)**. The primer sequences of the reference gene (CAC) and 10 genes of interest are reported in **Table 5-2.** Statistical analysis of the gene expression data was conducted on the delta Ct values between R and B, RB, and RBG treatments in pair-wise comparisons using students t-test (α=0.05).

Table 5-2 Primer sequences of primers designed for qRT-PCR

Gene_ID	Name	Forward primer (5' - 3')	Reverse primer (5' - 3')
Solyc08g006960.2	CAC	CCTCCGTTGTGATGTAACTGG	TTGGTGGAAAGTAACATCATCG
Solyc06g060830.2	HAT4	TCCTCATTCCTCGTCAGATCG	TCTCCTCAGTACAGTTCCCTTCT
Solyc09g074430.2	FLZ6	TCACAAGTGGCTTCAGGGAG	CCTCTTCTTGATAGCCCCACA
Solyc05g051580.2	DOT3	ACCTTAAGACTCATCCTTCACTGTC	CTCTGACAGCAAAACCTGCAT
Solyc07g052980.2	XTH16	GGATCATCTTTCTGGTACTGGGT	TGCAGTGACAGTTCCAGCAG
Solyc03g119530.2	LBD40 TF	ACGCCACTCTTTTCCTTGCT	CGATCTGAAAATAGCAGGACGC
Solyc05g009170.1	C2H2 TF	GGTGGTATAGCGGAGCCAAA	GGTGGTATAGCGGAGCCAAA
Solyc06g053290.1	SAUR59	TCCCCTGTTTATGCAGCTGTT	TCCCCTGTTTATGCAGCTGTT
Solyc10g052470.1	FSM1	TGAGAAGGCATTGGCTGTGT	TGTATTTGGGGAAGGGCACC
Solyc07g054980.1	MYBR1R2	TATGCCGGACTAGCGAGGTG	TCATTGTCCGATCTTCCTGGC
Solyc04g005100.2	MYB-D	CCGTGGACAGAAGAAGAGCA	AGCAGCACCCTGAACAGTAT
Solyc12g008900.1	CKX6	CACCTTCCAATCAAACCAAAATTGC	ACTCTAATTCCCCACTTCTAACTCT

5.3 Results

the qRT-PCR analysis was performed to identify the gene expression for leaf tissue of Micro-Tom grown under LEDs emitting either monochromatic red (R), monochromatic blue (B), red/blue (RB) or red/blue/green (RBG). Tissue was harvested at DAE 14, 21, and 28 for time-course analysis of gene expression of candidate genes of interest. The expression of these candidate genes in RNA-Seq samples (**Chapter 4)** was also validated by qRT-PCR.NA samples.

The relative gene expression of the 10 candidate genes of interest over the gene-expression time-course is presented in **Figure 5-2** as pair-wise comparison of the relative expression of R compared to B, RB, and RBG treatments. The expression profiles of from qRT-PCR validate the RNA-seq expression data for all 11 genes, with $\log_2$ fold change similar in the qRT-PCR data as observed in the RNA-sequencing differential expression analysis (See **Table 5-1** for RNA-seq DEA). Six candidate genes show strong consistency in differential gene expression patterns across time-course that is consistent with RNA-sequencing: XTH16, MYB-D, HAT4, CKX, and C2H2. XTH16 was up-regulated in almost all comparisons, albeit only significantly in RvB at time-points 1 and 2. MYB-D was significantly up-regulated in all time-points between RvB, and despite significant up-regulation at time-point 1, the up-regulation was only significant between RvRB and RvRBG at time-point 3 and in the RNA-Seq samples. HAT4 exhibited a similar expression pattern in RNA-Seq as in all other time-points, in which it was significantly down-regulated in RvB. CKX was consistently significantly up-regulated between R compared to B, RB, and RBG, but most substantially between RvB with >~6 $\log_2$fold change across each time-point. The expression profiles of the remaining 6 genes did not show consistent differential expression in line with that observed in the RNA-Seq, despite qRT-PCR confirming the differential expression of all of these genes in the RNA-Seq dataset. FSM1 was consistently down-regulated in R compared to B, RB, and RBG, however, this difference was moderate and not found to be significant. FLZ6, SAUR59, DOT3, and LBD exhibited significant differential expression only in the RNA-Seq sample, with no difference in expression observed across the time-course.

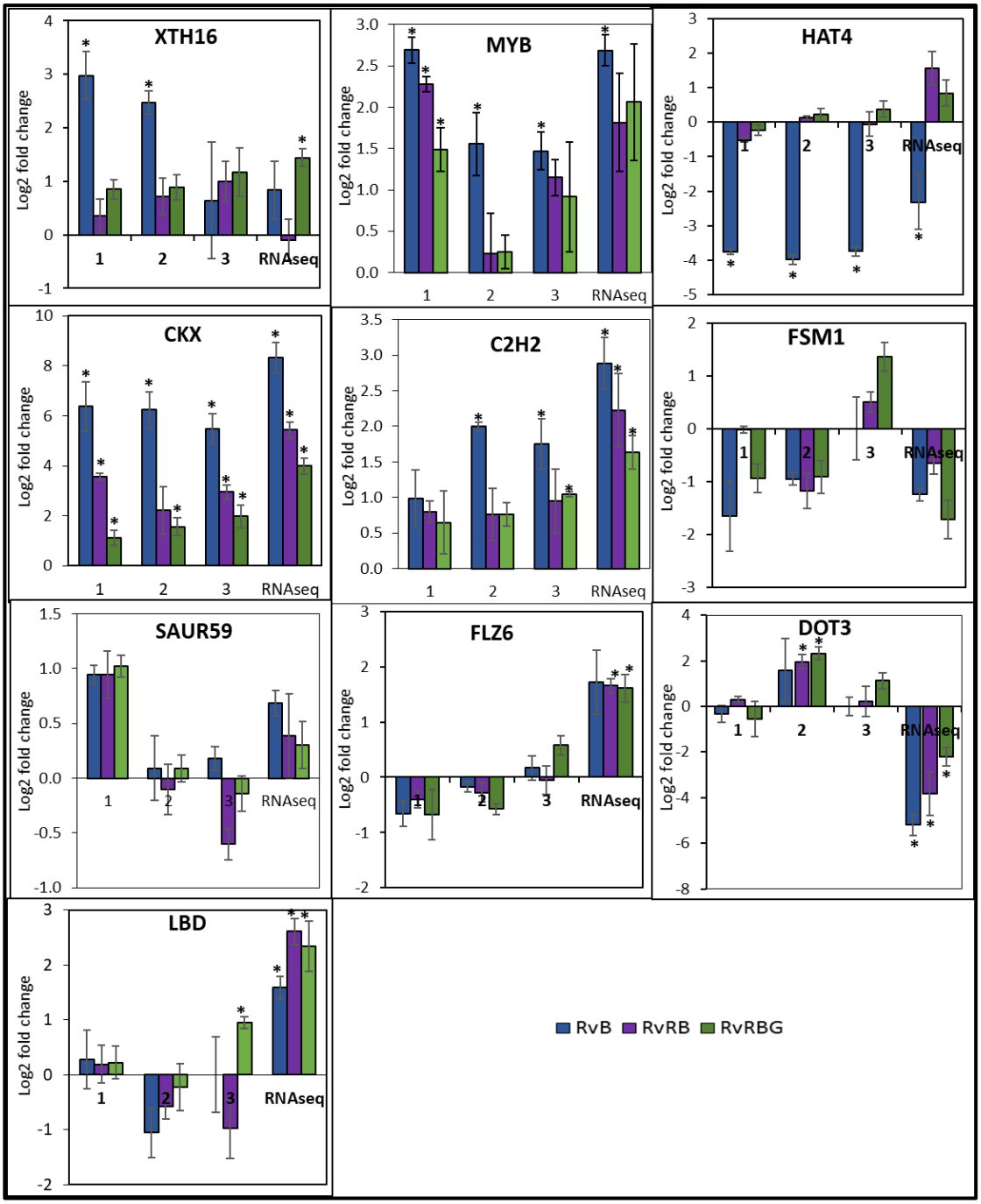


Figure 5-2 qRT-PCR gene expression analysis of candidate genes differentially expressed in micro-tom leaves under varying spectral qualities over time-course. 1= DAE 14, 2= DAE 21, DAE= 28, RNAseq= RNA samples sent for RNA sequencing. Expression is log2fold change of differential expression between R and B, RB, and RBG. Treatments: R= red; B= blue; RB= red/blue; RBG= Red/blue/green. Error bars indicate ±1 SE (n=3), significance (α=0.05) is indicated by *. XTH16= Solyc07g052980; MYB= Solyc07g054980.1; HAT4=Solyc06g060830.2; CKX=Solyc12g008900.1; C2H2= Solyc05g009170.1; FSM1= Solyc10g052470.1; DOT3= Solyc05g051580.2; LBD TF= Solyc03g119530.2; FLZ6= Solyc09g074430.2.

5.4 Discussion

The results in **Figure 5-2** show that XTH16, MYB-D, HAT4, CKX, C2H2 are consistently differential differentially expressed in both the gene expression time-course and RNA-sequencing data, exhibiting similar expression patterns across all time-points. This confirms these genes as consistently differentially regulation and makes them a candidate for transformation to investigate function. The importance of validating the consistent differential expression of candidate genes identified from RNA-Seq is evident from the fact that SAUR59, FLZ6 DOT3, and LBD did not exhibit similar expression patterns in the time-course RNA samples as it did in the qRT-PCR analysis of gene expression on the RNA samples used for RNA-Sequencing. Identification that XTH16, MYB-D, HAT4, CKX, and C2H2 genes are consistently differentially regulated under the different spectral qualities suggests these genes are regulated by light signalling genetic networks.

The majority of genes selection for expression quantification across the time-course were differentially regulated in the R transcriptome. The basis of this choice was that these plants exhibited the greatest differences in morphology, physiology, photosynthesis, and these traits ultimately reduced yield. Identifying genes which regulate these traits are of great interest. XTH16 was consistently significantly up-regulated in monochromatic red light (See **Figure 5-2**), and these plants also exhibited SAR type plant growth. Arabidopsis XTHs have been identified to be a key role in shade-avoidance induced SAR (Sasidharan et al., 2010), and it is possible the XTH16 also plays a role in the monochromatic red induced shade avoidance induced growth observed in this experiment (Chapter 3). Cytokinin catabolic gene CKX was also significantly upregulated in monochromatic R throughout the time-course.. given that CKX expression and cytokinin content was found to be regulated by tomato *cry1a*. over-expression and silenced transgenic lines, it is possible that CKX induced negative regulation of cytokinin content is involved in monochromatic R induced shade avoidance (C. C. Liu et al., 2018) MYB-D was the most highly upregulated gene in the RvB DEA and this gene was consistently differentially up-regulated by red light. C2H2

HAT4 is the only transcription factor selected which exhibited a differential expression pattern, as this gene was significantly up-regulated by blue light. Transcriptome analysis revealed an abundance of blue light specific transcriptional regulation including photosynthesis-related gene expression. The fact that the Arabidopsis homolog of this gene is a core light signalling component which is important to the shade avoidance transcriptional regulation of development (Iannacone et al., 2008) and given its differential expression identified in the RNA-Seq and validated in the time-course, elucidation of the function of this gene is of interest to identify whether it is an important regulator of shade avoidance in tomato.

5.4.1 Future work: characterization of gene function

The XTH16, MYB-D, HAT4, CKX, C2H2 genes will be characterized by RNAi-induced gene silencing to investigate gene function and the role of these gene in light signalling. International collaborator Yu Pan at The University of Southwest (Chongqing, China), will transform Micro-Tom expressing anti-sense copies of these genes under the expression of the constitutively expressed CaMV 35S promoter. Phenotyping of these transgenic lines under normal conditions as well as under varying spectral qualities will establish the importance of these genes in light signalling.

5.5 Conclusions

In summary, we identified several genes which exhibited consistent differential expression by spectral quality in Micro-Tom. The cell wall modifying enzyme xyloglucan endotransglucosylase/hydrolase 16 (XTH16) and cytokinin catabolic enzyme Cytokinin dehydrogenase/kinase 6 CKX6, putatively involved in negative regulation of cytokinin content and cell growth we consistently up-regulated in monochromatic red light. Homeobox transcription factor HAT4, orthologous to blue light stimulates transcription factor AtHAT4, was constitutively stimulated under monochromatic blue light. An MYB-D type myb4-like transcription factor MYBD was consistently differently regulated by spectral quality. C2H2 also exhibited the same R up-

regulated pattern, being significantly higher in time-points 2,3 and the RNA-Sequencing samples.

6 TRANSCRIPTOMIC ANALYSIS OF THE EFFECT OF SUPPLEMENTAL GREEN LIGHT ON MICRO-TOM

6.1 INTRODUCTION

Green light was largely overlooked as a source photosynthetically active radiation, due to the observation that isolated chlorophyll and simple photoautotrophic organisms showed reduced absorbance and lower photosynthetic efficiency than red and blue light. However, subsequent evidence has shown that whole leaf samples absorb a far greater proportion of green light than expected from the isolated chlorophyll models, which is attributed to the density of leaf tissue: Red and blue light are captured by upper-layers of leaf tissue, while green light penetrates further into the leaf and is absorbed by the deeper photosynthetic tissue (McCree, 1971; J. Sun et al., 1998; Terashima et al., 2009). Terashima and colleagues (2009) reported that supplementation of strong white light with green light increased leaf photosynthesis to a greater extent than supplementing with red light, as when PPFD is high, light in the upper chloroplast is dissipated as heat while green light drives photosynthesis in the lower parts of leaves which are not light saturated (Terashima et al, 2009). The potential for green light to access the deep photosynthetic tissue not accessible by green light, may be important in improving overall whole-canopy photosynthesis. Studies on lettuce have shown that plants grown under LED emitting red, blue, and green (24%) light accumulated greater biomass than those grown under dichromic red/blue or cool white fluorescent light (H. Kim et al., 2004).

6.1.1 Cryptochrome-dependent green light effect

The manner of cryptochrome absorption of green light was resolved with the identification of the model of cryptochrome activation. In the dark, cryptochrome contains a fully oxidized flavin adenine dinucleotide (FAD) which absorb light in the blue region of the visible light spectrum, converting it into a semi-reduced state and biologically active state (J. P. Bouly et al., 2007). While reversion of the cryptochrome semi-quinone state occurs in the dark, the partial reduction of the FAD

chromophore shifts its absorption profile into the green part of the light spectrum, and absorption of green light drives full reduction and inactivation of the cryptochrome. Prolonged darkness reverts the reduced FAD chromophore to its original oxidized inactive state (Banerjee et al., 2007; J. P. Bouly et al., 2007). The observation that the 'escape time' to reverse blue light activation of cryptochrome with green light closely matches the lifetime of cryptochrome semi-quinone state further confirms the role of green light in photoreversion the blue-light activated cryptochrome (Herbel, Orth, Wenzel, Ahmad, & Batschauer, 2013). Under this model, the relative quanta of blue/ green light control the activity state of the pool of plant cryptochrome in a manner analogous to that of the phytochrome in response to red / far-red ratio, and this has shown to be true in *Arabidopsis* as green light induces the accumulation of far-red associated shade avoidance transcripts (Sellaro et al., 2010; T. Zhang, Maruhnich, & Folta, 2011).

6.1.2 Other photoreceptor-dependent green light effects

Green light stimulates germination in *Arabidopsis* through PhyA and PhyB, and even small fluences of green light are able to maintain an active pool of phytochromes necessary to initiate a phytochrome-regulated transcriptional response (Dhingra, Bies, Lehner, & Folta, 2006; T. Zhang et al., 2011). However, this response is of little importance under moderate fluences of white light as the activation state of the phyB phytochrome pool will be maintained to a far greater extent by red light, while phyA activation is saturated at low fluence.

6.1.3 Aims and hypotheses

An investigation into molecular mechanisms of green light signalling has largely been limited to studies in the model plant species *Arabidopsis*, and are short studies which focus on photomorphogenesis. The only previous transcriptome-wide gene expression study on green light was 10 years ago, studying the effect of a single pulse of 100µmol m2 light to Arabidopsis seedlings (Dhingra et al., 2006). The effect of green light on plant growth and development has been underestimated. There have been no major studies into the effect of green light on genome-wide expression patterns, even after the revelation that green light reverses cryptochrome activation-

suggesting that the activity of photoreceptor regulated genes can be modified through modulation of *CRY* activity by R/G ratio. Terashima et al (2009) paper suggesting green light is a better supplemental source to improve photosynthesis at high irradiance than red, highlighting the potential importance of green light for improving photosynthesis and potentially yield. Considering that recent trends in physiological research suggest, green light is being re-investigated as an important wavelength for plant growth, a study into the effect of continuous supplemental green light on transcriptome will provide insight into the degree to which green light regulates transcription, and its importance for crop growth. Our aim is to characterize the transcriptomic response of *Solanum lycopersicum* c.v Micro-Tom to supplemental green light and understand to what extent its understanding of photosynthesis, metabolism and gene regulation.

6.2 METHODS

6.2.1 Plant materials and growth conditions

Micro-Tom plants were grown in a controlled environment growth room at 25 ^{o}f /20^{o}C (day/night), with germination and growing condition as reported in (See methods; **2.1**). Upon germination and prior to treatment initiation, Micro-Tom plants were grown under mixed R and B LED (RB) lighting for 25 days. At 25 DAE, plants were split into two groups; with the control plants returning to the mixed RB LED lighting as previously grown, while the treatment group was placed in a separate isolated chamber with LED light emitting a mixture of R, B, and G LED (RBG) light. See **Figure 6-1** for the spectral distribution of the LED for both control and treatment conditions.

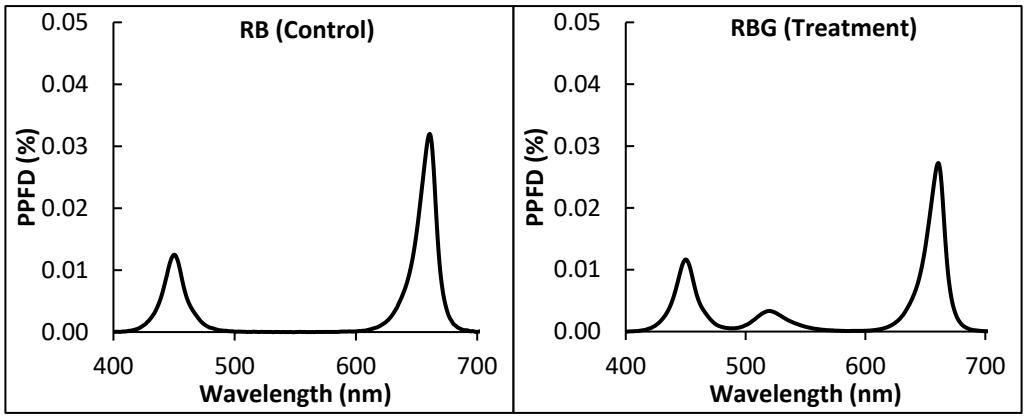


Figure 6-1 Spectral output of LED lights for both control and treatment conditions. Left is the control spectrum (RB), right is the treatment spectrum (RBG). PPFD percentage PPFD emitted at each wavelength/ sum of total PPFD across all wavelengths. Measurements were taken at 1nm intervals.

6.2.2 Sample collection and Illumina sequencing

Leaf samples were harvested from both the control and treatment groups 3 separate time-point: 4 hours, 1day +4 hours (1day), and 7 days+4 hours (7days) after treatment initiation. The leaf tissue samples were harvested at 3 pm each day to minimize the impact of the circadian rhythm on gene expression. At each time-point, one whole leaf was excised from six biologically independent plants, from which RNA was extracted and pooled to form three samples, each consisting of the total RNA from two leaves (See methods**; 2.3**). In total 18 samples (3 biological replicates, 3 time-points, 2 conditions) were prepared. Total RNA underwent polyA enrichment, followed by Illumina Total Strand PE-library preparation (See methods; **2.4**). Libraries were then sequenced at the Oxford Wellcome Trust genomics center on a single multiplexed lane using the Illumina HiSeq 4000.

6.2.3 Bioinformatics on RNA-Seq data

The complete methodology for Mapping of Illumina reads, quality assessment and unsupervised analysis, differential expression analysis, and gene enrichment analysis is as described in (See methods; **2.4**). For differential expression analysis, pair-wise comparisons between control and treatment samples at each time-point was conducted with significance threshold 0.05> FDR.

To test for between-sample variation, both PCA and hierarchical clustering was conducted on thelog-transformed filtered count data in pair-wise comparisons between samples harvested at the same time-point. Differential expression was conducted using EdgeR, with pair-wise comparisons made between treatment (RBG) and control (RB) samples for each of the three time-points, 1 (4hours), 2 (1day), and 3 (7days). The FDR threshold for calling significant differential expression set to 0.05 <FDR. Gene enrichment analysis was conducted using GOStats (Falcon & Gentleman, 2007) as described in () with enrichment lists refined and treemaps constructed using Revigo (Supek, Bošnjak, Škunca, & Šmuc, 2011). KEGG enrichment was also conducted using GOStats with Pathview (Kegg & Graphviz, 2014) used to visualize metabolic maps and overview heatmap of transcriptomic data.

6.3 RESULTS

6.3.1 Summary of RNA-Seq Libraries and Alignment to Genome

To understand the effect of supplemental green light on the transcriptome, Micro-tom plants were grown under RB LED lights for 25 days, after which they were split into two groups, with the control group remaining in the previous light conditions, while the treatment group were transferred to chamber with LED lights emitting RBG, and total RNAs were extracted for RNA-Seq transcriptomic analysis at 3 time-points: 4 hours, 1day, and 7days post-treatment initiation.

Table 6-1 shows the summary of sequencing and alignment of the RNA-Seq data generated on the 18 samples sequenced, displaying the number of raw reads generated from each library and the amount and proportion of these raw reads which were successfully mapped to the reference genome (*Solanum lycopersicum* SL2.5 genome) and assigned as counts to each gene. In total, 373 million Illumina sequencing reads were generated from the 18 RNA-Seq libraries, with an average of 20.7 million raw PE reads per sample. Raw reads were aligned against the *Solanum lycopersicum* genome using HiSat2, with all samples showing consistent alignment mapped reads above 98%. The uniquely mapped clean reads were counted using HTSeq, with an average of 17.9 million read counts unambiguously assigned to 25,771 genes, which is the conversion of raw reads 86.2% to gene counts. After filtering to remove lowly expressed genes, 18,835 genes were found to be expressed above one CPM in at least three samples.

.

Table 6-1 Summary of sequencing and alignment of RNA libraries.

Group	Time	#	Raw reads		Mapped reads		Total gene count	
			(millions)	(%)	(millions)	(%)	(millions)	(%)
Control	**1**	**1**	20.2	100	19.8	98.3	17.5	86.9
Control	**1**	**2**	18.9	100	18.6	98.3	16.4	87.0
Control	**1**	**3**	18.9	100	18.5	98.2	16.3	86.3
Control	**2**	**1**	17.4	100	17.1	98.2	15.1	86.9
Control	**2**	**2**	21.5	100	21.1	98.2	18.6	86.5
Control	**2**	**3**	24.2	100	23.8	98.1	20.9	86.5
Control	**3**	**1**	17.3	100	17.0	98.2	14.9	86.2
Control	**3**	**2**	20.7	100	20.3	98.2	17.8	86.0
Control	**3**	**3**	20.8	100	20.4	98.2	17.8	85.7
Treatment	**1**	**1**	17.3	100	17.0	98.3	15.0	86.7
Treatment	**1**	**2**	21.1	100	20.7	98.2	18.2	86.3
Treatment	**1**	**3**	23.1	100	22.7	98.2	19.9	85.8
Treatment	**2**	**1**	21.2	100	20.8	98.1	18.2	85.6
Treatment	**2**	**2**	23.7	100	23.2	98.1	20.5	86.4
Treatment	**2**	**3**	21.4	100	21.0	98.2	18.3	85.8
Treatment	**3**	**1**	21.3	100	20.9	98.1	18.2	85.7
Treatment	**3**	**2**	19.8	100	19.4	98.1	16.8	85.2
Treatment	**3**	**3**	24.7	100	24.3	98.2	21.2	85.7

*mapping to tomato genome. Control= RB; Treatment= RBG. Time: 1=4hours; 2=1 day; 3=7 days. # = rep. % is of raw reads.

6.3.2 Quality assessment of RNA-Seq libraries

Samples were library-normalized to eliminate differences in sequencing using EdgeR, and the library-normalized counts-per-million (CPM) data qualitative assessed in Noiseq. The sensitivity plot identifies what proportion of the genome is expressed and identifying the number of genes which will be filtered by using different CPM cut-offs. We can see that by not applying a cut-off 70% of the genome will be present while applying a cut-off of >1CPM reduces that 48.6% (18,835 genes). Further increases of the CPM to cut-off to >2CPM would only further remove 4% of genes. Interestingly, only 30% of the genome is highly expressed (>10 CPM). We assessed the need for a CPM cut-off by assessing the distribution of counts at different CPMs. The density plot of unfiltered (raw) counts data (**See Figure 8-1**) identifies two peaks in the proportion of genes at $\log_2$-CPM, with the highest proportion of genes at $\log_2$-CPM <-5 and a second smaller peak at log-CPM >5. The statistical vigour to detect differential expression is drastically reduced when the expression is

low. When filtered to remove genes which were below 1CPM in at least three samples, a normal distribution of expression was achieved with a single peak density of genes at ~5 log-CPM.

The distribution of gene counts against gene length and GC content was evaluated to assess for any biases between treatments (See **Figure 8-3**). The median GC content of the *Solanum lycopersicum* is 37.3%, with mean expression peaking around this range. No treatment specific GC bias was observable within the 25-48%, which is the GC content range which accounts for 97% of the tomato genome. The expected relationship between gene expression and gene length is present as expression increases linearly with gene length. The median transcript length of tomato genome is 1462bp. As expression increases past 2000bp although the all groups show the same trend in expression, differences in mean expression began to appear and this increased with expression

6.3.3 Unsupervised analysis of transcriptomic data

To understand the relationship between transcriptomes of the treatment and control samples throughout the time-course, principal component analysis (PCA) and hierarchical clustering were performed on both all the samples together and assessing each time-point separately (See **Figure 6-2**). The PCA shows a clear separation between the treatment and control cluster on the PC1 axis (See **Figure 6-2A**). PC1 explains 41% of the variance between samples and clearly explains the variance between treatment and control. Along the vertical axis of PC2, while two treatment samples cluster away from the control, the third treatment sample is aligned with the control samples. Hierarchical clustering of the T1 treatment and control samples (See **Figure 6-2B**) shows the discrete separation of treatment from control, with the three control transcriptomes clustering neatly together. Within the treatment group, while T1_1 and T1_2 cluster together, T1_3 was less similar.

Figure 6-2C & D shows the PCA and Hierarchical clustering, respectively, of treatment and control samples in the 1day time-point. Both the PCA and hierarchical clustering show that while the control samples cluster closely together, indicating high similarity, one of the treatment samples (T2_2) shows high similarity to the control samples and is placed within the control cluster along both PC1 and within the

hierarchical clustering tree. The other two treatment samples cluster on the opposite side of PC1 to the control cluster indicating strong dissimilarity, and this is evident as the dendrogram of the hierarchical clustering shows two discrete groups.

Finally, PCA and hierarchical clustering were conducted for time-point 3 samples - seven days after the treatment group supplementation with green light began (See **Figure 6**-2 **E & F**). The PCA shows the control group cluster tightly along both PC1 and PC2. PC1, which explains 55% of the variation between samples separates roughly separates treatment and control, with two treatment and control samples positioned around the center of the axis, and one treatment sample (T3_3) and control sample (C3_2) occupying extremes of the PC1 axis. PC2 which explains 13% of the variation between samples separates T3_2 and T3_1 from both the control samples and T3_3 which are on the opposite side of the axis. In summary, the first PC1 strongly separates T3_3 from the control samples and remaining treatment samples, while PC2 separates the remaining treatment samples from all others. This trend is evident in the hierarchical clustering, as T3_3 is the outlier, while the other two treatment samples cluster closely and the control samples cluster separately.

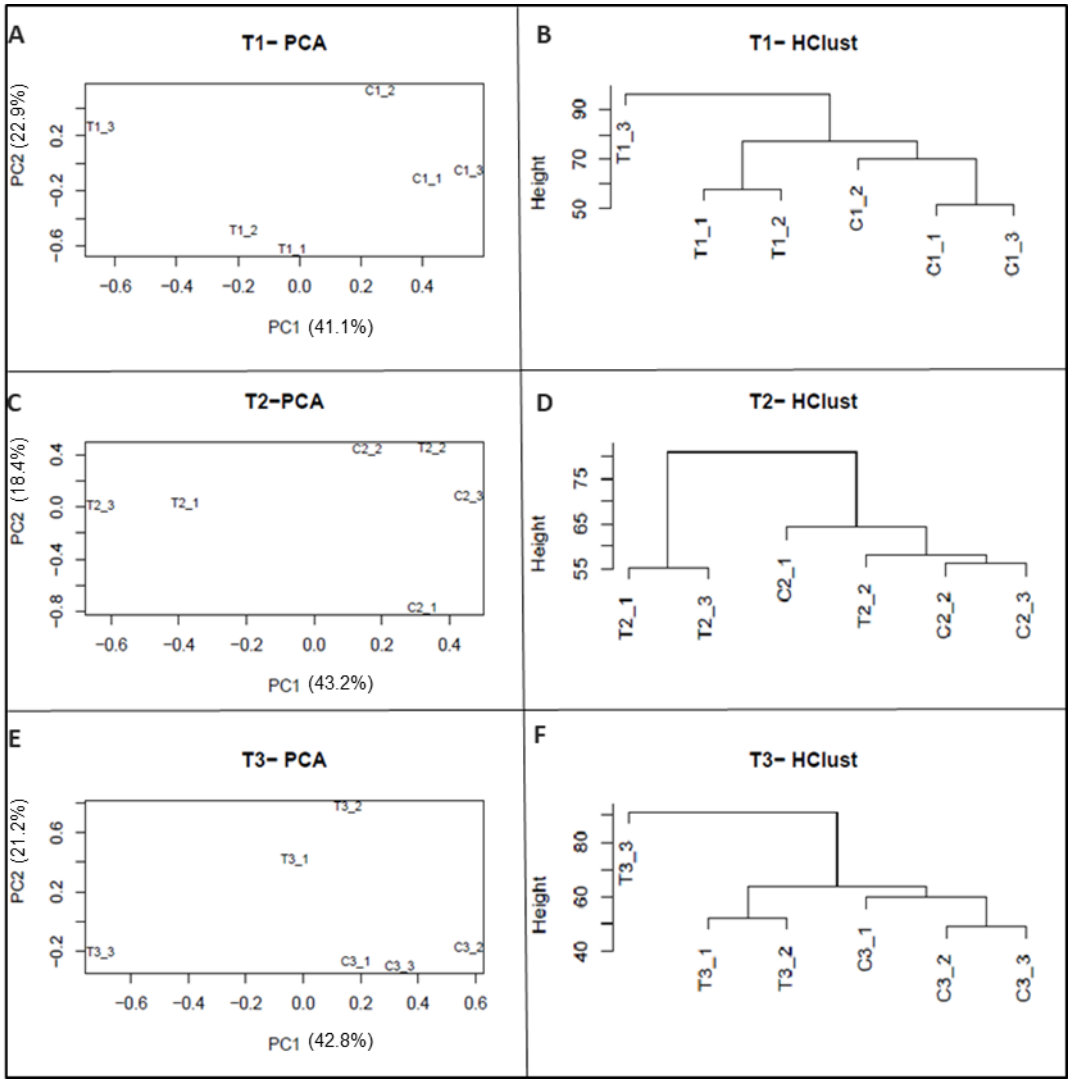


Figure 6-2 PCA and Hierarchical clustering of time-course data. Genetic distance between samples was calculated from the Euclidean distance between log-normalized count data, filtered to remove genes in which cpm <1. Principal Component Analysis was conducted between samples at time-point 1 (A), 2 (C), and 3 (E). Hierarchical clustering was also conducted using the same measure of genetic distance on both treatment and control samples, with each time-point 1 (B), 2, (D), and 3 (F) plotted separately.

6.3.4 Differential expression analysis

Differentially expressed genes were identified in pair-wise comparisons between control and treatment plants at each time-point to assess how the Micro-Tom leaf transcriptome was responding to green light supplementation over time. The EdgeR program was used to evaluate the significance of the difference in expression and to adjust for multiple testing. The volcano plots from differentially expressed genes of significance (*p.adj*) against $\log_2$ fold change for treatment vs control at each time-point is shown in **Figure 6-3**, **A-C**, and the summary of total DEGs in **Figure**

6-2, while in **Table 6-2** the top 10 up-and-down- regulate genes in each pair-wise comparison are presented. In total, of the 18,835 genes found to be expressed (CPM <1) in this experiment, 1530 unique genes were found to be differentially expressed in at least one time-point (*p. adj* <0.05). At 4hours after beginning supplementation the differences observed are the early-responsive genes, and 1190 genes are found to be significantly differentially expressed, with 447 up-regulated and 743 down-regulated (See **Figure 6-2A**). Of the DEGs at 4hours, 278 genes statistically significantly two-fold (SSTF; log_2 fold-change > 2, *p-adj* <0.05) differentially expressed, 100 genes up- and 178 down-regulated. The proportion of DE genes down-regulated is greater than those up-regulated; 62% and 64% of all DEGs and SSTF are down-regulated, respectively. This distribution is clearly visualized in the volcano plot (See **Figure 6-3A**) where there the trend is more DEGs on the negative side of the Log_2FC axis, as well as having a DEGs with lower significance values. The most highly up-regulated genes include (See **Table 6-2**): a Homeobox-leucine zipper transcription factor (Solyc03g082500.2), a CONSTANS-like zinc finger protein encoding gene (Solyc04g007470.2), and a calcium-dependent protein kinase17 (Solyc12g099790.1). Solyc03g082550.2 HB transcription factor is related to Arabidopsis (AtHB7) an ABA-responsive transcription factor involved in regulating growth in response to drought (Olsson, Engström, & Söderman, 2004), and this transcription factor was also found to be significantly down-regulated in the RBGvRB 1day comparison. CONSTANS family proteins are involved in regulating photoperiod in response to light and circadian clock signals (Valverde et al., 2004). CDKs transduce calcium signals and are integral to plant defense and induced in response to several hormones including ABA in *Arabidopsis* (W. Xu & Huang, 2017). The top down-regulated genes in treatment compared to control after 4hours were mostly chlorophyll a-b binding proteins, including CAB4 (Solyc06g069730.2) which was -2.9 log_2 fold down-regulated in RBG after 4 hours. Many of the CAB genes significantly down-regulated in TvC 4hours were also significantly down-regulated in the 1day and 7-day time-points (See **Table 6-2**).

Next, the differentially expressed genes between treatment and control one day after the treatment plants began supplementation with green light (**Figure 6-2B**). At one-day post treatment initiation, 305 genes were found to be differentially expressed, with 69 up-regulated and 236 down-regulated. Of these 305 genes, only 35 were

SSTF, 18 SSTF up-regulated and the remaining 17 down-regulated. The volcano plot visualizes this (**Figure 6-3B**), and we see that even those DEGs have relatively high *p-adj* values compared to those from four-hour time-point. Two of the most significantly up-regulated genes in the RBGvRB 1day comparison were phenylopanoid biosynthesis genes, with both Glutathione S-transferase (Solyc02g081340.2) and caffeoyl-CoA O-methyltransferase (Solyc09g082660.2) highly up-regulated, however, only at this time-point. In fact, this was a trend, as all genes significantly upregulated in the 1day time-point were only differentially expressed at this time. Three of the most highly down-regulated genes in RBGvRB at the one-day time point were Glutaredoxin (Solyc04g011840.1; Solyc04g011860.1; Solyc06g054570.1) which are involved in tolerance to oxidative stress.

Finally, the third time-point of transcriptome data from Micro-Tom plants taken seven days after green light supplementation began. The overview of the DE analysis at this time-point (**Figure 6-2C**) shows in total 270 genes were DE, with 24 up-regulated in RBG compared to RB, while the other 246 genes were significantly down-regulated. Using the STTF, 135 were identified as being differentially expressed, with only 8 of these up-regulated and the remaining 127 down-regulated, in RBG relative to RB. Looking at the volcano plot (**Figure 6-3C**) it is evident that not only are the vast majority of DE genes are down-regulated, but those DEGs that are down-regulated have substantially lower *p-adj* values. Evaluation of the top differentially expressed genes (See **Table 6-2**) revealed a few highly differentially expressed genes there were no genes of interest present.

Next, we looked at the Venn comparison of overlap between differentially expressed gene sets at each time-point between treatment and control transcriptomes (**Figure 6-2**). Of the 1530 unique genes differentially expressed in at least one time-point, 63% of these genes were only differentially expressed at the 4hour time-point. The greatest degree of overlap was between genes differentially expressed between 4 hours and 1 day (127 genes; 8.3%), with very few genes differentially expressed at all time-points or between any other comparisons.

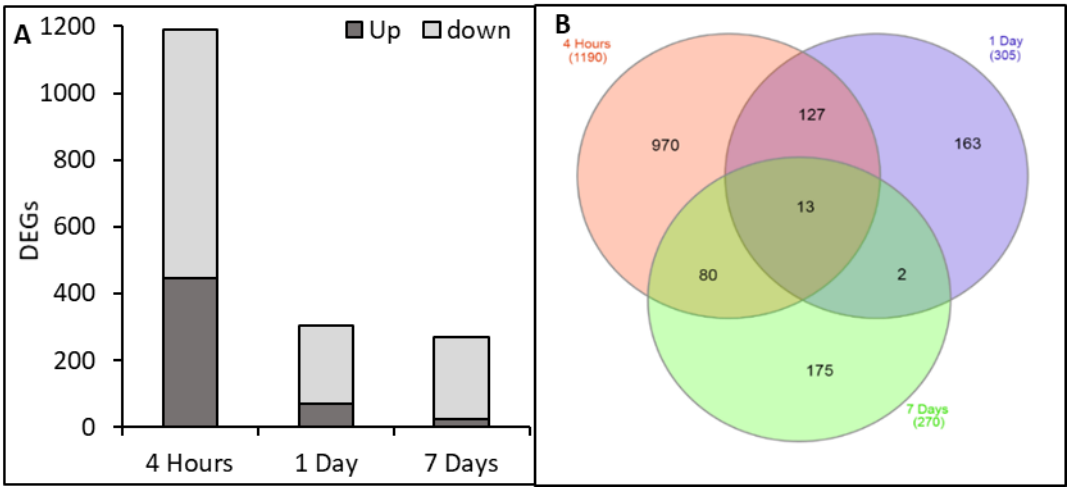


Figure 6-2 Summary of up and down-regulated genes between treatment and control at each time-point for all DEGs. A, DEGs at each time-point between treatment and control. B, Venn of overlap between DEGs between time-points

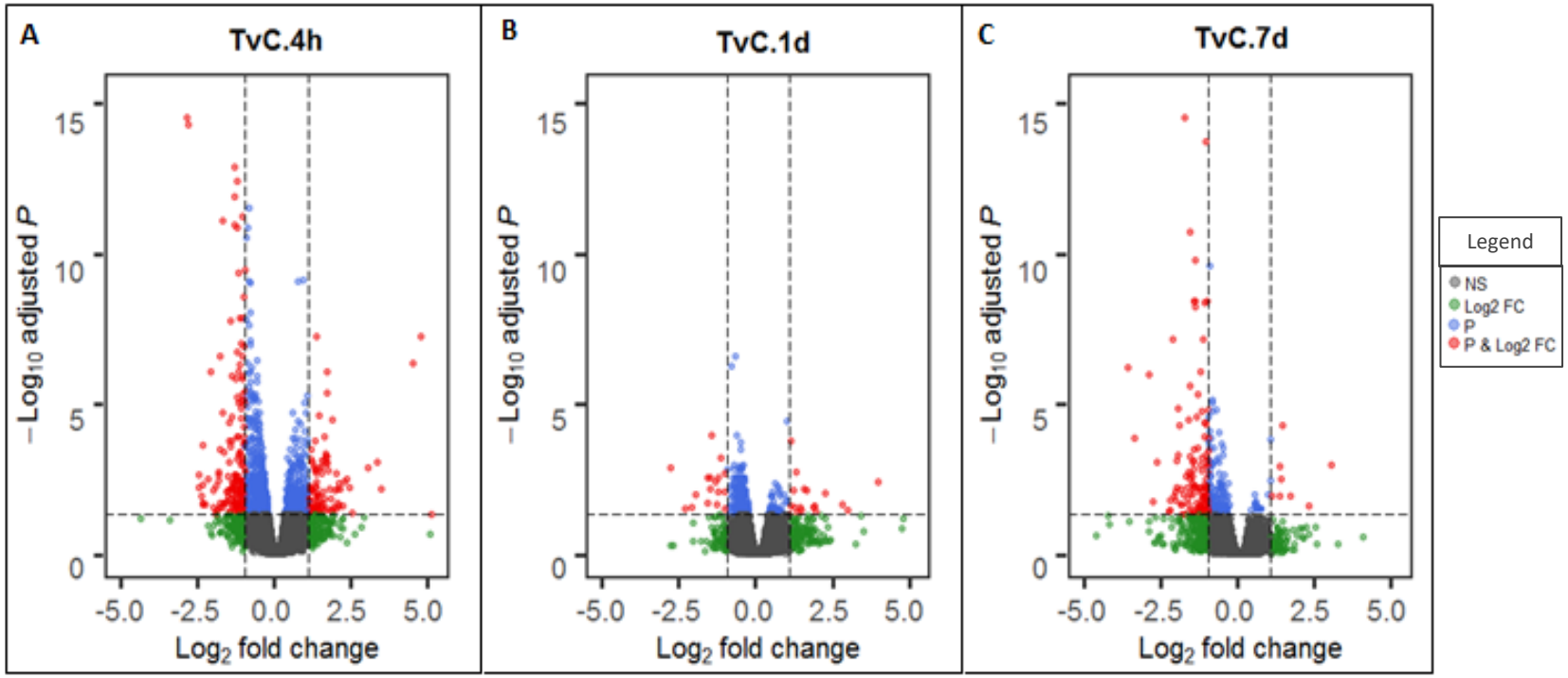


Figure 6-3Volcano plot of differential expression between Treatment and control throughout time-course. A, Treatment v Control 4 hours after treatment. B, Treatment v Control 1d after treatment. C, Treatment v Control 7d after treatment. Treatment (T) = RBG; Control (C) = RB; 4h= 4hours post-treatment start; 1d= 1day post treatment start; 7d= 7 days post treatment start. NS= Not significant; P= *p*-adjusted significance (FDR); log2 FC= log_2 fold-change of gene expression

6.3.5 TOP DEGs

Table 6-2 Top 10 differentially up- and down- regulated genes in RBGvRB at each time-point

#	Gene_ID	Description	TvC_4hour		TvC_1day		TvC_7day	
			Log_2FC	FDR	Log_2FC	FDR	Log_2FC	FDR
		TvC_4hour up-regulated						
1	Solyc01g057680.2	Hcr2-p4.1	**4.6**	**7.1E-08**	NS	NS	NS	NS
2	Solyc12g099790.1	Calcium-dependent protein kinase 17	**4.4**	**5.7E-07**	NS	NS	NS	NS
3	Solyc02g071560.2	Subtilisin-like protease	**3.2**	**9.8E-04**	NS	NS	NS	NS
4	Solyc09g005730.2	Plant-specific domain TIGR01589 family protein	**1.8**	**3.8E-05**	NS	NS	NS	NS
5	Solyc03g082550.2	Homeobox leucine zipper protein	**1.6**	**6.2E-04**	1.4	3.0E-02	NS	NS
6	Solyc04g007470.2	CONSTANS-like zinc finger protein	**1.6**	**5.2E-06**	NS	NS	NS	NS
7	Solyc02g067050.2	Uncharacterized ACR COG1678 family protein	**1.6**	**8.9E-04**	NS	NS	NS	NS
8	Solyc06g072620.2	MtN3-like protein	**1.6**	**1.0E-06**	NS	NS	1.0	1.2E-02
9	Solyc03g112300.2	Os11g0444900 protein	**1.6**	**6.2E-04**	NS	NS	NS	NS
10	Solyc05g009040.2	Receptor-like protein kinase	**1.6**	**5.0E-04**	NS	NS	NS	NS
		TvC_4hour down-regulated						
1	Solyc06g069730.2	Chlorophyll a-b binding protein 4, chloroplastic	**-2.9**	**5.1E-15**	NS	NS	-1.1	2.6E-02
2	Solyc02g070980.1	Chlorophyll a/b binding protein	**-2.8**	**8.5E-15**	-1.4	4.2E-03	-1.2	2.0E-02
3	Solyc02g070990.1	Chlorophyll a/b binding protein	**-2.8**	**5.5E-18**	-1.3	2.9E-03	-1.0	2.9E-02
4	Solyc02g070970.1	Chlorophyll a/b binding protein	**-2.5**	**2.2E-34**	-0.8	5.9E-03	-1.0	8.6E-05
5	Solyc02g063000.2	Glucosyltransferase	**-2.5**	**6.1E-03**	NS	NS	NS	NS
6	Solyc08g074620.1	Polyphenol oxidase	**-2.5**	**2.4E-03**	NS	NS	NS	NS
7	Solyc02g071000.1	Chlorophyll a/b binding protein	**-2.5**	**4.1E-26**	-1.0	1.6E-03	-1.1	4.6E-05
8	Solyc11g006250.1	GDSL esterase/lipase At5g33370	**-2.4**	**1.2E-02**	NS	NS	-2.8	1.9E-02

#	Gene_ID	Description	TvC_4hour		TvC_1day		TvC_7day	
			Log_2FC	FDR	Log_2FC	FDR	Log_2FC	FDR
9	Solyc05g005910.2	Peptide transporter	-2.4	2.2E-02	NS	NS	NS	NS
10	Solyc07g042400.2	Unknown Protein	-2.4	2.6E-04	NS	NS	-2.7	9.8E-04
		TvC_1day up-regulated						
1	Solyc06g068130.2	TPR domain protein	2.4	4.3E-02	3.8	4.2E-03	NS	NS
2	Solyc08g075570.2	Urea active transporter-like protein	NS	NS	2.8	3.7E-02	NS	NS
3	Solyc06g062420.2	Unknown Protein	1.8	2.8E-02	2.7	2.2E-02	NS	NS
4	Solyc02g072470.2	Receptor like kinase, RLK	NS	NS	2.2	1.0E-02	NS	NS
5	Solyc02g081340.2	Glutathione S-transferase	NS	NS	1.9	3.7E-02	NS	NS
6	Solyc03g123390.2	Hydrolase	NS	NS	1.8	2.4E-02	NS	NS
7	Solyc09g082660.2	Caffeoyl-CoA O-methyltransferase	NS	NS	1.8	2.9E-02	NS	NS
8	Solyc10g008410.1	RING finger protein 5	NS	NS	1.6	7.8E-03	NS	NS
9	Solyc11g062400.1	ATP binding / serine-threonine kinase	1.3	4.3E-03	1.5	7.0E-03	NS	NS
10	Solyc04g007350.2	Unknown Protein	NS	NS	1.4	3.5E-02	NS	NS
		TvC_1day down-regulated						
1	Solyc04g011840.1	Glutaredoxin	NS	NS	-2.8	1.4E-03	NS	NS
2	Solyc10g081810.1	Phosphatidylglycerol/phosphatidylinositol transfer protein	NS	NS	-2.3	3.0E-02	NS	NS
3	Solyc04g011860.1	Glutaredoxin	NS	NS	-2.1	2.9E-02	2.2	2.5E-02
4	Solyc01g098690.2	LRR receptor-like serine/threonine-protein kinase, RLP	NS	NS	-2.0	1.1E-02	NS	NS
5	Solyc10g074540.1	Expressed protein (Fragment)	NS	NS	-1.6	2.1E-02	NS	NS
6	Solyc06g067870.2	2-oxoglutarate-dependent dioxygenase	NS	NS	-1.6	2.9E-03	NS	NS
7	Solyc03g083160.1	Unknown Protein	NS	NS	-1.5	3.1E-03	NS	NS
8	Solyc04g079910.2	Coiled-coil domain-containing protein 109A	-1.8	3.5E-04	-1.5	7.5E-03	NS	NS
9	Solyc06g054570.1	Glutaredoxin family protein	-1.0	1.1E-02	-1.5	1.3E-04	NS	NS
10	Solyc02g070980.1	Chlorophyll a/b binding protein	-2.8	8.5E-15	-1.4	4.2E-03	-1.2	2.0E-02

#	Gene_ID	Description	TvC_4hour		TvC_1day		TvC_7day	
			Log_2FC	FDR	Log_2FC	FDR	Log_2FC	FDR
		TvC_7day up-regulated						
1	Solyc09g089540.2	Proteinase inhibitor I	1.9	3.3E-02	NS	NS	2.9	1.2E-03
2	Solyc04g011860.1	Glutaredoxin	NS	NS	-2.1	2.9E-02	2.2	2.5E-02
3	Solyc12g056160.1	Cation/H(+) antiporter 18	1.3	2.7E-02	NS	NS	1.6	1.2E-02
4	Solyc10g075110.1	Non-specific lipid-transfer protein	NS	NS	NS	NS	1.4	5.9E-05
5	Solyc12g014010.1	Glucosyltransferase	1.5	1.4E-04	NS	NS	1.3	3.3E-03
6	Solyc10g045240.1	Beta-glucosidase D4	NS	NS	NS	NS	1.3	1.4E-03
7	Solyc10g075090.1	Non-specific lipid-transfer protein	NS	NS	NS	NS	1.3	1.2E-02
8	Solyc06g072620.2	MtN3-like protein	1.6	1.0E-06	NS	NS	1.0	1.2E-02
9	Solyc05g050130.2	Acidic chitinase	NS	NS	NS	NS	1.0	3.9E-03
10	Solyc02g082850.2	Serine O-acetyltransferase	NS	NS	NS	NS	1.0	1.6E-04
		TvC_7day down-regulated						
1	Solyc11g050880.1	Katanin p60 ATPase-containing subunit	NS	NS	NS	NS	-9.3	3.1E-02
2	Solyc12g062200.1	Unknown Protein	NS	NS	NS	NS	-8.3	3.0E-02
3	Solyc04g025560.2	ADP-ribosylation factor	NS	NS	NS	NS	-7.6	4.5E-02
4	Solyc06g034360.1	Pectinesterase	NS	NS	NS	NS	-3.6	7.7E-07
5	Solyc08g069040.2	Peroxidase 1	NS	NS	NS	NS	-3.4	1.6E-04
6	Solyc08g077100.2	Baculoviral IAP repeat-containing protein 3	NS	NS	NS	NS	-2.9	1.3E-06
7	Solyc11g006250.1	GDSL esterase/lipase At5g33370	-2.4	1.2E-02	NS	NS	-2.8	1.9E-02
8	Solyc07g042400.2	Unknown Protein	-2.4	2.6E-04	NS	NS	-2.7	9.8E-04
9	Solyc08g067500.1	Non-specific lipid-transfer protein	NS	NS	NS	NS	-2.3	3.8E-02
10	Solyc03g120570.2	Proton-dependent oligopeptide transport family protein	NS	NS	NS	NS	-2.2	3.4E-02

6.3.6 Gene enrichment analysis of DE gene sets

GEA of treatment compared to control 4 hours after green light supplementation began

Genes down-regulated in the TvC comparison after 4 hours of green light supplementation were highly enriched in GO terms. In total, 78 biological process, 11 molecular function, 24 cellular component GO terms were enriched, as well as eight KEGG pathways (See Full gene enrichment tables

Table 8-1). **Figure 6-4** shows a tree map summary of enriched biological process terms, while the full table of enriched terms is represented in the supplementary tables. Tree-maps are useful tools for visualizing enrichment when a high number of terms are over-represented as they visualize significance through the relative size of the box given to each term while clustering related terms into groups. The single most highly enriched biological process terms were 'Photosynthesis light harvesting' (*p*= 7.9E-38), while other related photosynthesis terms such as 'photosynthesis', while several including Cellular Component terms such as 'chloroplast' and 'thylakoid membrane' were highly enriched. In addition to this the most highly enriched KEGG pathways related to Photosynthesis-antenna proteins', Carbon fixation in photosynthetic organism', and 'Photosynthesis'. The largest group of terms in the treemap is related to cellular aldehyde metabolism, with contains member terms including those related to pigment metabolism ('pigment metabolic process'; 'chlorophyll biosynthesis'), and KEGG enrichment supported this as 'Porphyrin and chlorophyll metabolism' pathway was highly enriched. Components involved in light signalling were both differentially expressed as both 'Response to red light' and 'Response to blue light' were over-represented. Other notable terms that were over-represented related to development such as 'Stomatal complex morphogenesis' and general control of the metabolism with 'Primary metabolism' and the KEGG 'Metabolic pathways' highly enriched.

Of the 447 genes up-regulated in RBG relative to RB 4 hours after supplementation of green light began, enrichment analysis revealed 38 BP; three MF; one CC, and two KEGG pathways were over-represented. The table of

enriched terms is presented in supplementary data (See **Table 8-2**). The most highly enriched MF term was ‘Transcription factor activity’ (p= 9.8E-08), while the only enriched term in the cellular component category was the ‘nucleus’ (p= 7.4E-04). The theme within the enriched biological process terms was the relationship towards defense and biotic stress, with ‘defense response, incompatible interaction ’, ‘immune system processes’, ‘regulation of plant-type hyper-sensitive response’ and several other similar terms significantly over-represented. The ‘Plant hormone signal transduction’ KEGG pathway was substantially enriched, while biological process terms relating to several hormones including ethylene (‘response to ethylene’), abscisic acid (‘abscisic acid-activated pathways’), and salicylic acid (‘systems acquire resistance, salicylic acid-mediated pathway’) were over-represented.

GEA of TvC 1 day after green light supplementation began

For the 236 genes downregulated in the treatment compared to the control after one day of green light supplementation, a large amount of enrichment was found with 55 BP, four MF, and 14 CC GO terms, as well as four KEGG pathways (See **Figure 6-5**; and full enrichment in **Table 8-3**). Substantial overlap between this enrichment and that of treatment v control at 4-hour time-point. The treemap shows visualizes the enrichment of biological process terms after filtering to remove redundancy (See **Figure 6-5**). Cellular aldehyde metabolism is the most highly enriched biological process (p= 1.4E-29), which is within the group containing ‘pigment metabolism’ and ‘chlorophyll biosynthetic process’. The KEGG pathways ‘Photosynthesis’ and ‘Photosynthesis – antennae proteins’ are significantly enriched, while the vast majority of enriched CC terms relate to the chloroplast, with chloroplast being the most significantly enriched (p=1.3E-49). In addition to this, a term related to the expression of plastid genes is enriched, such as ‘transcription from plastid promoter’. Both ‘response to blue light’ and ‘response to red light’ are significantly enriched in this gene set also. The most highly enriched MF is ‘structural constituents of the ribosome’, while the KEGG pathways ‘Ribosome’ is also over-represented. ‘Stomatal morphogenesis’ is enriched (p=7.8E-08). As only 69 genes were up-regulated in treatment compared to control after one day, this is not an adequate sample size for enrichment tests, and so no enrichment was conducted.

GEA of TvC after 7 days after green light supplementation began

The 246 genes down-regulated in the treatments against the control after seven days of green light supplementation, were analyzed for enrichment of GO and KEGG terms with eight BP, seven MF, eight CC GO terms, and three KEGG terms found to be over-represented. It is worth noting that on a gene set this size, enrichment can be skewed. The photosynthesis related terms ‘Photosynthesis, light harvesting’ and KEGG pathway ‘Photosynthesis –antenna proteins’ are enriched however the number of genes differentially expressed and significance of enrichment is greatly reduced compared to the 4hour time-point. As only 24 genes were up-regulated in RBGvRB after seven days, no enrichment was conducted.

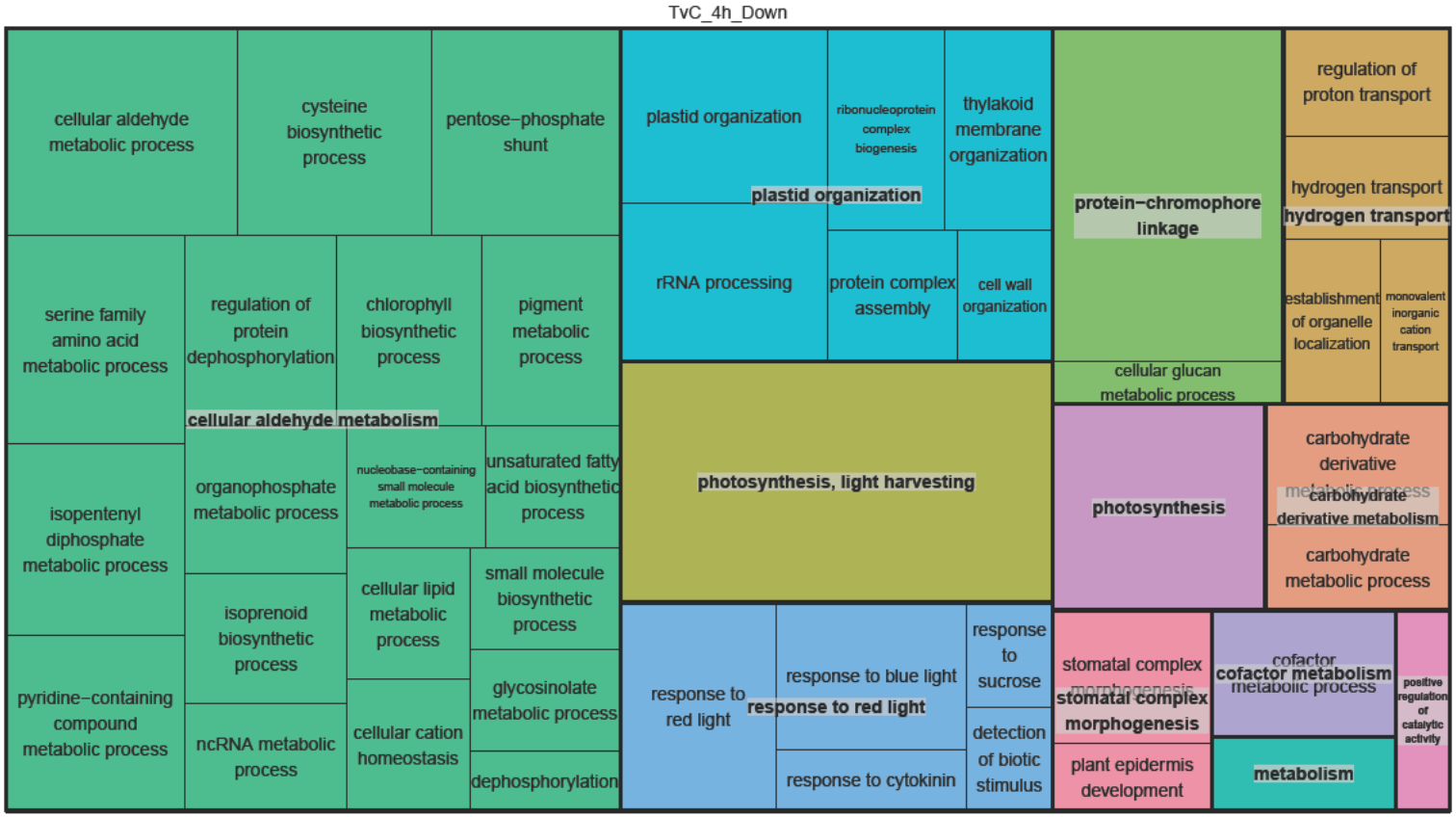


Figure 6-4. Tree-map of enriched Biological Process GO terms in down-regulated genes between TvC after 4hours. The size of each box represents the relative significance (-Log10PValue) of the enriched term relative to the sum of the significance of all terms Significance cut-off determined at p<0.0001, Redundant terms were removed using Revigo.

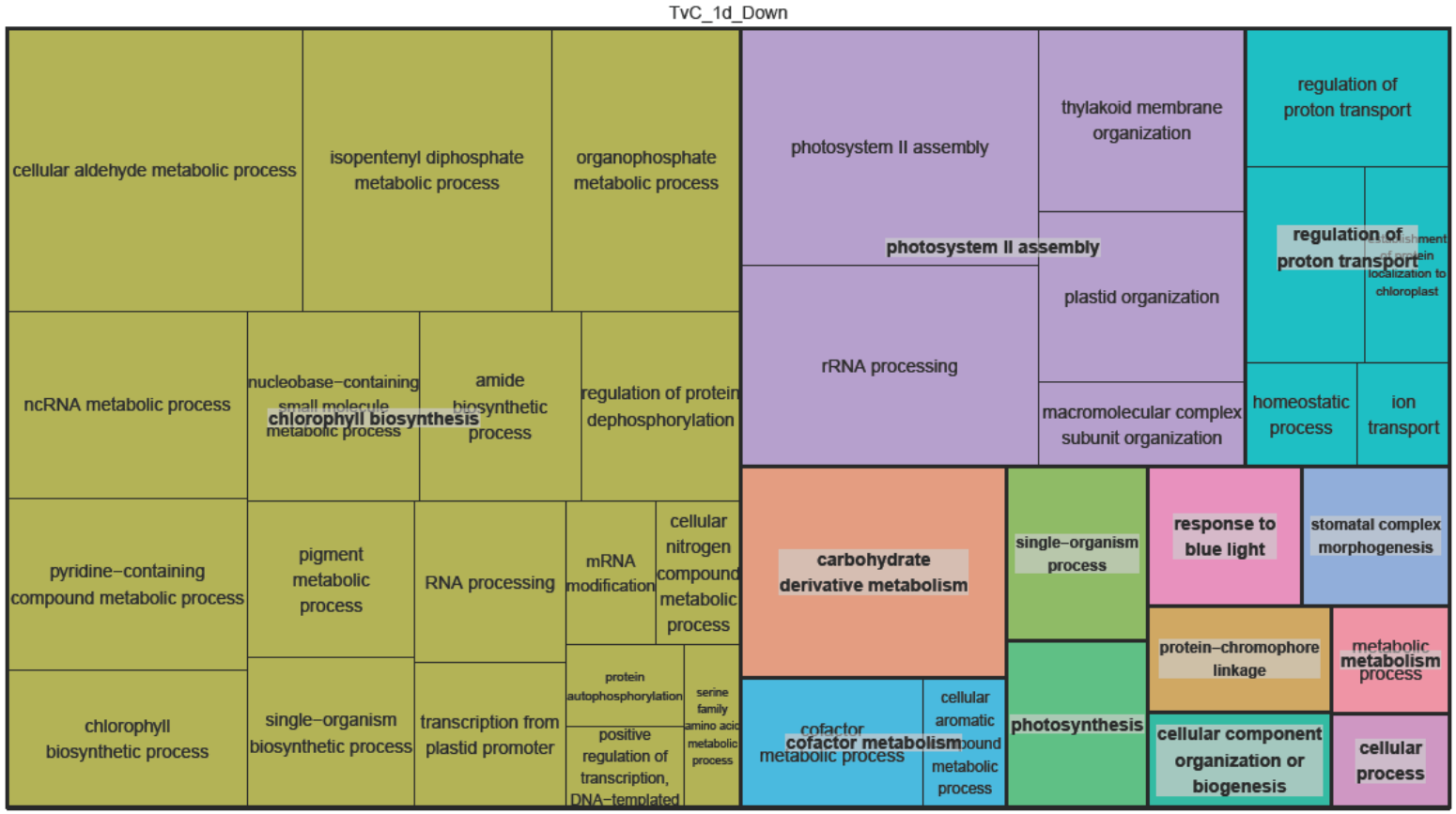


Figure 6-5 Tree-map of enriched Biological Process GO terms in down-regulated genes between TvC after 1 day. The size of each box represents the relative significance (-Log10PValue) of the enriched term relative to the sum of the significance of all terms Significance cut-off determined at p<0.0001, Redundant terms were removed using Revigo.

6.3.7 Pathways analysis

Photosynthesis

Photosynthesis-related GO terms and KEGG pathways were significantly enriched in down-regulated genes in TvC 4hour and 1day time-points. To better understand the effect of green light supplementation on the transcriptome, the expression was overlayed onto the KEGG photosynthesis-related heatmap. **Figure 6-7** has KEGG maps on the general light reaction of photosynthesis (top), and the specific genes which encode the light-harvesting complexes (bottom). Both heatmaps shows the general trend of a down-regulation in the expression of these photosynthesis-related genes in TvC and to a lesser extent the 1day time-point, with fewer and weaker down-regulation generally observed. Genes encoding light-harvesting complex proteins (also known as chlorophyll a/b binding proteins; CAB) were extensively down-regulated in RBG after 4 hours, and to a lesser extent, fewer genes were also differentially down-regulated in RBG compared to RB at 7 days. CAB12 (Solyc06g069730.2) was -2.9 log_2fold down-regulated in TvC 4 hours and TvC 7days, respectively. Similarly, CAB5 (Solyc12g006140.1) was -1.3log_2fold down-regulated in TvC 4 hours, and 7days, respectively. The only two CAB genes significantly down-regulated in the 1day time-point were CAB1a (Solyc02g070980.1) and CAB1b (Solyc02g070980.1), and these genes were significantly down-regulated in all comparisons, however, were twice a strongly down-regulated at 4 hours compared to 1 day and 7days.

The other half of the photosynthesis is the dark-reaction, which is represented in the KEGG ‘Carbon fixation in photosynthetic organisms’, which is an overview of the general pathways involved in the assimilation of CO_2 into organic compounds. Heatmap overlay of gene expression onto the Carbon fixation KEGG map (**Figure 6-8**) shows a similar trend to the previously discussed pathways, as with few exceptions the greatest number of differentially expressed genes and the most highly-downregulated genes are in the 4 hour time-point, followed by the 1 day time-point, with no DE genes in the TvC 7day time-point. The expression of some key genes in carbon fixation pathway is presented in **Table 6-3**. Three Rubisco sub-chain (Solyc02g063150.2, Solyc03g034220.2, and Solyc02g085950.2) encoding genes were significantly down-regulated in the TvC 4 hour time-point, with Solyc02g063150.2

most significantly down-regulated at -1.1 log_2fold change, however, these genes were not significantly down-regulated in the later time-points. Two fructose 1,6-bisphosphate aldolase (FBA6, Solyc07g065900.2; Solyc10g086730.1) genes were significantly down-regulated in both the TvC 4hour and 1day time-points. glyceraldehyde-3-phosphate dehydrogenase A (Solyc04g009030.2) and B (Solyc12g094640.1) were similarly differentially down-regulated in both TvC 4 hours and 1day time-points ~6log_2fold change Only one carbon fixation gene was up-regulated in this experiment in the time-series, which was phosphoenolpyruvate carboxylase 2 at the 4hour time-point, although this was only transient as no expression difference was observed in either the TvC 1day or 7 day comparisons.

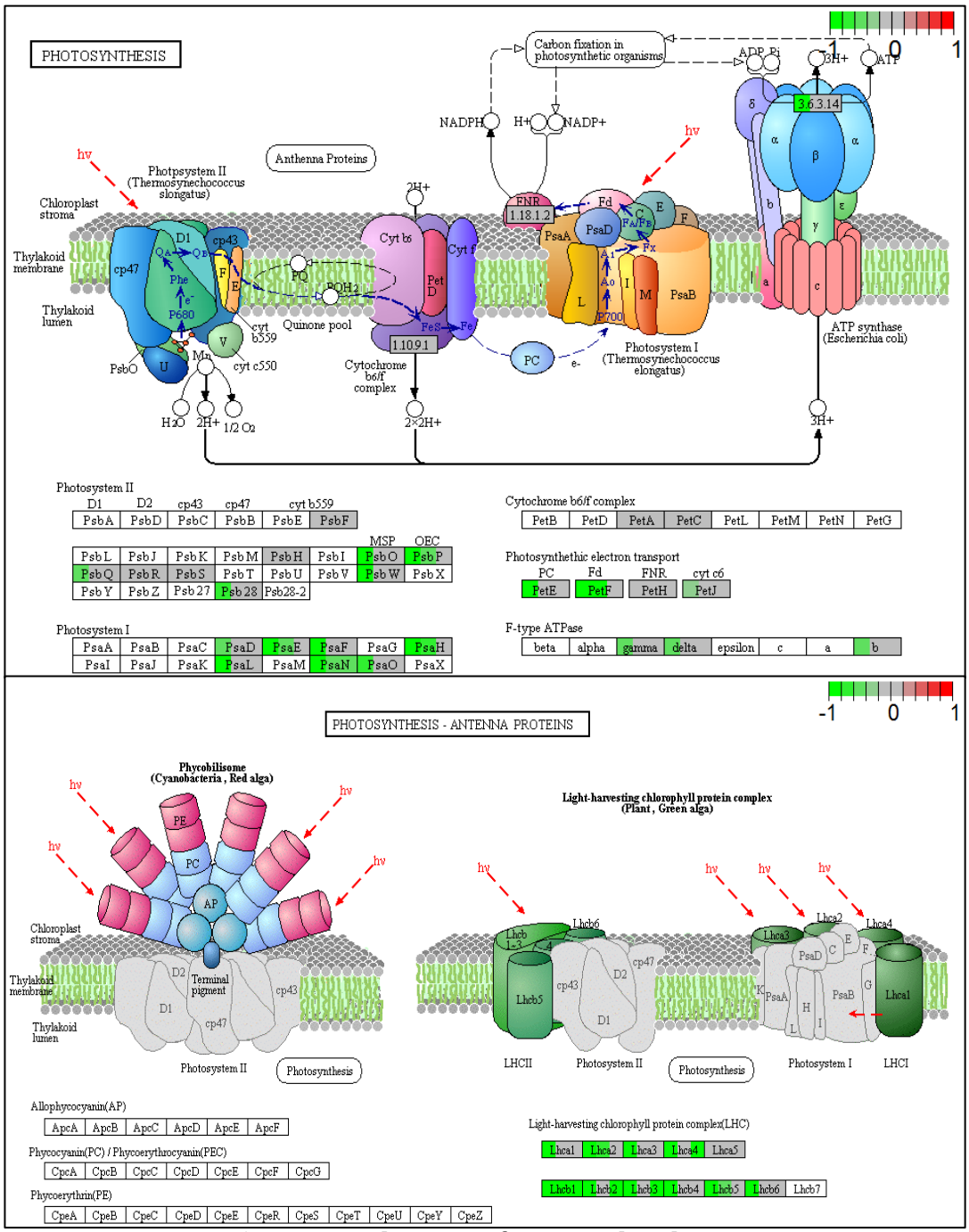


Figure 6-6 Key genes' expression heatmap of TvC overlayed onto KEGG photosynthesis pathway maps. Each circle represents a compound and each rectangle box represents an enzyme. The expression of each enzyme in multiple comparisons between TvC at 4 hours, 1 day, and 7 day time-points is represented in each enzyme as it is split into three sections, where: left= 4hour; centre= 1day; right= 7days. Expression is shown on 3-colour 'green-grey-red' scale, limits: -1 to 1 $\log_2$FC. Enzymes filled in white were not expressed in experiment.

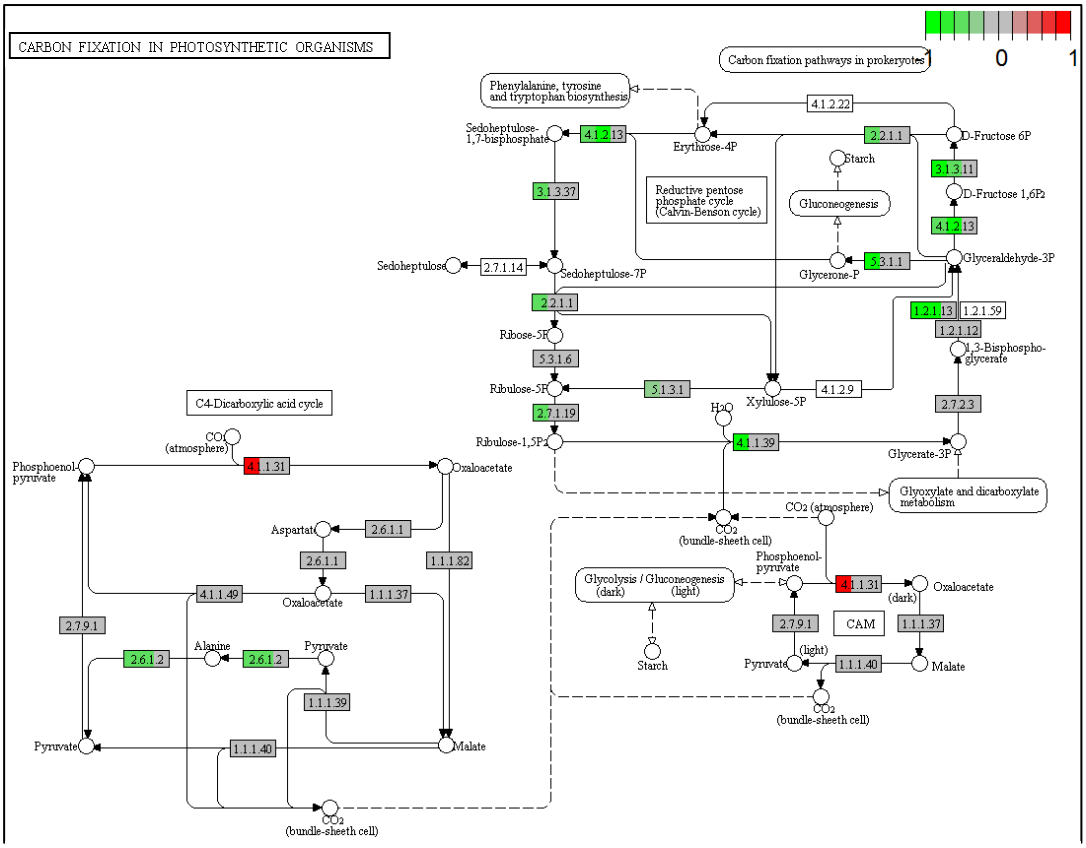


Figure 6-7 Key genes' expression heatmap of TvC overlayed onto KEGG 'carbon fixation in photosynthetic organisms' map. Each circle represents a compound and each rectangle box represents an enzyme. The expression of each enzyme in multiple comparisons between TvC at 4hours, 1day, and 7day time-points is represented in each enzyme as it is split into three sections, where: left= 4hour; centre= 1day; right= 7days. Expression is shown on 3-colour 'green-grey-red' scale, limits: -1 to 1 $\log_2$FC. Enzymes filled in white were not expressed in experiment.

Table 6-3Photosynthesis related gene expression

		TvC 4 hours		TvC 1day		TvC 7days	
Gene_ID	Descriptions	LogFC	FDR	Log_2FC	FDR	Log_2FC	FDR
Photosynthetic antennae encoding genes							
Solyc06g069730.2	CAB12; chlorophyll a-b binding protein Cab12	-2.9	5.1E-15	NS	NS	-1.1	2.6E-02
Solyc02g070980.1	Cab-1A; chlorophyll a/b-binding protein Cab-1A	-2.8	8.5E-15	-1.4	4.2E-03	-1.2	2.0E-02
Solyc02g070980.1	chlorophyll a-b binding protein 1B, chloroplastic	-2.8	5.5E-18	-1.3	2.9E-03	-1.0	2.9E-02
Solyc12g011280.1	chlorophyll a-b binding protein 8, chloroplastic	-1.3	2.0E-12	NS	NS	NS	NS
Solyc12g006140.1	CAB5; chlorophyll a-b binding protein 5, chloroplastic	-1.3	2.2E-07	NS	NS	-0.7	2.3E-02
Solyc07g047850.2	Chlorophyll a-b binding protein 4, chloroplastic	-1.2	6.1E-10	NS	NS	-0.7	1.5E-02
Solyc07g063600.2	chlorophyll a-b binding protein 13, chloroplastic-	-1.1	3.2E-07	NS	NS	-0.6	4.7E-02
Carbon fixation in photosynthetic organisms pathway genes							
Solyc02g063150.2	Ribulose bisphosphate carboxylase small chain	-1.1	7.2E-04	NS	NS	NS	NS
Solyc10g054870.1	triosephosphate isomerase, chloroplastic	-0.9	4.9E-02	NS	NS	NS	NS
Solyc03g034220.2	Ribulose bisphosphate carboxylase small chain	-0.7	1.2E-02	NS	NS	NS	NS
Solyc04g009030.2	glyceraldehyde-3-phosphate dehydrogenase A, chloroplastic	-0.7	9.8E-04	-0.6	2.3E-02	NS	NS
Solyc05g052600.2	SBPase; chloroplast sedoheptulose-1,7-bisphosphatase	-0.6	2.5E-03	NS	NS	NS	NS
Solyc12g094640.1	glyceraldehyde-3-phosphate dehydrogenase B, chloroplastic-like	-0.6	2.2E-02	-0.6	4.8E-02	NS	NS
Solyc02g085950.2	Ribulose bisphosphate carboxylase small chain	-0.5	4.3E-02	NS	NS	NS	NS
Solyc07g065900.2	SlFBA6; fructose 1,6-bisphosphate aldolase	-0.5	1.3E-02	-0.9	7.0E-07	NS	NS
Solyc05g013380.2	glutamate--glyoxylate aminotransferase 2	-0.4	1.4E-03	-0.5	4.2E-03	NS	NS
Solyc08g076220.2	phosphoribulokinase, chloroplastic	-0.4	4.4E-02	NS	NS	NS	NS
Solyc10g086730.1	fructose-1,6-bisphosphatase, chloroplastic	-0.4	3.0E-02	-0.6	1.5E-03	NS	NS
Solyc07g062530.2	ppc2; phosphoenolpyruvate carboxylase 2	1.1	3.2E-02	NS	NS	NS	NS
Solyc01g110360.2	SlFBA1; fructose 1,6-bisphosphate aldolase 1	NS	NS	-0.9	2.7E-02	NS	NS

Chlorophyll metabolism

Chlorophyll metabolism was also significantly enriched in the 4-hour time-points, and so as before the expression of genes was overlayed onto the 'Porphyrin and chlorophyll metabolism' heatmap (See **Figure 6-9**). There is a clear trend of down-regulation of chlorophyll metabolism genes in TvC 4hours and to a lesser extent TvC 1day, with no differential expression observable in TvC after 7days. The expression of several key differentially expressed genes annotated to the porphyrin and chlorophyll metabolism KEGG pathway is presented in **Table 6-4**. Geranylgeranyl diphosphate reductase (GGPR; Solyc03g115980.1) catalyzes the reduction of GGDP to phytyl diphosphate in one of the first committed steps for chlorophyll biosynthesis. GGPR was -1.1 log_2fold down-regulated in the TvC 4hour time-point. Protochlorophyllide reductase (Solyc12g013710.1), an enzyme catalyzing the formation of an important precursor of chlorophyll, protochlorophyllide, was significantly down-regulated -1.4 and -0.6 log2fold in TvC 4 hour and 1day, respectively. Two chlorophyll b biosynthesis genes, chlorophyllide a oxygenase, were found to be differentially regulated, with one (Solyc06g060310.2) down-regulated in both TvC 4 hours and 1day, and the other specifically down-regulated in only TvC 4hours time-point.

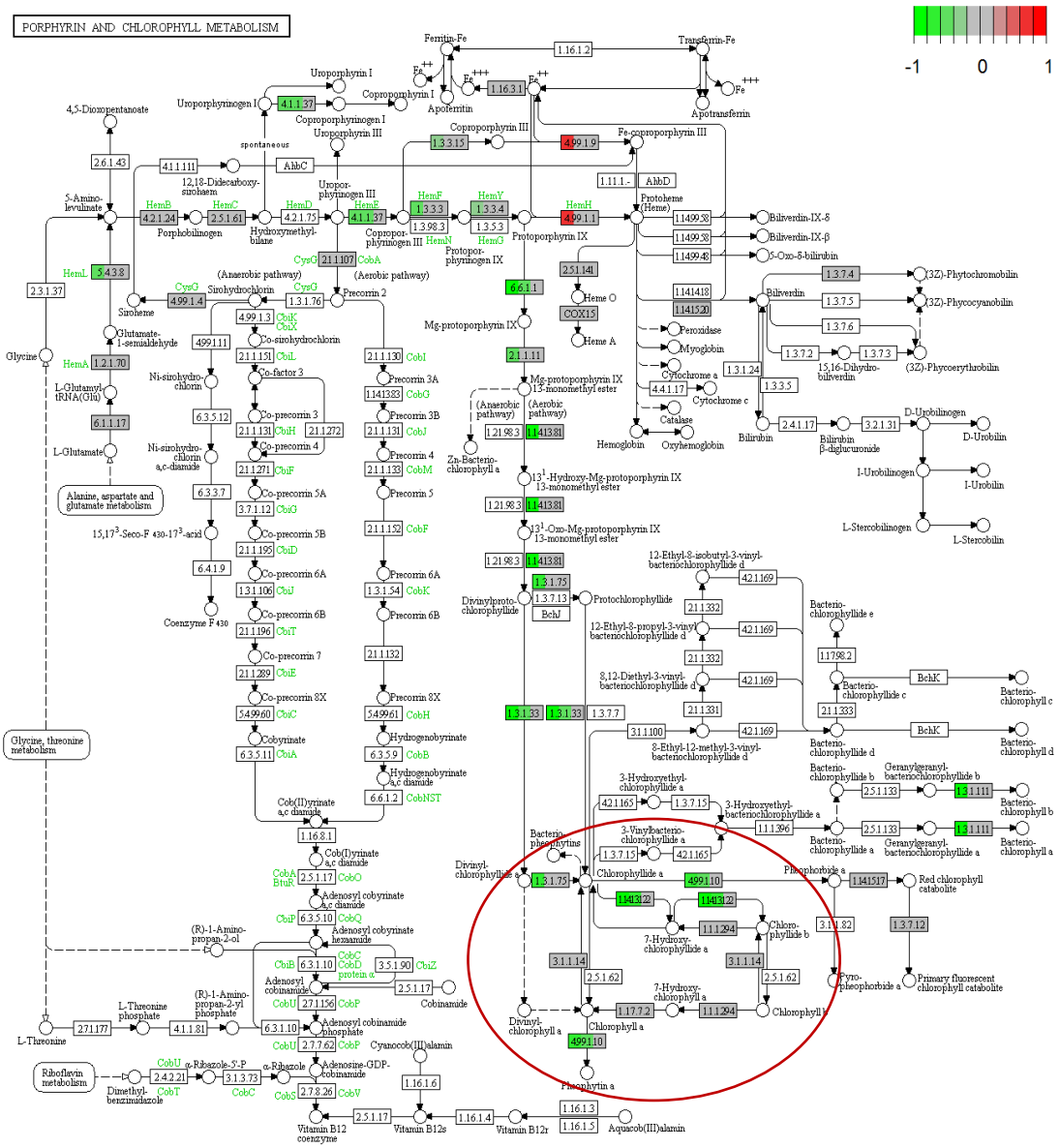


Figure 6-8 Heatmap overlay of time-course key genes' expression of TvC onto 'Porphyrin and Chlorophyll metabolism' KEGG map. Each circle represents a compound and each rectangle box represents an enzyme. The expression of each enzyme in multiple comparisons between TvC at 4hours, 1day, and 7day time-points is represented in each enzyme as it is split into three sections, where: left= 4hour; center = 1day; right= 7days. Expression is shown on 3-colour 'green-grey-red' scale, limits: -1 to 1 $\log_2$FC. Enzymes filled in white were not expressed in the experiment. The red circle outlines the specific part of the pathway in which chlorophyll a and b are metabolized from precursors.

Table 6-4 Porphyrin and chlorophyll metabolic genes

		TvC 4 hours		TvC 1day		TvC 7days	
Gene_ID	Descriptions	LogFC	FDR	LogFC	FDR	LogFC	FDR
Solyc04g015750	magnesium-chelatase subunit ChlH, chloroplastic	-1.5	2.2E-08	NS	NS	NS	NS
Solyc12g013710	protochlorophyllide reductase-like	-1.4	2.0E-13	-0.6	2.4E-02	NS	NS
Solyc06g060310	chlorophyllide a oxygenase, chloroplastic	-1.3	1.5E-11	-0.7	7.8E-03	NS	NS
Solyc10g006900	light dependent NADH:protochlorophyllide oxidoreductase 3	-1.2	6.3E-07	NS	NS	NS	NS
Solyc03g115980	geranylgeranyl diphosphate reductase, chloroplastic	-1.1	2.1E-04	NS	NS	NS	NS
Solyc11g012850	chlorophyllide a oxygenase, chloroplastic-like	-0.9	1.1E-06	NS	NS	NS	NS

Table 6-5 Plant hormone metabolism and signalling genes DE between RBG and RB

		TvC 4 hours		TvC 1day		TvC 7days	
Gene_ID	**Descriptions**	**Log_2FC**	**FDR**	**Log_2FC**	**FDR**	**Log_2FC**	**FDR**
	Hormone metabolism						
Solyc04g078900.2	CYP707A1; ABA 8'-hydroxylase	-0.6	4.5E-04	NS	NS	NS	NS
Solyc07g049530.2	ACO1; 1-aminocyclopropane-1-carboxylate oxidase 1	1.4	3.0E-02	NS	NS	NS	NS
	Hormone signalling						
Solyc01g110570.2	auxin-induced protein 15A-like	-1.7	2.3E-05	NS	NS	-1.4	6.0E-03
Solyc10g076790.1	LAX4 protein	-0.6	2.6E-02	NS	NS	NS	NS
Solyc07g042260.2	auxin response factor 7	-0.5	3.2E-04	NS	NS	NS	NS
Solyc02g092980.2	cycD3; cyclin D3.1	-0.5	2.8E-02	NS	NS	NS	NS
Solyc07g040690.2	NIM1; non-inducible immunity 1	0.6	3.1E-02	NS	NS	NS	NS
Solyc09g075440.2	ETR3; ethylene receptor neverripe	0.6	3.0E-02	NS	NS	NS	NS
Solyc01g104650.2	G-box-binding factor 4-like	0.6	2.7E-02	NS	NS	NS	NS
Solyc08g077780.2	serine/threonine-protein kinase SAPK3	0.7	1.9E-02	NS	NS	NS	NS
Solyc07g040990.2	Protein phosphatase 2C	0.7	3.3E-02	NS	NS	NS	NS
Solyc03g007230.2	probable protein phosphatase 2C 51	0.7	4.2E-02	NS	NS	NS	NS
Solyc04g008110.2	histidine kinase 4	1.0	3.7E-02	NS	NS	NS	NS
Solyc08g066350.1	histidine-containing phosphotransfer protein 4-like	1.0	1.5E-02	NS	NS	NS	NS
Solyc03g096670.2	PP2C-2; protein phosphatase 2C AHG3 homolog	1.4	3.5E-02	NS	NS	NS	NS

Plant hormone signalling

As phytohormone play an integral role in light signalling, the differential expression of genes annotated to hormone metabolism and signalling pathways was investigated. For metabolism, very hormone metabolic genes were notably differentially expressed in any comparison. The few exceptions being, ABA 8'hydroxylase which is involved in the catabolism of phytohormone abscisic acid (Solyc04g078900.2), and aminocyclopropane-1-carboxylate oxidase 1 (Solyc07g049530.2) which is involved in the biosynthesis of ethylene. Despite little difference in the expression of genes involved in hormone homeostasis, several signalling genes were found to be differentially expressed, however almost exclusively in the TvC 4 hour comparison. Auxin receptor LAX4 (Solyc10g076790.1) was the only gene differentially expressed in, being significantly down-regulated in both TvC 4 hour and TvC 7day comparisons. An auxin-induced protein-encoding gene (Solyc01g110570.2) and auxin-regulated factor 7 (Solyc07g042260.2) were significantly down-regulated, -0.6 and -0.5 $\log_2$fold change, respectively, in TvC 4hour. Conversely, three abscisic acid receptor PP2C encoding genes were significantly up-regulated in TvC 4 hours. Finally, ethylene receptor ETR3 was significantly down-regulated in TvC 4 hours.

6.4 DISCUSSION

6.4.1 Experimental context

Green light is an important environmental signal, however, its complete mechanism of action remains unclear. Green light mechanics can be separated into cryptochrome-dependent, and independent pathways. The cryptochrome dependent pathway is better resolved, with cryptochrome green light proven to cause photo-reversion of blue-light activated cryptochrome, attenuating signal and eliciting a SAR response in a blue/green ratio dependent manner (J. P. Bouly et al., 2007; Sellaro et al., 2010). Evidence of a second cryptochrome-independent mechanism of green light action stems from experiments showing green light response *cry* and *phy* mutant backgrounds. Both the cryptochrome-dependent and –independent pathways tend to

oppose typical light-driven physiological and developmental responses (Tingting Zhang & Folta, 2012). In chapter 3, we saw a significant increase in the height, leaf area, and biomass Micro-Tom seedlings grown under RBG compared to RB (See **Figures 3-1** and **Figure 3-2**). Through studying the transcriptional response of Micro-Tom leaf tissue to continuous green light supplementation by time-course we have sought to understand the immediate and long-term effects of green light on global gene expression.

6.4.2 Immediate transient response to green light supplementation

The trend in gene expression shows that there is an immediate transcriptional response to green light, with 1190 genes DE, of which the majority of which were down-regulated (62.4 %) by green light. There was extensive regulation of photosynthesis-related gene expression and chlorophyll metabolism, including core several CAB genes as well as genes involved in carbon fixation, including 3 Rubisco sub-units. A similar result was found in *Arabidopsis and Nicotiana tabacum*, where seedlings exposed green light exhibited an immediate (30minutes) down-regulation of plastid transcription, with a single pulse of green light sufficient to elicit this effect (Dhingra et al., 2006). A few hormone signalling genes were also differentially expressed 4hours after green light supplementation began. Abscisic acid catabolic gene, ABA 8'-hydroxylase was significantly down-regulated, while ABA signalling genes PP2C were significantly up-regulated. ABA has been shown to repress transcription of plastid gene expression, however, the up-regulation of PP2C and down-regulation of ABA catabolic gene expression suggests that ABA signalling is up-regulated in RBG while plastid transcription is down-regulated (Mochizuki et al., 2004). Auxin transport LAX4 and auxin-responsive factor 7 were significantly up-regulated by RBG, ARF7 is a growth-promoting factor. Green light has been shown to stimulate growth in *Arabidopsis* (Tingting Zhang & Folta, 2012), while we observed an increase in Micro-Tom seedlings exposed to RBG compared to RB light (See **Figure 3-1**). However, despite the early-induced changes in Micro-Tom transcriptome by supplemental green light, we found this to diminish over time. After one day, the number of genes differentially expressed between RBG and RB LED grown plants substantially reduced to 306 genes, and the proportion of genes down-regulated increases to 77.4%. The GO enrichment revealed the transcriptional

response involved many of the same significantly enriched processes as seen after four-hours albeit the significance of the enrichment was generally reduced. By the seventh day after continuous green light supplementation plants are expected to have acclimated to its new light environment, and in comparison between the RG and RB transcriptomes we see the lowest number of DE genes, 270, of which 91.1 % of the DE genes are down-regulated within plants grown under RBG compared to RB. Green light was found to cause a transient increase in stem elongation in etiolated *Arabidopsis* seedlings (Folta, 2004). This was also observed in cry1, cry2, phyA transgenic Arabidopsis lines, In our time-series of gene expression on plants after supplementary green light, we also observe a transient effect of green light, as early-responsive green light effect on differential expression reduces over the course of one day and a week to the point where only 270 genes weree differentially expressed after 7 days.

Given that the effect we observed of green light is transient, it is worth considering why. Often in a transcriptional network, negative feedback loops exist which act to deactivate a response to prevent excessive signalling in response to a continuous stimulus. This exists in plant photoreceptor signalling, the mutually assured destruction of phytochrome-PIF complexes reduces phytochrome levels, thereby dampening the effect of red light over time (W. Ni et al., 2014). Several important early-induced SAR related transcription factors have also been shown to modulate their own expression in negative feedback loops (Galstyan, Cifuentes-Esquivel, Bou-Torrent, & Martinez-Garcia, 2011; Hornitschek, Lorrain, Zoete, Michielin, & Fankhauser, 2009; L. Li et al., 2014). It is that the plant response to a fluctuating light environment is an immediate reduction in plastid gene expression, however, in the sustained shade, the plant acclimates and returns to normal growth. In fact, PhyA antagonistically regulates phyB response to low R: FR, reducing differential expression in response to 24 hours of shade (Devlin, 2003). Given that PhyA absorbs in the green region of the visible light spectra, it is possible that phyA is, in fact, responsible for the reduction in differential expression over time in this experiment.

6.4.3 Limitations of this experiment

As discussed in the introduction, a mechanism through which green light can alter development has been established, whereby it inhibits cryptochrome-dependent blue light regulation of gene expression through photoreversion of the cryptochrome (J. P. Bouly et al., 2007). In our experiment, we used only a moderate amount of green light; 18 µmol m^2s^{-1} which was 13% of the total PAR and a B: G ratio of 1.5. This is unlikely to drastically overturn cryptochrome activation status, and therefore a possible reason for the lack of a long-term transcriptional response to supplemental green light could be due to this. In *Arabidopsis*, reducing B: G ratio below 1 inhibited cryptochrome causing shade avoidance (Sellaro et al., 2010). However, it has yet to be established in tomato that there is a beneficial effect of green light under any conditions, and we found no morphological, physiological or yield difference when grown to harvest under our RB or RBG as used in this experiment. (See chapter 3). Green light has been shown to be beneficial to lettuce grown under continuous light, as the addition of proportion of green light (~18-20%) to red/blue LEDs enhanced photosynthesis and reduced the oxidative stress and photoinhibitory damage imposed by continuous light (Bian, Yang, et al., 2018). This directly contrasts to both our experiment and that observed in Arabidopsis and tobacco (Dhingra et al., 2006), as photosynthesis-related gene expression was enhanced under RBG compared to RB LED light. However, it remains to be seen whether this difference is species specific, or that the effect of green light on the transcriptome differs by photoperiod, or indirectly from the stress imposed by continuous light. The benefit of green light may be enhanced under continuous light, as green light penetrates further into leaf and canopy (Vogelmann & Han, 2000), potentially spreading the light experienced by the plant over more photosystems and thus reducing the excess light energy and photo-inhibitory damage/oxidative stress. More research needs to be conducted with a variety of green light proportions, at various intensities and photoperiod to establish whether green light can be beneficial and to quantify the effect of green light on the regulation of global gene expression.

6.5 Conclusions

In summary, we have identified the effect of supplemental green light on the transcriptome of Micro-Tom plants and found that while there is an immediate and substantial response to green light altering transcription of photosynthesis, metabolism, and developmental genes, this response is transient. The differential expression of genes upon supplementation with green light fades over the course of one week to the point at which little difference was observed between the transcriptomes was minimal. This transcriptomic study identifies that there is little long-term effect of supplemental green light on Micro-Tom transcriptome, which agrees with the phenotypic study reported in chapter 3 which found no significant differences in the physiological properties, photosynthesis, biomass, or yield of Micro-Tom grown from seed to harvest with or without supplemental green light.

7 GENERAL DISCUSSION AND CONCLUSIONS

7.1 Introduction

In this thesis, the influence of LED spectra on the growth, development, and yield of Tomato has been explored and combined with RNA-Seq transcriptomic studies to resolve the transcriptional mechanism that underpins the adaptive responses to light quality observed.

Light signalling is a complex process perceived by multiple families of photoreceptors which regulate a plethora of plant traits that ultimately determine yield. The post-translational and genetic signalling events involved in light signal perception and transduction control extensive transcriptional networks that alter the plant growth and developmental decisions, resource allocation and sensitivity to other exogenous and endogenous signals. Many of the integral signalling elements downstream of photoreceptors have been identified in model species *Arabidopsis*, however, the translation and application of this knowledge to crop species have been limited. Gaining greater insight into the molecular events in the model crop species tomato will allow comparative analysis between the research conducted in Arabidopsis to identify common and novel signalling elements. The aims of this project were to:

1. To analyze Micro-Tom growth, photosynthesis, physiological and morphological changes, under different LED light spectra and the effect of spectral quality in tomato.
2. To conduct RNA-Seq transcriptomic analysis in Micro-Tom tomato plants grown under different light qualities in order to identify important regulatory components and key genes involved in the adaptive responses to light and agronomically important traits
3. Investigate the effect of supplemental green light on the transcriptome of tomato to understand how green LED light to regulate tomato plant growth and development.

7.1.1 Blue light is essential for tomato development

The identification of key regulatory genes that influence plant architecture, cell growth, cell division, and photosynthesis are paramount to yield manipulation (Kharshiing & Sinha, 2014; C. C. Liu et al., 2018). In Chapter 3, the major phenotypes observed in this work were the shade avoidance type growth and photosynthetic dysfunction in monochromatic red grown Micro-Tom plants. Both of which been previously identified in *Arabidopsis*, and established as negatively regulated by the cryptochrome photoreceptor in a threshold response to low blue light (Keller et al., 2011; Keuskamp et al., 2011; Pedmale et al., 2017). In addition to these morphological and physiological phenotypes, the R grown Micro-Tom had significantly reduced leaf biomass and fruit yield, demonstrating that light quality significantly affects yield. As discussed in the literature review and throughout this thesis, the primary mechanisms through which red and blue light elicits changes in the plant development and influences growth is through phytochrome and cryptochrome-mediated regulation of the transcriptome, respectively. In this thesis, the most substantial response to varying LED spectra on tomato growth and yield was between the monochromatic red grown plants compared to those grown under any other LED spectra. The low-blue light response in Arabidopsis is regulated specifically by PIF4 and PIF5 (Pedmale et al., 2016). In Chapter 4, we identified PIF orthologs (PIF1a, PIF1b, and PIF3) which are significantly over-represented for target genes in the down-regulated RvB and RvRBG gene sets, implicating PIF family involvement in the controlling the genetic response to LBL in tomato. While there was limited PIF differential expression, it is well established that the primary mechanism in which PIF activity is regulated by shade is through post-translational interactions; inhibiting DNA-binding activity or regulating PIF abundance through targeting them for 26S proteasomal degradation (Jang, Henriques, Seo, Nagatani, & Chua, 2010). In addition to PIFs, light also regulates growth and development through regulation of hormone metabolism and signalling is. Moreover, that recent characterization of Tomato *cry1a* transgenic lines isolated that cryptochromes negatively regulate shade avoidance (C. C. Liu et al., 2018). Liu (2018) found that CRY1a negatively regulates cytokinin, gibberellin and jasmonate content and that this plays a critical role in mediating the regulation of cell cycle and plant growth. In our transcriptomic analysis (Chapter 4), Micro-Tom plants grown under monochromatic red light exhibited a coordinated up-

regulation of cytokinin catabolic genes (cytokinin oxidase; CKX6), gibberellin (GA20 oxidase1; GA2OX1) and jasmonate biosynthesis genes (Allene oxidase synthase, AOS; Allene oxidase cyclase, AOC), along with a down-regulation of gibberellin catabolic genes (Gibberellin 2 beta dioxygenase; GA2OX),which are also similarly differentially regulated in *cry1a* silenced plants (C. C. Liu et al., 2018). This supports Liu (2018) that blue-light activated CRY1 is a dominant photoreceptor involved in LBL modulate hormone abundance to control growth.

Analysis of the photosynthetic capacity of Micro-Tom grown under varying LED spectra identified that Micro-Tom grown under R has significantly lower quantum yield and maximum rate of photosynthetic efficiency as measured by chlorophyll fluorescence. Hogewoning showed that monochromatic red grown lettuce plants exhibited dysfunctional photosynthesis and reduced photosynthetic efficiency, and the addition of only 7% blue light was necessary to restore normal photosynthesis (Hogewoning et al., 2010). In chapter 4, we identified plants grown under monochromatic red light has a significant reduction in the photosynthesis-related gene expression, including photosynthetic-rate determine enzymes such as rubisco sub-unit (rbscS). Facella and colleagues recently identified that CRY2 is a master regulator of the transcription of photosynthesis encoding genes (Facella et al., 2017). A possible mechanism for the reduction in photosynthesis-related gene expression and subsequent reduction in photosynthetic rates could be the inactivation of CRY2 in R grown Micro-Tom due to the absence of blue light.

7.1.2 Defense-related gene expression

A key observation from the transcriptome data was the differential expression of core defense signalling genes. Jasmonic acid biosynthesis-related gene expression was significantly up-regulated in R. Additionally, key JA signalling genes JAZ1was significantly upregulated in R light. In Arabidopsis, phytochromes regulate JAZ to control defense related signalling, which is an integral module to phytochrome-regulation of the defense response to biotic stress (Campos et al., 2016). In addition to JA, reactive-oxygen species signalling was also differentially regulated by light. RBOH1 was significantly up-regulated in R light compared to both B and RBG.

RBOH-dependent H_2O_2 production is essential for systems-acquired resistance. Furthermore, in Arabidopsis, phytochromes regulate ABA-dependent ROS signalling. Night-time supplemental red light promotes *Solanum lycopersicum* resistance to *p. syringae* through the promotion of SA accumulation and up-regulation of defense related transcripts (Y. Yang et al., 2015). This research by Yang and colleagues (2015) highlighted a novel use of light signalling to reduce yield losses through improving biotic stress using night-time supplementation of red light. The identification of the molecular mechanisms regulating red light promotion of defense could also be exploited to breed for improved resistance to biotic stress.

7.1.3 Co-action of red and blue light necessary for pigment production

The investigated the importance of red and blue wavelengths individually and in combination was investigated through the use of monochromatic red, monochromatic blue and mixed RB and RBG LED spectra. Plants grown under RB and RBG had higher fruit biomass and fruit yield than either R or B, although it was only significant compared to R. Co-action of red and blue light necessary for to elicit a response has been described for over two decades (Ahmad et al., 1998). This concept suggests that both red and blue light are needed together to stimulate a response. In fact, that phytochrome- and cryptochrome photoreceptors transduce red and blue light signals through a partially overlapping signalling pathway (Keller et al., 2011), and therefore red and blue light signals can directly antagonistically or synergistically interact. We observed that in pigment metabolism both red and blue light signals were required for pigment accumulation. Both chlorophyll and carotenoid levels in RB, RBG, and Fl were significantly higher than in either R or B which had similar levels. (See chapter 3). Furthermore, in the transcriptomic analysis of Micro-Tom under the same spectral qualities, the expression of chlorophyll metabolic genes was significantly up-regulated in RBG compared to both R and B. However, the most pronounced effect of light on pigment metabolism was observed in anthocyanin, which was not detectable in plants grown under B light, and significantly increased in RBG and RB to R, with Fl significantly higher than all others. Interestingly, the expression of anthocyanin biosynthesis genes was highly correlated with the pattern of anthocyanin accumulation measured in the leaf material Moreover, a co-expression network module was discovered which also included the

known transcriptional regulator of anthocyanin metabolism, ANTHOCYANINLESS (Qiu et al., 2016). The co-expression network was so dense with interactions, that even using seed genes of interest, biological interpretation of the co-expressed modules was extremely difficult. This was likely because so the number of samples used in our transcriptomic analysis, 15, is not high enough to sufficiently improve the accuracy and reduce the number of co-expression interactions to a high enough level. Despite this, we did identify the one module described. In fact, at the top of the network, an ERF transcription factor APETELAe was found to be highly differentially expressed in our transcriptome, highly positively correlated between its expressions to anthocyanin content and co-expressed with anthocyanin biosynthesis genes. This highlights the potential of co-expression network modeling in identifying potential novel interactions and to resolve the expression of light signalling networks. With the reduction in the cost of RNA-Sequencing, it has become more affordable to run large scale transcriptomic studies including high sample number, and more complex experimental designs. Increasing the size and complexity of transcriptomic experiments will improve the accuracy of co-expression networks and this approach has great potential for the reconstruction of light signalling networks.

7.1.4 Green light had limited effect on morphology, physiology or gene expression

We aimed to characterize the effect of supplemental green light on tomato growth and signalling. In Chapter 3, we characterized the effect of combinations of RB (7:3) and RBG (7:3:1.5), to establish the effect of additional green light on tomato morphology, photosynthesis, and yield. The importance of green light is of great concern to the horticultural industry, as optimizing the LED spectra of their light is necessary to improve energy efficiency and maximize yield. Currently, green LEDs are less efficient than red and blue LEDs, and therefore the inclusion of green light in a customized spectrum for plant production needs to be evaluated in that any improvement in yield against the energy required to generate green wavelengths. We observed a significant increase in the height, leaf area, and biomass accumulation of Micro-Tom seedlings grown under RBG compared to RB (See **Figures 3-1** and **Figure 3-2**). Given green light has been established to inhibit blue-light activation of cryptochrome, and that cryptochrome-perceived blue light suppresses growth (Sellaro

et al., 2010), the observation that RBG seedlings were significantly taller indicated that this may be due to green light perceived signals. It was based on this information that we conducted Chapter 6 green light RNA-Sequencing, which was a time-course of gene expression following the addition of green light to plants grown under RB. While there was an immediate response to green light in plants switched to RBG from RB, with 1190 DE genes after 4hours of supplemental green light-responsive genes, within one day the differential expression had drastically reduced to 305, and after one week only 270 genes were DE between RBG and RB plants. Replacing 13% of RB with G is a relatively moderate amount of green light. In Chapter 3, further characterization of the RB and RBG grown Micro-Tom in mature plants did not identify any difference in morphology, physiology, photosynthesis or yield. In the RBG treatment, 13% of RB was replaced with G. It has been established in other crops, that green light can be beneficial to yield (Bian, Cheng, et al., 2018; Bian, Yang, et al., 2018; H. Kim et al., 2004), and regulates important developmental processes (Sellaro et al., 2010), In the future work section we propose how future investigation of the importance of green light should be systematically conducted.

7.1.5 Targeted improvement of crops

While light signalling has pleiotropic effects on throughout plant growth and development, the elucidation of genes further down-stream may enable the targeting of a subset of these responses. Identifying core regulatory genes responsible for controlling traits such as plant architecture, photosynthesis, resource allocation, and stress tolerance may enable the improvement of yield and manipulation of food quality. Shade is a prevalent signal in agriculture as to optimize land use efficiency crops are grown at high densities, and while shade avoidance responses are beneficial to individual to plants, competition between plants reduces overall productivity and yield of crop grown in monoculture as there is a reallocation of resource towards non-productive growth such as stem elongation and increased apical growth. The potential of suppression of SAR was evident in potato over-expressing p*hyb* which has increased yield at high densities (Hernán E Boccalandro et al., 2003). Specific manipulation of genes at tissue or development specific level may further enable the circumvention of negative side effects that may undermine the potential beneficial effects of these genes. However, this necessitates the thorough understanding of the

mechanisms which underlie this process as well as biotechnological techniques to facilitate precise and targeted crop manipulation.

The advancement of gene editing allows the possibility of precise alterations in crop genomes to elicit targeted specific modifications. However, in Europe as of 2018 after a ruling from the European Court of Justice gene editing is considered genetic modification and therefore banned. Despite this, the continued advancement of plant biotechnology combined with the elucidation of new genes targets for manipulation for crop improvement provides promise for producing more resilient, productive and nutritious crops in the face of rising food insecurity. While genome editing is currently not viable in Europe, these molecular markers can instead be used to look for natural genetic variation that exists between commercial and domestic varieties as well as wild relatives which could then be introgressed into commercial lines through conventional breeding approaches for crop improvement. The Tomato Genome Re-Sequencing Project recently completed the 'tomato 150 genome project', in which 83 tomato genotypes were sequenced (Aflitos Set al., 2014), providing a comprehensive resource to mine for identifying natural variation which can be utilized to identify and introgress beneficial traits into commercial varieties. In the future work section, we discuss how RNAi-mediated silenced transgenic lines of the candidate genes of interest should be characterized.

7.2 Limitations of this study

The purpose of this study has been to characterize the phenotypic effects of LED spectra on Solanum lycopersicum and identify the genetic mechanisms through which spectral quality controls plant growth and development. The cultivar Micro-Tom was chosen as the model species for this research owing to its compact size, which allowed us to grow it in small compartments under a strictly controlled environment. However, as Micro-Tom has mutations to both SELF-PRUNING (SP) gene which produces a determinate flowering phenotype, and DWARF (D) which disrupts brassinosteroid biosynthesis, it is possible the effect of LED spectra on this variety may differ from other cultivars. While phenotypic evidence in chapter 3 showed typical shade avoidance type plant responses, a similar study of the effect of

spectral quality on commercial cultivars would be useful to establish the phenotypes and transcriptomic differences observed in this study are the same seen in other varieties.

7.3 Future work

7.3.1 Functional characterization of candidate light signalling genes

This work provides a foundation for future study of potential light signalling components identified in chapters 4 and 5 through mutant analysis which was not possible during this project due to time constraints. The sequences of the genes of interest have been sent to collaborators in Southwest University, China for the generation of transgenic tomato lines by RNAi mediated gene silencing. Transgenic lines silenced for each of the chosen genes, the XYLOGLUCAN ENDOTRANSGLUCOSYLASE/HYDROLASE, C2H2 TRANSCRIPTION FACTOR, MYB RELATED TRANSCRIPTION FACTOR, HAT4 TRANSCRIPTION FACTOR, and CYTOKININ KINASE will be evaluated for different parameters related to growth, photosynthesis and carbon metabolism, crop yield and fruit quality. The importance of these genes in light signalling can be tested not only by growing transgenic lines in white light to identify phenotypic abnormalities, but also growing these plants under the varying spectral qualities as was done in chapters 3 and 4 to observe if any phenotypes observed in the wild-type plants under different light qualities have been abolished/exaggerated with the disruption of candidate gene expression. Further analyses will be conducted to understand the regulatory mechanisms involved in the phenotypic and metabolic abnormalities, which could include further RNA-Sequencing. This functional analysis will test the importance of candidate genes in light signalling and potentially identify molecular markers involved in the control of agronomically important plant traits.

7.3.2 Further understanding of the post-translational mechanisms at the apex of the transcriptional network

It is well established that the early signal transduction events downstream of both phytochrome and cryptochrome perception of light signals involve post-translational modifications. Phytochromes and cryptochromes directly interact with

several transcription factors as well as regulating the activity of E3 ubiquitin ligases, through which the abundance and activity of several transcription factors are modulated, regulating the transcriptional cascade that re-programs gene expression. Transcription factor target enrichment analysis in chapter 4 identified dozen of transcription factors which were enriched for differentially expressed target genes between the various light treatments. Many of these enriched target genes were not significantly differentially expressed, suggesting that if they truly are regulating transcription light regulates the transcription factors through post-transcriptional modifications. The enriched genes included several transcription factors which have homologs in Arabidopsis that are important light signalling components, the most important being the two PIFs, PIF1a and PIF1b. Investigation of the abundance of these proteins through western blots would identify if there is a quantitative change in protein level under different spectral qualities. While chromatin-immunoprecipitation of PIF1a and PIF1b would experimentally validate its target genes and prove the importance of these genes in tomato photoreceptor-mediated light signalling.

7.3.3 Quantitative investigation of effects of varying doses green light on Micro-Tom

In this thesis, the importance of the addition of green light to the LED spectra was investigated. However, the proportion of green light was limited to 13% of PAR and a B: G ratio of 2. While little evidence of phenotypic of the transcriptomic effect of green light on Micro-Tom, further work to could still be done to thoroughly investigate the importance of green light. A dose-study of increasing % green light as a proportion of total PAR from 0-50%, and reducing B: G ratio from 2-0.5 would thoroughly determine the quantitative effect of green light on Micro-Tom physiology and yield. In addition to testing the effect of different doses of green light, another future experiment to determine the effect of supplemental green light at different light intensities is necessary to determine the importance of green light particularly at higher light intensities. In Arabidopsis, supplemental green light drives photosynthesis more efficiently than red light in Arabidopsis under strong white light (Terashima et al., 2009). Green light has also been shown to be beneficial under continuous green light as it reduces the photoinhibitory damage caused by excess light (Bian, Yang, et al., 2018). Both high light and continuous light conditions result in

excess light energy and light stress which damages photosystems and reduces photosynthetic capacity and efficiency. Together these support the hypothesis that the greater penetration of green light as opposed to red or blue into the leaf distributes the light energy across a greater number of photosystems, reducing the excess light energy and enabling increased photosynthetic efficiency under conditions excess light environments. Studying the effect of supplemental green light at saturating light intensities or in continuous light systems will establish if Micro-Tom productivity can be improved by the addition of green light to LED spectra, or whether yield or energy efficiency can be maintained or improved by its exclusion.

7.4 Conclusions

These findings contribute to a better understanding of the molecular basis of the response of tomato to various spectral qualities, yielding insight into the mechanisms underpinning the adaptive response *of Solanum lycopersicum* to spectral quality. This study is the first to report the effects of LED spectral quality on yield in Micro-Tom using LED as sole-source lighting. Studying the molecular basis of light signalling in tomato enables the translation of decades worth of knowledge gained from model species *Arabidopsis* to an economically important crop and model fruit species. These data provide a basis for understanding light signalling in tomato, and the extensive transcriptional reprogramming which underpins the adaptive response of tomato morphology, biochemistry, and development in response to spectral quality. The results presented within on the effects of LED spectral quality on the leaf transcriptome as well as the effect of LED spectra on morphology, physiology, photosynthesis and yield in tomato are novel and have meaningful consequence for the identification of molecular markers which regulate important plant traits, which can be targeted for improved crop yield and quality. Transcriptomic analysis identified several genes which were consistently differentially regulated by light over time, which may be important genes light signalling genes and will be further characterized by RNAi-mediated gene silencing in tomato to elucidate the importance of these genes in the adaptive response of tomato to spectral quality.

The study of the effect of supplemental green light finds no agronomic benefit to the addition of green LEDs to commercial horticultural lighting and that while

supplemental green light-induced increase biomass and stem elongation in tomato seedlings, in phenotyping to harvest study it did not influence morphology, physiology, biomass or yield in mature plants at harvest. Transcriptomic analysis of global gene expression induced supplemental green light revealed that while Micro-Tom leaf transcriptome had a substantial early-response transcriptional response, over the course of a week this dissipated. Our study found no beneficial effect of supplemental green light on physiology, morphology, photosynthesis or yield, and further research into the relevance of green light for tomato growth should be conducted to inform the horticultural industry on optimization of LED spectra with or without green light.

8 Supplementary Information

8.1 Supplementary data for Chapter 6

8.1.1 Quality assessment of chapter 6 RNA-Seq data

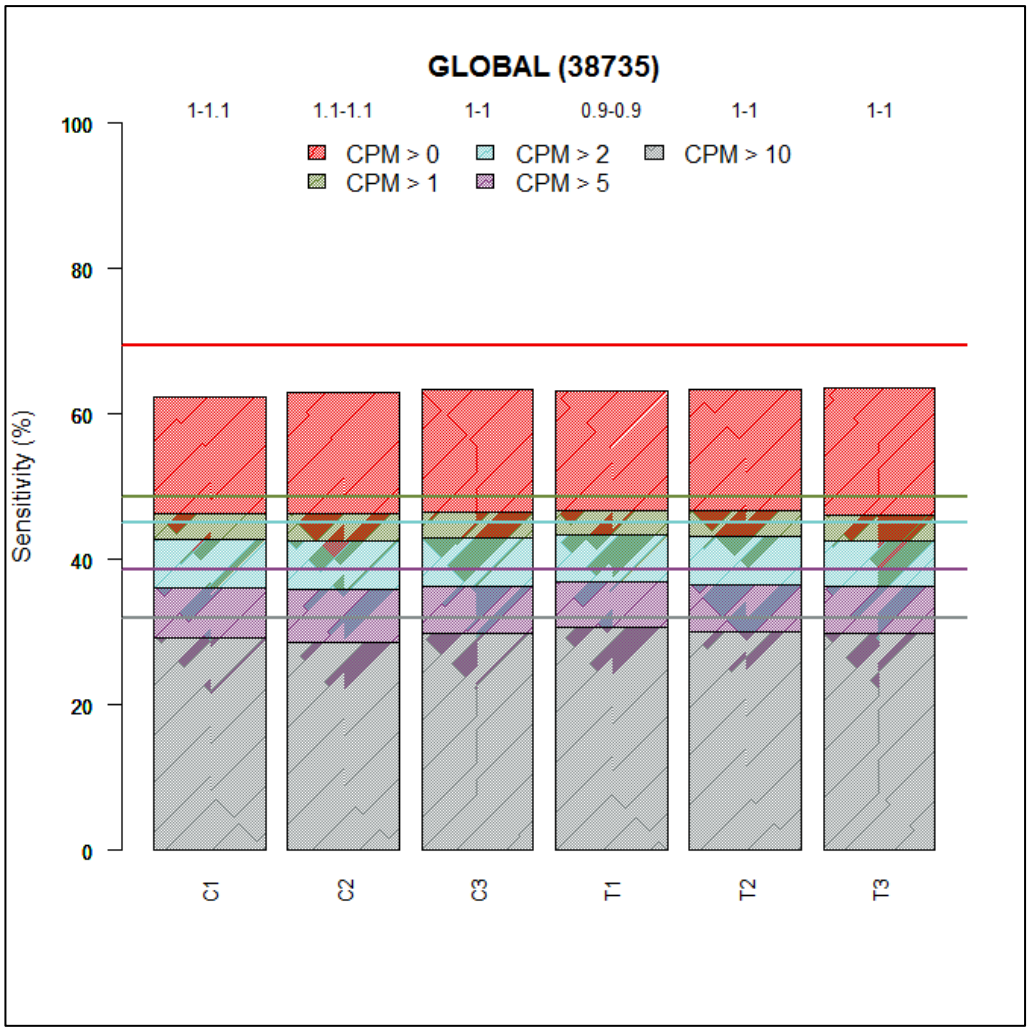


Figure 8-1 Sensitivity plot of normalized unfiltered transcriptome data. Bars on the graph represent each RNA-Seq treatment. Left-hand axis displays percentage sensitivity which is the proportion of genes which are present at different CPM cut-offs. Genes have been assigned into CPM cut-offs of >0, 1,2,5,10 as indicated by the legend. The colored horizontal lines indicate the percentage of genes with those CPM in at least one sample CPM cut-offs. Cut-offs are coloured CPM>0 = red, CPM >1 = green; CPM>2 = blue; CPM>5 = purple; CPM >10 = grey. Global refers to the total number of genes in the genome, and the numbers above each bar on the graph refer to the suggest CPM cut-off that should be employed on data. n=3

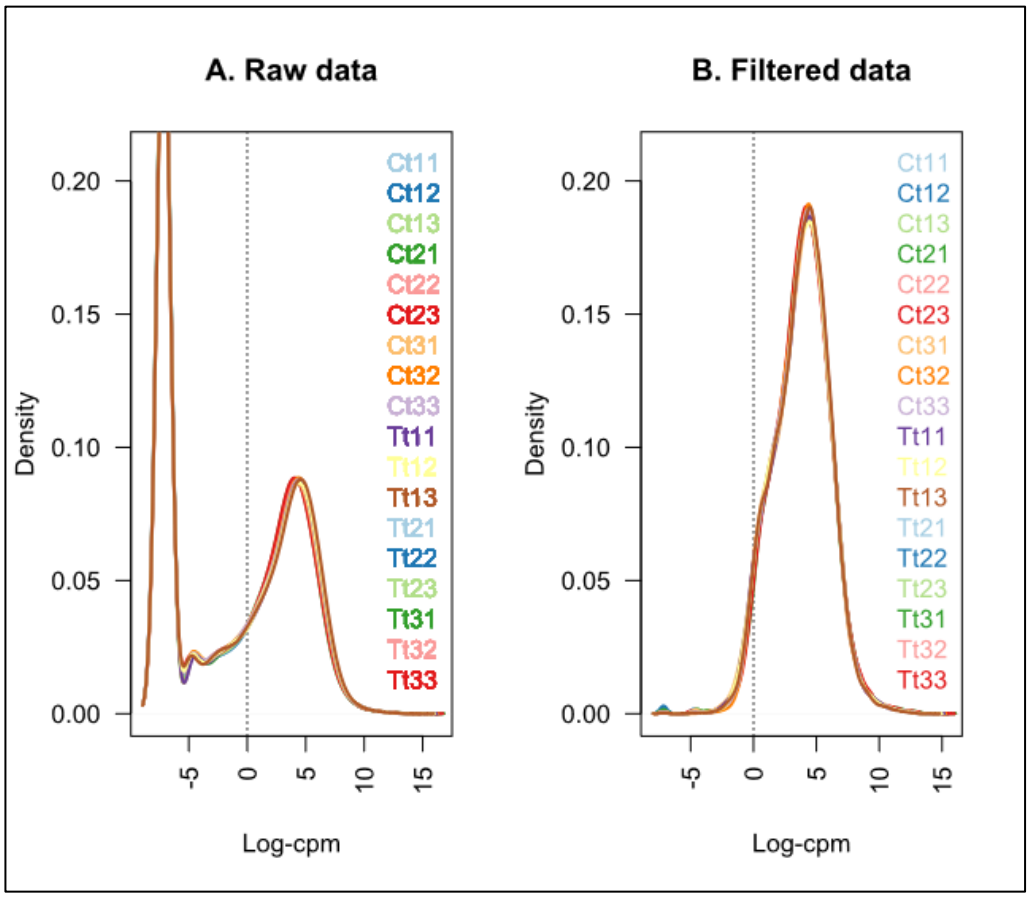


Figure 8-2 Density plot of the effect of filtering genes on log-CPM distribution on RNA-Seq transcriptomes. The density (proportion of genes) that fall within log-CPM bins is displayed for each sample before filtering (a) and after filtering to remove genes with CPM <1 (b). Treatment abbreviated so that T= Treatment and C= control; t1,t2,or t2 represent time-point 3hours, 1day or 7days, respectively; terminal digit 1,2, or 3 represent the biological replicate.

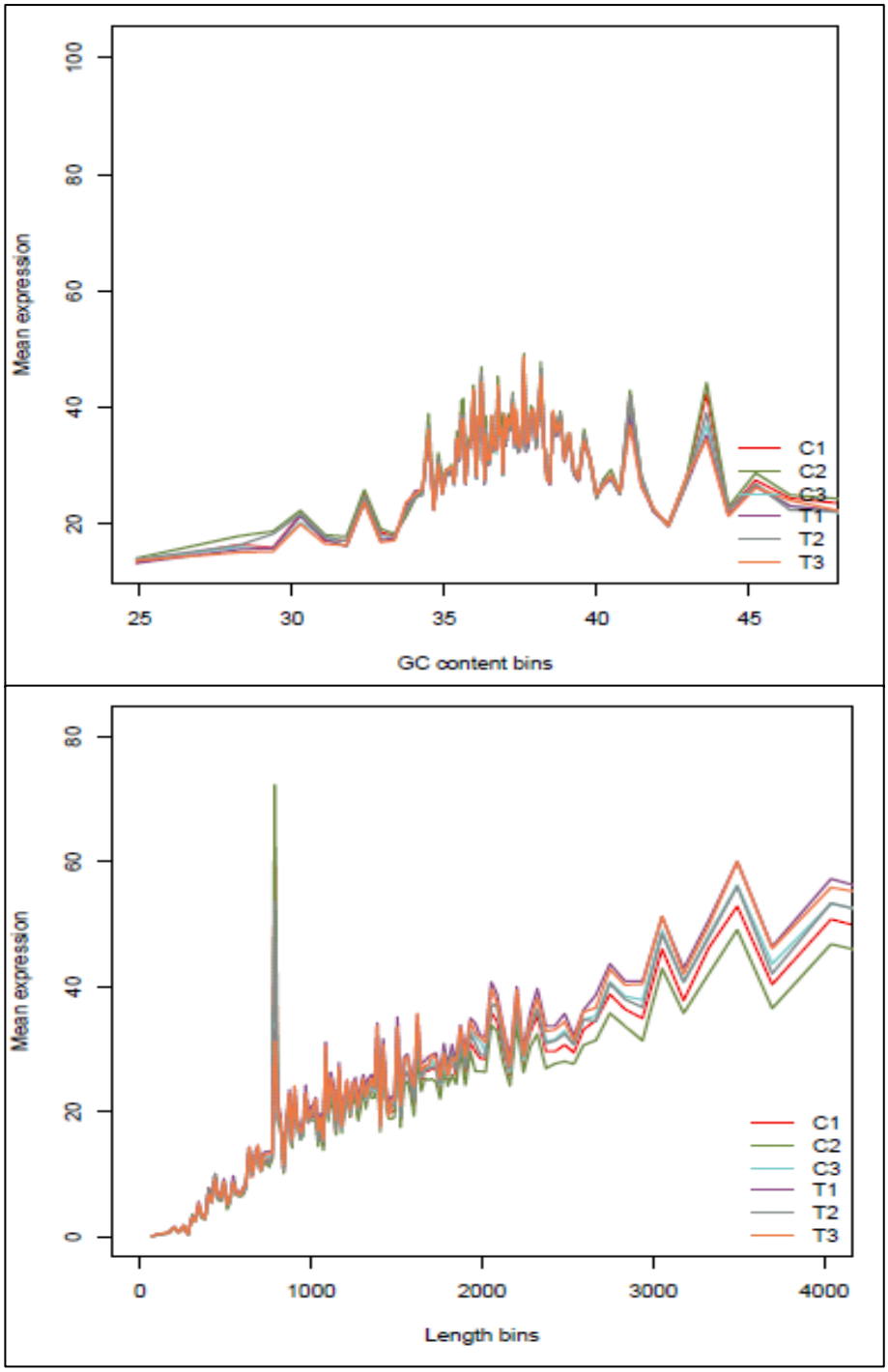


Figure 8-3 Mean expression for compared against GC content and gene length for transcriptomic data. C1= RB_4hour time-point; C2= RB_1day time-point**;** C3= RB_7days time-point; T1= RBG_4hour time-point; T2= RBG_1day time-point**;** T3= RBG_7days time-point**..**

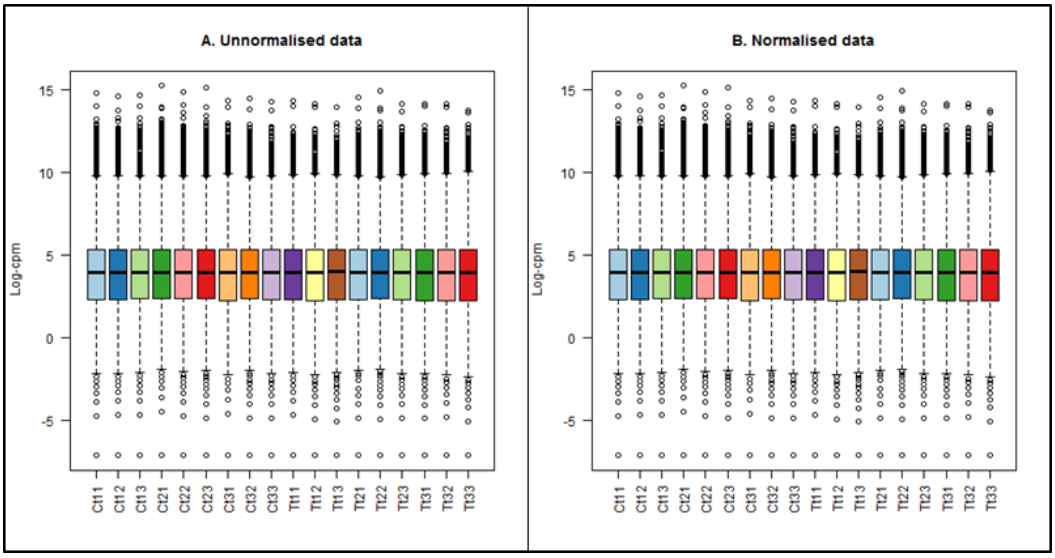


Figure 8-4 Normalization of RNA-Seq count data. Box plots show per sample logCPM distribution of filtered but un-normalized cpm data (a) and after TMM-normalization. Treatment abbreviated so that R=Red; B=Blue; RB= Red/Blue; RBG; Red/Blue/Green; F= Fluorescent. Filtering in EdgeR.

8.1.2 Full gene enrichment tables

Table 8-1 Enriched GO and KEGG terms significantly down-regulated in TvC_4h

ID	P-value	OR	Term
			Biological Process
GO:0009765	7.9E-38	96.2	photosynthesis, light harvesting
GO:0018298	4.8E-28	58.5	protein-chromophore linkage
GO:0006081	7.9E-18	5.1	cellular aldehyde metabolic process
GO:0015979	2.3E-16	14.0	photosynthesis
GO:0019344	5.2E-15	10.3	cysteine biosynthetic process
GO:0010207	5.7E-15	8.1	photosystem II assembly
GO:0006098	1.2E-14	6.8	pentose-phosphate shunt
GO:0009069	5.3E-14	7.2	serine family amino acid metabolic process
GO:0009657	1.1E-13	4.3	plastid organization
GO:0019288	3.9E-13	6.0	isopentenyl diphosphate biosynthetic process..
GO:0046490	6.1E-13	5.9	isopentenyl diphosphate metabolic process
GO:0006733	1.0E-12	4.2	oxidoreduction coenzyme metabolic process
GO:0046496	2.1E-12	4.3	nicotinamide nucleotide metabolic process
GO:0006364	2.3E-12	4.9	rRNA processing
GO:0019684	2.6E-12	11.0	photosynthesis, light reaction
GO:0010114	2.8E-12	19.0	response to red light
GO:0010218	5.2E-12	15.2	response to far red light
GO:0072524	6.6E-12	4.1	pyridine-containing compound metabolic process
GO:0033014	2.6E-11	6.7	tetrapyrrole biosynthetic process
GO:0009773	2.8E-11	17.7	photosynthetic electron transport in photosystem I
GO:0035304	6.5E-11	8.9	regulation of protein dephosphorylation
GO:0009637	1.1E-10	9.3	response to blue light
GO:0015995	1.7E-10	8.3	chlorophyll biosynthetic process
GO:0022900	2.2E-10	7.5	electron transport chain
GO:0042440	4.5E-10	4.1	pigment metabolic process
GO:0019637	3.3E-09	2.4	organophosphate metabolic process
GO:0022613	4.7E-09	3.5	ribonucleoprotein complex biogenesis
GO:0051186	5.8E-09	3.7	cofactor metabolic process
GO:1901135	1.2E-08	2.3	carbohydrate derivative metabolic process
GO:0010027	1.9E-08	4.2	thylakoid membrane organization
GO:0010103	2.6E-08	7.1	stomatal complex morphogenesis
GO:0008299	3.3E-08	4.4	isoprenoid biosynthetic process
GO:0008654	4.6E-08	3.3	phospholipid biosynthetic process
GO:1901607	5.3E-08	3.7	alpha-amino acid biosynthetic process
GO:0016117	5.8E-08	6.1	carotenoid biosynthetic process
GO:0006778	5.8E-08	4.2	porphyrin-containing compound metabolic process
GO:0016108	7.2E-08	6.0	tetraterpenoid metabolic process
GO:0009117	2.5E-07	2.5	nucleotide metabolic process
GO:0016114	2.7E-07	4.8	terpenoid biosynthetic process
GO:0010155	4.1E-07	9.4	regulation of proton transport

ID	P-value	OR	Term
GO:0019220	4.5E-07	4.6	regulation of phosphate metabolic process
GO:0034660	6.8E-07	2.6	ncRNA metabolic process
GO:0006082	7.0E-07	1.9	organic acid metabolic process
GO:0006818	7.8E-07	4.6	hydrogen transport
GO:0055086	8.8E-07	2.3	nucleobase-containing small molecule metabolic process
GO:0006461	9.4E-07	2.6	protein complex assembly
GO:0006636	1.4E-06	9.4	unsaturated fatty acid biosynthetic process
GO:0044255	1.8E-06	2.1	cellular lipid metabolic process
GO:0030003	1.9E-06	6.1	cellular cation homeostasis
GO:0051656	2.0E-06	4.8	establishment of organelle localization
GO:0005975	2.3E-06	1.9	carbohydrate metabolic process
GO:0044802	3.4E-06	2.8	single-organism membrane organization
GO:0044283	3.7E-06	2.1	small molecule biosynthetic process
GO:0019757	3.8E-06	6.3	glycosinolate metabolic process
GO:0009902	4.9E-06	4.7	chloroplast relocation
GO:0051644	4.9E-06	4.7	plastid localization
GO:0034622	6.3E-06	2.3	cellular macromolecular complex assembly
GO:0042548	6.8E-06	46.6	regulation of photosynthesis, light reaction
GO:0055082	1.0E-05	5.1	cellular chemical homeostasis
GO:0008152	1.6E-05	1.7	metabolic process
GO:0051188	2.2E-05	2.6	cofactor biosynthetic process
GO:0019761	2.5E-05	6.3	glucosinolate biosynthetic process
GO:0006546	2.7E-05	10.9	glycine catabolic process
GO:0071555	3.7E-05	2.6	cell wall organization
GO:0019752	7.2E-05	1.7	carboxylic acid metabolic process
GO:0009735	7.9E-05	6.0	response to cytokinin
GO:0072330	8.3E-05	2.6	monocarboxylic acid biosynthetic process
GO:0051049	8.4E-05	4.3	regulation of transport
GO:0015672	8.8E-05	2.9	monovalent inorganic cation transport
GO:0050801	1.0E-04	3.9	ion homeostasis
GO:0043085	1.3E-04	3.6	positive regulation of catalytic activity
GO:0090558	1.6E-04	2.7	plant epidermis development
GO:0022607	2.2E-04	1.9	cellular component assembly
GO:0006073	3.1E-04	2.3	cellular glucan metabolic process
GO:0016311	6.4E-04	2.4	dephosphorylation
GO:0009744	6.5E-04	4.3	response to sucrose
GO:0009595	6.9E-04	9.3	detection of biotic stimulus
GO:0019252	9.2E-04	2.9	starch biosynthetic process
			Molecular Function
GO:0016168	2.1E-33	111.0	chlorophyll binding
GO:0016491	5.0E-06	1.9	oxidoreductase activity
GO:0016630	7.7E-05	Inf	protochlorophyllide reductase activity
GO:0042132	1.0E-04	30.2	fructose 1,6-bisphosphate 1-phosphatase activity
GO:0030599	1.3E-04	6.3	pectinesterase activity
GO:0004553	1.3E-04	2.6	hydrolase activity, hydrolyzing O-glycosyl compounds

ID	P-value	OR	Term
GO:0016984	3.0E-04	67.8	ribulose-bisphosphate carboxylase activity
GO:0009055	3.1E-04	3.2	electron carrier activity
GO:0003824	3.3E-04	1.4	catalytic activity
GO:0016744	5.6E-04	15.1	transferase activity, transferring aldehyde or ketonic groups
GO:0004427	8.5E-04	12.9	inorganic diphosphatase activity
			Cellular Component
GO:0044435	6.7E-38	6.0	plastid part
GO:0009535	2.5E-36	12.9	chloroplast thylakoid membrane
GO:0042651	2.9E-36	12.4	thylakoid membrane
GO:0031984	5.0E-36	7.8	organelle subcompartment
GO:0009523	1.4E-35	93.3	photosystem II
GO:0034357	7.8E-33	98.8	photosynthetic membrane
GO:0009522	2.6E-30	130.3	photosystem I
GO:0009507	1.1E-16	3.5	chloroplast
GO:0009941	3.8E-16	4.8	chloroplast envelope
GO:0009538	1.5E-13	Inf	photosystem I reaction center
GO:0009579	1.5E-12	8.8	thylakoid
GO:0098796	9.1E-11	3.9	membrane protein complex
GO:0009534	1.6E-10	9.7	chloroplast thylakoid
GO:0009570	2.6E-10	3.5	chloroplast stroma
GO:0009654	4.5E-09	23.1	photosystem II oxygen evolving complex
GO:0031967	1.2E-08	2.7	organelle envelope
GO:0031977	5.1E-08	10.6	thylakoid lumen
GO:0005618	1.3E-06	3.6	cell wall
GO:0048046	1.5E-06	4.7	apoplast
GO:0044422	2.3E-06	1.7	organelle part
GO:0005737	5.0E-06	1.7	cytoplasm
GO:0019898	3.6E-05	6.9	extrinsic component of membrane
GO:0098807	1.1E-04	36.3	chloroplast thylakoid membrane protein complex
GO:0010319	2.2E-04	9.1	stromule
			KEGG pathways
00196	4.6E-27	404.3	Photosynthesis - antenna proteins
00195	2.1E-24	40.7	Photosynthesis
01100	3.2E-11	2.8	Metabolic pathways
00860	5.4E-10	11.9	Porphyrin and chlorophyll metabolism
00710	2.8E-07	7.1	Carbon fixation in photosynthetic organisms
00630	1.5E-05	5.5	Glyoxylate and dicarboxylate metabolism
01110	6.1E-05	2.0	Biosynthesis of secondary metabolites
01200	1.8E-04	4.4	Carbon metabolism

Table 8-2 Enriched GO and KEGG terms significantly up-regulated in TvC_4h

ID	P-value	OR	Term
			Biological Process
GO:0071495	4.2E-08	4.7	cellular response to endogenous stimulus
GO:0006468	1.2E-07	2.6	protein phosphorylation
GO:0070887	4.4E-07	3.5	cellular response to chemical stimulus
GO:0030968	7.3E-07	18.3	endoplasmic reticulum unfolded protein response
GO:0006986	1.0E-06	17.3	response to unfolded protein
GO:0035967	1.0E-06	17.3	cellular response to topologically incorrect protein
GO:0044700	2.4E-06	2.6	single organism signalling
GO:0007154	2.7E-06	2.5	cell communication
GO:0009814	4.9E-06	5.7	defense response, incompatible interaction
GO:0031348	2.9E-05	7.6	negative regulation of defense response
GO:2001141	3.2E-05	2.1	regulation of RNA biosynthetic process
GO:0006355	3.2E-05	2.1	regulation of transcription, DNA-templated
GO:0009737	5.1E-05	4.4	response to abscisic acid
GO:0071396	5.5E-05	5.3	cellular response to lipid
GO:0050794	5.6E-05	1.8	regulation of cellular process
GO:0009723	5.8E-05	6.8	response to ethylene
GO:0043069	6.5E-05	10.4	negative regulation of programmed cell death
GO:0071446	7.5E-05	6.6	cellular response to salicylic acid stimulus
GO:0009697	1.1E-04	9.3	salicylic acid biosynthetic process
GO:0000165	1.4E-04	8.9	MAPK cascade
GO:0019219	1.9E-04	1.9	regulation of nucleobase-containing compound metabolic process
GO:0007568	1.9E-04	8.3	aging
GO:0009862	1.9E-04	8.3	Systems acquired resistance, salicylic acid mediated signalling pathway
GO:0002376	1.9E-04	3.2	immune system process
GO:0097659	2.1E-04	1.9	nucleic acid-templated transcription
GO:0006914	2.6E-04	7.8	autophagy
GO:0034050	3.4E-04	5.2	host programmed cell death induced by symbiont
GO:0009873	4.0E-04	9.4	ethylene-activated signalling pathway
GO:0009738	4.9E-04	5.6	abscisic acid-activated signalling pathway
GO:0009889	5.2E-04	1.8	regulation of biosynthetic process
GO:0060255	5.9E-04	1.8	regulation of macromolecule metabolic process
GO:0050776	6.3E-04	4.7	regulation of immune response
GO:0010363	6.7E-04	5.3	regulation of plant-type hypersensitive response
GO:0097306	6.7E-04	5.3	cellular response to alcohol
GO:0008219	7.4E-04	4.1	cell death

ID	P-value	OR	Term
GO:0036211	8.3E-04	1.7	protein modification process
GO:0051707	9.1E-04	2.6	response to other organism
GO:0009755	9.2E-04	3.6	hormone-mediated signalling pathway
			Molecular Function
GO:0003700	9.8E-08	3.2	transcription factor activity, sequence-specific DNA binding
GO:0004672	1.4E-05	2.2	protein kinase activity
GO:0043565	8.0E-05	3.2	sequence-specific DNA binding
			Cellular Component
GO:0005634	7.4E-04	1.9	nucleus
			KEGG
04075	4.7E-06	5.2	Plant hormone signal transduction
04016	2.6E-05	6.1	MAPK signalling

Table 8-3 Enriched terms significantly down-regulated in TvC_1d genes

ID	Pvalue	OR	Term
			Biological Process
GO:0006081	1.4E-29	14.2	cellular aldehyde metabolic process
GO:0046490	3.7E-25	19.1	isopentenyl diphosphate metabolic process
GO:1901135	3.8E-20	6.0	carbohydrate derivative metabolic process
GO:0006098	8.5E-20	16.0	pentose-phosphate shunt
GO:0022613	4.5E-18	9.8	ribonucleoprotein complex biogenesis
GO:0034660	2.8E-16	7.4	ncRNA metabolic process
GO:0046496	1.9E-15	8.8	nicotinamide nucleotide metabolic process
GO:0072524	4.5E-15	8.5	pyridine-containing compound metabolic process
GO:0010027	9.6E-14	10.4	thylakoid membrane organization
GO:0033014	4.9E-13	13.5	tetrapyrrole biosynthetic process
GO:0009657	6.8E-13	8.7	plastid organization
GO:0015995	3.6E-12	16.9	chlorophyll biosynthetic process
GO:0055086	5.7E-12	5.0	nucleobase-containing small molecule metabolic process
GO:0051188	9.1E-12	6.8	cofactor biosynthetic process
GO:0034622	1.5E-11	5.4	cellular macromolecular complex assembly
GO:0044802	2.6E-11	6.7	single-organism membrane organization
GO:0035304	3.1E-11	16.3	regulation of protein dephosphorylation
GO:0009902	4.5E-11	13.6	chloroplast relocation
GO:0051644	4.5E-11	13.6	plastid localization
GO:1901566	8.3E-11	3.7	organonitrogen compound biosynthetic process
GO:0051656	9.4E-11	12.8	establishment of organelle localization
GO:0032787	1.1E-10	4.3	monocarboxylic acid metabolic process
GO:0022607	1.6E-10	4.3	cellular component assembly
GO:0032544	8.3E-10	170.2	plastid translation

ID	Pvalue	OR	Term
GO:0042440	1.0E-09	6.8	pigment metabolic process
GO:0010114	1.6E-09	24.7	response to red light
GO:0044711	2.5E-09	3.0	single-organism biosynthetic process
GO:0044699	3.5E-09	2.6	single-organism process
GO:0051186	6.8E-09	6.3	cofactor metabolic process
GO:0015979	7.2E-09	15.4	photosynthesis
GO:0019684	2.3E-08	13.5	photosynthesis, light reaction
GO:0009773	2.8E-08	21.8	photosynthetic electron transport in photosystem I
GO:0009637	3.9E-08	12.9	response to blue light
GO:0022900	4.5E-08	10.7	electron transport chain
GO:0010103	7.8E-08	11.8	stomatal complex morphogenesis
GO:0009765	1.2E-07	17.3	photosynthesis, light harvesting
GO:0051049	1.7E-07	10.7	regulation of transport
GO:0016311	5.2E-07	5.5	dephosphorylation
GO:0071840	8.7E-07	2.3	cellular component organization or biogenesis
GO:0072596	1.5E-06	15.3	establishment of protein localization to chloroplast
GO:0015672	2.9E-06	5.5	monovalent inorganic cation transport
GO:0032268	1.4E-05	4.4	regulation of cellular protein metabolic process
GO:0045038	2.2E-05	167.2	protein import into chloroplast thylakoid membrane
GO:0034641	6.4E-05	2.0	cellular nitrogen compound metabolic process
GO:0042592	9.3E-05	3.6	homeostatic process
GO:0009987	1.5E-04	2.1	cellular process
GO:0016117	2.4E-04	6.3	carotenoid biosynthetic process
GO:0016108	2.7E-04	6.2	tetraterpenoid metabolic process
GO:0016114	2.9E-04	5.2	terpenoid biosynthetic process
GO:0046777	4.3E-04	6.9	protein autophosphorylation
GO:0045893	4.9E-04	3.6	positive regulation of transcription, DNA-templated
GO:1902680	4.9E-04	3.6	positive regulation of RNA biosynthetic process
GO:0016053	7.7E-04	2.5	organic acid biosynthetic process
GO:0090558	9.5E-04	3.6	plant epidermis development
GO:0045454	9.9E-04	4.3	cell redox homeostasis
			Molecular Function
GO:0003735	1.2E-12	7.1	structural constituent of ribosome
GO:0016168	5.4E-10	27.3	chlorophyll binding
GO:0051540	2.8E-06	8.7	metal cluster binding
GO:0051537	4.9E-05	14.8	2 iron, 2 sulfur cluster binding
			Cellular Component
GO:0009507	1.3E-49	15.4	chloroplast
GO:0042651	1.3E-29	19.2	thylakoid membrane
GO:0031984	5.9E-25	8.9	organelle subcompartment
GO:0009941	2.6E-12	6.5	chloroplast envelope
GO:0031967	1.1E-07	3.8	organelle envelope
GO:0031977	2.6E-07	15.9	thylakoid lumen
GO:0034357	5.4E-07	18.2	photosynthetic membrane

ID	Pvalue	OR	Term
GO:0009654	1.1E-06	24.5	photosystem II oxygen evolving complex
GO:0098796	2.8E-05	3.7	membrane protein complex
GO:0080085	4.3E-04	Inf	signal recognition particle, chloroplast targeting
			KEGG Pathways
03010	1.1E-08	5.6	Ribosome
00196	7.3E-06	16.9	Photosynthesis - antenna proteins
00630	8.7E-06	9.6	Glyoxylate and dicarboxylate metabolism
00195	1.4E-05	10.9	Photosynthesis

Table 8-4 Enriched terms significantly up-regulated in TvC_1d genes

GOBPID	Pvalue	OR	Term
			Biological process
GO:0060147	1.2E-04	183.9	Regulation of posttranscriptional gene silencing
			Molecular Function
NA			
			Cellular Component
NA			
			KEGG Pathways
NA			

Table 8-5 Enriched terms significantly down-regulated in TvC_7d genes

ID	Pvalue	OR	Term
			Biological Process
GO:0009765	7.1E-17	42.9	photosynthesis, light harvesting
GO:0018298	4.1E-16	46.4	protein-chromophore linkage
GO:0045490	1.0E-07	23.7	pectin catabolic process
GO:0015979	1.8E-06	5.0	photosynthesis
GO:0010393	6.7E-06	11.6	galacturonan metabolic process
GO:0071555	1.3E-04	4.3	cell wall organization
GO:0002237	1.8E-04	16.9	response to molecule of bacterial origin
GO:0005975	5.3E-04	2.4	carbohydrate metabolic process
			Molecular Function
GO:0016168	1.4E-16	51.1	chlorophyll binding
GO:0030599	7.4E-06	15.2	pectinesterase activity
GO:0030570	1.3E-05	38.8	pectate lyase activity
GO:0016787	1.6E-05	2.2	hydrolase activity
GO:0045330	1.4E-04	18.3	aspartyl esterase activity
GO:0004857	4.6E-04	6.7	enzyme inhibitor activity
GO:0004553	8.9E-04	3.6	hydrolase activity, hydrolyzing O-glycosyl compounds
			Cellular Component
GO:0009522	9.5E-15	43.6	photosystem I
GO:0009523	3.5E-14	30.5	photosystem II
GO:0005618	6.4E-08	9.2	cell wall
GO:0034357	1.5E-07	7.0	photosynthetic membrane
GO:0098796	6.4E-07	5.7	membrane protein complex
GO:0016021	5.7E-06	3.0	integral component of membrane
GO:0005576	5.9E-06	6.3	extracellular region
GO:0031224	3.7E-04	13.8	intrinsic component of membrane
			KEGG Pathways
00196	5.2E-14	75.7	Photosynthesis - antenna proteins
00040	5.0E-05	15.6	Pentose and glucuronate interconversions
00901	3.3E-04	30.0	Indole alkaloid biosynthesis

Table 8-6 Enriched terms significantly up-regulated in TvC_7d genes

GOBPID	Pvalue	OR	Term
			Biological Process
GO:0072593	4.4E-05	25.5	reactive oxygen species metabolic process
			Molecular Function
NA			
			Cellular Component
NA			
			KEGG Pathways
NA			

8.2 RNA-Seq (Chapter 4)

8.2.1 Quality assessment of RNA-Seq data

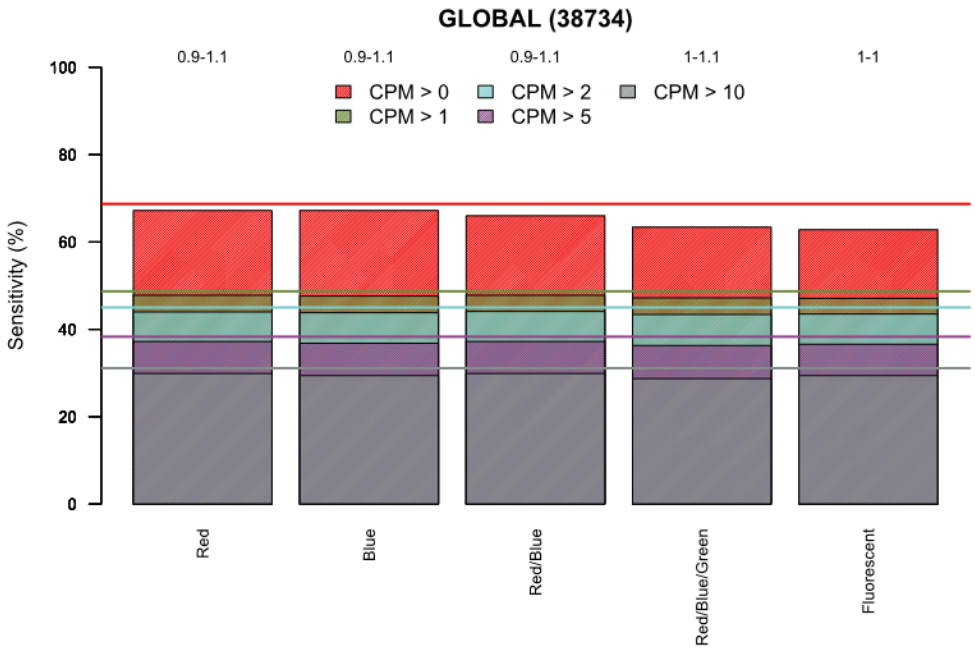


Figure 8-5 Sensitivity plot of % genes which fall into different count per million (CPM) ranges in RNA-Seq samples from Micro-Tom grown under different spectral qualities. Bars on the graph represent each RNA-Seq treatment. Left-hand axis displays percentage sensitivity which is the proportion of genes which are present at different CPM cut-offs. Genes have been assigned into CPM cut-offs of >0, 1,2,5,10 as indicated by the legend. The coloured horizontal lines indicate the percentage of genes with those CPM in at least one sample CPM cut-offs. Cut-offs are coloured CPM>0 = red, CPM >1 = green; CPM>2 = blue; CPM>5 = purple; CPM >10 = grey. Global refers to the total number of genes in the genome, and the numbers above each bar on the graph refer to the suggest CPM cut-off that should be employed on data. n=3.

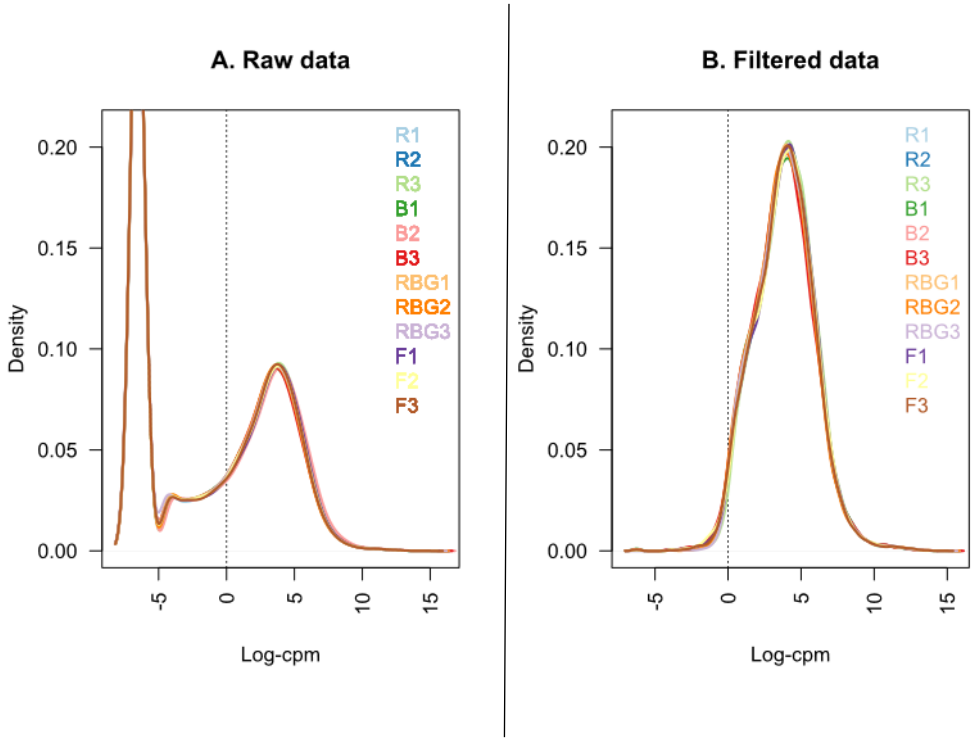


Figure 8-6 Effect of filtering on the log-CPM distribution of RNA-Seq samples from Micro-Tom grown under different spectral qualities. The density (proportion of genes) that fall within log-CPM bins is displayed for each sample before filtering (a) and after filtering to remove genes with CPM <1 (b). Treatment abbreviated so that R=Red; B=Blue; RB= Red/Blue; RBG; Red/Blue/Green; F= Fluorescent. Filtering in EdgeR.

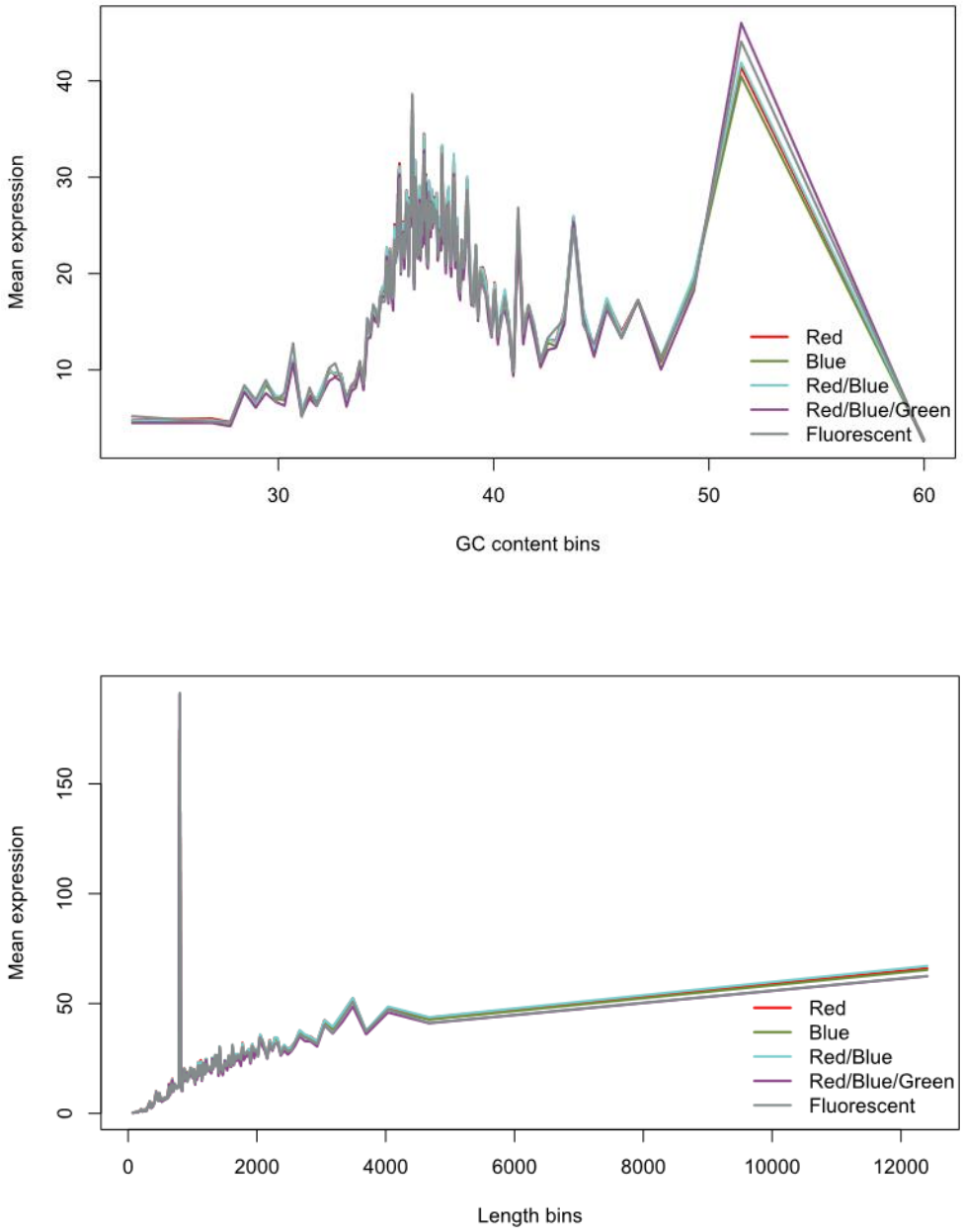


Figure 8-7 GC and length Bias in RNA-Seq samples from Micro-Tom grown under different spectral qualities. Top panel graph displays the mean expression of genes against GC content for reach treatment; bottom panel graph displays mean an expression of genes against gene length for each treatment. Each treatment n=3 samples. *Solanum lycopersicum* genome v2.5 was used for GC length and GC content annotation.

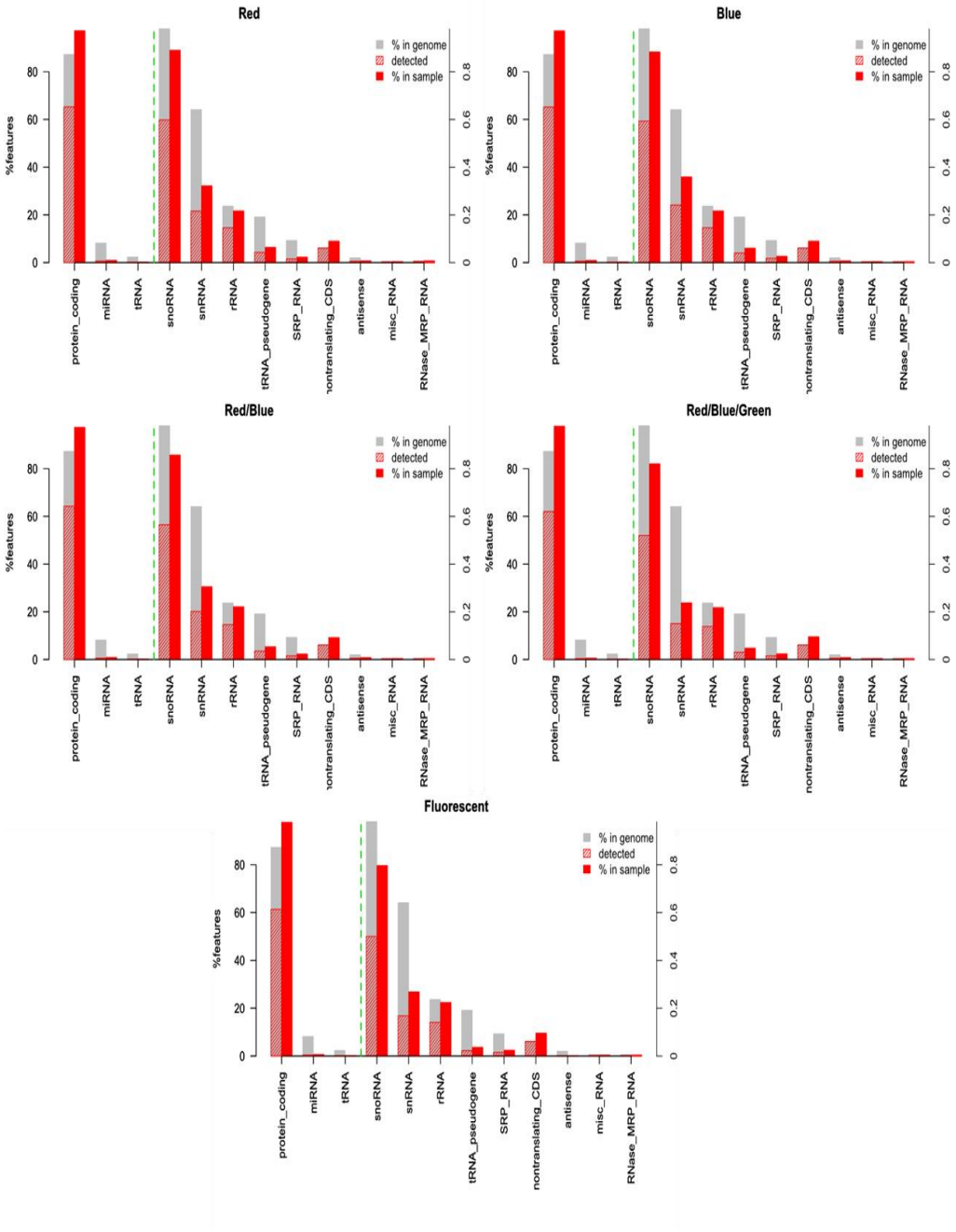


Figure 8-8 Biotype detection of RNA-Seq samples from Micro-Tom leaves grown under different spectral qualities. Grey bar indicates % of features annotated to each biotype in the genome, the striped bar is the % each biotype detected in the treatment, the solid coloured bar is the percentage of total counts assigned to each biotype. The solid grey and solid red bars are identical between treatments. The green vertical line separates the most abundant biotypes (with left-hand of the line corresponding to the left axis scale) from the rest (on right-hand of the dotted line, corresponding to the right axis). Both the left and right-axis are %features detected, where feature means gene. *Solanum lycopersicum* genome v2.5 was used for biotype annotation.

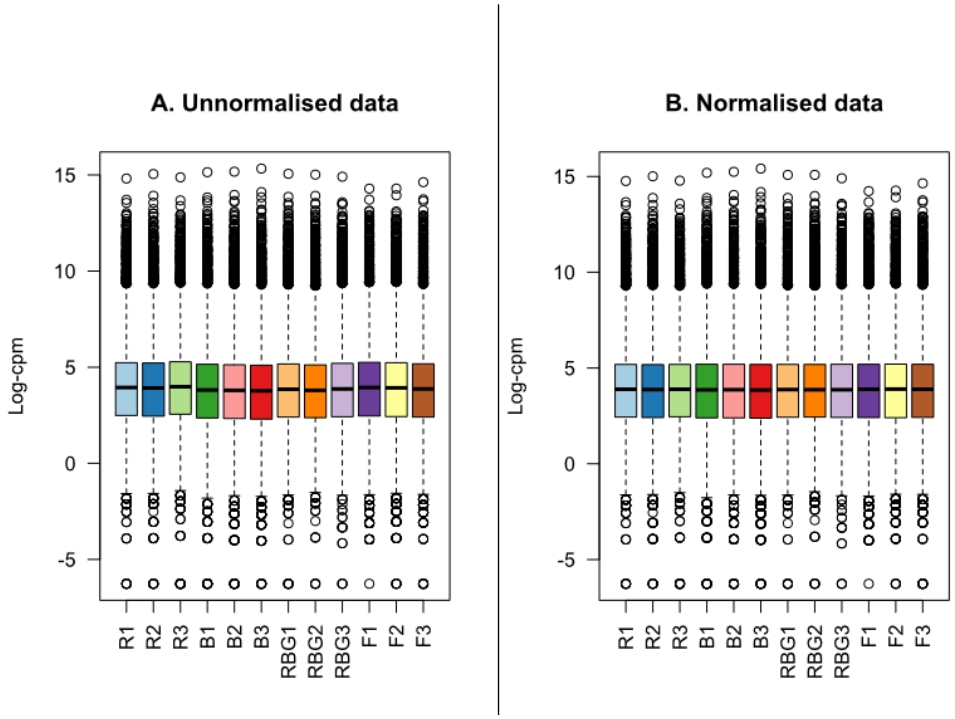


Figure 8-9 Effect of normalization on the log-CPM distribution of RNA-Seq samples from Micro-Tom grown under different spectral qualities. Box plots show per sample logCPM distribution of filtered but un-normalized cpm data (a) and after TMM-normalization. Treatment abbreviated so that R=Red; B=Blue; RB= Red/Blue; RBG; Red/Blue/Green; F= Fluorescent. Filtering in EdgeR.

8.2.2 Full gene enrichment tables

Table 8-7 RvB up-regulated gene functional enrichment

ID	P-value	O/R	Term
		Biological process	
GO:0006468	3.50E-26	2.85	protein phosphorylation
GO:0036211	4.68E-11	1.74	protein modification process
GO:0007154	1.13E-08	1.94	cell communication
GO:0006796	5.08E-08	1.58	phosphate-containing compound metabolic process
GO:0048544	1.40E-06	5.86	recognition of pollen
GO:0044700	1.02E-05	1.73	single organism signalling
GO:0009627	1.88E-04	3.13	systemic acquired resistance
GO:0043069	2.02E-04	5.05	negative regulation of programmed cell death
GO:0009751	3.34E-04	3.23	response to salicylic acid
GO:0010200	3.67E-04	4.59	response to chitin
GO:0009867	3.88E-04	3.55	jasmonic acid mediated signalling pathway
GO:0031348	4.78E-04	3.46	negative regulation of defense response
GO:0009863	5.36E-04	3.22	salicylic acid mediated signalling pathway
GO:0009696	6.31E-04	4.21	salicylic acid metabolic process
GO:0046189	6.31E-04	4.21	phenol-containing compound biosynthetic process
GO:0030968	6.39E-04	5.38	endoplasmic reticulum unfolded protein response
GO:0010941	8.20E-04	2.79	regulation of cell death
GO:0071229	8.38E-04	2.19	cellular response to acid chemical
GO:0035556	8.38E-04	1.86	intracellular signal transduction
GO:0006986	8.83E-04	5.04	response to unfolded protein
GO:0035967	8.83E-04	5.04	cellular response to topologically incorrect protein
GO:0010363	9.20E-04	3.01	regulation of plant-type hypersensitive response
		Molecular function	
GO:0004674	1.87E-19	3.32	protein serine/threonine kinase activity
GO:0016772	2.00E-14	2.01	transferase activity, transferring phosphorus…
GO:0005524	2.99E-10	1.68	ATP binding
GO:0043168	4.56E-09	1.54	anion binding
GO:0030554	6.87E-09	1.59	adenyl nucleotide binding
GO:0032555	1.71E-08	1.55	purine ribonucleotide binding
GO:0097367	6.93E-08	1.51	carbohydrate derivative binding
GO:0004672	6.68E-07	2.04	protein kinase activity
GO:0003824	1.91E-05	1.30	catalytic activity
GO:0000166	8.77E-05	1.33	nucleotide binding
GO:0015369	3.57E-04	38.75	calcium:proton antiporter activity
GO:0015276	3.79E-04	9.70	ligand-gated ion channel activity
GO:0005057	3.92E-04	5.98	signal transducer activity…
GO:0008289	4.36E-04	2.60	lipid binding
GO:0099600	4.79E-04	4.42	transmembrane receptor activity
GO:0004707	5.26E-04	6.79	MAP kinase activity
GO:0015085	7.97E-04	5.18	calcium ion transmembrane transporter activity

ID	P-value	O/R	Term
		Cellular compartment	
GO:0016021	2.18E-13	2.12	integral component of membrane
GO:0044425	4.62E-09	1.78	membrane part
GO:0005886	1.30E-04	1.80	plasma membrane
GO:0005783	1.87E-04	2.08	endoplasmic reticulum
		KEGG pathway	
04075	4.66E-10	3.95	Plant hormone signal transduction
04626	1.49E-09	4.93	Plant-pathogen interaction
04016	1.58E-08	4.61	MAPK signalling pathway - Plant
00905	4.86E-04	13.13	Brassinosteroid biosynthesis

Table 8-8 RvB down-regulated gene functional enrichment

ID	P-value	O/R	Term
			Biological process
GO:0010027	1.87E-40	10.88	thylakoid membrane organization
GO:0044802	1.72E-36	8.56	single-organism membrane organization
GO:0042440	2.22E-29	6.31	pigment metabolic process
GO:0006081	8.09E-29	5.05	cellular aldehyde metabolic process
GO:0019288	1.04E-28	8.36	isopentenyl diphosphate biosynthetic process, methylerythritol 4-phosphate pathway
GO:0046490	3.31E-28	8.10	isopentenyl diphosphate metabolic process
GO:0051644	2.27E-26	13.62	plastid localization
GO:0034660	1.19E-22	5.31	ncRNA metabolic process
GO:0019252	5.41E-20	7.22	starch biosynthetic process
GO:0006364	2.73E-19	4.83	rRNA processing
GO:0010207	1.53E-18	7.02	photosystem II assembly
GO:0042793	1.19E-17	12.20	transcription from plastid promoter
GO:0019637	8.05E-17	2.41	organophosphate metabolic process
GO:0000023	9.29E-17	7.32	maltose metabolic process
GO:0009657	2.08E-15	6.99	plastid organization
GO:0006733	2.53E-15	3.45	oxidoreduction coenzyme metabolic process
GO:0006082	3.01E-14	2.42	organic acid metabolic process
GO:0006778	7.25E-14	4.50	porphyrin-containing compound metabolic process
GO:0055114	1.44E-13	2.01	oxidation-reduction process
GO:0072524	2.65E-13	3.29	pyridine-containing compound metabolic process
GO:0044255	5.78E-13	2.17	cellular lipid metabolic process
GO:0022613	7.03E-13	3.24	ribonucleoprotein complex biogenesis
GO:0009311	8.52E-13	4.48	oligosaccharide metabolic process
GO:1901135	4.07E-11	2.10	carbohydrate derivative metabolic process
GO:0006655	1.35E-10	9.91	phosphatidylglycerol biosynthetic process
GO:0032787	1.36E-10	2.11	monocarboxylic acid metabolic process
GO:0016226	1.57E-10	5.31	iron-sulfur cluster assembly
GO:0016556	6.42E-10	5.31	mRNA modification
GO:0010155	1.72E-09	9.49	regulation of proton transport
GO:0035304	1.93E-09	5.67	regulation of protein dephosphorylation
GO:0010114	2.23E-09	10.34	response to red light
GO:0055086	2.25E-09	2.13	nucleobase-containing small molecule metabolic process
GO:0009073	2.92E-09	5.52	aromatic amino acid family biosynthetic process
GO:0009637	7.88E-09	5.70	response to blue light
GO:0044711	9.22E-09	2.09	single-organism biosynthetic process
GO:0009965	1.37E-08	4.12	leaf morphogenesis
GO:0016053	1.99E-08	2.07	organic acid biosynthetic process
GO:0045893	5.20E-08	2.75	positive regulation of transcription, DNA-templated
GO:0006636	1.03E-07	8.45	unsaturated fatty acid biosynthetic process
GO:0006546	1.04E-07	13.50	glycine catabolic process
GO:0072598	1.25E-07	7.43	protein localization to chloroplast
GO:0045036	1.25E-07	7.43	protein targeting to chloroplast

ID	P-value	O/R	Term
GO:0019757	3.02E-07	5.36	glycosinolate metabolic process
GO:0009069	3.11E-07	3.26	serine family amino acid metabolic process
GO:0051186	1.29E-06	2.39	cofactor metabolic process
GO:0015979	1.35E-06	3.85	photosynthesis
GO:0006461	1.57E-06	2.08	protein complex assembly
GO:0043085	2.26E-06	3.38	positive regulation of catalytic activity
GO:0044262	2.40E-06	1.97	cellular carbohydrate metabolic process
GO:0006818	5.24E-06	3.10	hydrogen transport
GO:0046173	5.64E-06	5.80	polyol biosynthetic process
GO:0043038	6.24E-06	4.31	amino acid activation
GO:0015672	7.58E-06	2.49	monovalent inorganic cation transport
GO:0006766	8.54E-06	4.18	vitamin metabolic process
GO:0044710	1.05E-05	1.73	single-organism metabolic process
GO:0005976	1.69E-05	1.85	polysaccharide metabolic process
GO:1901617	2.24E-05	2.42	organic hydroxy compound biosynthetic process
GO:0044283	2.72E-05	2.76	small molecule biosynthetic process
GO:0009695	3.59E-05	5.55	jasmonic acid biosynthetic process
GO:0051049	5.69E-05	3.33	regulation of transport
GO:0009106	5.75E-05	7.85	lipoate metabolic process
GO:0022900	6.15E-05	3.07	electron transport chain
GO:0071214	8.03E-05	3.71	cellular response to abiotic stimulus
GO:0048367	8.53E-05	1.66	shoot system development
GO:0000096	8.80E-05	2.33	sulfur amino acid metabolic process
GO:0065009	1.34E-04	2.26	regulation of molecular function
GO:0006725	1.70E-04	1.28	cellular aromatic compound metabolic process
GO:1901657	2.23E-04	2.59	glycosyl compound metabolic process
GO:0033015	3.12E-04	3.79	tetrapyrrole catabolic process
GO:0051187	3.12E-04	3.79	cofactor catabolic process
GO:0051606	3.82E-04	4.32	detection of stimulus
GO:0030091	4.02E-04	7.84	protein repair
GO:0055080	7.61E-04	2.67	cation homeostasis
GO:1901564	8.56E-04	1.35	organonitrogen compound metabolic process
GO:0046777	9.13E-04	2.95	protein autophosphorylation
			Molecular function
GO:0003824	2.72E-11	1.56	catalytic activity
GO:0016705	5.60E-11	2.88	oxidoreductase activity, acting on paired donors, with incorporation or reduction of molecular oxygen
GO:0004497	4.36E-10	3.44	monooxygenase activity
GO:0005506	6.51E-10	2.87	iron ion binding
GO:0016491	2.23E-08	1.96	oxidoreductase activity
GO:0061135	4.26E-07	7.68	endopeptidase regulator activity
GO:0004812	5.53E-07	5.28	aminoacyl-tRNA ligase activity
GO:0016829	1.71E-06	2.43	lyase activity
GO:0048037	2.93E-06	1.92	cofactor binding
GO:0020037	8.21E-06	2.26	heme binding

ID	P-value	O/R	Term
GO:0051536	1.07E-05	3.27	iron-sulfur cluster binding
GO:0008236	9.50E-05	2.30	serine-type peptidase activity
GO:0000996	2.04E-04	21.82	core DNA-dependent RNA polymerase binding promoter specificity activity
GO:0050660	2.16E-04	2.51	flavin adenine dinucleotide binding
GO:0016627	2.24E-04	3.26	oxidoreductase activity, acting on the CH-CH group of donors
GO:0015297	3.32E-04	2.78	antiporter activity
GO:0015103	3.81E-04	3.89	inorganic anion transmembrane transporter activity
GO:0001053	5.18E-04	34.88	plastid sigma factor activity
GO:0015238	5.54E-04	3.45	drug transmembrane transporter activity
GO:0015291	5.84E-04	3.66	secondary active transmembrane transporter activity
GO:0016667	6.93E-04	2.39	oxidoreductase activity, acting on a sulfur group of donors
GO:0016701	9.16E-04	3.70	oxidoreductase activity, acting on single donors with incorporation of molecular oxygen
			Cellular compartment
GO:0009507	3.16E-77	6.47	chloroplast
GO:0031984	2.39E-22	3.95	organelle subcompartment
GO:0005737	9.98E-22	2.16	cytoplasm
GO:0042651	5.98E-21	5.44	thylakoid membrane
GO:0031967	7.54E-21	3.32	organelle envelope
GO:0043231	1.15E-16	1.96	intracellular membrane-bounded organelle
GO:0009579	3.69E-16	8.51	thylakoid
GO:0044422	5.82E-14	1.88	organelle part
GO:0043596	1.52E-05	Inf	nuclear replication fork
GO:0009295	1.57E-05	7.01	nucleoid
GO:0009508	3.95E-05	14.44	plastid chromosome
GO:0005622	2.85E-04	1.38	intracellular
GO:0048046	4.44E-04	2.57	apoplast
			KEGG pathway
01110	1.98E-14	2.83	Biosynthesis of secondary metabolites
01100	3.82E-09	2.03	Metabolic pathways
00630	2.20E-08	6.21	Glyoxylate and dicarboxylate metabolism
00710	3.67E-07	5.55	Carbon fixation in photosynthetic organisms
00906	9.11E-07	7.93	Carotenoid biosynthesis
00260	2.15E-05	4.01	Glycine, serine and threonine metabolism
00941	3.88E-05	8.14	Flavonoid biosynthesis
01200	1.61E-04	3.61	Carbon metabolism

Table 8-9 RvRBG up-regulated functional enrichment

ID	P value	O/R	Term
			Biological process
GO:0006468	9.71E-20	2.70	protein phosphorylation

GO:0036211	6.53E-09	1.72	protein modification process
GO:0006796	1.03E-07	1.63	phosphate-containing compound metabolic process
GO:0071495	5.17E-05	2.34	cellular response to endogenous stimulus
GO:0009755	2.02E-04	2.22	hormone-mediated signalling pathway
GO:0010411	3.57E-04	6.90	xyloglucan metabolic process
GO:0009826	4.85E-04	2.91	unidimensional cell growth
GO:0048589	5.47E-04	2.20	developmental growth
GO:0071555	5.85E-04	2.06	cell wall organization
GO:0007154	7.35E-04	1.55	cell communication
GO:0030243	7.64E-04	2.88	cellulose metabolic process
			Molecular function
GO:0016772	1.05E-12	2.03	transferase activity, transferring phosphorus-containing groups
GO:0004672	4.62E-11	2.66	protein kinase activity
GO:0004674	5.04E-11	2.68	protein serine/threonine kinase activity
GO:0030554	1.45E-06	1.53	adenyl nucleotide binding
GO:0032555	2.47E-06	1.49	purine ribonucleotide binding
GO:0005524	2.64E-06	1.53	ATP binding
GO:0097367	8.72E-06	1.46	carbohydrate derivative binding
GO:0043168	2.18E-05	1.41	anion binding
GO:0003824	5.50E-05	1.31	catalytic activity
GO:0099600	4.24E-04	4.86	transmembrane receptor activity
GO:0016762	8.26E-04	5.78	xyloglucan:xyloglucosyl transferase activity
			Cellular compartment
GO:0016021	9.73E-13	2.15	integral component of membrane
GO:0016020	1.05E-10	1.99	membrane
GO:0005886	1.13E-06	2.17	plasma membrane
GO:0046658	1.04E-05	11.12	anchored component of plasma membrane
GO:0031224	1.97E-05	5.83	intrinsic component of membrane
GO:0005618	5.96E-05	2.72	cell wall
GO:0071944	2.06E-04	2.59	cell periphery
			KEGG pathway
04075	7.05E-06	3.23	Plant hormone signal transduction
04016	8.26E-04	3.02	MAPK signalling pathway - Plant

Table 8-10 RvRBG down-regulated genes functional enrichment

ID	Pvalue	O/R	Term
			Biological process
GO:0055114	5.04E-15	2.17	oxidation-reduction process
GO:0018298	1.26E-09	8.84	protein-chromophore linkage
GO:0009765	3.43E-09	8.07	photosynthesis, light harvesting
GO:0046173	3.99E-08	8.56	polyol biosynthetic process
GO:0010264	1.40E-07	9.52	myo-inositol hexakisphosphate biosynthetic process
GO:0042440	2.40E-07	2.78	pigment metabolic process
GO:0043647	1.06E-05	5.55	inositol phosphate metabolic process
GO:0008152	3.78E-05	1.43	metabolic process
GO:0010224	6.69E-05	6.01	response to UV-B
GO:0016117	1.14E-04	3.29	carotenoid biosynthetic process
GO:0016108	1.38E-04	3.23	tetraterpenoid metabolic process
GO:0016114	1.76E-04	2.66	terpenoid biosynthetic process
GO:0009637	2.67E-04	3.50	response to blue light
GO:0006778	3.27E-04	2.36	porphyrin-containing compound metabolic process
GO:0015995	3.60E-04	3.20	chlorophyll biosynthetic process
GO:0010155	4.46E-04	4.44	regulation of proton transport
GO:0019684	5.11E-04	2.16	photosynthesis, light reaction
GO:0031408	5.96E-04	5.44	oxylipin biosynthetic process
GO:0043085	6.15E-04	2.67	positive regulation of catalytic activity
GO:0009069	6.98E-04	2.42	serine family amino acid metabolic process
GO:0042493	7.03E-04	3.50	response to drug
GO:0006855	7.03E-04	3.50	drug transmembrane transport
GO:1901617	8.11E-04	2.16	organic hydroxy compound biosynthetic process
GO:0044283	8.42E-04	1.56	small molecule biosynthetic process
GO:0006546	8.90E-04	5.94	glycine catabolic process
GO:0009658	8.98E-04	2.10	chloroplast organization
			Molecular function
GO:0016705	6.40E-13	4.06	oxidoreductase activity, acting on paired donors..
GO:0004497	2.87E-11	3.90	monooxygenase activity
GO:0016168	2.68E-10	10.06	chlorophyll binding
GO:0005506	3.66E-10	3.06	iron ion binding
GO:0020037	3.49E-09	2.98	heme binding
GO:0016491	3.07E-06	1.73	oxidoreductase activity
GO:0003824	2.76E-05	1.34	catalytic activity
GO:0016706	3.81E-05	3.21	oxidoreductase activity, acting on paired donors..
GO:0003700	7.28E-05	1.76	transcription factor activity, sequence-specific DNA binding
GO:0004866	1.46E-04	5.27	endopeptidase inhibitor activity
GO:0061134	1.46E-04	5.27	peptidase regulator activity
GO:0016701	2.17E-04	4.46	oxidoreductase activity, acting on single donors with incorporation of molecular oxygen
GO:0048037	2.26E-04	1.74	cofactor binding
GO:0016628	2.38E-04	6.48	oxidoreductase activity, acting on the CH-CH group of donors, NAD or NADP as acceptor

ID	Pvalue	O/R	Term
GO:0016758	2.53E-04	1.88	transferase activity, transferring hexosyl groups
GO:0010277	2.69E-04	41.97	chlorophyllide a oxygenase [overall] activity
GO:0015297	3.85E-04	2.90	antiporter activity
GO:0015238	4.38E-04	3.72	drug transmembrane transporter activity
GO:0016829	8.70E-04	1.96	lyase activity
Cellular compartment			
GO:0044435	1.46E-09	2.32	plastid part
GO:0009507	2.40E-08	2.10	chloroplast
GO:0009523	3.56E-08	6.21	photosystem II
GO:0009941	6.41E-07	2.61	chloroplast envelope
GO:0044436	1.07E-05	2.40	thylakoid part
GO:0031984	6.99E-05	2.08	organelle sub-compartment
GO:0009535	7.05E-05	2.57	chloroplast thylakoid membrane
GO:0042651	2.11E-04	2.33	thylakoid membrane
GO:0031967	2.17E-04	1.85	organelle envelope
GO:0009534	3.29E-04	3.77	chloroplast thylakoid
GO:0009522	7.37E-04	3.65	photosystem I
GO:0009579	7.99E-04	3.16	thylakoid
KEGG pathway			
01110	3.09E-09	2.38	Biosynthesis of secondary metabolites
00196	8.75E-08	11.89	Photosynthesis - antenna proteins
01100	7.46E-07	1.88	Metabolic pathways
00941	9.84E-05	7.80	Flavonoid biosynthesis
00904	1.33E-04	12.80	Diterpenoid biosynthesis
00100	3.30E-04	6.13	Steroid biosynthesis

Table 8-11 BvRBG up-regulated genes functional enrichment

ID	Pvalue	O/R	Term
			Biological process
GO:0010027	7.25E-17	6.09	thylakoid membrane organization
GO:0044802	1.42E-14	5.05	single-organism membrane organization
GO:0009658	1.02E-12	7.11	chloroplast organization
GO:0006081	1.30E-10	3.31	cellular aldehyde metabolic process
GO:0006364	6.62E-10	3.81	rRNA processing
GO:0042793	3.37E-09	7.44	transcription from plastid promoter
GO:0016556	1.35E-08	5.80	mRNA modification
GO:0019288	2.25E-08	3.97	isopentenyl diphosphate biosynthetic process…
GO:0046490	3.19E-08	3.89	isopentenyl diphosphate metabolic process
GO:0015979	4.49E-08	2.78	photosynthesis
GO:0019252	4.86E-08	4.36	starch biosynthetic process
GO:0045893	1.17E-07	3.20	positive regulation of transcription, DNA-templated
GO:1902680	1.17E-07	3.20	positive regulation of RNA biosynthetic process
GO:0051644	2.57E-07	4.91	plastid localization
GO:0009902	2.57E-07	4.91	chloroplast relocation
GO:0045935	3.28E-07	3.03	positive regulation of nucleobase-containing compound metabolic process
GO:0000023	3.72E-07	4.52	maltose metabolic process
GO:0006073	5.56E-07	2.75	cellular glucan metabolic process
GO:0051656	6.15E-07	4.58	establishment of organelle localization
GO:0034660	6.76E-07	3.04	ncRNA metabolic process
GO:0022613	8.21E-07	2.74	ribonucleoprotein complex biogenesis
GO:0051186	1.01E-06	2.10	cofactor metabolic process
GO:0010207	1.48E-06	3.90	photosystem II assembly
GO:0006098	1.54E-06	3.48	pentose-phosphate shunt
GO:0008152	3.97E-06	1.60	metabolic process
GO:0009891	4.45E-06	2.64	positive regulation of biosynthetic process
GO:0071478	4.51E-06	8.42	cellular response to radiation
GO:0072598	4.93E-06	7.16	protein localization to chloroplast
GO:0045036	4.93E-06	7.16	protein targeting to chloroplast
GO:0006399	4.97E-06	3.13	tRNA metabolic process
GO:0008299	6.76E-06	2.50	isoprenoid biosynthetic process
GO:0005976	9.60E-06	2.14	polysaccharide metabolic process
GO:0010604	1.09E-05	2.52	positive regulation of macromolecule metabolic process
GO:0044711	1.11E-05	1.58	single-organism biosynthetic process
GO:0006655	1.27E-05	6.30	phosphatidylglycerol biosynthetic process
GO:0008654	1.91E-05	2.44	phospholipid biosynthetic process
GO:0042440	4.99E-05	2.51	pigment metabolic process
GO:0009311	5.04E-05	2.97	oligosaccharide metabolic process
GO:0009965	5.27E-05	3.44	leaf morphogenesis
GO:0009657	8.09E-05	3.45	plastid organization
GO:0009584	8.99E-05	56.81	detection of visible light
GO:0016226	9.52E-05	3.59	iron-sulfur cluster assembly

ID	Pvalue	O/R	Term
GO:0006796	9.73E-05	1.46	phosphate-containing compound metabolic process
GO:0044262	1.68E-04	1.95	cellular carbohydrate metabolic process
GO:0044281	1.98E-04	1.46	small molecule metabolic process
GO:0009585	2.38E-04	14.22	red, far-red light phototransduction
GO:0071489	2.45E-04	9.49	cellular response to red or far red light
GO:0033013	2.72E-04	2.59	tetrapyrrole metabolic process
GO:0015994	5.50E-04	2.74	chlorophyll metabolic process
GO:0009733	6.51E-04	2.53	response to auxin
GO:0009582	6.68E-04	10.15	detection of abiotic stimulus
GO:0006396	7.88E-04	1.63	RNA processing
GO:0033692	8.81E-04	2.02	cellular polysaccharide biosynthetic process
GO:1901360	9.36E-04	1.32	organic cyclic compound metabolic process
			Molecular function
GO:0003824	1.14E-05	1.42	catalytic activity
GO:0001053	6.34E-05	62.43	plastid sigma factor activity
GO:0000996	4.02E-04	20.81	core DNA-dependent RNA polymerase binding promoter specificity activity
GO:0009881	4.44E-04	11.16	photoreceptor activity
GO:0016491	7.96E-04	1.48	oxidoreductase activity
			Cellular compartment
GO:0009507	1.48E-34	4.63	chloroplast
GO:0044435	1.21E-12	2.81	plastid part
GO:0009508	3.08E-08	40.72	plastid chromosome
GO:0009579	9.54E-08	2.66	thylakoid
GO:0009570	1.05E-06	2.58	chloroplast stroma
GO:0043231	1.48E-05	1.55	intracellular membrane-bounded organelle
GO:0009534	1.91E-05	2.54	chloroplast thylakoid
GO:0031977	2.08E-05	6.65	thylakoid lumen
GO:0009505	7.83E-05	4.49	plant-type cell wall
GO:0042646	1.67E-04	15.45	plastid nucleoid
GO:0005576	3.49E-04	2.37	extracellular region
GO:0009941	4.31E-04	2.08	chloroplast envelope
GO:0005737	5.96E-04	1.40	cytoplasm
			KEGG pathway
04712	9.99E-06	9.92	Circadian rhythm - plant
01110	2.59E-05	2.36	Biosynthesis of secondary metabolites

Table 8-12 BvRBG down-regulated genes functional enrichment

ID	Pvalue	O/R	Term
			Biological process
GO:0006468	1.75E-09	2.05	protein phosphorylation
GO:0036211	1.14E-06	1.61	protein modification process
GO:0048544	1.25E-06	6.69	recognition of pollen
GO:0009765	8.18E-06	5.95	photosynthesis, light harvesting
GO:0031347	2.54E-05	3.14	regulation of defense response
GO:0018298	2.88E-05	5.64	protein-chromophore linkage
GO:0010363	3.17E-05	4.29	regulation of plant-type hypersensitive response
GO:0007154	5.32E-05	1.72	cell communication
GO:0008152	7.15E-05	1.49	metabolic process
GO:0050776	1.46E-04	3.43	regulation of immune response
GO:0009963	1.53E-04	10.71	positive regulation of flavonoid biosynthetic process
GO:0034050	2.14E-04	3.47	host programmed cell death induced by symbiont
GO:0046189	2.62E-04	5.16	phenol-containing compound biosynthetic process
GO:0010941	2.89E-04	3.36	regulation of cell death
GO:0006612	3.86E-04	3.25	protein targeting to membrane
GO:0009414	4.43E-04	3.20	response to water deprivation
GO:0071215	4.56E-04	3.59	cellular response to abscisic acid stimulus
GO:1901701	7.78E-04	2.10	cellular response to oxygen-containing compound
GO:0001101	9.19E-04	1.94	response to acid chemical
			Molecular function
GO:0004674	5.95E-10	2.62	protein serine/threonine kinase activity
GO:0003700	6.10E-08	2.26	transcription factor activity, sequence-specific DNA binding
GO:0016773	6.75E-08	1.85	phosphotransferase activity, alcohol group as acceptor
GO:0016301	1.61E-07	1.80	kinase activity
GO:0043565	9.49E-07	2.68	sequence-specific DNA binding
GO:0016168	2.65E-05	5.75	chlorophyll binding
GO:0004842	4.89E-05	2.81	ubiquitin-protein transferase activity
GO:0016705	4.99E-05	2.21	oxidoreductase activity, acting on paired donors, with incorporation or reduction of molecular oxygen
GO:0016740	5.14E-05	1.41	transferase activity
GO:0046906	4.72E-04	2.11	tetrapyrrole binding
GO:0004497	5.42E-04	2.33	monooxygenase activity
GO:0004190	6.84E-04	3.21	aspartic-type endopeptidase activity
			Cellular compartment
GO:0016021	3.30E-07	1.95	integral component of membrane
GO:0044421	1.62E-05	16.46	extracellular region part
GO:0009523	3.85E-05	5.20	photosystem II
GO:0044425	6.70E-04	1.53	membrane part
			KEGG pathway
04075	1.67E-06	3.46	Plant hormone signal transduction
00592	1.63E-05	8.11	alpha-Linolenic acid metabolism
00196	3.47E-05	8.61	Photosynthesis - antenna proteins

ID	Pvalue	O/R	Term
04016	2.19E-04	3.34	MAPK signalling pathway - Plant
04626	3.20E-04	3.20	Plant-pathogen interaction

Table 8-13 FlvLED shared DE genes GO and KEGG enrichment

Term_ID	Description	O/R	Pvalue
	Biological process		
GO:1901566	organonitrogen compound biosynthetic process	3.2	5.17E-55
GO:0010027	thylakoid membrane organization	6.2	2.40E-26
GO:0019288	isopentenyl diphosphate biosynthetic process…	5.5	2.70E-21
GO:0042793	transcription from plastid promoter	13.1	2.09E-18
GO:0006081	cellular aldehyde metabolic process	3.1	1.83E-17
GO:0006364	rRNA processing	3.5	3.41E-15
GO:0051644	plastid localization	6.4	5.16E-15
GO:0045036	protein targeting to chloroplast	17.1	1.26E-13
GO:0072598	protein localization to chloroplast	17.1	1.26E-13
GO:0010207	photosystem II assembly	4.4	8.55E-13
GO:0034660	ncRNA metabolic process	2.8	8.97E-11
GO:0034641	cellular nitrogen compound metabolic process	1.4	1.89E-10
GO:0033014	tetrapyrrole biosynthetic process	3.9	2.32E-10
GO:0009059	macromolecule biosynthetic process	1.4	3.56E-10
GO:0042440	pigment metabolic process	2.6	1.42E-09
GO:0043038	amino acid activation	5.4	4.06E-09
GO:0015979	photosynthesis	2.1	3.85E-08
GO:0055086	nucleobase-containing small molecule metabolic process	1.8	4.67E-08
GO:1901135	carbohydrate derivative metabolic process	1.6	3.01E-07
GO:0044281	small molecule metabolic process	1.6	9.25E-07
GO:0072524	pyridine-containing compound metabolic process	2.0	1.18E-06
GO:0009657	plastid organization	3.0	1.43E-06
GO:0008152	metabolic process	1.5	3.84E-06
GO:0010103	stomatal complex morphogenesis	3.3	4.88E-06
GO:0006414	translational elongation	5.9	5.51E-06
GO:0051186	cofactor metabolic process	2.0	7.93E-06
GO:0032392	DNA geometric change	Inf	8.51E-05
GO:0006091	generation of precursor metabolites and energy	1.6	1.17E-04
GO:0002181	cytoplasmic translation	6.9	1.19E-04
GO:0045727	positive regulation of translation	8.5	2.43E-04
GO:0006801	superoxide metabolic process	8.5	2.43E-04
GO:0019745	pentacyclic triterpenoid biosynthetic process	10.1	3.33E-04

Term_ID	Description	O/R	Pvalue
GO:0005984	disaccharide metabolic process	2.0	4.08E-04
GO:0048367	shoot system development	1.4	5.04E-04
GO:0044238	primary metabolic process	1.2	6.00E-04
	Molecular function		
GO:0003735	structural constituent of ribosome	8.2	1.49E-71
GO:0004812	aminoacyl-tRNA ligase activity	5.6	6.47E-09
GO:0019843	rRNA binding	7.3	1.89E-08
GO:0003723	RNA binding	1.7	1.06E-06
GO:0016491	oxidoreductase activity	1.4	2.29E-06
GO:0016829	lyase activity	1.8	1.81E-04
GO:0016853	isomerase activity	1.8	2.11E-04
GO:0016209	antioxidant activity	2.4	2.71E-04
GO:0048037	cofactor binding	1.5	8.59E-04
	Cellular component		
GO:0005840	ribosome	7.9	6.99E-68
GO:0009507	chloroplast	2.8	4.35E-33
GO:0043228	non-membrane-bounded organelle	2.5	9.29E-29
GO:0005737	cytoplasm	1.9	9.38E-28
GO:0009579	thylakoid	2.2	1.28E-10
GO:0031967	organelle envelope	2.0	1.55E-09
GO:0031977	thylakoid lumen	5.8	1.04E-06
GO:0042555	MCM complex	Inf	9.24E-05
GO:0031984	organelle subcompartment	1.6	1.25E-04
GO:0044464	cell part	1.3	1.57E-04
GO:0005852	eukaryotic translation initiation factor 3 complex	4.5	9.67E-04
	KEGG pathway		
03010	Ribosome	10.5	4.49E-66
00100	Steroid biosynthesis	6.3	3.41E-05
00970	Aminoacyl-tRNA biosynthesis	3.8	4.23E-05
01110	Biosynthesis of secondary metabolites	1.4	5.62E-04
00710	Carbon fixation in photosynthetic organisms	2.7	7.18E-04

9 References

Abdurakhmonov, I. Y., Buriev, Z. T., Saha, S., Jenkins, J. N., Abdukarimov, A., & Pepper, A. E. (2014). Phytochrome RNAi enhances major fibre quality and agronomic traits of the cotton Gossypium hirsutum L. *Nature Communications*, *5*, 1–10. https://doi.org/10.1038/ncomms4062

Achard, P. (2003). Ethylene Regulates Arabidopsis Development via the Modulation of DELLA Protein Growth Repressor Function. *The Plant Cell Online*, *15*(12), 2816–2825. https://doi.org/10.1105/tpc.015685

Aflitos S., Schijlen E., de Jong H., de Ridder D., Smit S., Finkers R., Wang J., Zhang G., Li N., Mao L., Bakker F., Dirks R., Breit T., Gravendeel, P. S. (2014). Exploring genetic variation in the tomato (Solanum section Lycopersicon) clade by whole-genome sequencing. *Plant J*, *80*(1), 136–148.

Aflitos S., Schijlen E., de Jong H., de Ridder D., Smit S., Finkers R., Wang J., Zhang G., Li N., Mao L., Bakker F., Dirks R., Breit T., Gravendeel, P. S., Aflitos, S., Schijlen, E., De Jong, H., De Ridder, D., Smit, S., … Peters, S. (2014). Exploring genetic variation in the tomato (Solanum section Lycopersicon) clade by whole-genome sequencing. *Plant Journal*, *80*(1), 136–148. https://doi.org/10.1111/tpj.12616

Ahmad, M., & Cashmore, A. R. (1993). HY4 gene of A. thaliana encodes a protein with characteristics of a blue-light photoreceptor. *Nature*, *366*(6451), 162–166. https://doi.org/10.1038/366162a0

Ahmad, M., Jarillo, J. A., Smirnova, O., & Cashmore, A. R. (1998). Cryptochrome blue-light photoreceptors of Arabidopsis implicated in phototropism. *Nature*, *392*(6677), 720–723. https://doi.org/10.1038/33701

Al-Sady, B., Ni, W., Kircher, S., Schäfer, E., & Quail, P. H. (2006). Photoactivated Phytochrome Induces Rapid PIF3 Phosphorylation Prior to Proteasome-Mediated Degradation. *Molecular Cell*, *23*(3), 439–446. https://doi.org/10.1016/j.molcel.2006.06.011

Alabadi, D. (2004). Gibberellins Repress Photomorphogenesis in Darkness. *Plant Physiology*, *134*(3), 1050–1057. https://doi.org/10.1104/pp.103.035451

Anders, S., Pyl, P. T., & Huber, W. (2015). HTSeq-A Python framework to work with high-throughput sequencing data. *Bioinformatics*, *31*(2), 166–169. https://doi.org/10.1093/bioinformatics/btu638

Ariel, F. D., Manavella, P. A., Dezar, C. A., & Chan, R. L. (2007). The true story of the HD-Zip family. *Trends in Plant Science*, *12*(9), 419–426. https://doi.org/10.1016/j.tplants.2007.08.003

Ashikari, M. (2005). Cytokinin Oxidase Regulates Rice Grain Production. *Science*, *309*(5735), 741–745. https://doi.org/10.1126/science.1113373

Bai, M. Y., Shang, J. X., Oh, E., Fan, M., Bai, Y., Zentella, R., … Wang, Z. Y.

(2012). Brassinosteroid, gibberellin and phytochrome impinge on a common transcription module in Arabidopsis. *Nature Cell Biology*, *14*(8), 810–817. https://doi.org/10.1038/ncb2546

Baker, N. R. (2008). Chlorophyll Fluorescence: A Probe of Photosynthesis In Vivo. *Annual Review of Plant Biology*, *59*(1), 89–113. https://doi.org/10.1146/annurev.arplant.59.032607.092759

Ballaré, C. L. (2014). Light Regulation of Plant Defense. *Annual Review of Plant Biology*, *65*(1), 335–363. https://doi.org/10.1146/annurev-arplant-050213-040145

Ballaré, C. L., & Casal, J. J. (2000). Light signals perceived by crop and weed plants. *Field Crops Research*, *67*(2), 149–160. https://doi.org/10.1016/S0378-4290(00)00090-3

Banerjee, R., Schleicher, E., Meier, S., Mun, R., Pokorny, R., Ahmad, M., … Batschauer, A. (2007). The Signalling State of Arabidopsis Cryptochrome 2 Contains Flavin Semiquinone, *282*(20), 14916–14922. https://doi.org/10.1074/jbc.M700616200

Barrero, J. M., Downie, A. B., Xu, Q., & Gubler, F. (2014). A Role for Barley CRYPTOCHROME1 in Light Regulation of Grain Dormancy and Germination. *The Plant Cell*, *26*(3), 1094–1104. https://doi.org/10.1105/tpc.113.121830

Bartholomew, D. M., Bartley, G. E., & Scolnik, P. A. (1991). Abscisic Acid Control of rbcS and cab Transcription in Tomato Leaves. *Plant Physiology*, *96*(1), 291–296. https://doi.org/10.1104/pp.96.1.291

Baxter, A., Mittler, R., & Suzuki, N. (2014). ROS as key players in plant stress signalling. *Journal of Experimental Botany*, *65*(5), 1229–1240. https://doi.org/10.1093/jxb/ert375

Bian, Z., Cheng, R., Wang, Y., Yang, Q., & Lu, C. (2018). Effect of green light on nitrate reduction and edible quality of hydroponically grown lettuce (Lactuca sativa L.) under short-term continuous light from red and blue light-emitting diodes. *Environmental and Experimental Botany*, *153*(May), 63–71. https://doi.org/10.1016/j.envexpbot.2018.05.010

Bian, Z., Yang, Q., Li, T., Cheng, R., Barnett, Y., & Lu, C. (2018). Study of the beneficial effects of green light on lettuce grown under short-term continuous red and blue light-emitting diodes. *Physiologia Plantarum*. https://doi.org/10.1111/ppl.12713

Boccalandro, H. E., Giordano, C. V., Ploschuk, E. L., Piccoli, P. N., Bottini, R., & Casal, J. J. (2012). Phototropins But Not Cryptochromes Mediate the Blue Light-Specific Promotion of Stomatal Conductance, While Both Enhance Photosynthesis and Transpiration under Full Sunlight. *Plant Physiology*, *158*(3), 1475–1484. https://doi.org/10.1104/pp.111.187237

Boccalandro, H. E., Ploschuk, E. L., Yanovsky, M. J., Sánchez, R. a, Gatz, C., & Casal, J. J. (2003). Increased phytochrome B alleviates density effects on tuber yield of field potato crops. *Plant Physiology*, *133*(4), 1539–1546. https://doi.org/10.1104/pp.103.029579

Bouly, J. P., Schleicher, E., Dionisio-Sese, M., Vandenbussche, F., Van Der Straeten, D., Bakrim, N., … Ahmad, M. (2007). Cryptochrome blue light photoreceptors are activated through interconversion of flavin redox states. *Journal of Biological Chemistry*, *282*(13), 9383–9391. https://doi.org/10.1074/jbc.M609842200

Bouly, J., Schleicher, E., Dionisio-sese, M., Vandenbussche, F., Straeten, D. Van Der, Bakrim, N., … Ahmad, M. (2007). through Interconversion of Flavin Redox States * □, *282*(13), 9383–9391. https://doi.org/10.1074/jbc.M609842200

Brown, C. S., Schuerger, a C., & Sager, J. C. (1995). Growth and photomorphogenesis of pepper plants under red light-emitting diodes with supplemental blue or far-red lighting. *Journal of the American Society for Horticultural Science. American Society for Horticultural Science*, *120*(5), 808–813.

Bukhov, N. G., Drozdova, I. S., Bondar, V. V., & Mokronosov, A. T. (1992). Blue, red and blue plus red light control of chlorophyll content and CO2 gas exchange in barley leaves: Quantitative description of the effects of light quality and fluence rate. *Physiologia Plantarum*, *85*(4), 632–638. https://doi.org/10.1111/j.1399-3054.1992.tb04765.x

Bula, R. J., Morrow, R. C., Tibbitts, T. W., Barta, D. J., Ignatius, R. W., & Martin, T. S. (1991). Light-emitting diodes as a radiation source for plants. *HortScience*, *26*(2), 203–205.

Butler, W. L., Hendricks, S. B., & Siegelman, H. W. (1964). ACTTON SPECTRA OF PHYTOCHROME IN VITRO*. *Photochemistry and Photobiology*, *3*(4), 521–528. https://doi.org/10.1111/j.1751-1097.1964.tb08171.x

Cagnola, J. I., Ploschuk, E., Benech-Arnold, T., Finlayson, S. A., & Casal, J. J. (2012). Stem Transcriptome Reveals Mechanisms to Reduce the Energetic Cost of Shade-Avoidance Responses in Tomato. *Plant Physiology*, *160*(2), 1110–1119. https://doi.org/10.1104/pp.112.201921

Cai, B., Li, Q., Xu, Y., Yang, L., Bi, H., & Ai, X. (2016). Genome-wide analysis of the fructose 1,6-bisphosphate aldolase (FBA) gene family and functional characterization of FBA7 in tomato. *Plant Physiology and Biochemistry*, *108*, 251–265. https://doi.org/10.1016/j.plaphy.2016.07.019

Campos, M. L., Yoshida, Y., Major, I. T., De Oliveira Ferreira, D., Weraduwage, S. M., Froehlich, J. E., … Howe, G. A. (2016). Rewiring of jasmonate and phytochrome B signalling uncouples plant growth-defense tradeoffs. *Nature Communications*, *7*, 1–10. https://doi.org/10.1038/ncomms12570

Carabelli, M., Morellit, G., Whitelamt, G., & Ruberti, I. D. a. (1996). Homeobox Gene in Green Plants, *93*(April), 3530–3535.

Carabelli, M., Possenti, M., Sessa, G., Ciolfi, A., Sassi, M., Morelli, G., & Ruberti, I. (2007). Canopy shade causes a rapid and transient arrest in leaf development through auxin-induced cytokinin oxidase activity service Canopy shade causes a rapid and transient arrest in leaf development through auxin-induced cytokinin oxidase activity. *Genes & Development*, 1863–1868. https://doi.org/10.1101/gad.432607

Carlson, M. (2016). KEGG.db: A set of annotation maps for KEGG. *R Package Version 3.2.2.*

Carvalho, R. F., Campos, M. L., Pino, L. E., Crestana, S. L., Zsögön, A., Lima, J. E., … Peres, L. E. P. (2011). Convergence of developmental mutants into a single tomato model system: "Micro-Tom" as an effective toolkit for plant development research. *Plant Methods*, *7*(1), 1–14. https://doi.org/10.1186/1746-4811-7-18

Cashmore, A. R., Jarillo, J. A., Wu, Y.-J., & Liu, D. (1999). Cryptochromes: blue-light receptors for plants and animals. *Science*, *284*(5415), 760–765. https://doi.org/10.1126/science.284.5415.760

Cecchini, N. M., Monteoliva, M. I., & Alvarez, M. E. (2011). Proline Dehydrogenase Contributes to Pathogen Defense in Arabidopsis. *Plant Physiology*, *155*(4), 1947–1959. https://doi.org/10.1104/pp.110.167163

Čermák, T., Baltes, N. J., Čegan, R., Zhang, Y., & Voytas, D. F. (2015). High-frequency, precise modification of the tomato genome. *Genome Biology*, *16*(1). https://doi.org/10.1186/s13059-015-0796-9

Cerrudo, I., Caliri-Ortiz, M. E., Keller, M. M., Degano, M. E., Demkura, P. V., & Ballaré, C. L. (2017). Exploring growth-defence trade-offs in Arabidopsis: phytochrome B inactivation requires JAZ10 to suppress plant immunity but not to trigger shade-avoidance responses. *Plant Cell and Environment*, *40*(5), 635–644. https://doi.org/10.1111/pce.12877

Chapman, E. J., Greenham, K., Castillejo, C., Sartor, R., Bialy, A., Sun, T. ping, & Estelle, M. (2012). Hypocotyl transcriptome reveals auxin regulation of growth-promoting genes through GA-dependent and -independent pathways. *PLoS ONE*, *7*(5). https://doi.org/10.1371/journal.pone.0036210

Chatterjee, A., & Kundu, S. (2015). Revisiting the chlorophyll biosynthesis pathway using genome scale metabolic model of Oryza sativa japonica. *Scientific Reports*, *5*(April), 1–15. https://doi.org/10.1038/srep14975

Chatterjee, M., Sharma, P., & Khurana, J. P. (2006). Cryptochrome 1 from Brassica napus is up-regulated by blue light and controls hypocotyl/stem growth and anthocyanin accumulation. *Plant Physiology*, *141*(1), 61–74. https://doi.org/10.1104/pp.105.076323

Chen, S., Wang, X., Zhang, L., Lin, S., Liu, D., Wang, Q., … El-tanbouly, R. (2016). Identi fi cation and characterization of tomato gibberellin 2-oxidases (GA2oxs) and effects of fruit-speci fi c SlGA2ox1 overexpression on fruit and seed growth and development, (September), 1–9. https://doi.org/10.1038/hortres.2016.59

Cheng, Y., Dai, X., & Zhao, Y. (2006). Auxin biosynthesis by the YUCCA flavin monooxygenases controls the formation of floral organs and vascular tissues in Arabidopsis. *Genes and Development*, *20*(13), 1790–1799. https://doi.org/10.1101/gad.1415106

Chrispeels, H. E., Oettinger, H., Janvier, N., & Tague, B. W. (2000). AtZFP1, encoding Arabidopsis thaliana C2H2zinc-finger protein 1, is expressed downstream of photomorphogenic activation. *Plant Molecular Biology*, *42*(2), 279–290. https://doi.org/10.1023/A:1006352809700

Christie, J. M., Blackwood, L., Petersen, J., & Sullivan, S. (2015). Plant flavoprotein photoreceptors. *Plant and Cell Physiology*, *56*(3), 401–413. https://doi.org/10.1093/pcp/pcu196

Christie, J., Suetsugu, N., Sullivan, S., & Wada, M. (2017). Shining Light on the Function of NPH3/RPT2-like Proteins in Phototropin Signalling. *Plant Physiology*, pp.00835.2017. https://doi.org/10.1104/pp.17.00835

Clack, T., Mathews, S., & Sharrock, R. A. (1994). The phytochrome apoprotein family in Arabidopsis is encoded by five genes: the sequences and expression of PHYD and PHYE. *Plant Molecular Biology*, *25*(3), 413–427. https://doi.org/10.1007/BF00043870

Costa, B. S., Jungandreas, A., Jakob, T., Weisheit, W., Mittag, M., & Wilhelm, C. (2012). Blue light is essential for high light acclimation and photoprotection in the diatom Phaeodactylum tricornutum. *Journal of Experimental Botany*, *64*(2), 483–493. https://doi.org/10.1093/jxb/err313

De Lucas, M., Davière, J. M., Rodríguez-Falcón, M., Pontin, M., Iglesias-Pedraz, J. M., Lorrain, S., … Prat, S. (2008). A molecular framework for light and gibberellin control of cell elongation. *Nature*, *451*(7177), 480–484. https://doi.org/10.1038/nature06520

de Lucas, M., & Prat, S. (2014). PIFs get BRright: PHYTOCHROME INTERACTING FACTORs as integrators of light and hormonal signals. *New Phytologist*, *202*(4). https://doi.org/10.1111/nph.12725

De Smet, R., & Marchal, K. (2010). Advantages and limitations of current network inference methods. *Nature Reviews Microbiology*, *8*(10), 717–729. https://doi.org/10.1038/nrmicro2419

de Wit, M., Keuskamp, D. H., Bongers, F. J., Hornitschek, P., Gommers, C. M. M., Reinen, E., … Pierik, R. (2016). Integration of Phytochrome and Cryptochrome Signals Determines Plant Growth during Competition for Light. *Current Biology*, *26*(24), 3320–3326. https://doi.org/10.1016/j.cub.2016.10.031

De Wit, M., Spoel, S. H., Sanchez-Perez, G. F., Gommers, C. M. M., Pieterse, C. M. J., Voesenek, L. A. C. J., & Pierik, R. (2013). Perception of low red: Far-red ratio compromises both salicylic acid- and jasmonic acid-dependent pathogen defences in Arabidopsis. *Plant Journal*, *75*(1), 90–103. https://doi.org/10.1111/tpj.12203

Demarsy, E., Schepens, I., Okajima, K., Hersch, M., Bergmann, S., Christie, J., … Fankhauser, C. (2012). Phytochrome Kinase Substrate 4 is phosphorylated by the phototropin 1 photoreceptor. *EMBO Journal*, *31*(16), 3457–3467. https://doi.org/10.1038/emboj.2012.186

Department for Environment Food and Rural Affairs. (2017). Horticulture Statistics 2017, (May), 1–2.

Devlin, P. F. (2003). A Genomic Analysis of the Shade Avoidance Response in Arabidopsis. *Plant Physiology*, *133*(4), 1617–1629. https://doi.org/10.1104/pp.103.034397

Dhingra, A., Bies, D. H., Lehner, K. R., & Folta, K. M. (2006). Green light adjusts the

plastid transcriptome during early photomorphogenic development. *Plant Physiology*, *142*(3), 1256–1266. https://doi.org/10.1104/pp.106.088351

Ding, Z., Li, S., An, X., Liu, X., Qin, H., & Wang, D. (2009). Transgenic expression of MYB15 confers enhanced sensitivity to abscisic acid and improved drought tolerance in Arabidopsis thaliana. *Journal of Genetics and Genomics*, *36*(1), 17–29. https://doi.org/10.1016/S1673-8527(09)60003-5

Dorais, M., Ehret, D. L., & Papadopoulos, A. P. (2008). Tomato (Solanum lycopersicum) health components: From the seed to the consumer. *Phytochemistry Reviews*, *7*(2), 231–250. https://doi.org/10.1007/s11101-007-9085-x

Du, H., Wu, N., Fu, J., & Lizhong, X. (2012). A GH3 family member, OsGH3-2, modulates auxin and abscisic acid levels and differentially affects drought and cold tolerance in rice. *Journal of Experimental Botany*, *63*(18), 6467–6480. https://doi.org/10.1093/jxb/err313

Durinck, S., Moreau, Y., Kasprzyk, A., Davis, S., De Moor, B., Brazma, A., & Huber, W. (2005). BioMart and Bioconductor: A powerful link between biological databases and microarray data analysis. *Bioinformatics*, *21*(16), 3439–3440. https://doi.org/10.1093/bioinformatics/bti525

Eda, M., Matsumoto, T., Ishimaru, M., & Tada, T. (2016). Structural and functional analysis of tomato β-galactosidase 4: insight into the substrate specificity of the fruit softening-related enzyme. *The Plant Journal : For Cell and Molecular Biology*, *86*(4), 300–307. https://doi.org/10.1111/tpj.13160

Endo, M., Tanigawa, Y., Murakami, T., Araki, T., & Nagatani, A. (2013). PHYTOCHROME-DEPENDENT LATE-FLOWERING accelerates flowering through physical interactions with phytochrome B and CONSTANS. *Proceedings of the National Academy of Sciences*, *110*(44), 18017–18022. https://doi.org/10.1073/pnas.1310631110

Expósito-Rodríguez, M., Borges, A. A., Borges-Pérez, A., & Pérez, J. A. (2008). Selection of internal control genes for quantitative real-time RT-PCR studies during tomato development process. *BMC Plant Biology*, *8*, 1–12. https://doi.org/10.1186/1471-2229-8-131

Expósito-Rodríguez, M., Borges, A. A., Borges-Pérez, A., & Pérez, J. A. (2011). Gene structure and spatiotemporal expression profile of tomato genes encoding YUCCA-like flavin monooxygenases: The ToFZY gene family. *Plant Physiology and Biochemistry*, *49*(7), 782–791. https://doi.org/10.1016/j.plaphy.2011.02.022

Facella, P., Carbone, F., Placido, A., & Perrotta, G. (2017). Cryptochrome 2 extensively regulates transcription of the chloroplast genome in tomato. *FEBS Open Bio*, *7*(4), 456–471. https://doi.org/10.1002/2211-5463.12082

Facella, P., Lopez, L., Carbone, F., Galbraith, D. W., Giuliano, G., & Perrotta, G. (2008). Diurnal and circadian rhythms in the tomato transcriptome and their modulation by cryptochrome photoreceptors. *PLoS ONE*, *3*(7). https://doi.org/10.1371/journal.pone.0002798

Falcon, S., & Gentleman, R. (2007). Using GOstats to test gene lists for GO term

association. *Bioinformatics*, *23*(2), 257–258. https://doi.org/10.1093/bioinformatics/btl567

Farber, M., Attia, Z., & Weiss, D. (2016). Cytokinin activity increases stomatal density and transpiration rate in tomato. *Journal of Experimental Botany*, *67*(22), 6351–6362. https://doi.org/10.1093/jxb/erw398

Feng, S., Martinez, C., Gusmaroli, G., Wang, Y., Zhou, J., Wang, F., … Deng, X. W. (2008). Coordinated regulation of Arabidopsis thaliana development by light and gibberellins. *Nature*. https://doi.org/10.1038/nature06448

Folta, K. M. (2004). Green light stimulates early stem elongation, antagonizing light-mediated growth inhibition. *Plant Physiology*, *135*(3), 1407–1416. https://doi.org/10.1104/pp.104.038893

Folta, K. M., & Maruhnich, S. A. (2007). Green light: A signal to slow down or stop. *Journal of Experimental Botany*, *58*(12), 3099–3111. https://doi.org/10.1093/jxb/erm130

Fu, X., & Harberd, N. P. (2003). Auxin promotes Arabidopsis root growth by modulating gibberellin response. *Nature*, *421*(6924), 740–743. https://doi.org/10.1038/nature01387

Galstyan, A., Cifuentes-Esquivel, N., Bou-Torrent, J., & Martinez-Garcia, J. F. (2011). The shade avoidance syndrome in Arabidopsis: A fundamental role for atypical basic helix-loop-helix proteins as transcriptional cofactors. *Plant Journal*, *66*(2), 258–267. https://doi.org/10.1111/j.1365-313X.2011.04485.x

Galuszka, P., Frébortová, J., Werner, T., Yamada, M., Strnad, M., Schmülling, T., & Frébort, I. (2004). Cytokinin oxidase/dehydrogenase genes in barley and wheat: Cloning and heterologous expression. *European Journal of Biochemistry*, *271*(20), 3990–4002. https://doi.org/10.1111/j.1432-1033.2004.04334.x

Galvão, V. C., & Fankhauser, C. (2015). Sensing the light environment in plants: photoreceptors and early signalling steps. *Current Opinion in Neurobiology*, *34*(Figure 1), 46–53. https://doi.org/10.1016/j.conb.2015.01.013

García-Martinez, J. L., & Gil, J. (2001). Light regulation of gibberellin biosynthesis and mode of action. *Journal of Plant Growth Regulation*, *20*(4), 354–368. https://doi.org/10.1007/s003440010033

Garg, A. K., Sawers, R. J. H., Wang, H., Kim, J. K., Walker, J. M., Brutnell, T. P., … Wu, R. J. (2006). Light-regulated overexpression of an Arabidopsis phytochrome A gene in rice alters plant architecture and increases grain yield. *Planta*, *223*(4), 627–636. https://doi.org/10.1007/s00425-005-0101-3

Giliberto, L., Perrotta, G., Pallara, P., Weller, J. L., Fraser, P. D., Bramley, P. M., … Giuliano, G. (2005). Manipulation of the blue light photoreceptor cryptochrome 2 in tomato affects vegetative development, flowering time, and fruit antioxidant content. *Plant Physiology*, *137*(1), 199–208. https://doi.org/10.1104/pp.104.051987

Goins, G. D., Yorio, N. C., Sanwo, M. M., & Brown, C. S. (1997). Photomorphogenesis, photosynthesis, and seed yield of wheat plants grown under red light-emitting diodes (LEDs) with and without supplemental blue

lighting. *Journal of Experimental Botany*, *48*(312), 1407–1413. https://doi.org/10.1093/jxb/48.7.1407

Griebel, T., & Zeier, J. (2008). Light Regulation and Daytime Dependency of Inducible Plant Defenses in Arabidopsis: Phytochrome Signalling Controls Systemic Acquired Resistance Rather Than Local Defense. *Plant Physiology*, *147*(2), 790–801. https://doi.org/10.1104/pp.108.119503

Gubler, F., Hughes, T., Waterhouse, P., & Jacobsen, J. (2008). Regulation of Dormancy in Barley by Blue Light and After-Ripening: Effects on Abscisic Acid and Gibberellin Metabolism. *Plant Physiology*, *147*(2), 886–896. https://doi.org/10.1104/pp.107.115469

Gururani, M. A., Ganesan, M., & Song, P.-S. (2015). Photo-biotechnology as a tool to improve agronomic traits in crops. *Biotechnology Advances*, *33*(1), 53–63. https://doi.org/10.1016/j.biotechadv.2014.12.005

Haitz, R., & Tsao, J. Y. (2011). Solid-state lighting: "The case" 10 years after and future prospects. *Physica Status Solidi (A) Applications and Materials Science*, *208*(1), 17–29. https://doi.org/10.1002/pssa.201026349

Harari-Steinberg, O., Ohad, I., & Chamovitz, D. (2007). Dissection of the Light Signal Transduction Pathways Regulating the Two Early Light-Induced Protein Genes in Arabidopsis. *Plant Physiology*, *1*, 5–8. https://doi.org/10.1104/pp.010270.986

Hauser, B. A., & Pratt, L. H. (1997). Planta, 379–387.

Heim, M. a., Jakoby, M., Werber, M., Martin, C., Weisshaar, B., & Bailey, P. C. (2003). The basic helix-loop-helix transcription factor family in plants: A genome-wide study of protein structure and functional diversity. *Molecular Biology and Evolution*, *20*(5), 735–747. https://doi.org/10.1093/molbev/msg088

Hennig, L., Stoddart, W. M., Dieterle, M., Whitelam, G. C., & Schäfer, E. (2002). Phytochrome E controls light-induced germination of Arabidopsis. *Plant Physiology*, *128*(1), 194–200. https://doi.org/10.1104/pp.010559

Herbel, V., Orth, C., Wenzel, R., Ahmad, M., & Batschauer, A. (2013). Life-times of Arabidopsis cryptochrome signalling states in vivo, *12144*, 583–592. https://doi.org/10.1111/tpj.12144

Hernández, R., Eguchi, T., Deveci, M., & Kubota, C. (2016). Tomato seedling physiological responses under different percentages of blue and red photon flux ratios using LEDs and cool white fluorescent lamps. *Scientia Horticulturae*, *213*(November), 270–280. https://doi.org/10.1016/j.scienta.2016.11.005

Hernández, R., & Kubota, C. (2016). Physiological responses of cucumber seedlings under different blue and red photon flux ratios using LEDs. *Environmental and Experimental Botany*, *121*, 66–74. https://doi.org/10.1016/j.envexpbot.2015.04.001

Heschel, M. S., Selby, J., Butler, C., Whitelam, G. C., Sharrock, R. a., & Donohue, K. (2007). A new role for phytochromes in temperature-dependent germination. *New Phytologist*, *174*(4), 735–741. https://doi.org/10.1111/j.1469-8137.2007.02044.x

Hirose, F., Inagaki, N., Hanada, A., Yamaguchi, S., Kamiya, Y., Miyao, A., … Takano, M. (2012). Cryptochrome and phytochrome cooperatively but independently reduce active gibberellin content in rice seedlings under light irradiation. *Plant and Cell Physiology*, *53*(9), 1570–1582. https://doi.org/10.1093/pcp/pcs097

Hogewoning, S. W., Trouwborst, G., Maljaars, H., Poorter, H., van Ieperen, W., & Harbinson, J. (2010). Blue light dose-responses of leaf photosynthesis, morphology, and chemical composition of Cucumis sativus grown under different combinations of red and blue light. *Journal of Experimental Botany*, *61*(11), 3107–3117. https://doi.org/10.1093/jxb/erq132

Holtkotte, X., Ponnu, J., Ahmad, M., & Hoecker, U. (2017). The blue light-induced interaction of cryptochrome 1 with COP1 requires SPA proteins during Arabidopsis light signalling. *PLoS Genetics*, *13*(10), 1–15. https://doi.org/10.1371/journal.pgen.1007044

Hornitschek, P., Kohnen, M. V., Lorrain, S., Rougemont, J., Ljung, K., López-Vidriero, I., … Fankhauser, C. (2012). Phytochrome interacting factors 4 and 5 control seedling growth in changing light conditions by directly controlling auxin signalling. *Plant Journal*, *71*(5), 699–711. https://doi.org/10.1111/j.1365-313X.2012.05033.x

Hornitschek, P., Lorrain, S., Zoete, V., Michielin, O., & Fankhauser, C. (2009). Inhibition of the shade avoidance response by formation of non-DNA binding bHLH heterodimers. *The EMBO Journal*, *28*(24), 3893–3902. https://doi.org/10.1038/emboj.2009.306

Hsieh, W.-P., Hsieh, H.-L., & Wu, S.-H. (2012). *Arabidopsis* bZIP16 Transcription Factor Integrates Light and Hormone Signalling Pathways to Regulate Early Seedling Development. *The Plant Cell*, *24*(10), 3997–4011. https://doi.org/10.1105/tpc.112.105478

Husaineid, S. S. H., Kok, R. A., Schreuder, M. E. L., Hanumappa, M., Cordonnier-Pratt, M. M., Pratt, L. H., … Van Der Krol, A. R. (2007). Overexpression of homologous phytochrome genes in tomato: Exploring the limits in photoperception. *Journal of Experimental Botany*, *58*(3), 615–626. https://doi.org/10.1093/jxb/erl253

Hyodo, H., Yamakawa, S., Takeda, Y., Tsuduki, M., Yokota, A., Nishitani, K., & Kohchi, T. (2003). Active gene expression of a xyloglucan endotransglucosylase/hydrolase gene, XTH9, in inflorescence apices is related to cell elongation in Arabidopsis thaliana. *Plant Molecular Biology*, *52*(2), 473–482. https://doi.org/10.1023/A:1023904217641

Iannacone, R., Mittempergher, F., Morelli, G., Panio, G., Perito, A., Ruberti, I., … Cellini, F. (2008). INFLUENCE OF AN ARABIDOPSIS DOMINANT NEGATIVE ATHB2 MUTANT ON TOMATO PLANT DEVELOPMENT. In *Acta Horticulturae* (pp. 263–276). International Society for Horticultural Science (ISHS), Leuven, Belgium. https://doi.org/10.17660/ActaHortic.2008.789.36

Iglesias, M. J., Sellaro, R., Zurbriggen, M. D., & Casal, J. J. (2018). Multiple links between shade avoidance and auxin networks. *Journal of Experimental Botany*, *69*(2), 213–228. https://doi.org/10.1093/jxb/erx295

Imaizumi, T., Schultz, T. F., Harmon, F. G., Ho, L. A., & Kay, S. A. (2005). {FKF}1 {F}-{Box} {Protein} {Mediates} {Cyclic} {Degradation} of a {Repressor} of {CONSTANS} in {Arabidopsis}. *Science*, *309*(5732), 293–297. https://doi.org/10.1126/science.1110586

Inoue, S., & Kinoshita, T. (2017). Blue Light Regulation of Stomatal Opening and the Plasma Membrane H $^{+}$ -ATPase. *Plant Physiology*, *174*(2), 531–538. https://doi.org/10.1104/pp.17.00166

Iwakawa, H., Ueno, Y., Semiarti, E., Onouchi, H., Kojima, S., Tsukaya, H., … Machida, Y. (2002). The ASYMMETRIC LEAVES2 gene of Arabidopsis thaliana, required for formation of a symmetric flat leaf lamina, encodes a member of a novel family of proteins characterized by cysteine repeats and a leucine zipper. *Plant and Cell Physiology*, *43*(5), 467–478. https://doi.org/10.1093/pcp/pcf077

Jackson, S. D., & Prat, S. (1996). Control of tuberisation in potato by gibberellins and phytochrome B.

Jang, I.-C., Henriques, R., Seo, H. S., Nagatani, A., & Chua, N.-H. (2010). Arabidopsis PHYTOCHROME INTERACTING FACTOR Proteins Promote Phytochrome B Polyubiquitination by COP1 E3 Ligase in the Nucleus. *The Plant Cell Online*, *22*(7), 2370–2383. https://doi.org/10.1105/tpc.109.072520

Jarillo, J. A., Capel, J., Tang, R. H., Yang, H. Q., Alonso, J. M., Ecker, J. R., & Cashmore, A. R. (2001). An Arabidopsis circadian clock component interacts with both CRY1 and phyB. *Nature*, *410*(6827), 487–490. https://doi.org/10.1038/35068589

Jiao, Y., Yang, H., Ma, L., Sun, N., Yu, H., Liu, T., … Deng, X. (2003). A Genome-Wide Analysis of Blue-Light Regulation of Arabidopsis Transcription Factor Gene Expression during Seedling Development 1 [w]. *Plant Physiology*, *133*(December), 1480–1493. https://doi.org/10.1104/pp.103.029439.chromosome

Jung, J. H., Domijan, M., Klose, C., Biswas, S., Ezer, D., Gao, M., … Wigge, P. A. (2016). Phytochromes function as thermosensors in Arabidopsis. *Science*, *354*(6314), 886–889. https://doi.org/10.1126/science.aaf6005

Kagawa, T., Sakai, T., Suetsugu, N., Oikawa, K., Ishiguro, S., Kato, T., … Wada, M. (2001). Arabidopsis NPL1: a phototropin homolog controlling the chloroplast high-light avoidance response. *Science (New York, N.Y.)*, *291*, 2138–2141. https://doi.org/10.1126/science.291.5511.2138

Kang, C.-Y., Lian, H.-L., Wang, F.-F., Huang, J.-R., & Yang, H.-Q. (2009). Cryptochromes, phytochromes, and COP1 regulate light-controlled stomatal development in Arabidopsis. *The Plant Cell*, *21*(9), 2624–2641. https://doi.org/10.1105/tpc.109.069765

Karlova, R., Rosin, F. M., Busscher-Lange, J., Parapunova, V., Do, P. T., Fernie, A. R., … de Maagd, R. A. (2011). Transcriptome and Metabolite Profiling Show That APETALA2a Is a Major Regulator of Tomato Fruit Ripening. *The Plant Cell*, *23*(3), 923–941. https://doi.org/10.1029/RS025i004p00299

Kegg, E., & Graphviz, E. (2014). Pathview: An R package for pathway based data

integration and visualization. *Biocondictor*, *29*(14), 8–10. https://doi.org/10.1093/bioinformatics/btt285.2

Keller, M. M., Jaillais, Y., Pedmale, U. V., Moreno, J. E., Chory, J., & Ballaré, C. L. (2011). Cryptochrome 1 and phytochrome B control shade-avoidance responses in Arabidopsis via partially independent hormonal cascades. *Plant Journal*, *67*(2), 195–207. https://doi.org/10.1111/j.1365-313X.2011.04598.x

Keuskamp, D. H., Pollmann, S., Voesenek, L. A. C. J., Peeters, A. J. M., & Pierik, R. (2010). Auxin transport through PIN-FORMED 3 (PIN3) controls shade avoidance and fitness during competition. *Proceedings of the National Academy of Sciences*, *107*(52), 22740–22744. https://doi.org/10.1073/pnas.1013457108

Keuskamp, D. H., Sasidharan, R., Vos, I., Peeters, A. J. M., Voesenek, L. A. C. J., & Pierik, R. (2011). Blue-light-mediated shade avoidance requires combined auxin and brassinosteroid action in Arabidopsis seedlings. *Plant Journal*, *67*(2), 208–217. https://doi.org/10.1111/j.1365-313X.2011.04597.x

Khanna, R. (2006). Functional Profiling Reveals That Only a Small Number of Phytochrome-Regulated Early-Response Genes in Arabidopsis Are Necessary for Optimal Deetiolation. *The Plant Cell Online*, *18*(9), 2157–2171. https://doi.org/10.1105/tpc.106.042200

Khanna, R., Huq, E., Kikis, E. a, Al-Sady, B., Lanzatella, C., & Quail, P. H. (2004). A novel molecular recognition motif Nnecessary for targeting photoactivated phytochrome signalling to specific Basic Helix-Loop-Helix transcription factors. *The Plant Cell*, *16*(11), 3033–3044. https://doi.org/10.1105/tpc.104.025643.1

Kharshiing, E., & Sinha, S. P. (2014). Plant Productivity: Can Photoreceptors Light the Way? *Journal of Plant Growth Regulation*, *34*(1), 206–214. https://doi.org/10.1007/s00344-014-9454-9

Kim, D., Langmead, B., & Salzberg, S. L. (2015). HISAT: a fast spliced aligner with low memory requirements. *Nat Methods*, *12*(4), 357–360. https://doi.org/10.1038/nmeth.3317.HISAT

Kim, H., Goins, G. D., Wheeler, R. M., Sager, J. C., Burrows, J., Koss, L., … Quincy, C. (2004). Green-light Supplementation for Enhanced Lettuce Growth under Red- and Blue-light-emitting Diodes, *39*(7), 1617–1622.

Kim, K.-M., Kim, J.-Y., & Kim, J.-I. (2009). Morphological Traits of S598A Sweetpotato as an Industrial Starch Crop. *Korean Journal of Crop Science*, *54*.

Kim, W.-Y., Geng, R., & Somers, D. E. (2003). Circadian phase-specific degradation of the F-box protein ZTL is mediated by the proteasome. *Proceedings of the National Academy of Sciences*, *100*(8), 4933–4938. https://doi.org/10.1073/pnas.0736949100

Kim, W. Y., Fujiwara, S., Suh, S. S., Kim, J., Kim, Y., Han, L., … Somers, D. E. (2007). ZEITLUPE is a circadian photoreceptor stabilized by GIGANTEA in blue light. *Nature*, *449*(7160), 356–360. https://doi.org/10.1038/nature06132

Kinoshita, T., Doi, M., & Suetsugu, N. (2001). Regulation of Stomatal Opening. *Nature*, *414*(December), 0–4.

Kircher, S. (2002). Nucleocytoplasmic Partitioning of the Plant Photoreceptors

Phytochrome A, B, C, D, and E Is Regulated Differentially by Light and Exhibits a Diurnal Rhythm. *The Plant Cell Online*, *14*(7), 1541–1555. https://doi.org/10.1105/tpc.001156

Kircher, S., Kozma-Bognar, L., Kim, L., Adam, E., Harter, K., Schafer, E., & Nagy, F. (1999). Light quality-dependent nuclear import of the plant photoreceptors phytochrome A and B. *The Plant Cell*, *11*(8), 1445–1456. https://doi.org/10.1105/tpc.11.8.1445

Kleine, T., Kindgren, P., Benedict, C., Hendrickson, L., & Strand, A. (2007). Genome-wide gene expression analysis reveals a critical role for CRYPTOCHROME1 in the response of Arabidopsis to high irradiance. *Plant Physiology*, *144*(3), 1391–1406. https://doi.org/10.1104/pp.107.098293

Kleiner, O., Kircher, S., Harter, K., & Batschauer, a. (1999). Nuclear localization of the Arabidopsis blue light receptor cryptochrome 2. *Plant Journal*, *19*(3), 289–296. https://doi.org/10.1046/j.1365-313X.1999.00535.x

Koini, M. A., Alvey, L., Allen, T., Tilley, C. A., Harberd, N. P., Whitelam, G. C., & Franklin, K. A. (2009). High Temperature-Mediated Adaptations in Plant Architecture Require the bHLH Transcription Factor PIF4. *Current Biology*, *19*(5), 408–413. https://doi.org/10.1016/j.cub.2009.01.046

Kong, S.-G., Lee, D.-S., Kwak, S.-N., Kim, J.-K., Sohn, J.-K., & Kim, I.-S. (2004). Characterization of sunlight-grown transgenic rice plants expressing Arabidopsis phytochrome A. *Molecular Breeding*, *14*(1), 35–45. https://doi.org/10.1023/B:MOLB.0000037993.79486.7b

Kong, S. G., Suetsugu, N., Kikuchi, S., Nakai, M., Nagatani, A., & Wada, M. (2013). Both phototropin 1 and 2 localize on the chloroplast outer membrane with distinct localization activity. *Plant and Cell Physiology*, *54*(1), 80–92. https://doi.org/10.1093/pcp/pcs151

Kong, S. G., Suzuki, T., Tamura, K., Mochizuki, N., Hara-Nishimura, I., & Nagatani, A. (2006). Blue light-induced association of phototropin 2 with the Golgi apparatus. *Plant Journal*, *45*(6), 994–1005. https://doi.org/10.1111/j.1365-313X.2006.02667.x

Kossmann, J., & Sonnewald, U. (1991). Reduction of the chloroplastic fructose-l , 6-bisphosphatase in transgenic potato plants impairs photosynthesis and plant growth, *6*(1994), 637–650.

Kunihiro, A., Yamashino, T., Nakamichi, N., Niwa, Y., Nakanishi, H., & Mizuno, T. (2011). PHYTOCHROME-INTERACTING FACTOR 4 and 5 (PIF4 and PIF5) activate the Homeobox ATHB2 and auxin-inducible IAA29 genes in the coincidence mechanism underlying photoperiodic control of plant growth of Arabidopsis thaliana. *Plant and Cell Physiology*, *52*(8), 1315–1329. https://doi.org/10.1093/pcp/pcr076

Kuno, N. (2003). The Novel MYB Protein EARLY-PHYTOCHROME-RESPONSIVE1 Is a Component of a Slave Circadian Oscillator in Arabidopsis. *The Plant Cell Online*, *15*(10), 2476–2488. https://doi.org/10.1105/tpc.014217

Kurepin, L. V., Emery, R. J. N., Pharis, R. P., & Reid, D. M. (2007). The interaction of light quality and irradiance with gibberellins, cytokinins and auxin in

regulating growth of Helianthus annuus hypocotyls. *Plant, Cell and Environment*, *30*(2), 147–155. https://doi.org/10.1111/j.1365-3040.2006.01612.x

Lanoue, J., Leonardos, E. D., Ma, X., & Grodzinski, B. (2017). The Effect of Spectral Quality on Daily Patterns of Gas Exchange, Biomass Gain, and Water-Use-Efficiency in Tomatoes and Lisianthus: An Assessment of Whole Plant Measurements. *Frontiers in Plant Science*, *8*(June), 1–15. https://doi.org/10.3389/fpls.2017.01076

Lau, O. S., & Deng, X. W. (2010). Plant hormone signalling lightens up: integrators of light and hormones. *Current Opinion in Plant Biology*, *13*(5), 571–577. https://doi.org/10.1016/j.pbi.2010.07.001

Lee, K., Han, K. S., Kwon, Y. S., Lee, J. H., Kim, S. H., Chung, W. S., … Bae, D. W. (2009). Identification of potential DREB2C targets in Arabidopsis thaliana plants overexpressing DREB2C using proteomic analysis. *Molecules and Cells*, *28*(4), 383–388. https://doi.org/10.1007/s10059-009-0154-4

Lee, S. Y., Kwon, J. K., Park, K. S., & Choi, H. G. (2014). The effect of LED light source on the growth and yield of greenhouse grown tomato. *Acta Horticulturae*, *1037*, 789–794. https://doi.org/10.17660/ActaHortic.2014.1037.104

Legris, M., Klose, C., Burgie, E. S., Rojas, C. C., Neme, M., Hiltbrunner, A., … Casal, J. J. (2016). Phytochrome B integrates light and temperature signals in Arabidopsis. *Science*, *354*(6314), 897–900. https://doi.org/10.1126/science.aaf5656

Leivar, P., Monte, E., Oka, Y., Liu, T., Carle, C., Castillon, A., … Quail, P. H. (2008). Multiple Phytochrome-Interacting bHLH Transcription Factors Repress Premature Seedling Photomorphogenesis in Darkness. *Current Biology*, *18*(23), 1815–1823. https://doi.org/10.1016/j.cub.2008.10.058

Leivar, P., & Quail, P. H. (2011). PIFs: Pivotal components in a cellular signalling hub. *Trends in Plant Science*, *16*(1), 19–28. https://doi.org/10.1016/j.tplants.2010.08.003

Leivar, P., Tepperman, J. M., Monte, E., Calderon, R. H., Liu, T. L., & Quail, P. H. (2009). Definition of Early Transcriptional Circuitry Involved in Light-Induced Reversal of PIF-Imposed Repression of Photomorphogenesis in Young Arabidopsis Seedlings. *The Plant Cell*. https://doi.org/10.1105/tpc.109.070672

LI-COR. (1989). *LI-1800 Portable Spectrometer Instruction Manual*.

Li, C.-X., Xu, Z.-G., Dong, R.-Q., Chang, S.-X., Wang, L.-Z., Khalil-Ur-Rehman, M., & Tao, J.-M. (2017). An RNA-Seq Analysis of Grape Plantlets Grown in vitro Reveals Different Responses to Blue, Green, Red LED Light, and White Fluorescent Light. *Frontiers in Plant Science*, *8*(January). https://doi.org/10.3389/fpls.2017.00078

Li, H., Handsaker, B., Wysoker, A., Fennell, T., Ruan, J., Homer, N., … Durbin, R. (2009). The Sequence Alignment/Map format and SAMtools. *Bioinformatics*, *25*(16), 2078–2079. https://doi.org/10.1093/bioinformatics/btp352

Li, J., Li, G., Wang, H., & Deng, X. W. (2011). Phytochrome Signalling Mechanisms Phytochrome Signalling Mechanisms. *Review Literature And Arts Of The*

Americas, (9), 1–26. https://doi.org/10.1199/tab.0148

Li, J., Nagpal, P., Vitart, V., McMorris, T. C., & Chory, J. (1996). A role for Brassinosteroids in light-dependant development of Arabidopsis. *Science*, *272*(April), 398–401.

Li, J., Wei, H., & Zhao, P. X. (2013). DeGNServer: Deciphering genome-scale gene networks through high performance reverse engineering analysis. *BioMed Research International*, *2013*(Mi). https://doi.org/10.1155/2013/856325

Li, J., Zhao-Hui, C., Batoux, M., Nekrasov, V., Roux, M., Chinchilla, D., … Jones, J. D. G. (2009). Specific ER quality control components required for biogenesis of the plant innate immune receptor EFR. *Proceedings of the National Academy of Sciences*, *106*(37), 15973–15978. https://doi.org/10.1073/pnas.0905532106

Li, L., Ljung, K., Breton, G., Li, L., Ljung, K., Breton, G., … Chory, J. (2012). Linking photoreceptor excitation to changes in plant architecture Linking photoreceptor excitation to changes in plant architecture. *Genes & Development*, *26*, 785–790. https://doi.org/10.1101/gad.187849.112

Li, L., Zhang, Q., Pedmale, U. V., Nito, K., Fu, W., Lin, L., … Chory, J. (2014). PIL1 participates in a negative feedback loop that regulates its own gene expression in response to shade. *Molecular Plant*, *7*(10), 1582–1585. https://doi.org/10.1093/mp/ssu068

Li, Q. F., Wang, C., Jiang, L., Li, S., Sun, S. S. M., & He, J. X. (2012). An interaction between BZR1 and DELLAs mediates direct signalling crosstalk between brassinosteroids and gibberellins in Arabidopsis. *Science Signalling*, *5*(244). https://doi.org/10.1126/scisignal.2002908

Liscum, E., & Briggs, W. R. (1995). Mutations in the NPH1 locus of Arabidopsis disrupt the perception of phototropic stimuli. *The Plant Cell*, *7*(4), 473–485. https://doi.org/10.1105/tpc.7.4.473

Liu, B., Zuo, Z., Liu, H., Liu, X., & Lin, C. (2011). Arabidopsis cryptochrome 1 interacts with SPA1 to suppress COP1 activity in response to blue light. *Genes and Development*, *25*(10), 1029–1034. https://doi.org/10.1101/gad.2025011

Liu, C. C., Ahammed, G. J., Wang, G. T., Xu, C. J., Chen, K. S., Zhou, Y. H., & Yu, J. Q. (2018). Tomato CRY1a plays a critical role in the regulation of phytohormone homeostasis, plant development, and carotenoid metabolism in fruits. *Plant Cell and Environment*, *41*(2), 354–366. https://doi.org/10.1111/pce.13092

Liu, J., Zhang, F., Zhou, J., Chen, F., Wang, B., & Xie, X. (2012). Phytochrome B control of total leaf area and stomatal density affects drought tolerance in rice. *Plant Molecular Biology*, *78*(3), 289–300. https://doi.org/10.1007/s11103-011-9860-3

Liu, X. Y., Chang, T. T., Guo, S. R., Xu, Z. G., & Li, J. (2011). Effect of different light quality of LED on growth and photosynthetic character in cherry tomato seedling. *Acta Horticulturae*, *907*, 325–330. https://doi.org/10.17660/ActaHortic.2011.907.53

Liu Xiaoying. (2012). Regulation of the growth and photosynthesis of cherry tomato

seedlings by different light irradiations of light emitting diodes (LED). *African Journal of Biotechnology*, *11*(22), 6169–6177. https://doi.org/10.5897/AJB11.1191

Liu, Y., Dawson, W., Prati, D., Haeuser, E., Feng, Y., & Van Kleunen, M. (2016). Does greater specific leaf area plasticity help plants to maintain a high performance when shaded? *Annals of Botany*, *118*(7), 1329–1336. https://doi.org/10.1093/aob/mcw180

Llorente, B., D'Andrea, L., Ruiz-Sola, M. A., Botterweg, E., Pulido, P., Andilla, J., … Rodriguez-Concepcion, M. (2016). Tomato fruit carotenoid biosynthesis is adjusted to actual ripening progression by a light-dependent mechanism. *Plant Journal*, *85*(1), 107–119. https://doi.org/10.1111/tpj.13094

Lopez, L., Carbone, F., Bianco, L., Giuliano, G., Facella, P., & Perrotta, G. (2012). Tomato plants overexpressing cryptochrome 2 reveal altered expression of energy and stress-related gene products in response to diurnal cues. *Plant, Cell and Environment*, *35*(5), 994–1012. https://doi.org/10.1111/j.1365-3040.2011.02467.x

Lorrain, S., Allen, T., Duek, P. D., Whitelam, G. C., & Fankhauser, C. (2008). Phytochrome-mediated inhibition of shade avoidance involves degradation of growth-promoting bHLH transcription factors. *Plant Journal*, *53*(2), 312–323. https://doi.org/10.1111/j.1365-313X.2007.03341.x

Luo, W., & Brouwer, C. (2013). Pathview: An R/Bioconductor package for pathway-based data integration and visualization. *Bioinformatics*, *29*(14), 1830–1831. https://doi.org/10.1093/bioinformatics/btt285

Ma, L., Li, J., Qu, L., Hager, J., Chen, Z., Zhao, H., & Deng, X. W. (2001). Light control of Arabidopsis development entails coordinated regulation of genome expression and cellular pathways. *The Plant Cell*, *13*(12), 2589–2607. https://doi.org/10.1105/tpc.010229

MacHemer, K., Shaiman, O., Salts, Y., Shabtai, S., Sobolev, I., Belausov, E., … Barg, R. (2011). Interplay of MYB factors in differential cell expansion, and consequences for tomato fruit development. *Plant Journal*, *68*(2), 337–350. https://doi.org/10.1111/j.1365-313X.2011.04690.x

Massa, G. D., Kim, H. H., Wheeler, R. M., & Mitchell, C. a. (2008). Plant productivity in response to LED lighting. *HortScience*, *43*(7), 1951–1956.

Mathews, S., & Sharrock, R. A. (1997). Phytochrome gene diversity. *Plant, Cell and Environment*, *20*(6), 666–671. https://doi.org/10.1046/j.1365-3040.1997.d01-117.x

Matsuda, R., Ohashi-Kaneko, K., Fujiwara, K., & Kurata, K. (2008). Effects of Blue Light Deficiency on Acclimation of Light Energy Partitioning in PSII and CO2 Assimilation Capacity to High Irradiance in Spinach Leaves. *Plant and Cell Physiology*, *49*(4), 664–670. https://doi.org/10.1093/pcp/pcn041

Mawphlang, O. I. L., & Kharshiing, E. V. (2017). photoreceptor mediated plant growth response crop engineering. *Frontier in Plant Science*, *8*.

McCree, K. J. (1971). The action spectrum, absorptance and quantum yield of

photosynthesis in crop plants. *Agricultural Meteorology*, *9*(C), 191–216. https://doi.org/10.1016/0002-1571(71)90022-7

Mochizuki, T., Onda, Y., Fujiwara, E., Wada, M., & Toyoshima, Y. (2004). Two independent light signals cooperate in the activation of the plastid psbD blue light-responsive promoter in Arabidopsis. *FEBS Letters*, *571*(1–3), 26–30. https://doi.org/10.1016/j.febslet.2004.06.052

Morrow, R. C. (2008). LED lighting in horticulture. *HortScience*, *43*(7), 1947–1950.

Muller, P. (2001). Non-Photochemical Quenching. A Response to Excess Light Energy. *Plant Physiology*, *125*(4), 1558–1566. https://doi.org/10.1104/pp.125.4.1558

Mulo, P. (2011). Chloroplast-targeted ferredoxin-NADP+ oxidoreductase (FNR): Structure, function and location. *Biochimica et Biophysica Acta - Bioenergetics*, *1807*(8), 927–934. https://doi.org/10.1016/j.bbabio.2010.10.001

Murchie, E. H., & Lawson, T. (2013). Chlorophyll fluorescence analysis: A guide to good practice and understanding some new applications. *Journal of Experimental Botany*, *64*(13), 3983–3998. https://doi.org/10.1093/jxb/ert208

Murchie, E. H., & Niyogi, K. K. (2010). Manipulation of Photoprotection to Improve Plant Photosynthesis. *Plant Physiology*, *155*(1), 86–92. https://doi.org/10.1104/pp.110.168831

Nelson, J. A., & Bugbee, B. (2014). Economic analysis of greenhouse lighting: Light emitting diodes vs. high intensity discharge fixtures. *PLoS ONE*, *9*(6). https://doi.org/10.1371/journal.pone.0099010

Ni, M., Tepperman, J. M., & Quail, P. H. (1998). PIF3, a phytochrome-interacting factor necessary for normal photoinduced signal transduction, is a novel basic helix-loop-helix protein. *Cell*, *95*(5), 657–667. https://doi.org/10.1016/S0092-8674(00)81636-0

Ni, W., Xu, S. L., Tepperman, J. M., Stanley, D. J., Maltby, D. A., Gross, J. D., … Quail, P. H. (2014). A mutually assured destruction mechanism attenuates light signalling in Arabidopsis. *Science*, *344*(6188), 1160–1164. https://doi.org/10.1126/science.1250778

Ni, Z., Kim, E.-D., & Chen, Z. J. (2009). Chlorophyll and starch assays. Retrieved from http://dx.doi.org/10.1038/nprot.2009.12

Nozue, K., Tat, A. V., Kumar Devisetty, U., Robinson, M., Mumbach, M. R., Ichihashi, Y., … Maloof, J. N. (2015). Shade Avoidance Components and Pathways in Adult Plants Revealed by Phenotypic Profiling. *PLoS Genetics*, *11*(4), 1–26. https://doi.org/10.1371/journal.pgen.1004953

Oh, E., Yamaguchi, S., Hu, J., Yusuke, J., Jung, B., Paik, I., … Choi, G. (2007). PIL5, a Phytochrome-Interacting bHLH Protein, Regulates Gibberellin Responsiveness by Binding Directly to the GAI and RGA Promoters in Arabidopsis Seeds. *The Plant Cell Online*, *19*(4), 1192–1208. https://doi.org/10.1105/tpc.107.050153

Oh, E., Zhu, J. Y., Bai, M. Y., Arenhart, R. A., Sun, Y., & Wang, Z. Y. (2014). Cell elongation is regulated through a central circuit of interacting transcription factors in the Arabidopsis hypocotyl. *ELife*, *2014*(3), 1–19.

https://doi.org/10.7554/eLife.03031

Oh, E., Zhu, J. Y., & Wang, Z. Y. (2012). Interaction between BZR1 and PIF4 integrates brassinosteroid and environmental responses. *Nature Cell Biology*, *14*(8), 802–809. https://doi.org/10.1038/ncb2545

Ohashi-Kaneko, K., Matsuda, R., Goto, E., Fujiwara, K., & Kurata, K. (2006). Growth of rice plants under red light with or without supplemental blue light. *Soil Science and Plant Nutrition*, *52*(4), 444–452. https://doi.org/10.1111/j.1747-0765.2006.00063.x

Ohgishi, M., Oka, A., Morelli, G., Ruberti, I., & Aoyama, T. (2001). Negative autoregulation of the Arabidopsis homeobox gene ATHB-2. *Plant Journal*, *25*(4), 389–398. https://doi.org/10.1046/j.1365-313X.2001.00966.x

Okushima, Y., Fukaki, H., Onoda, M., Theologis, A., & Tasaka, M. (2007). ARF7 and ARF19 Regulate Lateral Root Formation via Direct Activation of LBD/ASL Genes in Arabidopsis. *The Plant Cell Online*, *19*(1), 118–130. https://doi.org/10.1105/tpc.106.047761

Olimpieri, I., Caccia, R., Picarella, M. E., Pucci, A., Santangelo, E., Soressi, G. P., & Mazzucato, A. (2011). Constitutive co-suppression of the GA 20-oxidase1 gene in tomato leads to severe defects in vegetative and reproductive development. *Plant Science*, *180*(3), 496–503. https://doi.org/10.1016/j.plantsci.2010.11.004

Olle, M., & Viršile, A. (2013). The effects of light-emitting diode lighting on greenhouse plant growth and quality. *Agricultural and Food Science*, *22*(2), 223–234.

Olsson, A. S. B., Engström, P., & Söderman, E. (2004). The homeobox genes ATHB12 and ATHB7 encode potential regulators of growth in response to water deficit in Arabidopsis. *Plant Molecular Biology*, *55*(5), 663–677. https://doi.org/10.1007/s11103-004-1581-4

Onda, Y., Yagi, Y., Saito, Y., Takenaka, N., & Toyoshima, Y. (2008). Light induction of Arabidopsis SIG1 and SIG5 transcripts in mature leaves: Differential roles of cryptochrome 1 and cryptochrome 2 and dual function of SIG5 in the recognition of plastid promoters. *Plant Journal*, *55*(6), 968–978. https://doi.org/10.1111/j.1365-313X.2008.03567.x

Park, J. E., Seo, P. J., Lee, A. K., Jung, J. H., Kim, Y. S., & Park, C. M. (2007). An Arabidopsis GH3 gene, encoding an auxin-conjugating enzyme, mediates phytochrome B-regulated light signals in hypocotyl growth. *Plant and Cell Physiology*, *48*(8), 1236–1241. https://doi.org/10.1093/pcp/pcm086

Pedmale, U. V, Huang, S. C., Zander, M., Cole, B. J., Hetzel, J., Ljung, K., … Cole, B. J. (2017). HHS Public Access, *164*(0), 233–245. https://doi.org/10.1016/j.cell.2015.12.018.Cryptochromes

Pedmale, U. V, Huang, S. S. C., Zander, M., Cole, B. J., Hetzel, J., Ljung, K., … Chory, J. (2016). Cryptochromes Interact Directly with PIFs to Control Plant Growth in Limiting Blue Light. *Cell*, *164*(1–2), 233–245. https://doi.org/10.1016/j.cell.2015.12.018

Petricka, J. J., Clay, N. K., & Nelson, T. M. (2008). Vein patterning screens and the

defectively organized tributaries mutants in Arabidopsis thaliana. *Plant Journal*, *56*(2), 251–263. https://doi.org/10.1111/j.1365-313X.2008.03595.x

Phipson, B., Lee, S., Majewski, I., Alexander, W., & Smyth, G. (2015). limma powers differential expression analyses for RNA-sequencing and microarray studies. *Nucleic Acids Research*, *43*(7), E47.

Puthiyaveetil, S., Ibrahim, I. M., Jelicić, B., Tomasić, A., Fulgosi, H., & Allen, J. F. (2010). Transcriptional control of photosynthesis genes: the evolutionarily conserved regulatory mechanism in plastid genome function. *Genome Biology and Evolution*, *2*, 888–896. https://doi.org/10.1093/gbe/evq073

Qiu, Z., Wang, X., Gao, J., Guo, Y., Huang, Z., & Du, Y. (2016). The tomato Hoffman's anthocyaninless gene encodes a bHLH transcription factor involved in anthocyanin biosynthesis that is developmentally regulated and induced by low temperatures. *PLoS ONE*, *11*(3), 1–22. https://doi.org/10.1371/journal.pone.0151067

Quail, P. H. (2002). Phytochrome photosensory signalling networks. *Nature Reviews. Molecular Cell Biology*, *3*(2), 85–93. https://doi.org/10.1038/nrm728

Quint, M., Delker, C., Franklin, K. A., Wigge, P. A., Halliday, K. J., & Van Zanten, M. (2016). Molecular and genetic control of plant thermomorphogenesis. *Nature Plants*, *2*(January), 1–9. https://doi.org/10.1038/nplants.2015.190

Rai, A. C., Singh, M., & Shah, K. (2013). Engineering drought tolerant tomato plants over-expressing BcZAT12 gene encoding a C2H2zinc finger transcription factor. *Phytochemistry*, *85*, 44–50. https://doi.org/10.1016/j.phytochem.2012.09.007

Ramakers, C., Ruijter, J. M., Lekanne Deprez, R. H., & Moorman, A. F. M. (2003). Assumption-free analysis of quantitative real-time polymerase chain reaction (PCR) data. *Neuroscience Letters*, *339*(1), 62–66. https://doi.org/10.1016/S0304-3940(02)01423-4

Rao, A. Q., Irfan, M., Saleem, Z., Nasir, I. A., Riazuddin, S., & Husnain, T. (2011). Overexpression of the phytochrome B gene from Arabidopsis thaliana increases plant growth and yield of cotton (Gossypium hirsutum). *Journal of Zhejiang University SCIENCE B*, *12*(4), 326–334. https://doi.org/10.1631/jzus.B1000168

Rao, X., Huang, X., Zhou, Z., & Lin, X. (2013). An improvement of the 2ˆ(-delta delta CT) method for quantitative real-time polymerase chain reaction data analysis. *Biostatistics, Bioinformatics and Biomathematics*, *3*(3), 71–85. https://doi.org/10.1016/j.biotechadv.2011.08.021.Secreted

Rawat, R., Schwartz, J., Jones, M. A., Sairanen, I., Cheng, Y., Andersson, C. R., … Harmer, S. L. (2009). REVEILLE1, a Myb-like transcription factor, integrates the circadian clock and auxin pathways. *Proceedings of the National Academy of Sciences*, *106*(39), 16883–16888. https://doi.org/10.1073/pnas.0813035106

Robinson, M. D., McCarthy, D., Chen, Y., & Smyth, G. K. (2013). edgeR: differential expression analysis of digital gene expression data User's Guide, (October 2018), 1–75.

Robinson, M. D., McCarthy, D. J., & Smyth, G. K. (2009). edgeR: A Bioconductor package for differential expression analysis of digital gene expression data.

Bioinformatics, *26*(1), 139–140. https://doi.org/10.1093/bioinformatics/btp616

Robson, P. R., McCormac, a C., Irvine, a S., & Smith, H. (1996). Genetic engineering of harvest index in tobacco through overexpression of a phytochrome gene. *Nature Biotechnology*, *14*(8), 995–998. https://doi.org/10.1038/nbt0896-995

Rosado, D., Gramegna, G., Cruz, A., Lira, B. S., Freschi, L., De Setta, N., & Rossi, M. (2016). Phytochrome Interacting Factors (PIFs) in Solanum lycopersicum: Diversity, evolutionary history and expression profiling during different developmental processes. *PLoS ONE*. https://doi.org/10.1371/journal.pone.0165929

Rubin, G., Tohge, T., Matsuda, F., Saito, K., & Scheible, W.-R. (2009). Members of the LBD Family of Transcription Factors Repress Anthocyanin Synthesis and Affect Additional Nitrogen Responses in Arabidopsis. *The Plant Cell*, *21*(11), 3567–3584. https://doi.org/10.1105/tpc.109.067041

Ruppel, N. J., Kropp, K. N., Davis, P. A., Martin, A. E., Luesse, D. R., & Hangarter, R. P. (2013). Mutations in geranylgeranyl diphosphate synthase 1 affect chloroplast development in arabidopsis thaliana (Brassicaceae). *American Journal of Botany*, *100*(10), 2074–2084. https://doi.org/10.3732/ajb.1300124

Saijo, Y., Sullivan, J. a, Wang, H., Yang, J., Shen, Y., Rubio, V., … Hoecker, U. (2003). The COP1 − SPA1 interaction defines a critical step in phytochrome A-mediated regulation of HY5 activity service The COP1 – SPA1 interaction defines a critical step in phytochrome A-mediated regulation of HY5 activity. *Genes & Development*, (203), 2642–2647. https://doi.org/10.1101/gad.1122903

Sakai, T., Kagawa, T., Kasahara, M., Swartz, T. E., Christie, J. M., Briggs, W. R., … Okada, K. (2001). Arabidopsis nph1 and npl1: blue light receptors that mediate both phototropism and chloroplast relocation. *Proceedings of the National Academy of Sciences of the United States of America*, *98*(12), 6969–6974. https://doi.org/10.1073/pnas.101137598

Sakamoto, K., & Briggs, W. (2002). Cellular and subcellular localization of Phototropin 1. *The Plant Cell*, *14*(August), 1723–1735. https://doi.org/10.1105/tpc.003293.Phot1

Sasidharan, R., Chinnappa, C. C., Staal, M., Elzenga, J. T. M., Yokoyama, R., Nishitani, K., … Pierik, R. (2010). Light Quality-Mediated Petiole Elongation in Arabidopsis during Shade Avoidance Involves Cell Wall Modification by Xyloglucan Endotransglucosylase/Hydrolases. *PLANT PHYSIOLOGY*. https://doi.org/10.1104/pp.110.162057

Sato, S., Tabata, S., Hirakawa, H., Asamizu, E., Shirasawa, K., Isobe, S., … Klein Lankhorst, R. M. (2012). The tomato genome sequence provides insights into fleshy fruit evolution. *Nature*, *485*(7400), 635–641. https://doi.org/10.1038/nature11119

Schena, M., Lloyd, A. M., & Davis, R. W. (1993). The HAT4 gene of Arabidopsis encodes a developmental regulator. *Genes and Development*, *7*(3), 367–379. https://doi.org/10.1101/gad.7.3.367

Schomburg, F. M., Bizzell, C., Lee, D. J., Zeevart, J. A. D., & Amasino, R. (2003).

Overexpression of a Novel Class of Gibberellin 2-Oxidases Decreases Gibberellin Levels and Creates Dwarf Plants, *15*(November), 1–2. https://doi.org/10.1105/tpc.005975.2

Sellaro, R., Crepy, M., Trupkin, S. A., Karayekov, E., Buchovsky, A. S., Rossi, C., … Jose, J. (2010). Cryptochrome as a sensor of the blue/green ratio of natural radiation in Arabidopsis. *Plant Physiology*, *154*(1), 401–409. https://doi.org/10.1104/pp.110.160820

Sellaro, R., Hoecker, U., Yanovsky, M., Chory, J., & Casal, J. J. (2009). Synergism of Red and Blue Light in the Control of Arabidopsis Gene Expression and Development. *Current Biology*, *19*(14), 1216–1220. https://doi.org/10.1016/j.cub.2009.05.062

Sessa, G., Carabelli, M., Sassi, M., Ciolfi, A., Possenti, M., Mittempergher, F., … Ruberti, I. (2005). A dynamic balance between gene activation and repression regulates the shade avoidance response in Arabidopsis. *Genes & …*, *19*(23), 2811–2815. https://doi.org/10.1101/gad.364005.GENES

Sharma, P., Chatterjee, M., Burman, N., & Khurana, J. (2014). CRY1 regulates growth and devlopment in Brassica through alteration in expression of genes involved in light phytohormone and stress. *Plant, Cell & Environment*, *37*, 961–977.

Sheehan, M. J., Kennedy, L. M., Costich, D. E., & Brutnell, T. P. (2007). Subfunctionalization of PhyB1 and PhyB2 in the control of seedling and mature plant traits in maize. *Plant Journal*, *49*(2), 338–353. https://doi.org/10.1111/j.1365-313X.2006.02962.x

Shin, Y. K., Yum, H., Kim, E. S., Cho, H., Gothandam, K. M., Hyun, J., & Chung, Y. Y. (2006). BcXTH1, a Brassica campestris homologue of Arabidopsis XTH9, is associated with cell expansion. *Planta*, *224*(1), 32–41. https://doi.org/10.1007/s00425-005-0189-5

Shinomura, T., Nagatani, a, Hanzawa, H., Kubota, M., Watanabe, M., & Furuya, M. (1996). Action spectra for phytochrome A- and B-specific photoinduction of seed germination in Arabidopsis thaliana. *Proceedings of the National Academy of Sciences of the United States of America*, *93*(15), 8129–8133. https://doi.org/10.1073/pnas.93.15.8129

Smith, H. (1982). Light Quality, Photoperception, and Plant Strategy. *Annual Review of Plant Physiology*, *33*(1), 481–518. https://doi.org/10.1146/annurev.pp.33.060182.002405

Smith, H., & Whitelam, G. C. (1997). The shade avoidance syndrome: multiple responses mediated by multiple phytochromes. *Plant Cell and Environment*, *20*, 840–844. https://doi.org/10.1046/j.1365-3040.1997.d01-104.x

Son, K. H., & Oh, M. M. (2013). Leaf shape, growth, and antioxidant phenolic compounds of two lettuce cultivars grown under various combinations of blue and red light-emitting diodes. *HortScience*, *48*(8), 988–995.

Song, & Imaizumi, T. (2012). FKF1 Conveys Timing Information for, *1045*, 1045–1050. https://doi.org/10.1126/science.1219644

Spartz, A. K., Lee, S. H., Wenger, J. P., Gonzalez, N., Itoh, H., Inzé, D., … Gray, W. M. (2012). The SAUR19 subfamily of SMALL AUXIN UP RNA genes promote cell expansion. *Plant Journal*, *70*(6), 978–990. https://doi.org/10.1111/j.1365-313X.2012.04946.x

Stamm, P., & Kumar, P. P. (2010). The phytohormone signal network regulating elongation growth during shade avoidance. *Journal of Experimental Botany*, *61*(11), 2889–2903. https://doi.org/10.1093/jxb/erq147

Steindler, C., Matteucci, a, Sessa, G., Weimar, T., Ohgishi, M., Aoyama, T., … Ruberti, I. (1999). Shade avoidance responses are mediated by the ATHB-2 HD-zip protein, a negative regulator of gene expression. *Development (Cambridge, England)*, *126*(19), 4235–4245.

Stuart, J. M., Segal, E., Koller, D., & Kim, S. K. (2003). A gene-coexpression network for global discovery of conserved genetic modules. *Science*, *302*(5643), 249–255. https://doi.org/10.1126/science.1087447

Sun, J., Nishio, J. N., & Vogelmann, T. C. (1998). Green light drives CO2 fixation deep within leaves. *Plant and Cell Physiology*, *39*(10), 1020–1026. https://doi.org/10.1093/oxfordjournals.pcp.a029298

Sun, L., Zhang, A., Zhou, Z., Zhao, Y., Yan, A., Bao, S., … Gan, Y. (2015). *GLABROUS INFLORESCENCE STEMS3* (*GIS3*) regulates trichome initiation and development in *Arabidopsis*. *New Phytologist*, *206*(1), 220–230. https://doi.org/10.1111/nph.13218

Sun, N., Wang, J., Gao, Z., Dong, J., He, H., Terzaghi, W., … Chen, H. (2016). *Arabidopsis* SAURs are critical for differential light regulation of the development of various organs. *Proceedings of the National Academy of Sciences*, *113*(21), 6071–6076. https://doi.org/10.1073/pnas.1604782113

Sun, T. P. (2011). The molecular mechanism and evolution of the GA-GID1-DELLA signalling module in plants. *Current Biology*, *21*(9), R338–R345. https://doi.org/10.1016/j.cub.2011.02.036

Supek, F., Bošnjak, M., Škunca, N., & Šmuc, T. (2011). Revigo summarizes and visualizes long lists of gene ontology terms. *PLoS ONE*, *6*(7). https://doi.org/10.1371/journal.pone.0021800

Takemiya, A., Sugiyama, N., Fujimoto, H., Tsutsumi, T., Yamauchi, S., Hiyama, A., … Shimazaki, K. I. (2013). Phosphorylation of BLUS1 kinase by phototropins is a primary step in stomatal opening. *Nature Communications*, *4*(May), 1–8. https://doi.org/10.1038/ncomms3094

Talbott, L. D., Shmayevich, I. J., Chung, Y., Hammad, J. W., & Zeiger, E. (2003). Blue light and phytochrome-mediated stomatal opening in the \textit{npq1} and \textit{phot1 phot 2} mutants of {Arabidopsis}. *Plant Physiology*, *133*(December), 1522–1529. https://doi.org/10.1104/pp.103.029587

Tepperman, J. M., Hudson, M. E., Khanna, R., Zhu, T., Chang, S. H., Wang, X., & Quail, P. H. (2004). Expression profiling of phyB mutant demonstrates substantial contribution of other phytochromes to red-light-regulated gene expression during seedling de-etiolation. *Plant Journal*, *38*(5), 725–739. https://doi.org/10.1111/j.1365-313X.2004.02084.x

Tepperman, J. M., Zhu, T., Chang, H. S., Wang, X., & Quail, P. H. (2001). Multiple transcription-factor genes are early targets of phytochrome A signalling. *Proceedings of the National Academy of Sciences of the United States of America*, *98*(16), 9437–9442. https://doi.org/10.1073/pnas.161300998

Terashima, I., Fujita, T., Inoue, T., Chow, W. S., & Oguchi, R. (2009). Green Light Drives Leaf Photosynthesis More Efficiently than Red Light in Strong White Light : Revisiting the Enigmatic Question of Why Leaves are Green. *Plant & Cell Physiology*, *50*(4), 684–697. https://doi.org/10.1093/pcp/pcp034

Tewolde, F. T., Lu, N., Shiina, K., Maruo, T., Takagaki, M., Kozai, T., & Yamori, W. (2016). Nighttime Supplemental LED Inter-lighting Improves Growth and Yield of Single-Truss Tomatoes by Enhancing Photosynthesis in Both Winter and Summer. *Frontiers in Plant Science*, *7*(April), 1–10. https://doi.org/10.3389/fpls.2016.00448

Thiele, a, Herold, M., Lenk, I., Quail, P. H., & Gatz, C. (1999). Heterologous expression of Arabidopsis phytochrome B in transgenic potato influences photosynthetic performance and tuber development. *Plant Physiology*, *120*(1), 73–82. https://doi.org/10.1104/pp.120.1.73

Tobeña-Santamaria, R., Bliek, M., Ljung, K., Sandberg, G., Mol, J. N. ., Souer, E., & Koes, R. (2002). FLOOZY of petunia is a flavin and flower architecture for the specification of leaf mono-oxygenase-like protein required for the specification of leaf and flower achitecture. *GENES & DEVELOPMENT*, *16*(May), 753–763. https://doi.org/10.1101/gad.219502.in

Toledo-Ortiz, G., Johansson, H., Lee, K. P., Bou-Torrent, J., Stewart, K., Steel, G., … Halliday, K. J. (2014). The HY5-PIF Regulatory Module Coordinates Light and Temperature Control of Photosynthetic Gene Transcription. *PLoS Genetics*, *10*(6). https://doi.org/10.1371/journal.pgen.1004416

Usami, T., Mochizuki, N., Kondo, M., Nishimura, M., & Nagatani, A. (2004). Cryptochromes and phytochromes synergistically regulate Arabidopsis root greening under blue light. *Plant and Cell Physiology*, *45*(12), 1798–1808. https://doi.org/10.1093/pcp/pch205

Valverde, F., Mouradov, A., Soppe, W., Ravenscroft, D., Samach, A., & Coupland, G. (2004). Photoreceptor regulation of CONSTANS protein in photoperiodic flowering. *Science (New York, N.Y.)*, *303*(5660), 1003–1006. https://doi.org/10.1126/science.1091761

Vogelmann, T. C., & Han, T. (2000). Measurement of chlorophyll fluorescence profiles in leaves. *Plant, Cell, and Environment*, *23*, 1303–1311.

W, E. P. D., Dhingra, A., Bies, D. H., Lehner, K. R., & Folta, K. M. (2006). Green Light Adjusts the Plastid Transcriptome during, *142*(November), 1256–1266. https://doi.org/10.1104/pp/106.088351

Wan, Y. L., Eisinger, W., Ehrhardt, D., Kubitscheck, U., Baluska, F., & Briggs, W. (2008). The subcellular localization and blue-light-induced movement of phototropin 1-GFP in etiolated seedlings of Arabidopsis thaliana. *Molecular Plant*, *1*(1), 103–117. https://doi.org/10.1093/mp/ssm011

Wang, F., Wu, N., Zhang, L., Ahammed, G. J., Chen, X., Xiang, X., … Zhou, Y.

(2017). Light Signalling-dependent Regulation of Photoinhibition and Photoprotection in Tomato. *Plant Physiology*, *176*(February), pp.01143.2017. https://doi.org/10.1104/pp.17.01143

Wang, X. Y., Xu, X. M., & Cui, J. (2015). The importance of blue light for leaf area expansion, development of photosynthetic apparatus, and chloroplast ultrastructure of Cucumis sativus grown under weak light. *Photosynthetica*, *53*(2), 213–222. https://doi.org/10.1007/s11099-015-0083-8

Wang, Z., Gerstein, M., & Snyder, M. (2009). RNA-Seq: a revolutionary tool for transcriptomics. *Nature Reviews. Genetics*, *10*(1), 57–63. https://doi.org/10.1038/nrg2484

Weller, J. L., Beauchamp, N., Kerckhoffs, L. H. J., Damien Platten, J., & Reid, J. B. (2001). Interaction of phytochromes A and B in the control of de-etiolation and flowering in pea. *Plant Journal*, *26*(3), 283–294. https://doi.org/10.1046/j.1365-313X.2001.01027.x

Weller, J. L., Perrotta, G., Schreuder, M. E. L., Van Tuinen, A., Koornneef, M., Giuliano, G., & Kendrick, R. E. (2001). Genetic dissection of blue-light sensing in tomato using mutants deficient in cryptochrome 1 and phytochromes A, B1 and B2. *Plant Journal*, *25*, 427–440. https://doi.org/10.1046/j.1365-313X.2001.00978.x

Weller, J. L., Schreuder, M. E. L. L., Smith, H., Koornneef, M., & Kendrick, R. E. (2000). Physiological interactions of phytochromes A, B1 and B2 in the control of development in tomato. *Plant Journal*. https://doi.org/10.1046/j.1365-313X.2000.00879.x

Werner, T., Motyka, V., Strnad, M., & Schmülling, T. (2001). Regulation of plant growth by cytokinin. *Proceedings of the National Academy of Sciences of the United States of America*, *98*(18), 10487–10492. https://doi.org/10.1073/pnas.171304098

Wieczorek, P., Wrzesińska, B., & Obrepalska-Steplowska, A. (2013). Assessment of reference gene stability influenced by extremely divergent disease symptoms in Solanum lycopersicum L. *Journal of Virological Methods*, *194*(1–2), 161–168. https://doi.org/10.1016/j.jviromet.2013.08.010

Wu, F.-Q., Xin, Q., Cao, Z., Liu, Z.-Q., Du, S.-Y., Mei, C., … Zhang, D.-P. (2009). The Magnesium-Chelatase H Subunit Binds Abscisic Acid and Functions in Abscisic Acid Signalling: New Evidence in Arabidopsis. *Plant Physiology*, *150*(4), 1940–1954. https://doi.org/10.1104/pp.109.140731

Xu, F., He, S., Zhang, J., Mao, Z., Wang, W., Li, T., … Yang, H. Q. (2018). Photoactivated CRY1 and phyB Interact Directly with AUX/IAA Proteins to Inhibit Auxin Signalling in Arabidopsis. *Molecular Plant*. https://doi.org/10.1016/j.molp.2017.12.003

Xu, W., & Huang, W. (2017). Calcium-Dependent Protein Kinases in Phytohormone Signalling Pathways. *International Journal of Molecular Sciences*. https://doi.org/10.1016/j.cub.2015.10.018

Yamamoto, Y., Kamiya, N., Morinaka, Y., Matsuoka, M., & Sazuka, T. (2007). Auxin Biosynthesis by the YUCCA Genes in Rice. *Plant Physiology*, *143*(3),

1362–1371. https://doi.org/10.1104/pp.106.091561

Yang, D.-L., Yao, J., Mei, C.-S., Tong, X.-H., Zeng, L.-J., Li, Q., … He, S. Y. (2012). Plant hormone jasmonate prioritizes defense over growth by interfering with gibberellin signalling cascade. *Proceedings of the National Academy of Sciences*, *109*(19), E1192–E1200. https://doi.org/10.1073/pnas.1201616109

Yang, D., Seaton, D. D., Krahmer, J., & Halliday, K. J. (2016). Photoreceptor effects on plant biomass, resource allocation, and metabolic state. *Proceedings of the National Academy of Sciences*, *113*(27), 7667–7672. https://doi.org/10.1073/pnas.1601309113

Yang, F. O., Mao, J. F., Wang, J., Zhang, S., & Li, Y. (2015). Transcriptome analysis reveals that red and blue light regulate growth and phytohormone metabolism in Norway spruce [Picea abies (L.) Karst.]. *PLoS ONE*, *10*(8), 1–19. https://doi.org/10.1371/journal.pone.0127896

Yang, H. Q., Wu, Y. J., Tang, R. H., Liu, D., Liu, Y., & Cashmore, A. R. (2000). The C termini of Arabidopsis cryptochromes mediate a constitutive light response. *Cell*, *103*(5), 815–827. https://doi.org/10.1016/S0092-8674(00)00184-7

Yang, J., Lin, R., Sullivan, J., Hoecker, U., Liu, B., Xu, L., … Wang, H. (2005). Light Regulates COP1-Mediated Degradation of HFR1, a Transcription Factor Essential for Light Signalling in Arabidopsis. *The Plant Cell Online*, *17*(3), 804–821. https://doi.org/10.1105/tpc.104.030205

Yang, Y., Wang, M., Yin, Y., Onac, E., Zhou, G., Peng, S., … Zhou, Y. (2015). RNA-seq analysis reveals the role of red light in resistance against Pseudomonas syringae pv . tomato DC3000 in tomato plants, 1–16. https://doi.org/10.1186/s12864-015-1228-7

Yin, Y., Vafeados, D., Tao, Y., Yoshida, S., Asami, T., & Chory, J. (2005). A new class of transcription factors mediates brassinosteroid-regulated gene expression in Arabidopsis. *Cell*, *120*(2), 249–259. https://doi.org/10.1016/j.cell.2004.11.044

Yorio, N. C., Goins, G. D., Kagie, H. R., Wheeler, R. M., & Sager, J. C. (2001). Improving spinach, radish, and lettuce growth under red light-emitting diodes (LEDs) with blue light supplementation. *HortScience*, *36*(2), 380–383.

Yu, J. W., Rubio, V., Lee, N. Y., Bai, S., Lee, S. Y., Kim, S. S., … Deng, X. W. (2008). COP1 and ELF3 Control Circadian Function and Photoperiodic Flowering by Regulating GI Stability. *Molecular Cell*, *32*(5), 617–630. https://doi.org/10.1016/j.molcel.2008.09.026

Zhang, H., Burr, J., & Zhao, F. (2017). A comparative life cycle assessment (LCA) of lighting technologies for greenhouse crop production. *Journal of Cleaner Production*, *140*, 705–713. https://doi.org/10.1016/j.jclepro.2016.01.014

Zhang, H., He, H., Wang, X., Wang, X., Yang, X., Li, L., & Deng, X. W. (2011). Genome-wide mapping of the HY5-mediated genenetworks in Arabidopsis that involve both transcriptional and post-transcriptional regulation. *Plant Journal*, *65*(3), 346–358. https://doi.org/10.1111/j.1365-313X.2010.04426.x

Zhang, T., & Folta, K. M. (2012). Green light signalling and adaptive response. *Plant Signalling & Behavior*, *7*(1), 75–78. https://doi.org/10.4161/psb.7.1.18635

Zhang, T., Maruhnich, S. a., & Folta, K. M. (2011). Green Light Induces Shade Avoidance Symptoms. *Plant Physiology*, *157*(3), 1528–1536. https://doi.org/10.1104/pp.111.180661

Zhang, T., Maruhnich, S. a., & Folta, K. M. (2011). Green Light Induces Shade Avoidance Symptoms. *Plant Physiology*, *157*(3), 1528–1536. https://doi.org/10.1104/pp.111.180661

Zhang, Y., Mayba, O., Pfeiffer, A., Shi, H., Tepperman, J. M., Speed, T. P., & Quail, P. H. (2013). A Quartet of PIF bHLH Factors Provides a Transcriptionally Centered Signalling Hub That Regulates Seedling Morphogenesis through Differential Expression-Patterning of Shared Target Genes in Arabidopsis. *PLoS Genetics*, *9*(1), 11–13. https://doi.org/10.1371/journal.pgen.1003244

Zhao, A., Fang, Y., Chen, X., Zhao, S., Dong, W., Lin, Y., … Liu, L. (2014). Crystal structure of Arabidopsis glutamyl-tRNA reductase in complex with its stimulator protein. *Proceedings of the National Academy of Sciences*, *111*(18), 6630–6635. https://doi.org/10.1073/pnas.1400166111

Zhao, X., Yu, X., Foo, E., Symons, G. M., Lopez, J., Bendehakkalu, K. T., … Lin, C. (2007). A Study of Gibberellin Homeostasis and Cryptochrome-Mediated Blue Light Inhibition of Hypocotyl Elongation. *Plant Physiology*, *145*(1), 106–118. https://doi.org/10.1104/pp.107.099838

Zhou, P., Song, M., Yang, Q., Su, L., Hou, P., Guo, L., … Yang, J. (2014). Both PHYTOCHROME RAPIDLY REGULATED1 (PAR1) and PAR2 Promote Seedling Photomorphogenesis in Multiple Light Signalling Pathways. *Plant Physiology*, *164*(2), 841–852. https://doi.org/10.1104/pp.113.227231

Zhou, T., Meng, L., Ma, Y., Liu, Q., Zhang, Y., Yang, Z., … Bian, M. (2018). Overexpression of sweet sorghum cryptochrome 1a confers hypersensitivity to blue light, abscisic acid and salinity in Arabidopsis. *Plant Cell Reports*, *37*(2), 251–264. https://doi.org/10.1007/s00299-017-2227-8

Zuo, Z. C., Meng, Y. Y., Yu, X. H., Zhang, Z. L., Feng, D. S., Sun, S. F., … Lin, C. T. (2012). A study of the blue-light-dependent phosphorylation, degradation, and photobody formation of Arabidopsis CRY2. *Molecular Plant*, *5*(3), 726–733. https://doi.org/10.1093/mp/sss007